IL
NUOVO CIMENTO
ORGANO DELLA SOCIETÀ ITALIANA DI FISICA
SOTTO GLI AUSPICI DEL CONSIGLIO NAZIONALE DELLE RICERCHE

VOL. XVI, N. 2 *Serie decima* 16 Aprile 1960

Excited Nucleon Interpretation of High Energy Nuclear Interactions.

F. J. M. FARLEY
CERN - Geneva

(ricevuto il 24 Giugno 1959)

Summary. — An analysis of the kinematics of the excited nucleon model leads to three relationships which are found to be in fair agreement with the experimental data: i) inelasticity-n_s relation; ii) backward angle-n_s relation and iii) forward angle-primary energy relation. A simple statistical treatment of the excited nucleon itself gives a good fit to the transverse momentum distribution in the jets.

1. – Introduction.

Models of high energy nucleon-nucleon encounters, leading to multiple meson production (cosmic ray jets), fall into two broad classes. In the first [1] the mesons are evaporated from a highly excited region stationary in the centre of mass system of the collision (C-space). The strong backward-forward collimation of the mesons in C-space is then discussed in terms of angular momentum conservation or shock waves in the meson gas. In the second [2]

[1] E. FERMI: *Phys. Rev.*, **81**, 683 (1951); W. HEISENBERG: *Zeits. f. Phys.*, **133**, 65 (1952); L. D. LANDAU: *Dokl. Akad. Nauk SSSR*, **12**, 51 (1953); S. Z. BELEN'KIJ and L. D. LANDAU: *Suppl. Nuovo Cimento*, **3**, 15 (1956); D. ITO and H. TANAKA: *Suppl. Nuovo Cimento*, **7**, 91 (1958).

[2] S. TAKAGI: *Progr. Theor. Phys.*, **7**, 123 (1952); H. J. BHABHA: *Proc. Roy. Soc.*, A **219**, 293 (1953); W. L. KRAUSHAAR and L. J. MARKS: *Phys. Rev.*, **93**, 326 (1954); E. FRIEDLÄNDER: *Acta Phys. Acad. Sci. Hungar.*, **6**, 237 (1956); G. T. ZACEPIN: *Suppl. Nuovo Cimento*, **8**, 746 (1958).

the mesons are emitted from excited nucleons (*) moving away from each other after the interaction. Here, with isotropic emission from the moving nucleons (N-space), the collimation of mesons in C-space arises simply as a kinematic effect. Recently it has been suggested (3) that the mesons may be emitted isotropically from moving regions which are separating less fast than the nucleons, *i.e.* from a space intermediate between C-space and N-space.

In the present discussion it is assumed that the mesons are emitted isotropically from two excited nucleons, and furthermore that the total energy in C-space of each excited nucleon after the interaction is the same as its energy before the collision, *i.e.* no energy is left in C-space and there is no exchange between the nucleons. This model leads to definite predictions which are compared with experimental observations on cosmic ray jets and on air showers.

Consider two nucleons of total energy E and rest mass E_0 approaching each other in C-space. Let their velocity be β_c and let $\gamma_c = (1-\beta_c^2)^{-\frac{1}{2}}$. β_c is also the velocity of C-space relative to the laboratory (L-space) for the collision of an incoming primary nucleon (E_p, β_p, γ_p) with a nucleon stationary in the laboratory. We have

$$E = \gamma_c E_0 , \tag{1}$$

$$\gamma_c = \sqrt{\tfrac{1}{2}(\gamma_p + 1)} . \tag{2}$$

After the interaction suppose that the rest mass of each nucleon is increased to αE, the total energy of each being unchanged. Conservation of momentum then requires α to be the same for each nucleon. Suppose that in this process the velocity of each nucleon in C-space is reduced to β, and that $\gamma = (1-\beta^2)^{-\frac{1}{2}}$. According to our assumption, the original energy

$$E = \gamma \times \alpha E ,$$

$$\left\{ \begin{array}{l} \therefore \alpha = 1/\gamma = (1-\beta^2)^{\frac{1}{2}} \\ \beta = (1-\alpha^2)^{\frac{1}{2}} . \end{array} \right. \tag{3}$$

(*) By excited nucleon we mean a strong local concentration of field energy which is eventually radiated in the form of particles including at least one baryon.

(3) G. Cocconi: *Phys. Rev.*, **111**, 1699 (1958); P. Ciok, T. Coghen, J. Gierula, R. Hołyński, A. Jurak, M. Mięsowicz, T. Saniewska and J. Pernegr: *Nuovo Cimento*, **10**, 741 (1958); Z. Koba and S. Takagi: *Nuovo Cimento*, **10**, 755 (1958); K. Niu: *Nuovo Cimento*, **10**, 994 (1958); J. Burmeister, K. Lanius and H. W. Meier: *Nuovo Cimento*, **11**, 12 (1959).

2. – Inelasticity-n_s relation.

The excitation energy of each nucleon is $(\alpha E - E_0)$ and we suppose this to give rise to the emission of m mesons, E_1 being the energy of a meson in N-space. Therefore

$$m\bar{E}_1 = \alpha E - E_0 \,. \tag{4}$$

Assuming that $\frac{1}{3}$ of the mesons are neutral, the number of charged shower particles from both nucleons is

$$n_s = 2m \times \tfrac{2}{3} = 4m/3 \,. \tag{5}$$

The inelasticity of the collision, K, is found by transforming the energies of the mesons to C-space. For an individual meson, energy E_1 and momentum p_1 in N-space, the energy in C-space is

$$E_1^c = \gamma(E_1 + \beta p_{1x}) \,,$$

x being the direction of motion of N-space relative to C-space. Therefore the mean energy of the mesons in C-space is

$$\bar{E}_1^c = \gamma \bar{E}_1 \tag{6}$$

conservation of parity requiring forward-backward symmetry for the meson emission by an excited nucleon with the result that $\bar{p}_{1x}$ is zero on the average. After the collision we are left finally in C-space with m mesons of mean energy $\gamma\bar{E}_1$, and an unexcited nucleon of energy γE_0. Therefore the inelasticity K is

$$K = \frac{\gamma \cdot m\bar{E}_1}{E} = \frac{\gamma \cdot m\bar{E}_1}{\gamma(m\bar{E}_1 + E_0)} = \frac{m\bar{E}_1}{m\bar{E}_1 + E_0} \,. \tag{7}$$

Equations (5) and (7) imply a unique relationship between the inelasticity K and the number of charged shower particles n_s, independent of the incident energy E, but with $\bar{E}_1$ as a parameter. $\bar{E}_1$ is, however, related to the mean transverse momentum $\bar{p}_T$ of the shower particles. For isotropic emission in N-space

$$\bar{p}_T = \frac{\pi}{4} \cdot \bar{p} = \frac{\pi}{4c} \cdot \bar{E}_1 \tag{8}$$

in relativistic approximation.

The relationship between K and n_s is shown in Fig. 1 for various values of $\bar{E}_1$, together with some calculations from experimental data (see Appendix). There is a general trend of agreement for low values of n_s, and the correspon-

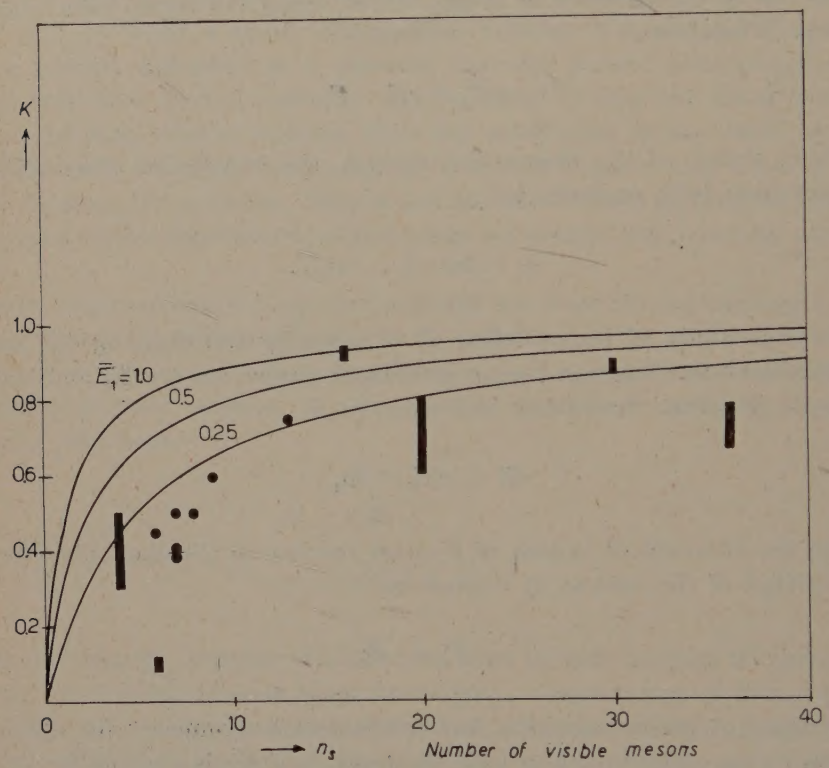

Fig. 1. – Inelasticity K, versus n_s. Experimental data from Appendix I. High energy points ■, low energy points ●.

dence between the Bristol double interaction event at 40 000 GeV [4] with the low energy (~ 50 GeV) data of BIRGER *et al.* [5] supports the conclusion that K for a given n_s is independent of primary energy. There is, however, definite disagreement between the prediction that K should be close to 1 for large values of n_s, and the general conclusions of the Bristol group [4] that K is low for all n_s at high primary energies.

---

[4] B. EDWARDS, J. LOSTY, D. H. PERKINS, K. PINKAU and J. REYNOLDS: *Phil. Mag.*, **3**, 237 (1958).

[5] N. G. BIRGER, V. V. GRIGOROV, G. B. GUSEVA, G. B. ZHDANOV, S. A. SLAVATINSKII and G. M. STASHKOV: *Journ. Exp. Teor. Fiz.*, **31**, 971 (1956).

Further evidence on the inelasticity of high energy interactions comes from extensive air showers. Averaging over the interactions in the nuclear cascade an inelasticity $K = 0.3$ is required to fit the data ([6,7]). Cloud chamber observations ([8]) indicate that low multiplicity events are overwhelmingly the most frequent. Therefore, one expects this value of K to correspond to events giving 1-3 visible mesons, in agreement with the graph of Fig. 1.

3. – Backward angle-n_s relation.

In the experimental data the primary energy can be estimated only from the observed angles of emission of the shower particles. To find the inelasticity this estimate of primary energy is combined with an estimate of total shower particle energy based either on multiple scattering of the tracks, or again on the angular distribution plus the assumption that all tracks have the same transverse momentum ([4]). It is therefore of interest to examine directly the predictions of the present model as to the angular distribution of the shower particles. This leads to a direct relationship between the angles and the number of shower particles n_s independent of energy, and provides an experimental test which is free from the uncertainties which arise in estimating K.

To obtain the angles of the mesons in the laboratory (L-space) it is first necessary to find the velocities of the excited nucleons in this frame, β_f for the nucleon travelling forward in C-space which emits the narrow cone of shower particles, β_b for the backward travelling nucleon which emits the wide cone.

Using the velocity addition theorem one finds

$$(9) \qquad \begin{cases} \gamma_f = (1-\beta_f^2)^{-\frac{1}{2}} = \gamma\gamma_c(1+\beta\beta_c)\,, \\ \gamma_b = (1-\beta_b^2)^{-\frac{1}{2}} = \gamma\gamma_c(1-\beta\beta_c)\,. \end{cases}$$

Therefore

$$(10) \qquad \beta\beta_c = \frac{\gamma_f - \gamma_b}{\gamma_f + \gamma_b}\,.$$

Therefore

$$(11) \qquad \gamma\gamma_c = \tfrac{1}{2}(\gamma_b + \gamma_f)\,.$$

([6]) G. Cocconi: *Suppl. Nuovo Cimento*, **8**, 560 (1958); G. T. Zacepin: *Oxford Conference on Extensive Air Showers* (1956); A. T. Abrosimov, V. I. Zacepin, V. I. Soloveva, G. B. Kristiansen and P. S. Chinin: *Izv. Akad. Nauk. SSSR (Phys.)*, **19**, 677 (1955); O. A. Guzhavina, V. V. Gizhavin and G. T. Zacepin: *Journ. Exp. Teor. Fiz.*, **31**, 819 (1956).

([7]) G. Cocconi: *Handb. d. Phys.*, **46**, (in the press).

([8]) M. Deuschmann: *Zeits. f. Naturfor.*, **9a**, 6, 477 (1954).

For high energy interactions which produce more than a few mesons $\beta_c \sim 1$, but β is considerably smaller. As a first approximation set $\beta_c = 1$ in Eq. (10):

$$\beta = \frac{\gamma_f - \gamma_b}{\gamma_f + \gamma_b}.$$

Therefore

$$\gamma = (1 - \beta^2)^{-\frac{1}{2}} = \frac{\gamma_f + \gamma_b}{2(\gamma_f \gamma_b)^{\frac{1}{2}}}. \tag{12}$$

And substituting in (11)

$$\gamma_c = (\gamma_f \gamma_b)^{\frac{1}{2}}. \tag{13}$$

Equations (12) and (13) determine the collision in C-space in terms of the observable motions of the excited nucleons in L-space as given by γ_b and γ_f, in the cases in which $\gamma_b \gg 1$.

For grazing collisions which leave the struck nucleon almost stationary, $\gamma_b \sim 1$, the approximation is not valid. To obtain a more general solution we use $\alpha = 1/\gamma$, $\alpha_c = 1/\gamma_c$, etc. We have

$$\left\{ \begin{aligned} (\alpha + \alpha_c)^2 &= 2\alpha\alpha_c + \alpha^2 + \alpha_c^2 \\ &= (1 + \alpha\alpha_c)^2 - \beta^2 \beta_c^2 . \end{aligned} \right. \tag{14}$$

But from (10) and (11)

$$\beta\beta_c = \frac{\alpha_b - \alpha_f}{\alpha_b + \alpha_f}, \tag{15}$$

$$\alpha\alpha_c = \frac{2\alpha_b \alpha_f}{\alpha_b + \alpha_f}. \tag{16}$$

And substituting in (14)

$$\alpha + \alpha_c = \frac{2(\alpha_b \alpha_f)^{\frac{1}{2}}}{\alpha_b + \alpha_f} (1 + \alpha_b)^{\frac{1}{2}} (1 + \alpha_f)^{\frac{1}{2}} \tag{17}$$

and similarly

$$\alpha - \alpha_c = \frac{2(\alpha_b \alpha_f)^{\frac{1}{2}}}{\alpha_b + \alpha_f} (1 - \alpha)^{\frac{1}{2}} (1 - \alpha_f)^{\frac{1}{2}}, \tag{18}$$

hence

$$\alpha = \frac{(\alpha_b \alpha_f)^{\frac{1}{2}}}{\alpha_b + \alpha_f} \{(1 + \alpha_b)^{\frac{1}{2}} (1 + \alpha_f)^{\frac{1}{2}} + (1 - \alpha_b)^{\frac{1}{2}} (1 - \alpha_f)^{\frac{1}{2}}\} \tag{19}$$

$$\alpha_c = \frac{(\alpha_b \alpha_f)^{\frac{1}{2}}}{\alpha_b + \alpha_f} \{(1 + \alpha_b)^{\frac{1}{2}} (1 + \alpha_f)^{\frac{1}{2}} - (1 - \alpha_b)^{\frac{1}{2}} (1 - \alpha_f)^{\frac{1}{2}}\}. \tag{20}$$

These equations reduce to (12) and (13) if $\alpha_f < \alpha_b \ll 1$. To relate these quantities to the number of mesons produced, remember that the total energy evolved from each nucleon as mesons in the C-system is equal to the incoming nucleon energy minus the final energy of the de-excited nucleon; therefore using (6)

$$\gamma \cdot m\bar{E}_1 = \gamma_c E_0 - \gamma E_0$$

$$\therefore m = \frac{E_0}{E_1}\left\{\frac{\gamma_c}{\gamma} - 1\right\} = \frac{E_0}{E_1}\left\{\frac{\alpha}{\alpha_c} - 1\right\}. \tag{21}$$

But from (19) and (20)

$$\frac{\alpha}{\alpha_c} = \frac{1 + \alpha_b\alpha_f + \beta_b\beta_f}{\alpha_b + \alpha_f}. \tag{22}$$

Therefore

$$n_s = \frac{4m}{3} = \frac{4E_0}{3\bar{E}_1}\,\frac{(1-\alpha_b)(1-\alpha_f) + \beta_b\beta_f}{\alpha_b + \alpha_f}. \tag{23}$$

The parameters α_f and α_b (with the related β_f and β_b) specify the motion of the two excited nucleons in the laboratory and can be determined from the observed angles of emission of the shower particles in the narrow and wide cones respectively, see below. Equation (23) therefore relates the number of shower particles n_s to the angular information. In almost every case $\beta_f > 0.99$ and α_f is small: therefore

$$n_s \sim \frac{4E_0}{3\bar{E}_1}\cdot\frac{1 - \alpha_b - \alpha_f + \beta_b}{\alpha_b + \alpha_f}, \tag{24}$$

$$n_s \sim \frac{4E_0}{3\bar{E}_1}\cdot\frac{1 - \alpha_b + \beta_b}{\alpha_b}. \tag{25}$$

The form (25) shows that n_s is determined very largely by the angles in the wide cone. As these angles can be measured accurately, Eq. (25) provides a good test of the excited nucleon model. The relation between n_s and α_b is plotted in Fig. 2 as a function of $\bar{E}_1$. This shows that a wide backward cone (α_b large) should be associated with a small number of shower particles (n_s small), and vice versa.

Before comparing these graphs with experiment, one must see how α_b and α_f can be estimated for each event from the observed distribution of shower particles with respect to the laboratory angle of emission φ. The observations are conveniently displayed, following EDWARDS *et al.* [4], by marking the position of each shower particle on a scale of log tg.φ as in

Fig. 4. The excited nucleon model makes quite definite predictions about the distribution of points on this diagram.

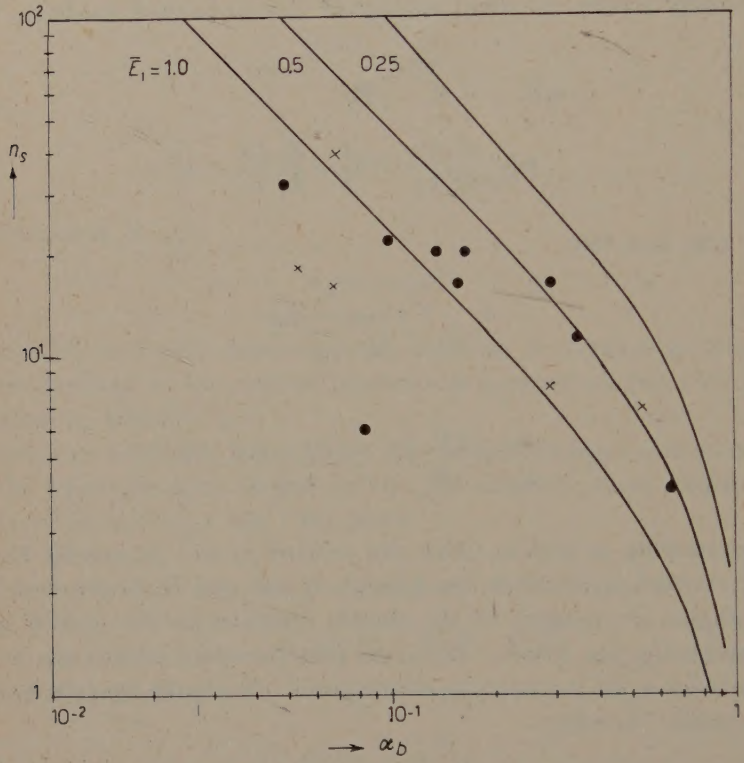

Fig. 2. – n_s versus the mean angle of the backward cone, α_b, and experimental data for the events depicted in Fig. 4.

Consider, for example, the backward nucleon. For a meson emitted at angle ϑ in N-space at velocity β_1

$$\gamma_b \operatorname{tg} \varphi = \frac{\sin \vartheta}{q + \cos \vartheta}, \tag{26}$$

where $q = \beta_b/\beta_1$. For isotropic emission from the moving nucleon the intensity versus $\log(\gamma_b \operatorname{tg} \varphi)$ is given in Fig. 3 for various values of q. For the simplest case, $q = 1$, the distribution is symmetrical and at the centre $\log \operatorname{tg} \varphi = -\log \gamma_b = \log \alpha_b$. In this case therefore $\log \gamma_b = -\overline{\log \operatorname{tg} \varphi}$, the formula of CASTAGNOLI *et al* [9]. Similar considerations apply to the forward cone and

[9] C. CASTAGNOLI, G. CORTINI, C. FRANZINETTI, A. MANFREDINI and D. MORENO: *Nuovo Cimento*, **10**, 1539 (1953).

according to (13), $\log \gamma_c = \frac{1}{2}(\log \gamma_b + \log \gamma_f) = -(\overline{\log \operatorname{tg} \varphi})_{\text{overall-mean}}$ in agreement with the usual formula. This shows that the Castagnoli formula is valid on the excited nucleon model if there are equal numbers of particles in the wide and narrow cones, and in so far as (13) is a good approximation to (20) and $q = 1$.

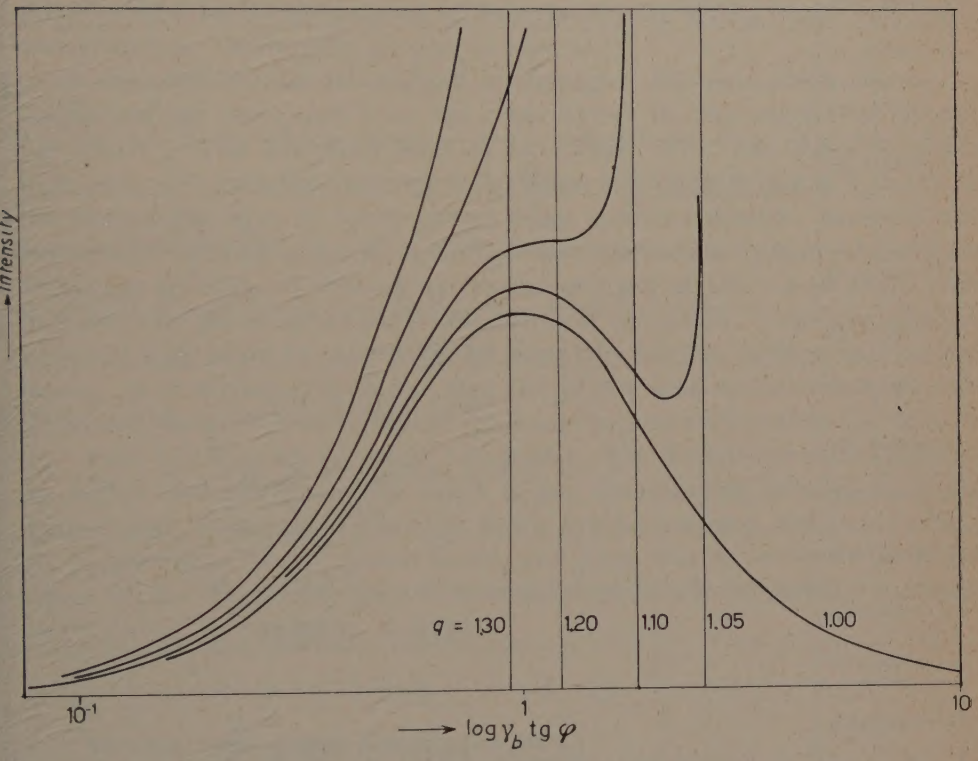

Fig. 3. – Probability distribution in $\log(\gamma_b \operatorname{tg} \varphi)$ for various values of q.

In practice, one must expect q values greater than 1, because β_1 will often be less than β_b. As indicated in Fig. 3 this gives rise to a shift of the distribution towards smaller values of $\log(\gamma_b \operatorname{tg} \varphi)$ with the result that the simple estimate of the α_b will be too low, γ_f too high, but the error will be not more than a factor 2. As this applies both to γ_b and γ_f the over-all value of γ_c would be over-estimated by the same factor.

Note that the width of the distribution (for $q = 1$) is such that half the particles are contained within a factor 3.3 in $\operatorname{tg} \varphi$ and 90% within a factor 10.

Returning to Fig. 4, one sees for many jets two distinct groups of particles corresponding to the backward and forward nucleons, and the width

of the groups and the distribution within the groups is in rough agreement with the predictions of Fig. 3.

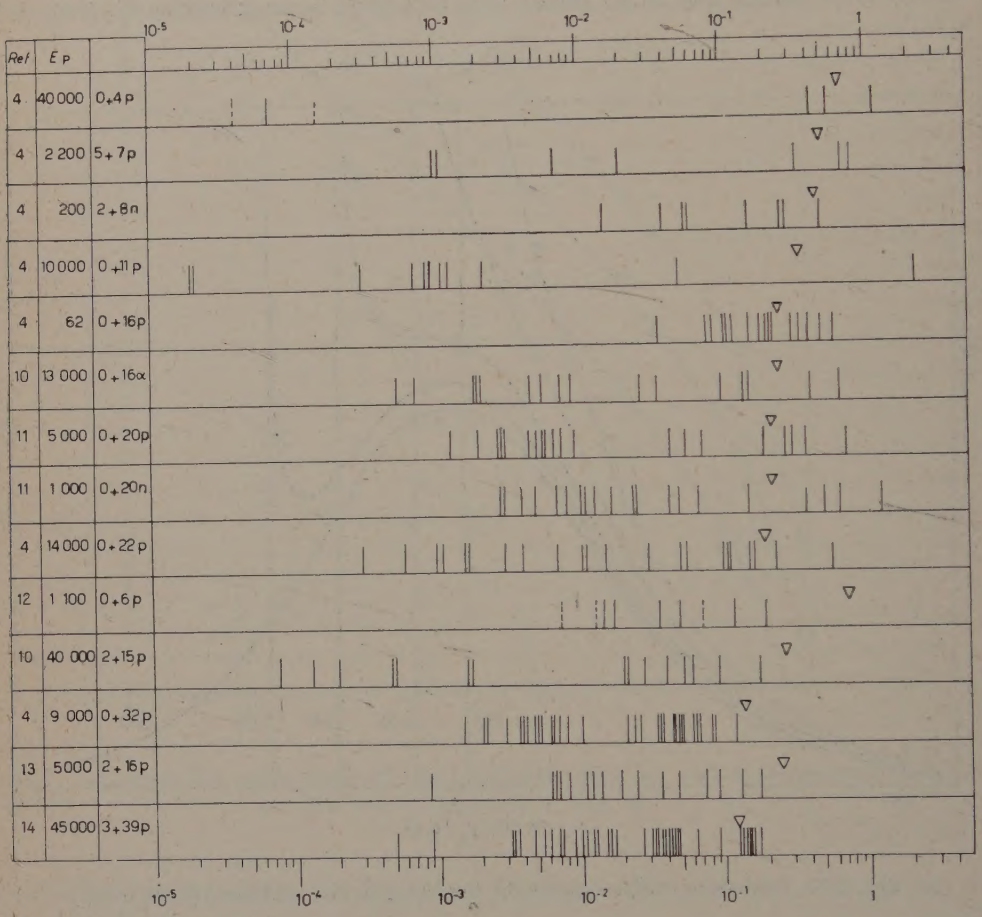

Fig. 4. – $\log \operatorname{tg} \varphi$ display of 14 events. Arrow marks the expected centre of the wide cone read from Fig. 2 for $\overline{E}_1 = 0.5$ and for the observed number of shower particles.

---

(10) R. G. Glasser, D. M. Haskin, M. Schein and J. J. Lord: *Phys. Rev.*, **99**, 1555 (1955).

(11) M. W. Teucher, D. M. Haskin and M. Schein: *Phys. Rev.*, **111**, 1384 (1958); M. Schein: *Proc. of the VII Rochester Conference* (New York, 1957).

(12) V. D. Hopper, S. Biswas and J. F. Darby: *Phys. Rev.*, **84**, 457 (1951).

(13) E. G. Boos, A. Kh. Vinitskii, Zh. S. Takibaev and I. Ia. Chasnikov: *Journ. Exp. Teor. Fiz.*, **34**, 622 (1958).

(14) A. Debenedetti, C. M. Garelli, L. Tallone and M. Vigone: *Nuovo Cimento*, **4**, 1142 (1956).

The separation of the backward and forward groups in the diagram gives a measure of γ, corresponding to the velocity of separation of the excited nucleons after the collision (see Eq. (12)). Qualitatively the observations corroborate the model in that after a glancing collision the excited nucleons separate with a large value of γ, but have small excitation. Thus when there are few mesons they occur in two well-separated groups. But a strong collision giving many mesons leaves the excited nucleons separating slowly, small value of γ, and gives two overlapping groups in Fig. 4.

A quantitative test is obtained by applying Eq. (25) which relates the position of the wide angle cone (as given by α_b) to the number of shower particles n_s. This has been done in two ways. First the value of α_b has been estimated from the observed interactions and plotted against n_s in Fig. 2, the interactions with no heavy prongs being plotted distinctly. Secondly, the theoretical value of α_b for $\bar{E}_1 = 0.5$ has been marked for each event in Fig. 4. There are six cases of striking agreement grouped at the top of Fig. 4, but in other cases the observed angles are definitely too small. It must be recalled, however, that many of the events are certainly not free nucleon-nucleon collisions. It is encouraging to find that the events with no heavy prongs tend to lie on a smooth curve in Fig. 2. This corresponds very well to the theoretical curve for $\bar{E}_1 = 0.5$ for small values of n_s, but deviates towards larger $\bar{E}_1$ for higher multiplicities. The result is not unreasonable because at higher multiplicities, corresponding to more highly excited nucleons, one would expect the proportion of heavy mesons to rise and these will be emitted with larger values of E_1. The higher transverse momentum of heavier particles has been demonstrated by EDWARDS *et al.* [4].

4. – Forward angle-primary energy relation.

A further check on the model can be obtained by comparing the angles in the forward cone with data on the core size in extensive air showers. One assumes that the majority of interactions are glancing collisions giving rise to only a few mesons: this is *a priori* likely, and is supported by cloud chamber experiments on penetrating showers [8]. In this case the excitation of the incident nucleon will be of the order $(0 \div 1)$ GeV, and as the total energy is conserved $\gamma_f \sim (\frac{1}{2} - 1) \times \gamma_p$. Therefore the median angle of the forward cone

$$\alpha_f = \frac{1}{\gamma_f} \sim (1 - 2) \cdot \frac{E_0}{E_p} = (1 - 2) \cdot 10^{-5} \tag{27}$$

for a primary energy of 10^{14} eV. According to COCCONI [7] the experimental data require the angular spread in the primary interation at this energy to

be less than $3.3 \cdot 10^{-5}$, in good agreement with the model. Note that the agreement would be less good if the mesons are emitted from a space moving slower than the residual nucleon as recently proposed [3], because α_f would then be correspondingly larger. The figures allow only a small adjustment in this direction.

Other theories of high energy interaction predict much larger angles in the forward cone and are at variance with the data [7,15].

5. – Momentum and angular momentum.

Consider the interaction in C-space. Before the interaction the momentum of each nucleon is $(E^2 - E_0^2)^{\frac{1}{2}}$, and after the interaction it is $(E^2 - \alpha^2 E^2)^{\frac{1}{2}}$ according to our assumptions. Therefore the change in the magnitude of the momentum during the interaction is

$$\Delta p = (E^2 - E_0^2)^{\frac{1}{2}} - \beta E \sim E(1 - \beta) \sim \tfrac{1}{2}\alpha^2 E \,, \tag{28}$$

if α is small.

Recalling from Eqs. (4) and (5) that $n_s \simeq 4\alpha E/3\bar{E}_1$ one finds

$$\Delta p = 9 n_s^2 \bar{E}_1^2 / 32 E \sim n_s^2 / 14 E \,. \tag{29}$$

For the Turin jet [14] $n_s = 39$, $E = 50$ (a case favourable to large Δp), this gives $\Delta p \sim 2.5$ GeV/c.

It is reasonable to expect an exchange of transverse momentum between the two nucleons of the order Δp. This scattering during the interaction would lead to a small difference in the mean direction of the wide and narrow cones. But in this example each cone has about 30 particles (including π^0) with mean transverse momentum of order 0.3 GeV/c, leading to an uncertainty of order $0.3 \cdot \sqrt{30} \sim 1.7$ GeV/c in defining the transverse momentum of the excited nucleon. It seems that the scattering effect will usually be masked by the uncertainty in the experimental information. Its detection would be favoured in a low energy event, giving many shower particles (n_s^2/E large), but as this would be a case of head-on collision one expects a small effect.

Given the change of linear momentum Δp the change in the angular momentum of each nucleon about the centre of mass is $b \cdot \Delta p = bE(1 - \beta)$, where b is the impact parameter. Conservation of angular momentum requires that each excited nucleon has a spin angular momentum of this value as seen from

(15) S. Z. Belen'kij and L. D. Landau: loc. cit.; G. Cocconi: *Suppl. Nuovo Cimento*, **8**, 560 (1958).

C-space; but using the Lorentz transformation of angular momentum ([16]), this is reduced to $bE(1-\beta)/\gamma = b\alpha E(1-\beta)$ when referred to N-space. On the other hand, the maximum angular momentum that can be carried away by the evaporated mesons is αER, where R is the nuclear radius (αE being the excitation energy). The ratio of these angular momenta, $\varrho = b(1-\beta)/R$, measures the extent of the constraint that angular momentum conservation places on the evaporation process. One expects $b < R$, so $\varrho < (1-\beta) = \frac{1}{2}\alpha^2$. As α is seldom larger than 0.5, it is seen that angular momentum conservation is not an important constraint. This result differs from that of KRAUSHAAR and MARKS ([2]).

In units of $\hbar$ the spin angular momentum l of the excited nucleon is $b\alpha(1-\beta)/\lambda\!\!\!^{-}$, where $2\pi\lambda\!\!\!^{-}$ is the de Broglie wave-length of the incident nucleon in C-space. In the case of the Turin jet ([14]), for example, $\alpha = 0.3$, $\lambda\!\!\!^{-} = 6 \cdot 10^{-16}$ cm, which with $b = 10^{-13}$ cm gives $l = 2.3$, a very small value for a nucleon with an excitation energy of 15 GeV.

6. – Statistical treatment of the excited nucleon.

The discussion so far has been largely concerned with the kinematics of the excited nucleon model. The energy E_1 of the mesons emitted by the excited nucleons has entered as a parameter, an average value near 0.5 being suitable to fit the experimental results.

More speculatively one may try to form a picture of the excited nucleon itself. It is found that a simple statistical model of meson emission can predict correctly the average value of E_1, and also gives a good fit to the transverse momentum distribution in experimental jets.

Consider a nucleon with excitation energy E_x above its ground state, and suppose that this surplus energy is emitted in the form of m mesons. The volume of phase-space available for the m mesons is given by FERMI ([17])

$$S_m = \frac{(4\pi R^3/3)^m}{\pi^{2m}\hbar^{3m}c^{3m}[(3m-1)!]} E_x^{(3m-1)}, \tag{30}$$

where R is the radius of the excited nucleon. This formula contains the condition that the total energy of the emitted particles shall add up to E_x, but conservation of momentum is not included. The emitted particles are assumed to be completely relativistic. It is assumed that the final de-excited nucleon

([16]) K. OCHIAI: *Theory of Relativity* (in Japanese) (Tokyo, 1941), p. 89.
([17]) E. FERMI: *Progr. Theor. Phys.*, **5**, 570 (1950).

carries negligible kinetic energy, but takes up the residual linear momentum; its phase-space factor is neglected, *i.e.* in this approximation its mass is infinite. With $R = 1.4$ fermi and with energies expressed in GeV, Eq. (30) reduces to

$$S_m = 620(150)^m E_x^{(\Sigma m-1)}/(3m-1)! \,. \tag{31}$$

For a given excitation energy E_x, Eq. (31) gives the relative probability for the emission of various numbers of mesons. The mean energy is then

$$\bar{E}_1 = \frac{\sum S_m E_x/m}{\sum S_m} \,. \tag{32}$$

The probability curves defined by (31) for various values of E_x are shown in Fig. 5, and the values obtained for $\bar{E}_1$ are given in Table I. The mean

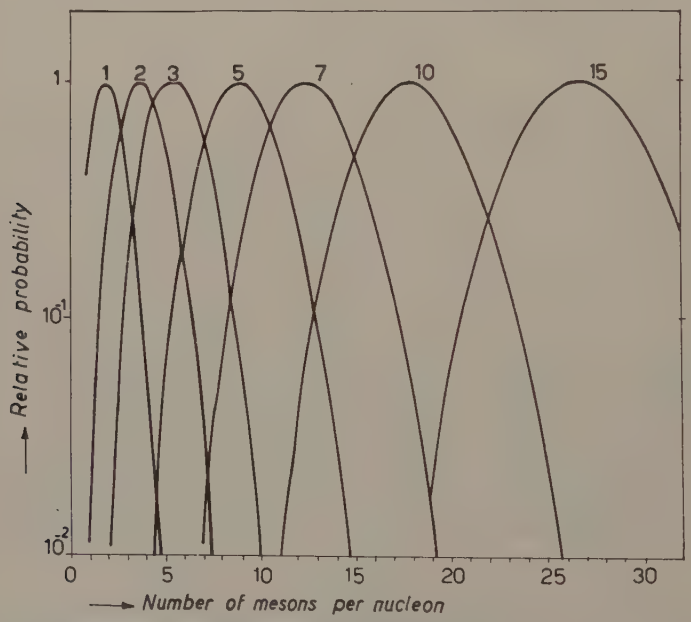

Fig. 5. - Number spectrum of mesons evaporated from an excited nucleon for various excitation energies.

energy $\bar{E}_1$ of the emitted mesons is remarkably constant, and almost independent of the degree of excitation. This explains why the transverse momentum is the same for jets of various energies and multiplicities, and why in general a single value of $\bar{E}_1$ will fit the data for a wide variety of events. The value of $\bar{E}_1$ depends on the value assumed for the radius R of the excited nucleon, but the usual value 1.4 fermi gives a good fit to the experimental

data. If one assumes that heavy mesons would be emitted from an excited focus of correspondingly smaller radius, one would find a larger value of $\bar{E}_1$ and larger transverse momentum for these particles as obtained experimentally by the Bristol group ([4]).

TABLE I.

Excitation energy, E_x (GeV)	Mean meson energy, E_1 (GeV)	Most probable number of mesons per nucleon
1	0.556	2
2	0.565	4
3	0.565	5
5	0.565	9
7	0.565	13
10	0.565	18
15	0.565	27

To find the energy spectrum of the emitted mesons one writes down the phase-space available for one meson to be emitted with energy in the range E_1 to $(E_1+\mathrm{d}E_1)$ and the others to take up the remaining energy (E_x-E_1). This is

$$S(m, E_1)\,\mathrm{d}E_1 = \frac{(4\pi R^3/3)^m}{\pi^{2m}\hbar^{3m}c^{3m}} \cdot \frac{E_1^2(E_x-E_1)^{(3m-4)}}{2(3m-4)!}\,\mathrm{d}E_1\,, \tag{33}$$

$$= 310(150)^m \frac{E_1^2(E_x-E_1)^{(3m-4)}}{(3m-4)!}\,\mathrm{d}E_1\,, \tag{34}$$

in the practical case.

For a given excitation energy the E_1 spectrum specified by (34) has been calculated for each value of m. The spectra are automatically weighted by (34) in proportion to the probability of having m mesons emitted, with the result that they can be added directly to give the over-all spectra shown in Fig. 6. The individual spectra are shown in Fig. 7, for a particular value of E_x. The transverse momentum spectrum, derived from the energy spectrum assuming isotropic emission from the excited nucleon, is shown in Fig. 8, and gives excellent agreement with the experimental results.

The derivation of these results from the statistical model has involved some important simplifying assumptions. It has been assumed that the emitted particles are highly relativistic. This will give errors in the low energy region of the spectrum, but they should be small in general because kinetic energies

greater tham m_0c^2 predominate. Conservation of momentum, angular momentum, and isotopic spin are also neglected, and the effect of these factors on the relative probabilities is hard to estimate.

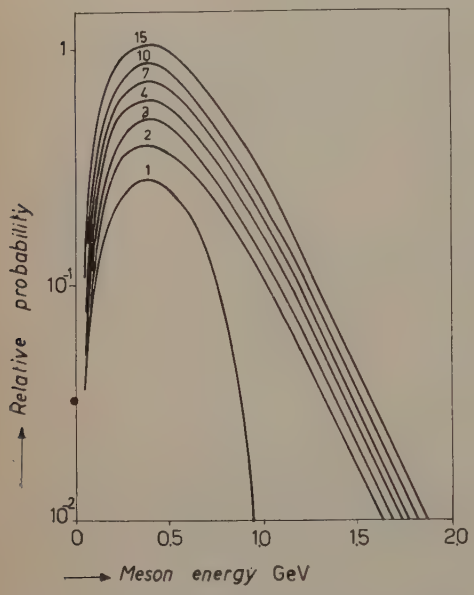

Fig. 6. – Energy spectrum of mesons in N-space for various excitation energies.

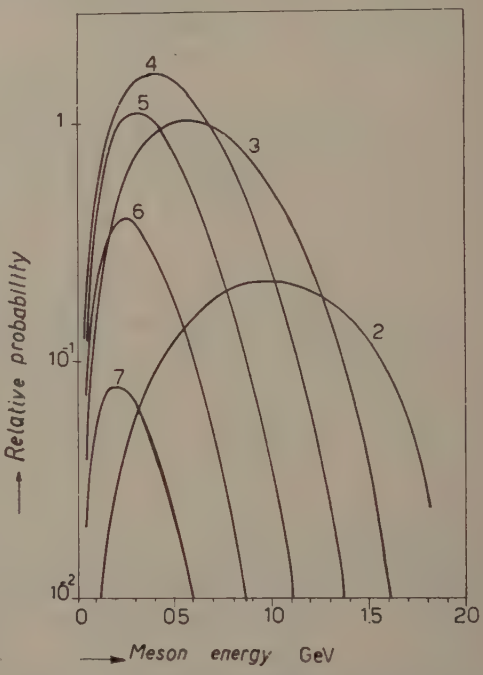

Fig. 7. – Partial energy spectra for $E_x = 2$ GeV, with various values of m.

The assumption that the residual nucleon remains at rest cannot be true because this would have zero probability. But one can see that the error is not large. According to FERMI the kinetic energy is divided roughly equally among the available particles, so one would expect the nucleon kinetic energy

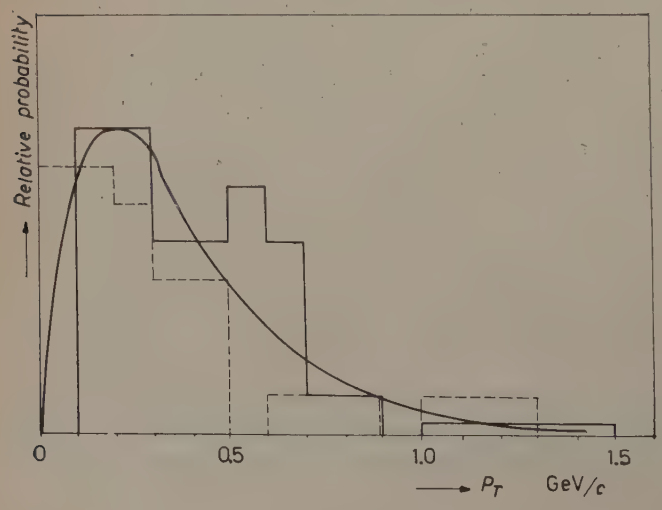

Fig. 8. – Histograms of transverse momentum spectrum from Turin jet [14] (dotted), and from ENGLER [18] (solid line), compared with theoretical curve.

to be about 0.5 GeV. This will not reduce appreciably the energy available for mesons except in the cases of lowest multiplicity and therefore will not greatly change the multiplicities.

The fact that the residual nucleon will have some velocity in the frame of the original excited nucleon, N-space, can lead to a violation of the kinematic laws deduced above. In particular, as the departure may be in different directions for the two excited nucleons produced after the collision the symmetry of the shower particles in C-space may be destroyed. The effect is probably small compared with experimental uncertainties due to the non-observation of neutral particles, and in any case should not lead to a systematic error.

7. – Nucleon-nucleus collision.

Some very speculative remarks about the nucleon-nucleus collision are here added. One may suppose that here again the fundamental process is excitation of the incident nucleon and of the struck nucleons, followed by meson emission. As the excited nucleon emits mesons of mean energy $\bar{E}_1$, one expects a mean lifetime of order $\hbar/\bar{E}_1$ for this process. Allowing for the time dilation, the mean free path of the incident nucleon before de-excitation is therefore $c\gamma_f\hbar/\bar{E}_1$. With $\gamma_f \sim E_p/m\bar{E}_1$, m being the number of mesons emitted by the excited nucleon, we obtain for the mean free path λ before emission of the *first* meson

$$\lambda = c\hbar E_p/m^2\bar{E}_1^2 = 1.2\cdot 10^{-13}\, E_p/m^2 \,. \tag{35}$$

where the primary energy E_p is expressed in GeV. This shows that when a nucleon collides with a heavy nucleus the incident nucleon, now excited, will leave the nucleus before emitting any mesons provided that $E_p/m^2 > 10$, say. If equation (5) is approximately valid for the nucleon-nucleus collision, this requirement is the same as $E_l/n_s^2 > 5$, a condition often fulfilled in experimental jets, especially at high energy.

In a high energy event, therefore, one may expect the incident nucleon to leave the nucleus before it emits any mesons, and a high energy meson-nucleon cascade will not be developed in the nucleus. In this case the narrow cone of shower particles would be emitted from the incident nucleon exactly as in the nucleon-nucleon collision. The struck volume of the nucleus would be left in an excited state, and would later emit mesons in a much more complex manner. If this emission had a strong forward collimation one could perhaps explain the absence of particles at large angles noticed in the events in the lower part of Fig. 4 which do not fit the model for nucleon-nucleon collision.

([18]) A. ENGLER: *Proc. of the VII Rochester Conference* (New York, 1957).

* * *

I wish to thank Prof. M. SCHEIN, Dr. D. H. PERKINS and Dr. E. LOHRMANN for communications concerning their experimental results, and Prof. G. MOLIERE, Dr. Y. YAMAGUCHI and Dr. R. HAGEDORN for stimulating discussions.

APPENDIX

Data for Fig. 1.

n_s	E_p (GeV)	K	Reference
4 (*)	40000	0.3÷0.5	(18)
6	1000	0.1	(12)
20 (*)	5000	0.6÷0.8	(11)
30 (*)	1250 (**)	0.88	(19)
36	4000	0.66÷0.78	(11)
16 (*)	13000	0.87	(20)
6	6.6	0.45	
7	10.8	0.5	
7	22	0.4	
7	29	0.4	(5)
8	22	0.5	
9	49	0.6	
13	29	0.75	

(*) Double interaction.
(**) Calculated from secondary energies.

(19) E. LOHRMANN: *Nuovo Cimento*, **3**, 822 (1956).
(20) G. BOZÓKI, G. DOMOKOS, E. FENYVES, E. GOMBOSI, K. LANIUS and H. W. MEIER: *Magyar Tudomanyos Akadémia Kösponti Fizikai Kutató Intézetének Kösleményei*, **6**, 105 (1958).

RIASSUNTO (*)

Un'analisi della cinematica del modello del nucleone eccitato porta a tre relazioni che si riscontrano in buon accordo con i dati sperimentali: 1) relazione anelasticità-n_s; 2) relazione angolo di rinculo-n_s; 3) relazione angolo in avanti-energia primaria. Un semplice trattamento statistico dello stesso nucleone eccitato dà una buona approssimazione con la distribuzione dell'impulso trasversale nel getto.

(*) *Traduzione a cura della Redazione.*

IL NUOVO CIMENTO Vol. XVI, N. 2 16 Aprile 1960

Integral Representation of a Double Commutator.

K. J. Le Couteur

Research School of Physical Sciences, Australian National University - Canberra

(ricevuto il 27 Giugno 1959)

Summary. Dyson's integral representation for the vacuum expectation value of a double commutator is put into a form consistent with the Jacobi identity.

Introduction.

If x_1, x_2, x_3 are three space time points and $A(x)$, $B(x)$, $C(x)$ three scalar fields, the vacuum expectation value of the double commutator of the field operators is denoted by

$$D(y, z) = D_{A.B.C.}(y, z) = \langle [C(x_3), [B(x_2), A(x_1)]] \rangle_0 , \tag{1}$$

where

$$y = x_1 - x_2 , \qquad z = x_2 - x_3 , \qquad y + z = x_1 - x_3 . \tag{2}$$

By an extension of Lehmann's [1] original investigation of the single commutator, Dyson [2] has established an integral representation for the expectation value of a double commutator. His result is

$$D_{C.B.A}(y, z) = \int_0^\infty \mathrm{d}s \int_0^\infty \mathrm{d}t \int_0^1 \mathrm{d}\lambda \psi_{CBA}(s, t, \lambda) \Delta_s(y) \Delta_t(z + \lambda y) , \tag{3}$$

---

(1) H. Lehmann: *Nuovo Cimento*, **11**, 342 (1954).
(2) F. J. Dyson: *Phys. Rev.*, **111**, 717 (1958).

where $\Delta_s(y)$ is the invariant commutator function for a free field of mass $s^{\frac{1}{2}}$ and ψ is an undetermined function of the real parameters s, t, λ.

This representation embodies only the assumptions that A, B, C commute at points separated by a space-like interval and that there are no negative energy states: it does not take account of two basic symmetry properties of the commutator, which will now be imposed as conditions on $\psi(s, t, \lambda)$.

1. – Antisymmetry.

Because the single commutator is antisymmetric

$$\big[C(x_3), [B(x_2), A(x_1)]\big] + \big[C(x_3), [A(x_1), B(x_2)]\big] \equiv 0$$

and so in the notation (1)

$$D_{CBA}(y, z) + D_{CAB}(-y, y+z) \equiv 0 \,. \tag{4}$$

Now from (3)

$$D_{CAB}(-y, y+z) = -\int_0^\infty \mathrm{d}s \int_0^\infty \mathrm{d}t \int_0^1 \mathrm{d}\lambda' \psi_{CAB}(s, t, 1-\lambda') \Delta_s(y) \Delta_t(z + \lambda' y) \,, \tag{5}$$

and so (4) is satisfied if

$$\psi_{CAB}(s, t, 1-\lambda) = \psi_{CBA}(s, t, \lambda) \,. \tag{6}$$

The simplest, though not the most general, solution of (6) is

$$\psi_{CBA}(s, t, \lambda) = \psi_{CBA}(s, t)\, \delta(\lambda) + \psi_{CAB}(s, t)\, \delta(1-\lambda) \,, \tag{7}$$

which gives

$$D_{CBA}(y, z) = \int_0^\infty \mathrm{d}s \int_0^\infty \mathrm{d}t\, \Delta_s(y) [\psi_{CBA}(s, t) \Delta_t(z) + \psi_{CAB}(s, t) \Delta_t(y+z)] \,. \tag{8}$$

2. – Jacobi's identity.

The Jacobi identity requires

$$D_{CBA}(y, z) + D_{BAC}(-y-z, y) + D_{ACB}(z, -y-z) \equiv 0 \,, \tag{9}$$

and is satisfied by (8) provided

$$(10)\qquad \int_0^\infty \mathrm{d}s \int_0^\infty \mathrm{d}t \,\{\Delta_s(y)[\psi_{CBA}(s,t)\Delta_t(z)+\psi_{CAB}(s,t)\Delta_t(y+z)]-$$

$$-\Delta_s(y+z)[\psi_{BAC}(s,t)\Delta_t(y)-\psi_{BCA}(s,t)\Delta_t(z)]-\Delta_s(z)[\psi_{ACB}\Delta_t(y+z)+\psi_{ABC}\Delta_t(y)]\}=0\,,$$

which is so if

$$(11)\qquad \psi_{CBA}(s,t)=\psi_{ABC}(t,s)\,,$$

and similarly for the other permutations of A, B, C.

Therefore, with the simmetry condition (11), equation (8) gives a possible representation of the double commutator.

RIASSUNTO (*)

La rappresentazione integrale di Dyson per il valore di aspettazione del vuoto di un commutatore doppio viene posta in una forma compatibile con la identità di Jacobi.

(*) *Traduzione a cura della Redazione.*

IL NUOVO CIMENTO Vol. XVI, N. 2 16 Aprile 1960

On the Symmetries of Strong and Weak Interactions (*).

F. GÜRSEY (**)

Brookhaven National Laboratory - Upton, N. Y.

(ricevuto il 17 Settembre 1959)

Summary. — A model of strong interactions is proposed which admits a group $(G_4 \times H)$ in the limit of a suitably defined doublet approximation, G_4 being a 4-dimensional extension of the isotopic spin group and H the hypercharge gauge group. Weak interactions having phenomenological chirality invariance properties or obeying the $\Delta I = \frac{1}{2}$ rule are shown to be invariant under an unitary subgroup of the group $(G_4 \times H)$.

1. – Introduction.

Recently phenomenological interaction forms have been proposed to take into account the rather intricate symmetry properties of the weak interactions of strongly interacting particles ([1-3]). The empirical rules strongly suggested by experiment are the $\Delta I = \frac{1}{2}$ rule ([4,5]) and an extension of the γ_5 invariance which will allow only left handed fields in Λ decay, but both left handed and

(*) Work performed under the auspices of the U. S. Atomic Energy Commission and the International Cooperation Administration.

(**) On leave from the University of Istanbul. Now at the Institute for Advanced Study, Princeton, New Jersey.

([1]) B. D'ESPAGNAT and J. PRENTKI: *Nucl. Phys.*, **11**, 700 (1959); *Phys. Rev.*, **114** 1366 (1959).

([2]) B. T. FELD: *Hyperon decays and symmetry properties of the weak interactions*, preprint.

([3]) J. C. PATI and S. ONEDA: *An attempt at universal four-fermion interaction*, preprint.

([4]) R. L. COOL, B. CORK, J. W. CRONIN and W. A. WENZEL: *Phys. Rev.*, **119**, 912 (1959).

([5]) F. S. CRAWFORD, M. CRESTI, R. L. DOUGLAS, M. L. GOOD, G. R. KALBFLEISCH, M. L. STEVENSON and H. K. TICHO: *Phys. Rev. Lett.*, **2**, 266 (1959).

right handed fields in Σ decay ([6]). Since γ_5 invariance is known to hold rigorously in pure leptonic processes and approximately when strongly interacting particles are present, higher symmetries for the latter have been invoked (see Ref. ([1-3])) to allow some of the symmetries of weak processes to survive in baryon and meson decays.

In the present note we would like to draw attention to a possible 4-dimensional extension G_4 of the isotopic spin group G_3, such that G_4, together with the hypercharge gauge group H contains charge independence, strangeness selection rules and the empirical symmetries of weak interactions as various subgroups. Hence, if G_4 is approximately valid for strong interactions, one may hope that renormalization effects will be small for any interaction invariant under a subgroup of G_4 and especially for weak interactions. The model treated here should be regarded as an illustration of the possibility that the symmetries of weak interactions may be essentially contained in those of strong interactions and certainly not as a definite proposal for a theory of elementary particles.

To facilitate the discussion of the invariance properties, we divide the strong Lagrangian into a part L rigorously invariant under G_4 and a part L' invariant only under G_3 and which acts as a perturbation on L. We call it (DP) for « doublet perturbation » since it will be seen that G_4 invariance implies a «doublet approximation» (DA) for the baryons (equal masses and same space-time structure for Λ and Σ which allows reshuffling of their components into two doublets N_2 and N_3). This is hardly surprising since PAIS ([7]) has shown that the weakest symmetry beyond charge independence must imply the (DA) (global symmetry is not assumed). However, a (DP) must also exist in order to avoid any contradiction with experiment ([8]). The difference with the 4-dimensional group considered by PAIS is that G_4 affects the nucleon states (and also the cascade particle states).

In Section **2** we show that for a certain class of non-linear meson-nucleon interactions, the pion-nuclear system possesses 4-dimensional symmetry which includes the γ_5 transformation as a subgroup. In Section **3**, the transformation properties of all baryons and the K-mesons under the group G_4 are defined. Section **4** deals with some specific weak interactions which are shown to be invariant under an unitary subgroup of G_4 and the hypercharge group H, provided the $\Delta I = \frac{1}{2}$ rule and the phenomenological γ_5 invariance properties are satisfied.

([6]) S. A. BLUDMAN: *Phenomenological analysis of hyperon decay rates and asymmetries*. Gatlinburg Conference on Weak Interactions (Oct. 1958); *Bull. Am. Phys. Soc.*, **9**, 83 (1959); also *Phys. Rev.*, **115**, 468 (1959).

([7]) A. PAIS: *Phys. Rev.*, **110**, 1480 (1958).

([8]) A. PAIS: *Phys. Rev.*, **110**, 574 (1958); **112**, 624 (1958).

1959

2. – 4-dimensional symmetry of the π-$\mathcal{N}$ system in the doublet approximation.

The only new rotation group that can be defined for the π-$\mathcal{N}$ system (excluding transformations that mix nucleons and antinucleons) is the following transformation for the nucleon operator ψ:

$$G_3': \quad \psi \to \exp[i\gamma_5 \boldsymbol{\tau}\cdot\boldsymbol{\omega}]\psi \,. \qquad \left[\psi = \begin{pmatrix} p \\ n \end{pmatrix}\right]. \tag{1}$$

This group has the same form as the Dyson-Foldy transformation and does not leave the free nucleon equation invariant unless $m = 0$. The equation transformed with the value $\boldsymbol{\omega}' = \boldsymbol{a}$ of the transformation parameters will read

$$\gamma_\mu \partial_\mu \psi = m \exp[2i\gamma_5 \boldsymbol{\tau}\cdot\boldsymbol{a}]\psi \,. \tag{2}$$

Now, following the method Nishijima [9] devised in order to ensure the γ_5 gauge invariance, we replace the parameters a in (2) by a dynamical field by putting

$$\boldsymbol{a} = f\boldsymbol{\varphi} = g\,\boldsymbol{\varphi}/2m \,, \tag{3}$$

where f is a universal length and g a dimensionless constant. Expanding in powers of f we obtain the equation

$$\gamma_\mu \partial_\mu \psi = m \exp[2if\gamma_5 \boldsymbol{\tau}\cdot\boldsymbol{\varphi}]\psi = m\psi + ig\gamma_5 \boldsymbol{\tau}\cdot\boldsymbol{\varphi}\,\psi - (g^2\varphi^2/2m)\psi + \ldots \,, \tag{4}$$

$\boldsymbol{\varphi}$ is pseudoscalar, has isotopic spin 1 and can be identified with the pion field. f is then the pseudovector coupling constant. The interaction (4) which is related to the non-linear form of the pseudovector interaction (after the Dyson-Foldy transformation has been performed) has been considered by GLAUBER [10] in connection with multiple meson production, and its mathematical structure which implies an inherent non locality associated with the length f has been investigated by many authors [11-14].

---

[9] K. NISHIJIMA: *Nuovo Cimento*, **11**, 910 (1959).
[10] R. J. GLAUBER: *Phys. Rev.*, **84**, 395 (1951).
[11] R. ARNOWITT and S. DESER: *Phys. Rev.*, **100**, 349 (1955).
[12] J. S. R. CHISHOLM: *Phil. Mag.*, **1**, 338 (1956).
[13] J. S. R CHISHOLM and G. M. DIXON: *Nuovo Cimento*, **9**, 125 (1958).
[14] W. GÜTTINGER: *Nuovo Cimento*, **10**, 1 (1958).

Equation (4) may also be written in the form

$$\begin{cases} \gamma_\mu \partial_\mu \psi_L = m\bar{\Phi}\psi_R \,, \\ \gamma_\mu \partial_\mu \psi_R = m\bar{\Phi}\psi_L \,, \end{cases} \tag{5}$$

where

$$\begin{cases} \Phi = \exp[2if\boldsymbol{\tau}\cdot\boldsymbol{\varphi}] \,, & \bar{\Phi} = \exp[-2if\boldsymbol{\tau}\cdot\boldsymbol{\varphi}] \,, \\ \psi_L = \tfrac{1}{2}(1+\gamma_5)\psi \,, & \psi_R = \tfrac{1}{2}(1-\gamma_5)\psi \,, \end{cases} \tag{6}$$

and

$$\Phi\bar{\Phi} = \bar{\Phi}\Phi = 1 \,. \tag{7}$$

Now a 4-dimensional internal rotation group G_4 arises from the possibility of performing independent isotopic spin rotations on the left handed and right handed nucleons independently. These two 3-dimensional groups obviously commute and they are defined by

$$G_3^{(1)}: \quad \psi_L \to \exp[i\boldsymbol{\tau}\cdot\boldsymbol{\mu}]\psi_L \,, \qquad \Phi \to \Phi \exp[-i\boldsymbol{\tau}\cdot\boldsymbol{\mu}] \,, \qquad \psi_R \to \psi_R \,, \tag{8}$$

and

$$G_3^{(2)}: \quad \psi_R \to \exp[i\boldsymbol{\tau}\cdot\boldsymbol{\nu}]\psi_R \,, \qquad \Phi \to \exp[i\boldsymbol{\tau}\cdot\boldsymbol{\nu}]\Phi \,, \qquad \psi_L \to \psi_L \,, \tag{9}$$

so that the whole group may be written as

$$\begin{cases} G_4: \quad \psi' = \exp\left[i\left\{\dfrac{1+\gamma_5}{2}\,\boldsymbol{\tau}\cdot\boldsymbol{\mu} + \dfrac{1-\gamma_5}{2}\,\boldsymbol{\tau}\cdot\boldsymbol{\nu}\right\}\right]\psi \,, \\ \qquad\quad \Phi' = \exp[i(2f\boldsymbol{\tau}\cdot\boldsymbol{\varphi}')] = \exp[i\boldsymbol{\tau}\cdot\boldsymbol{\nu}]\Phi\exp[-i\boldsymbol{\tau}\cdot\boldsymbol{\mu}] \,. \end{cases} \tag{10}$$

We note that the pseudoscalar nature of the pion and 4-dimensional invariance are intimately related, since only in this case we can construct a unitary matrix Φ as a function of $\boldsymbol{\Phi}$, such that it is transformed into another unitary matrix by means of 4-dimensional rotations [15]. The isotopic spin group

---

[15] The group G_4 has been previously introduced by the author: F. GÜRSEY: *Bull. Am. Phys. Soc.*, **3**, 10, 245 (1958); also *Nucl. Phys.*, **8**, 675 (1958). It arose as a natural generalization of the Pauli transformations studied in F. GÜRSEY: *Nuovo Cimento*, **7**, 411 (1958). The subgroup $G_3^{(1)}$ has been considered by S. A. BLUDMAN: *Nuovo Cimento*, **9**, 433 (1958) in connection with weak interactions. It should not be confused with the rotation group

$$\psi \to a\psi + b\psi^G, \qquad ((a)^2 + (b)^2 = 1),$$

that mixes nucleons and antinucleons. The latter unlike $G_3^{(1)}$, leaves the free nucleon equation invariant, but is violated by local pion-nucleon interactions. It was introduced by O. HARA, Y. FUJII and Y. OHNUCI [*Progr. Theor. Phys.*, **19**, 129 (1958)] and further discussed by B. TOUSCHEK [*Nuovo Cimento*, **8**, 181 (1958)], A. GAMBA and E. C. G. SUDARSHAN [*Nuovo Cimento*, **10**, 407 (1958)] and E. J. SCHREMP [*Phys. Rev.*, **113**, 936 (1959)].

G_3 is obtained by taking $\boldsymbol{\mu}=\boldsymbol{\nu}=\boldsymbol{\omega}$ and the subgroup G_3' of eq. (1) corresponds to the case $\boldsymbol{\mu}=-\boldsymbol{\nu}=\boldsymbol{\omega}'$. However, unlike $G_3^{(1)}$ and $G_3^{(2)}$ the rotational subgroups G_3 and G_3' do not commute. We also observe at this point that G_3 commutes with CP, C and P, but the subgroups $G_3^{(1)}$ and $G_3^{(2)}$ separately commute only with CP and not with C or P.

Now, the pion kinetic energy term in the strong Lagrangian can also be made invariant under G_4 if we make the substitution

$$(\partial_\mu \boldsymbol{\varphi})^2 \to -\tfrac{1}{4} f^{-2} \operatorname{Tr}\left[(\partial_\mu \Phi)(\partial_\mu \bar{\Phi})\right]^2 . \tag{11}$$

The first term in the expansion in powers of f is the usual pion kinetic energy. The additional terms represent pion-pion interactions. However, the pion bare mass term in the Lagrangian cannot be made invariant under G_4. It must arise as the result of a (DP) referred to above. Since the (DP) is invariant under G_3 it will generate a pion mass term which will be strongly renormalized by the pion-pion interactions. Therefore a sizable renormalized pion mass is not incompatible with a (DP). Since the (DP) must also give rise to the $\Lambda-\Sigma$ mass difference δ, in our doublet approximation not only δ but also the pion mass relative to the masses of other strongly interacting particles must be neglected.

The γ_5 transformation arises naturally in this model. Let us consider the discrete subgroup of G_4 by taking $\nu_3=\pi$, $\nu_1=\nu_2=0$ in $G_3^{(2)}$ as defined by eq. (9). We obtain

$$\psi \to \gamma_5 \psi , \qquad \Phi \to -\Phi . \tag{12}$$

Hence the change of sign in m contemplated in the mass reversal transformation ([16]) is here transferred to the matrix Φ, while m remains unchanged. The transformation (12) unlike the mass reversal is a unitary transformation (*). Since in the (DA) other strong interactions will not disturb G_4 invariance, the γ_5 invarianec as defined by (12) will also remain valid in this approximation.

([16]) J. J. Sakurai: *Nuovo Cimento*, **7**, 649 (1958).

(*) *Note added in proof.* – The unitary character of the general transformation (10) is clear for ψ_L and ψ_R. To see that it is true for the pion field, we use the operator identity given in Ref. ([10]) and in the appendix of a paper by G. Barton [*Nuovo Cimento*: **13**, 363 (1959)], namely,

$$(\exp[\alpha])(\exp[\beta]) = \exp[\alpha+\beta]\exp\left[\tfrac{1}{2}(\alpha,\beta)\right] ,$$

which is walid when $[\alpha,\beta]$ commutes with α and β. Now introduce two sets of commuting Pauli operators $\boldsymbol{\tau}$ and $\boldsymbol{\rho}$ and define $\boldsymbol{s}=\frac{1}{2}(\boldsymbol{\rho}+\boldsymbol{\tau})$. Further put $\boldsymbol{\varphi}=\boldsymbol{\varphi}(x)$ and $\boldsymbol{\varphi}'=\boldsymbol{\varphi}(x')$. Then assume commutation relations of the usual form for free particles so that

$$[\varphi_m, \varphi_n'] = i\delta_{mn} D'(x-x') ,$$

Hence a γ_5-invariant weak Lagrangian will remain so in presence of strong interactions in the limit of (DA). However the (DP) will induce simultaneously a pion mass, a shift of the baryon masses, a separation of the Λ-Σ system and corrections to the $(V-A)$ form of the weak interactions.

Before concluding this section, the remark should be made that the 4-dimensional symmetry we have considered is not dependent on the form of the unitaty 2×2 matrix Φ of eq. (5). We can take in general

$$\Phi = h(2f\boldsymbol{\tau}\cdot\boldsymbol{\varphi}) , \tag{13}$$

where $h(\lambda)$ is a differentiable function of the variable λ such that

$$h(0) = h'(0) = 1 \quad \text{and} \quad hh^* = 1 \quad (h^* = h(-\lambda)) . \tag{14}$$

Special cases of interest are $h(\lambda) = \exp[i\lambda]$, which leads to eq. (6) and

$$h(\lambda) = (1 + i\lambda)(1 - i\lambda)^{-1} , \tag{15}$$

which leads to a non-linear pion-nucleon interaction considered by STECH, ROLLNIK and KRAMER ([17]) in connection with γ_5 invariance (*).

3. – Group representations of strange particles.

The representations of G_4 can be labelled by two numbers m and n according to their transformation properties under $G_3^{(1)}$ (parameters $\boldsymbol{\mu}$) and $G_3^{(2)}$ (parameters $\boldsymbol{\nu}$) of eq. (8), (9). Since the left handed and right handed spinor fields

---

$D'(x - x')$ being a c-number which vanishes for space-like separation of x and x'. These are equivalent to the explicitly covariant equation

$$(\exp[2if\boldsymbol{s}\cdot\boldsymbol{\varphi}])\exp[-2if\boldsymbol{s}\cdot\boldsymbol{\varphi}'] = \left\{\exp[2if\boldsymbol{s}\cdot(\boldsymbol{\varphi}-\boldsymbol{\varphi})']\right\}\exp\left\{[-2if^2\boldsymbol{s}\cdot\boldsymbol{s}D'(x-x')]\right\} .$$

Under G_4, the left hand side behaves like a self dual antisymmetrical tensor since if gets multiplied to the left by $\exp[i\boldsymbol{s}\cdot\boldsymbol{\mu}]$ and to the right by $\exp[-i\boldsymbol{s}\cdot\boldsymbol{\mu}]$. The exponential factor containing $D'(x-x')$ is invariant under G_4.

([17]) B. STECH, H. ROLLNIK and B. STECH: *Zeits. f. Phys.*, **159**, 564 (1959).

(*) ***Note added in proof.*** – Another choice is $h(\lambda) = \sqrt{1-\lambda^2} + i\lambda$. In this case the traceless part of the matrix Φ is just proportional to the pion field, so that that part of the interaction is a Yukawa coupling. Note, however, that the usual commutation relations for $\boldsymbol{\varphi}$ exhibit four dimensional symmetry only to the order f^3. In general four dimensional invariance requires modification of the commutation relations for the $\boldsymbol{\varphi}$ field. If we do not explicitly relate $\boldsymbol{\varphi}$ to Φ, we can write invariant commutation relations directly for the free Φ field, namely $[\Phi_\mu(x), \Phi_\mu(x')] = i\delta_{\mu\nu}D(x-x')$ with the subsidiary condition $\sum_\nu \Phi_\nu\Phi_\nu - 1)|\Psi\rangle = 0$ for all states.

belong to different representations, we shall consider separately the representations of the 8 left handed and the 8 right handed baryons in the corresponding internal space E_4. We have

$$\psi_L : (\tfrac{1}{2}, 0) , \qquad \psi_R : (0, \tfrac{1}{2}) , \tag{16}$$

$$\Phi = (\tfrac{1}{2}, \tfrac{1}{2}) , \tag{17}$$

so that the left handed and right handed nucleons are respectively spinors of the first and second kind and the 4 components of Φ, namely Tr Φ and Tr $(\tau_n \Phi)$ form a 4-vector in E_4. For the cascade doublet we take

$$\Xi_L = (0, \tfrac{1}{2}) , \qquad \Xi_R = (\tfrac{1}{2}, 0) . \tag{18}$$

This representation implies that Ξ interacts with the pion according to the equation

$$\gamma_\mu \partial_\mu \psi_\Xi = m_\Xi \exp [- 2i\gamma_5 \boldsymbol{\tau} \cdot \boldsymbol{\varphi}] \psi_\Xi . \tag{19}$$

Now, in the (DA) the Λ and Σ hyperons form a degenerate multiplet. We assume that they belong to tensor representations of G_4 and make the assignments

$$Y_L : (\tfrac{1}{2}, \tfrac{1}{2}) , \tag{20}$$

$$\Lambda_R = (0, 0) , \qquad \boldsymbol{\Sigma}_R = (0, 1) . \tag{21}$$

Y_L is a 4-vector the 4-th component of which is Λ_L while the remaining components represent $\boldsymbol{\Sigma}_L$. A G_4-invariant hyperon-pion equation can easily be written in terms of the matrices

$$Y_L = \Lambda_L + i\boldsymbol{\tau} \cdot \boldsymbol{\Sigma}_L , \qquad Y_R = \Lambda_R + i\boldsymbol{\tau} \cdot \boldsymbol{\Sigma}_R , \tag{22}$$

which transform according to

$$Y_L \to \exp [i\boldsymbol{\tau} \cdot \boldsymbol{\mu}] \, Y_L \exp [- i\boldsymbol{\tau} \cdot \boldsymbol{\nu}] , \qquad Y_R \to \exp [i\boldsymbol{\tau} \cdot \boldsymbol{\nu}] \, Y_R \exp [- i\boldsymbol{\tau} \cdot \boldsymbol{\nu}] . \tag{23}$$

Hence the following equation of motion is invariant under G_4:

$$\begin{cases} \gamma_\mu \partial_\mu Y_L = m_Y \bar{\Phi} Y_R , \\ \gamma_\mu \partial_\mu Y_R = m_Y \Phi Y_L , \end{cases} \tag{24}$$

where Φ is defined by (6). It may be noted that the transformation law for

the matrix

$$Y'_L = \Lambda_L - i\boldsymbol{\tau}\cdot\boldsymbol{\Sigma}_L , \tag{25}$$

is

$$Y'_L \to \exp[i\boldsymbol{\tau}\cdot\boldsymbol{\nu}]\, Y'_L \exp[-i\boldsymbol{\tau}\cdot\boldsymbol{\mu}] . \tag{26}$$

The matrix Y'_R similarly defined transforms like Y_R.

For the K-meson doublet we take

$$K = (0, \tfrac{1}{2}) . \tag{27}$$

We have not assumed reflection invariance in E_4. This corresponds to the fact that the representations $(\frac{1}{2}, 0)$ for bosons and $(1, 0)$ for baryons are missing. There is an analogous situation in Space-Time where the $(\frac{1}{2}, 0)$ representation of the Lorentz group corresponds to the neutrino, but the representation $(0, \frac{1}{2})$ with the same lepton number is missing. In the (DA) the hyperons Λ_L, Σ_L and Y_R must have the same mass m_Y, otherwise parity would be violated. When the (DP) is switched on, invariance remains only with respect to the hypercharge gauge group and to the isotopic spin group G_3 which both commute with the parity operation. Then the Λ-Σ mass is split. The form of possible K-baryon interactions invariant under G_4 will be studied in a separate publication We simply remark here that the representations adopted above imply that if the Y-$\mathcal{N}$-K interaction is non derivative then the Y-Ξ-K interaction must be derivative in order to preserve invariance under G_4 (*). However, linear interactions in Φ must be non derivative and this, in the (DA), implies separate C and P conservation if CP is conserved [18] in pionic interaction.

The hypercharge gauge transformation

$$H: \quad \psi \to \exp[iu]\psi , \qquad \Xi \to \exp[-iu]\Xi , \qquad K \to \exp[iu]K , \tag{28}$$

with the other fields unchanged, is known to be a consequence of the conservation of charge and the third component of the isotopic spin. Alternatively we may derive the existence of such a gauge group, assuming like D'Espagnat and Prentki [19], interactions linear in Φ, and G_3 invariance for strongly interacting particles.

Hence we can enlarge the group G_4 to $G_4 \times H$ as the group of strong interactions in the (DA).

(*) *Note added in proof.* – In this case a 4-dimensionally invariant equation of motion for the nucleon is:

$$\gamma_\mu \partial_\mu \psi = \exp[2if\gamma_5 \boldsymbol{\tau}\cdot\boldsymbol{\varphi}]\,[m\psi + ig_K \gamma_5 Y K] .$$

[18] G. Feinberg and F. Gürsey: *Phys. Rev.*, **114**, 1153 (1959).

[19] B. D'Espagnat and J. Prentki: *Nucl. Phys.*, **1**, 33 (1956).

4. – Weak interactions.

We recall that the full group $(G_4 \times H)$ admits H, G_3, $G_3^{(1)}$ and $G_3^{(2)}$ as subgroups. The first two commute with C and P unlike the other two which commute only with CP. When the (DP) is switched on G_4 invariance is lost and we require strong interactions to be invariant under H and G_3. Interactions invariant under $G_3^{(1)}$ or $G_3^{(2)}$ only, necessarily violate parity. Hence we may try to describe weak interactions by means of these two groups. Two kinds of weak interactions may exist: Class I is invariant under $G_3^{(1)}$ (eq. (8)) and Class II is invariant under $G_3^{(2)}$ (eq. (9)). Since charge must also be conserved in each case we can enlarge the 3-parameter groups $G_3^{(1)}$ and $G_3^{(2)}$ to 4-parameter unitary groups which will also describe charge conservation. In the first case we consider the unitary subgroup $U^{(1)}$ of $(G_4 \times H)$ obtained by taking $\nu_1 = \nu_2 = 0$, $\nu_3 = u$. Then the transformation properties of various fields under $U^{(1)}$ are given by

$$
(29)\quad \begin{cases}
U^{(1)}\colon\ \psi_L \to \exp[iu]\exp[i\boldsymbol{\tau}\cdot\boldsymbol{\mu}]\psi_L\,, & \psi_R \to \exp[i(1+\tau_3)u]\psi_R\,, \\
\Xi_L \to \exp[-i(1-\tau_3)u]\Xi_L\,, & \Xi_R \to \exp[-iu]\exp[i\boldsymbol{\tau}\cdot\boldsymbol{\mu}]\Xi_R\,, \\
Y_L \to \exp[i\boldsymbol{\tau}\cdot\boldsymbol{\mu}]Y_L\exp[-i\tau_3 u]\,, & Y_R \to \exp[i\tau_3 u]Y_R\exp[-i\tau_3 u], \\
\bar{\Phi} \to \exp[i\boldsymbol{\tau}\cdot\boldsymbol{\mu}]\,\bar{\Phi}\,\exp[-i\tau_3 u]\,, & K \to \exp[iu]\exp[i\tau_3 u]K\,,
\end{cases}
$$

Similarly, we can define another unitary group associated with $G_3^{(2)}$, namely

$$
(30)\quad \begin{cases}
U^{(2)}\colon\ \psi_L \to \exp[i(1+\tau_3)u]\psi_L\,, & \psi_R \to [\exp[iu]\exp[i\boldsymbol{\tau}\cdot\boldsymbol{\nu}]\psi_R\,, \\
\Xi_L \to \exp[-iu]\exp[i\boldsymbol{\tau}\cdot\boldsymbol{\nu}]\Xi_L\,, & \Xi_R \to \exp[-i(1-\tau_3)u]\Xi_R\,, \\
Y_L \to \exp[i\tau_3 u]\,Y_L\exp[-i\boldsymbol{\tau}\cdot\boldsymbol{\nu}], & Y_R \to \exp[i\boldsymbol{\tau}\cdot\boldsymbol{\nu}]\,Y_R\exp[-i\boldsymbol{\tau}\cdot\boldsymbol{\nu}], \\
\bar{\Phi} \to \exp[i\tau_3 u]\,\bar{\Phi}\exp[-i\boldsymbol{\tau}\cdot\boldsymbol{\nu}]\,, & K \to \exp[iu]\exp[i\boldsymbol{\tau}\cdot\boldsymbol{\nu}]\,.
\end{cases}
$$

To include leptons in the scheme we may define the transformation properties of the lepton current

$$
(31)\qquad j = (\bar{e}+\bar{\mu})\gamma_\mu\nu = \tfrac{1}{2}(\bar{e}+\bar{\mu})\gamma_\mu(1+\gamma_5)\nu\,,
$$

as

$$
(32)\qquad U^{(1)}\colon\quad j_\mu \to \exp[2iu]j_\mu\,.
$$

This can be justified by remarking that the transformation for ψ_L is equivalent to a charge gauge transformation with $2u$ as the gauge parameter.

An example of Class I interaction is the decay of the K-meson into pions. Noticing that under $U^{(1)}$ the matrix

$$\theta = \begin{pmatrix} \overline{K}^0 & K^+ \\ -K^- & K^0 \end{pmatrix} = K_1^0 + i\boldsymbol{\tau}\cdot\mathbf{K}, \tag{33}$$

obeys the transformation law

$$U^{(1)}: \quad \theta \to \exp[i\tau_3 u]\theta \exp[-i\tau_3 u], \tag{34}$$

we can immediately construct an interaction term invariant under $U^{(1)}$ by taking

$$L_K = aGf^{-3}\,\mathrm{Tr}\{(\Phi\partial_\mu\overline{\Phi})[\partial_\mu\theta + K_1^0(\Phi\partial_\mu\overline{\Phi})]\} + \mathrm{H.C.}, \tag{35}$$

where a is a dimensionless coupling constant and G the Fermi constant. Expanding Φ we have approximately

$$L_K \approx 4aGf^{-1}\left[K_1^0(\partial_\mu\boldsymbol{\varphi})^2 + \tfrac{1}{2}f^{-1}(\partial_\mu\mathbf{K})\cdot(\partial_\mu\boldsymbol{\varphi}) - (\partial_\mu\mathbf{K})\cdot(\boldsymbol{\varphi}\cdot\partial_\mu\boldsymbol{\varphi}) + \right. \tag{36}$$
$$\left. + \tfrac{1}{3}f(\partial_\mu\mathbf{K})\cdot(\varphi^2\,\partial_\mu\boldsymbol{\varphi} - 2\boldsymbol{\varphi}\,\partial_\mu\varphi^2)\right].$$

The first and fourth terms of (36) lead respectively to the 2-pion decay of K_1^0 and the 3-pion decay of K_2^0 and K^+. The $\Delta I = \frac{1}{2}$ rule is seen to hold for K decay in the (DA) since L_K transforms like an isotopic spinor.

Hyperon decays involving ψ_L and ψ_R may be also regarded as belonging to Class I. In fact we can describe the pionic decay of the hyperons Λ and Σ by requiring invariance under $U^{(1)}$. Such an interaction is

$$L_Y = a'Gf^{-2}\,\mathrm{Tr}\left\{(\overline{\Phi}\,\partial_\mu\Phi)Y_L\begin{pmatrix}0 & 0\\ \overline{p}_L & \overline{n}_L\end{pmatrix}\gamma_\mu + \right. \tag{37}$$
$$\left. + (\Phi\,\partial_\mu\overline{\Phi})\left[Y'_L\begin{pmatrix}\overline{n}_L & 0\\ -\overline{p} & 0\end{pmatrix} + Y'_R\begin{pmatrix}0 & 0\\ \overline{p}_R & \overline{n}_R\end{pmatrix} + Y_R\begin{pmatrix}\overline{n}_R & 0\\ -\overline{p}_R & 0\end{pmatrix}\right]\gamma_\mu\right\} + \mathrm{H.C.}$$

Again a' is a dimensionless coupling constant. The compatibility of (37) with the $\Delta I = \frac{1}{2}$ rule can be seen by comparing it with the general interaction obeying that rule and written in matrix form ([20]). That the asymmetries are correctly described may be seen by writing out explicitly the interaction (37). We obtain on expanding Φ in powers of f,

$$L_Y \approx 4a'Gf^{-2}\{(\sqrt{2}\,\overline{p}_L\gamma_\mu\Lambda_L\partial_\mu\varphi^+ - \overline{n}_L\,\gamma_\mu\,\Lambda_L\partial_\mu\varphi^0) + \tag{38}$$
$$+ (\overline{n}_L\gamma_\mu\Sigma_L^0\,\partial_\mu\varphi^0 - \sqrt{2}\,\overline{p}_R\gamma_\mu\Sigma_R^0\partial_\mu\varphi^+) + \sqrt{2}\,\overline{p}_R\gamma_\mu\Sigma_R^+\partial_\mu\varphi^0 +$$
$$+ (\overline{n}_L\gamma_\mu\Sigma_L^- - \overline{n}_R\gamma_\mu\Sigma_R^-)\partial_\mu\varphi^+ + (\overline{n}_L\gamma_\mu\Sigma_L^+ + \overline{n}_R\gamma_\mu\Sigma_R^+)\partial_\mu\varphi^- + \mathrm{H.C.}\}.$$

([20]) See for instance, K. NAKAGAWA: *Nucl. Phys.*, **10**, 20 (1959) and ref. ([6]).

This gives $V-A$ interaction for Λ decay and also for the π^0 mode of Σ^+ decay, V for the π^+ mode of Σ^+ and A for the Σ^- decay. The universality of the weak interactions (equality of the coupling constants) and the possible forms of the interaction arising from the product of a current with itself will be discussed in a separate paper.

* * *

In conclusion the author would like to thank Prof. A. PAIS, Dr. G. FEINBERG, Dr. R. BEHRENDS and Prof. Y. NAMBU for stimulating discussions. He would also like to express his sincere thanks to Dr. S. A. GOUDSMIT for hospitality at the Brookhaven National Laboratory. His thanks are also due to Prof. R. J. OPPENHEIMER for hospitality at the Institute where this work was initiated and a grant from the National Science Foundation is gratefully acknowledged.

RIASSUNTO (*)

Si propone per le interazioni forti un modello che, nei limiti di un'approssimazione di doppietto opportunamente definita, ammette un gruppo $(G_4 \times H)$, essendo G_4 una estensione quadridimensionale del gruppo di spin isotopico e H il gruppo di gauge dell'ipercarica. Si dimostra che le interazioni deboli, che abbiano proprietà fenomenologiche d'invarianza della chiralità o obbediscano alla regola $\Delta I = \frac{1}{2}$, sono invarianti rispetto a un sottogruppo unitario del gruppo $(G_4 \times H)$.

(*) *Traduzione a cura della Redazione.*

Emission of Hyperfragments in Capture Stars of Negative Hyperons at Rest.

G. Dascola, C. Lamborizio, S. Mora and I. Ortalli

Istituto di Fisica dell'Università - Parma

(ricevuto il 30 Novembre 1959)

Summary. — Five hyperfragments, emitted from a total of 137 Σ^--stars at rest, have been observed. The estimate of the emission probability of such events is $(1.2\pm0.5)\%$ and results somewhat lower than the similar estimate for the hyperfragments from the K^--stars at rest observed in the same stack $(3.4\pm0.6)\%$.

1. – Introduction.

As known, a negative Σ hyperon interacting at rest with a proton may originate the following reactions:

$$\Sigma^- + p \to \Lambda^0 + n + 80 \text{ MeV}, \tag{1}$$

$$\Sigma^- + p \to \Sigma^0 + n + 8 \text{ MeV}. \tag{2}$$

If these reactions take place in a nucleus, the second one is strongly depressed by the Pauli exclusion principle owing to the low Q-value of the reaction [1]. On the other hand, if the produced Σ^0 hyperon remains inside the nucleus, a Λ^0 hyperon originates from the interaction of the Σ^0 with a nucleon ($\Sigma^0 + \mathcal{N} \to \Lambda^0 + \mathcal{N} + 72$ MeV) or from the Σ^0-decay (much less probable process).

(1) N. N. Biswas and M. Ceccarelli: *Nuovo Cimento*, 8, 599 (1958).

The reactions (1), (2) in the emulsion nuclei produce anyway a star whose visible energy is in general much lower than the Q of the reaction, unless the Λ^0 is trapped in the nucleus and then disintegrates. In some cases the Λ^0 may come out from the nucleus, surrounded by some nucleons, forming a hyperfragment.

Hyperfragments emitted from Σ^--capture stars in nuclei of photographic emulsion have been observed by several authors ([2-6]). However, to date only one datum exists ([5]) about the emission frequency of such events (2 hyperfragments in 94 Σ^--stars at rest).

The purpose of the present research is that of giving further data for the estimate of hyperfragment emission frequency from Σ^--capture interactions. Besides these events, also the hyperfragments directly emitted from K^--stars at rest are selected, in order to compare the hyperfragment emission from Σ^-- and K^--captures.

2. – Interactions from Σ^--captures at rest.

In this research we had at our disposal a stack of Ilford G-5 photographic emulsions exposed to the 80 MeV K^--beam of the Berkeley-bevatron.

In the whole stack 4565 K^--stars, with at least one prong, have been found. Every gray or black track coming out from the interactions has been followed in order to find, at the end of its range, the interactions with one or more prongs: 370 secondary interactions from baryons and nuclei have been found ($\Sigma^\pm$-decays excluded).

In order to identify, among these interactions, the Σ^--captures at rest, a lower limit of 150 μm has been chosen for the range of the connecting track. Moreover, it is to be noted that, with such cut-off, the probability of confusion between non-mesic hyperfragments and Σ^--stars has been highly reduced.

Thus, 109 events have been found, which could be interpreted as Σ^--stars at rest with one or more prongs (in this number doubtful 1 prong Σ^--stars are not included). In order to obtain the total number of Σ^--stars at rest with visible prongs, one must evaluate, on the other hand, the number of those with the primary range below the cut-off. For this purpose we have consi-

---

([2]) M. Ceccarelli, N. Dallaporta, M. Grilli, M. Merlin, G. Salandin, B. Sechi and M. Ladu: *Nuovo Cimento*, **2**, 542 (1955).

([3]) M. Schein, D. M. Haskin and D. Leenov: *Phys. Rev.*, **100**, 1455 (1955).

([4]) P. Rosselet, R. Weill and M. Gaillaud: *Nuovo Cimento*, **3**, 505 (1956).

([5]) K^--Stack Collaboration: *Intern. Conference on Mesons and Recently Discovered Particles* (Padua-Venice, 1957, II-79, II-5).

([6]) J. Hornbostel and G. T. Zorn: *Phys. Rev.*, **109**, 165 (1958).

dered the distribution of the observed stars, with the Σ^--range longer than 150 μm, versus the Σ^--energy (Fig. 1).

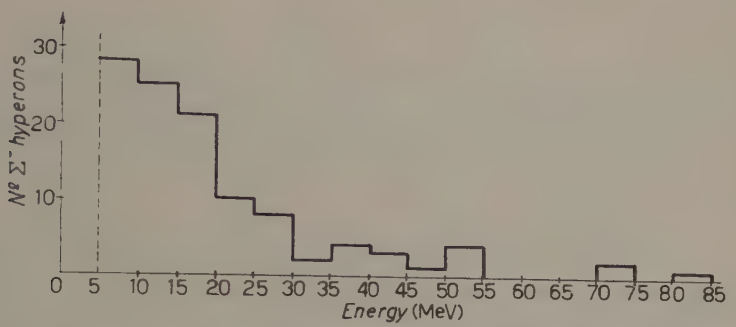

Fig. 1. – Energy specrum of the Σ^- hyperons giving visible stars at rest.

Extrapolating this distribution, according to the shape of the spectrum of Σ^- from K^--stars, one deduces that the number of the stars with the Σ^--range shorter than 150 μm (5 MeV) should be about equal to the number of the Σ^--stars in the first reported interval, *i.e.* 28.

In conclusion the total number of Σ^--capture stars at rest, with one or more prongs, results 137.

3. – Frequency and probability of hyperfragment emission from Σ^--capture stars at rest.

Among the prongs of the 109 observed Σ^--stars, 5 hyperfragments have been identified, of which one underwent mesonic decay and the other 4 decayed non-mesonically. On the other hand, no hyperfragment has been observed among the prongs of the interactions connected to the K^--stars by a track of range shorter than 150 μm.

Thus, we obtain for the emission frequency of hyperfragments from Σ^--stars at rest, with visible prongs, a value $(5/137) = (3.6 \pm 1.6)\%$ (*).

Moreover, in order to evaluate the hyperfragment emission probability from Σ^--stars at rest (ratio of the number of observed hyperfragments to the total number of cases in which a Λ^0 is produced), one must add to the already considered stars (137) the number of zero-prong stars. Computing this number according to the known percentage [3], we obtain an emission probability $(5/417) = (1.2 \pm 0.5)\%$.

(*) Such emission frequency does not take into account the hyperfragments with a range so short that it is not possible to observe them.

4. – Frequency and probability of hyperfragment emission from K^--capture stars at rest.

In order to find the number of hyperfragments emitted in K^--stars at rest, the 370 secondary interactions, mentioned in Section 2, have been taken again into account. These events have been classified according to the nature of the connecting track, as indicated in Table I.

TABLE I. – *Classification of the 370 secondary interactions according to the nature of the connecting track.*

Events identified:	
Stars from Σ^- with range $> 150\ \mu m$	109
Hammer tracks from ^8Li, ...	13
Hyperfrag. { mesonic	27 { 21 from K^- at rest; 6 from K^- in flight
Hyperfrag. { non-mes. with range $> 150\ \mu m$	1
Events in flight from unidentified track with range $> 150\ \mu m$	75
Events from unidentified track with range $< 150\ \mu m$	145 { 127 from K^- at rest; 18 from K^- in flight

The originated events from unidentified connecting track with range shorter than 150 μm have been then subdivided as in Table II: one deduces at last that 112 events must be attributed to non-mesic hyperfragments.

It may be therefore deduced from the two tables that the total number of mesic and non-mesic hyperfragments, emitted in K^--stars at rest, is 120.

Since among the 4 565 K^--stars observed in the whole stack, with at least one prong, 3779 stars are originated by K^- mesons at rest, the emission frequency of hyperfragments from K^--stars at rest is $(120/3\,779) = (3.2 \pm 0.5)\,\%$ (*).

Moreover, in order to estimate the hyperfragment emission probability from K^--stars at rest, one must add to the number of the already observed stars the K_{e^-}-number and then detract the number of interactions in which a Σ hyperon is emitted.

(*) See footnote at pag. 247.

TABLE II. – *Deduced classification of the* 145 *events due to unidentified track with range.* < 150 μm.

Stars from Σ^- at rest (see sect. **2**)	28
Stars in flight from unidentified track [a]	5
Stars from π^- at rest [b]	—
Non-mesonic hyperfragment decays [c]	112 { 98 from K^- at rest [d] 14 from K^- in flight [d]

[a] The number reported has been obtained extrapolating the distribution of the connecting track lenghts to the interval $(0 \div 150)$ μm.

[b] The contribution of the π^--stars is considered negligible according to the known π^--energy spectrum in K^--stars at rest [7].

[c] The number reported is the difference between the total number 145 and the sum of the first three categories.

[d] This subdivision is deduced from the similar one observed for all the 145 events (see Tab. I).

According to the classification reported in Table III, the hyperfragment emission probability in K^--stars at rest is $(120/3551) = (3.4 \pm 0.6)\%$.

TABLE III. – *Classification of the* K^-*-stars at rest.*

K^--stars with 1 or more prongs	3779	K^--stars with hyperon decays	309
K_{e} (17% of the whole)	774	K^--stars with Σ^--stars (Σ_{e}^- included)	359
Total number of K^--stars at rest	4553	K^--stars with Σ^0 (*)	334
		Total number of $\Sigma^{+,-,0}$	1002

(*) The number of Σ^0 hyperons is taken, following isotopic spin arguments [8], equal to $\frac{1}{2}[N(\Sigma^+) + N(\Sigma^-)]$.

This value actually is lower than that already determined by other authors [8,9]; such a difference may be attributed mainly to the different criteria adopted for the computation of the emission probability.

---

[7] See, *e.g.*: K^--COLLABORATION: *Nuovo Cimento*, **14**, 315 (1959).

[8] W. F. FRY, J. SCHNEPS, G. A. SNOW, M. S. SWAMI and D. C. WOLD: *Phys. Rev.*, **107**, 257 (1957).

[9] Y. EISENBERG, W. KOCH, M. NIKOLIĆ, M. SCHNEEBERGER and H. WINZELER: *Nuovo Cimento*, **11**, 351 (1959).

However, the above reported value of the hyperfragments emission probability from K^--stars at rest, results much greater than the one evaluated (Section 3) from Σ^--stars at rest $(1.2 \pm 0.5)\%$ (*).

* * *

We wish to thank Prof. MORPURGO for useful advice and the Bologna group for having furnished the stack and for a partial scanning of the plates.

(*) In the mentioned paper of FRY *et al.*, a value 0/115 of the hyperfragment formation probability, from Σ^--stars at rest, was found, no hyperfragment being observed from 50 Σ^--stars at rest.

RIASSUNTO

Sono stati osservati 5 iperframmenti emessi da un totale di 137 stelle da Σ^- a riposo. La probabilità di emissione di tali eventi risulta $(1.2 \pm 0.5)\%$ ed è alquanto inferiore alla probabilità di emissione di iperframmenti delle stelle di K^- a riposo osservate nello stesso pacco di emulsioni $(3.4 \pm 0.6)\%$.

IL NUOVO CIMENTO Vol. XVI, N. 2 16 Aprile 1960

The Theory of Photon Packets and the Lennuier Effect.

L. M. Falicov (*)

Instituto de Fisica, San Carlos de Bariloche, Rio Negro (**).

(ricevuto il 6 Dicembre 1959)

Summary. — The quantum electromagnetic field of radiation is studied for the case of a spectral distribution of energy and momentum. Packets of photons are introduced and classified. Some of their coherence properties are discussed by associating equivalent classical fields with each packet. The emission and dispersion of such packets are studied with special emphasis on the fluorescence resonance of frequencies near the atomic frequency. A scattered packet is shown to contain frequencies not present in the incident radiation, as found experimentally by R. Lennuier, and the apparent non-conservation of energy is seen to be a consequence of the Heisenberg uncertainty principle.

1. – Introduction.

Since the very beginning of wave mechanics, quantum phenomena concerning electromagnetic waves have been widely studied. However, no complete formulation of the problem has been given to cover the situation when the wave contains a range of wave vectors k, except for some special problems such as the natural line breadth. The existence of experimental data, such as those obtained by R. Lennuier (1) on resonance fluorescence, shows the need for such a formalism to describe processes involving non-monochromatic radiation.

We first introduce a formalism for photon packets in Section 2. These involve linear combination of many-photon functions, but since in physical

(*) This work is part of the thesis submitted to Cuyo National University, Argentina, in candidacy for the degree of Doctor in Physics.

(**) Present address: Cavendish Laboratory, Cambridge, U.K.

(1) R. Lennuier: *Ann. Phys.*, **2**, 233 (Paris, 1947).

processes the number of photons is conserved or changes by a definite number (one or two) we do not mix states with different numbers of photons. Some of the properties of the photon packets can be discussed by introducing the associated electromagnetic fields, as was first done by BECK [2] in a different context. This is necessary in order to define the momentum distribution of an arbitrary photon packet. In the limit of large numbers of photons, the associated fields also allow us to give a meaning to the classical concept of a coherent radiation, and to extend this concept to packets with a small number of photons.

The formalism is first applied to photon emission by an atom in Section **3**, and it is shown explicitly for the first time that a system containing a large number of similar radiating atoms gives a beam of coherent radiation as is very well known experimentally in classical optics. The second application (Section **4**) is to dispersion phenomena in which a packet changes its original distribution. This is applied in Section **5** to the dispersion of a one-photon packet by a bound electron (resonance fluorescence). LENNUIER observed that the scattered resonance fluorescence radiation contains frequencies not present in the incident radiation. This phenomenon is discussed in detail and the apparent non-conservation of energy is seen to be a consequence of the Heisenberg uncertainty principle.

2. – Photon packets.

When the radiation field is quantized and the photons are introduced, it is necessary to have a system of generalized functions to describe the field. We shall be interested in states of the field

$$\Gamma_k^n|0\rangle\,, \tag{1}$$

$$\Gamma_k^n = (\text{const.})\exp\left[-in\omega_k t\right](a_k^+)^n\,,$$

where a_k^+ is the creation operator of the photon k, k a multiple index that defines the wave vector and polarization; $|0\rangle$ is the state vector of the vacuum; the constant is chosen in order to normalize (1) to unity.

The state representing an arbitrary one-photon packet is therefore written

$$\Gamma^1|0\rangle = \sum_k \lambda_k \Gamma_k^1|0\rangle\,, \tag{2}$$

---

[2] G. BECK: *Nuovo Cimento*, **1**, 70 (1950).

where the λ_k's satisfy the normalization relation

$$\sum_k |\lambda_k|^2 = 1 . \tag{3}$$

In future we shall drop $|0\rangle$ and use Γ to represent states of the system. Γ^1 is not an eigenstate of the energy and k vector, but has a momentum and polarization distribution

$$f(k) = |\lambda_k|^2 .$$

An n-photon packet is similarly defined by

$$\Gamma^n = \sum_{[n_i]} L_n(n_1, n_2, n_3, \ldots)\Gamma_{k_1}^{n_1}\Gamma_{k_2}^{n_2}\Gamma_{k_3}^{n_3}\cdots , \tag{4}$$

where

$$L_n(n_1, n_2, n_3, \ldots) = 0$$

if

$$\sum_i n_i \neq n$$

and

$$\sum_{[n_i]} |L_n(n_i)|^2 = 1 . \tag{5}$$

We shall restrict the name photon packet to states such as (4) which contain a definite number n of photons, *i.e.* are eigenstates of the photon number operator $\sum_k a_k^+ a_k$.

As mentioned in the introduction, it is useful to associate a classical field with a photon packet. We first define the spectral distribution operator

$$D = \sum_{kk'} a_k^+ a_{k'} \exp\left[-i(\boldsymbol{k} - \boldsymbol{k}')\boldsymbol{r}\right] . \tag{6}$$

This is, for a photon packet, the diagonal part of the square of the vector potential operator, except that we omit for convenience a numerical coefficient $2\pi c^2\hbar(\omega_k\omega_{k'})^{-\frac{1}{2}}$ and the null field divergence. Similarly D is related to the energy density and the action density of the system except for some coefficients. The Fourier components of this operator, namely $D(k, k') = a_k^+ a_{k'}$, have for a photon packet Γ^n the expectation value

$$\begin{cases} \langle D(k, k')\rangle_n = \sum_{[n_i]} n_k |L_n(n_i)|^2 & k = k', \\ \qquad\qquad = \sum_{[n_i]} \left[(n_k + 1)n_{k'}\right]^{\frac{1}{2}} L_n^*(n_i) L_n(n_i + \delta_{ki} - \delta_{k'i}) & k \neq k'. \end{cases} \tag{7}$$

Now a general electromagnetic field can be expressed in terms of the vector potential

$$(8) \qquad \boldsymbol{A}_c = \sum_k \boldsymbol{e}_k \sqrt{4\pi c^2} \left[q_k \exp\left[ik_\mu x_\mu\right] + q_k^* \exp\left[-ik_\mu x_\mu\right]\right] \qquad \mu = x, y, z, ict.$$

where $\boldsymbol{e}_k$ and q_k are respectively the polarization versor and the amplitude of the k Fourier component. It is convenient to define the classical quantity

$$(9) \qquad \boldsymbol{D}_c = 2/\hbar \sum_{k,k'} \sqrt{\omega_k \omega_{k'}}\, q_k^* q_{k'} \exp\left[i(k'_\mu - k_\mu)x_\mu\right],$$

which is essentially the intensity of the field, and is the classical dynamical variable corresponding to the operator $\boldsymbol{D}$ (6). Its Fourier coefficients are similarly

$$(10) \qquad \boldsymbol{D}_c(k, k') = 2/\hbar \sqrt{\omega_k \omega_{k'}}\, q_k^* q_{k'},$$

Thus the classical field which we shall associate to each photon packet is defined by the condition

$$(11) \qquad \langle \boldsymbol{D}(k, k') \rangle_n = \boldsymbol{D}_c(k, k') .$$

Although (11) always defines $\boldsymbol{D}_c$ the set of equations (10) do not necessarily have a solution for the q's and thus it is not always possible to invert (9) and (8) to derive the corresponding $\boldsymbol{A}_c$. Although $\boldsymbol{A}_c$ is completely arbitrary, $\boldsymbol{D}_c$ has to have the form of the square of an arbitrary vector and is not itself arbitrary. It is of course necessary to work with the intensities of the field $\boldsymbol{D}$ and $\boldsymbol{D}_c$ rather than with the corresponding $\boldsymbol{A}$ and $\boldsymbol{A}_c$ because $\langle \boldsymbol{A} \rangle$ is always zero. Physically (11) always defines the spectral distribution of the energy, but this distribution does not always correspond to a single field $\boldsymbol{A}_c$ of well determined intensity and phase. In fact, if a quantum field admits its classical associate *i.e.* if $\boldsymbol{D}_c$ corresponds to a single $\boldsymbol{A}_c$, it means that the quantum packet corresponds to a coherent field in which the Fourier components are well defined in magnitude and relative phase. Inspection shows that packets satisfying this condition are:

a) Packets containing only one state k but any number of photons;

b) One-photon packets;

c) Packets of n photons having the same distribution as a one-photon packet.

The last is the most general case and includes the previous two as particular cases. Two packets are said to have equivalent distribution when the expec-

tation values of the D operator are proportional, the factor of proportionality being the ratio of the total number of photons. If the one-photon packet is expressed by (2), it can easily be shown that a packet of n photons has an equivalent distribution if and only if

$$L_n(n_i) = \frac{n!}{n_1!\, n_2!\, n_3! \ldots n_n! \ldots} \lambda_1^{n_1} \lambda_2^{n_2} \lambda_3^{n_3} \ldots \lambda_n^{n_n} \ldots . \tag{12}$$

Only these packets correspond to one coherent radiation field.

For a more general packet, it may be possible to associate M classical fields in such a way that the expectation value of D is equal to the sum of the M classical D_c magnitudes. Consider for example the packet

$$\Gamma^2 = \sum_{kk'} \lambda_k \mu_{k'} \Gamma_k^1 \Gamma_{k'}^1$$

such that $\lambda_k \neq 0$ only if $\mu_k = 0$ and vice versa. This two-photon packet is the superposition of the two one-photon packets defined by λ_k and μ_k with non-overlapping spectral distribution. With it we can associate two classical fields, *i.e.* those belonging to the two one-photon packets, but on going through the analysis it is found that the relative phase of these two fields is completely arbitrary. If the two packets are not orthogonal ($\sum_k \lambda_k^* \mu_k \neq 0$), then even the two fields are to some extent arbitrary. However, as will appear later, the physically important fact is the minimum number of separate fields required.

3. – Photon emission.

In this section we shall consider the emission of a photon by an electron making a transition between two bound states of energy E_1 and E_2, and apply the general theory of damping phenomena formulated by HEITLER [3].

In the case of spontaneous emission, the general theory gives immediately the formation of the photon packet

$$\Gamma^1 = \sum_k \alpha_k \Gamma_k^1 , \tag{13}$$

where

$$\alpha_k = \frac{AH_{k,0}}{\hbar(\omega_k - \omega_0 + i\gamma/2)} ,$$

---

[3] W. HEITLER: *Quantum Theory of Radiation*, 3rd edition (Oxford, 1954), p. 163, 181, 196.

$H_{k,0}$ is the matrix element of the interaction Hamiltonian between the electron and the electromagnetic field, taken between the state k, consisting of the electron in the ground state and one photon k and the state 0, consisting of the electron in the excited state and no photon; ω_0 is the frequency defined by $\hbar\omega_0 = E_1 - E_2$ and γ is the natural line breadth; A is some normalization factor.

A more interesting case is the emission by an atom in the presence of the one-photon packet (3) with distribution λ_k, *i.e.* stimulated emission. The result in this case is a packet of two photons with expansion coefficients

$$\text{(14)} \qquad \begin{cases} L_2(n_k = 1,\ n_{k'} = 1) = A(\lambda_k \alpha_{k'} + \lambda_{k'} \alpha_k) \\ L_2(n_k = 2) = A\sqrt{2}\,\lambda_k \alpha_k\,, \end{cases}$$

where α_k is again given by (13) and A is the normalization facor

$$\text{(15)} \qquad A^2 = [1 + |\beta|^2]^{-1}$$

and

$$\text{(16)} \qquad \beta = \sum_k \alpha_k^* \lambda_k$$

is the scalar product of the two one-photon packets α_k and λ_k. This two-photon packet has, in general, two associated fields that can be taken to be the fields associated with the one-photon packets (*).

$$\text{(17)} \qquad \begin{cases} \nu_{1k} = \left[\dfrac{1 - |\beta|^2}{1 + |\beta|^2}\right]^{\frac{1}{2}} \alpha_k \exp[i\varphi_1]\,, \\ \nu_{2k} = \left[\dfrac{1}{1 + |\beta|^2}\right]^{\frac{1}{2}} [\beta\alpha_k + \lambda_k] \exp[i\varphi_2]\,. \end{cases}$$

If $|\beta| \neq 1$ then (17) shows that the associated fields contain two arbitrary phases φ_1 and φ_2. Physically, with arbitrary incident radiation, the emitted packet is partly phase incoherent with the incident one. If $|\beta| = 1$, (17) reduces to one classical field, *i.e.* the emitted radiation coherent with incident. The condition $|\beta| = 1$ implies that the incident photon is equal to the photon emitted in vacuum (**).

(*) As mentioned before, the association is not unique, and in this case, for example, an exchange of α_k and λ_k in (17) yields another possible association.

(**) $|\beta| = 1$ implies $\lambda_k = \alpha_k \exp[i\varphi]$. The arbitrary constant phase difference has no physical significance and is completely undetermined since the phase is the canonical conjugate variable of the number of photons which is diagonal in our case.

Similarly, if the incident packet is a coherent n-photon packet with spectral distribution equal to the photon (13) emitted in the vacuum, it is found that the emission of an additional photon is stimulated. This photon is added coherently to the wave. Instead of the factor $\sqrt{2}$ in (14), a factor $\sqrt{(n_k+1)}$ comes in, corresponding to the usual enhancement factor for stimulated emission. A packet of the form (12) is built up, so that the emitted photon is added coherently to the wave. Thus the emission from an assembly of many radiating identical atoms results in a final coherent n-photons packet with one coherent associated classical field, as is well known experimentally from classical interference experiments.

4. – Dispersion of photon packets.

In this section we shall study phenomena in which packets change their structure, *i.e.* the scattering of photons by electrons. As regards scattering by free electrons (Compton effect), the calculations are quite straightforward with the following results. With any type of incident packet, it is verified that the scattered packet contains only wave vectors consistent with the conservation of energy and momentum. The main result of interest is that the scattered photon is incoherent with the unscattered part of the incident packet, even when the incident packet is coherent.

As regards scattering by a bound electron, consider an incident one-photon packet with spectral distribution λ_k containing frequencies in the region of the excitation frequency ω_0 to an excited state of the electron. The outgoing packet contains some unscattered incident radiation plus a dispersed component. As is shown in the Appendix, the dispersed part has spectral distribution

$$\mu_k = \frac{AH_{k,0}}{\omega_k - \omega_0 + i\gamma_0/2} \cdot \sum_{k'} \frac{\lambda_{k'} H_{0,k'}}{\omega_k - \omega_{k'} + i\gamma_{k'}/2}, \tag{18}$$

where

$$\gamma_{k'} = \frac{2i}{\hbar^2} \frac{|H_{k',0}|^2}{\omega_k - \omega_0 + i\gamma_0/2}, \tag{19}$$

$H_{k\,0}$ is the matrix element for the emission of a photon k from the atom when it goes from the excited state to the ground state; γ_0 is the natural line width of the excited state.

Eq. (18) has been evaluated for several different initial distributions and the results are summarized as follows:

i) For an incident monochromatic packet of frequency ω near ω_0, the outgoing packet is practically monochromatic with line width γ_k ($\ll \gamma_0$) defined by (19).

ii) If the ingoing packet is a « white » beam, *i.e.* it has a uniform distribution over a very wide range containing ω_0, the dispersed photon has the same distribution as the natural line emitted by the atom in the excited state, *i.e.* a line with natural width γ_0 centred about ω_0.

iii) If the original packet has the same distribution as a packet emitted in vacuum by the atom in the state concerned, *i.e.* a line with maximum at ω_0 and width γ_0, then the dispersed radiation has a stronger maximum at ω_0 and is somewhat narrower than the incoming one. The intensity distribution is in fact proportional to the square of the spectral distribution of the incident radiation.

iv) If the excitation packet has a maximum at ω near ω_0 and a natural width γ, the fluorescent packet shows two maxima, the first near ω_0, the second near ω. The distribution is in fact just proportional to the distribution of case ii) above multiplied by the intensity distribution of the incident packet, as one would expect.

Cases i) and ii) are the well-known cases of excitation by a very sharp line and excitation by an uniform distribution respectively, discussed by HEITLER. However the present formalism allows one to make explicit calculations for the first time for cases iii) and iv).

5. – The Lennuier effect.

Our most important application of formula (18) is the account for the effects observed by LENNUIER. In his experiments, mercury $\lambda = 2537$ Å radiation was obtained from a hot source containing several isotopes, so that the line was very broad with a width of about $4.7 \cdot 10^{-2}$ Å. The central part of the band containing the fundamental frequency was then eliminated by means of a suitable filter. This beam, with the characteristic frequency missing, was used to excite another sample of mercury, and the fluorescence radiation was analysed after eliminating the coherent radiation due to normal dispersion. The outgoing beam showed three maxima instead of two, the third being at the fundamental atomic frequency. The appearance in the final state of frequencies not found in the original radiation and the apparent non-conservation of energy were at first sight very puzzling. However, we shall show that the effect can be deduced directly with the use of eq. (18).

The exact shape of the incoming packet is in general very complicated. However, the most important fact of the appearance of the third maximum can be explained with a simple approximation to the real distribution. We have chosen $|\lambda_k|$ to have a distribution consisting of two triangles with maxima at $\omega_0 \pm 2\gamma_0$, each one of total width $2\gamma_0$ as shown in Fig. 1. The total width

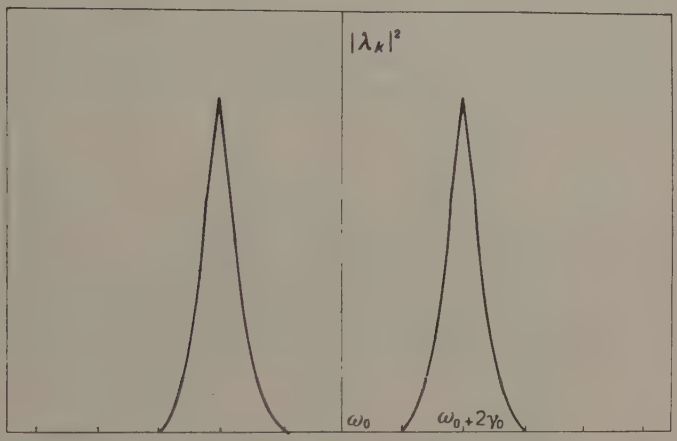

Fig. 1. Approximate intensity distribution of the incident radiation in Lennuier's experiment.

of the spectrum, $6\gamma_0$, represents the width of the original broad line, and the missing central frequencies in a range $2\gamma_0$ about ω_0 are those eliminated by the filter. We assume a constant phase in each of the two regions of the spectrum, but a phase difference of φ between the two parts. When this distribution is substituted into (18), the value of the summation depends sensitively on the phase difference φ between the two parts. The resultant spectra for the two extreme cases $\varphi = 0$ and π are plotted in Figs. 2 and 3 and it is seen that while the first spectrum resembles the incident radiation, the second one shows a very high peak at ω_0. In the actual Lennuier experiment, the two zones of the initial spectrum probably came from the emission by different isotopes. The phase difference between them is therefore quite arbitrary and the observed spectrum is the intensity distribution averaged over all φ. The resultant spectrum is shown in Fig. 4 and displays the three maxima of approximately the same height as observed by LENNUIER.

The appearance of the third maximum can be explained simply by the Heisenberg uncertainty principle. When the atom is excited by a monochromatic wave that is spread through all space, the time at which the excitation takes place is completely unknown. Consequently the energy can be exactly determined and the outgoing packet is therefore practically mono-

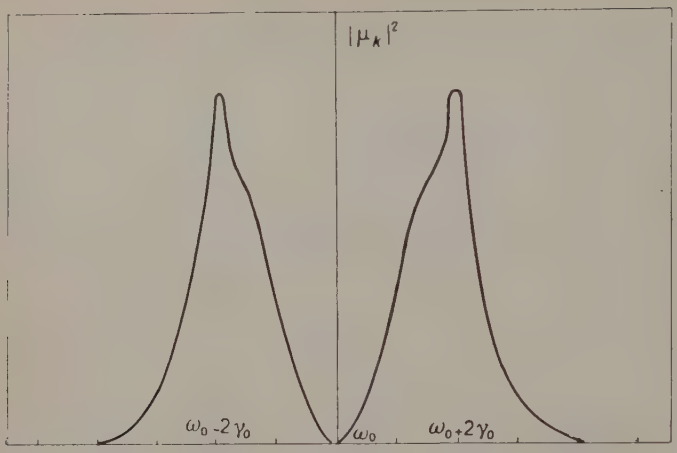

Fig. 2. – Fluorescent packet for $\varphi = 0$.

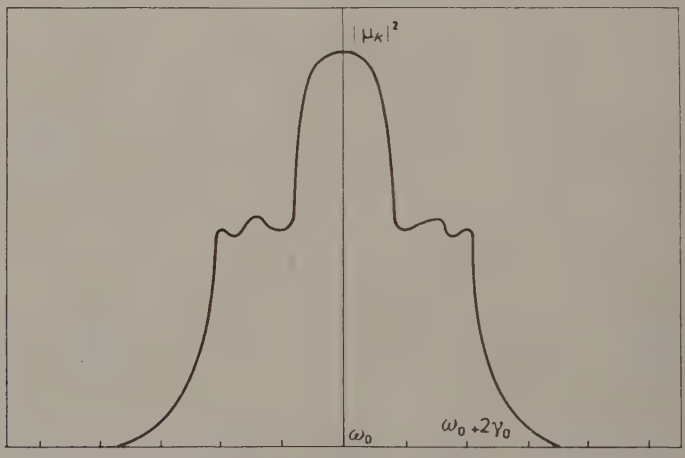

Fig. 3. – Fluorescent packet for $\varphi = \pi$.

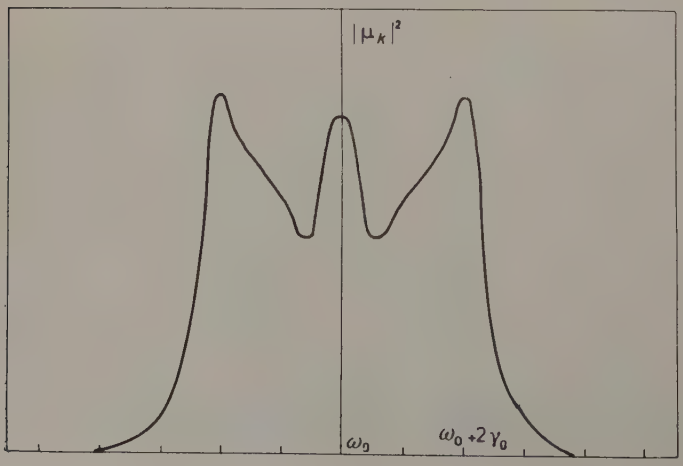

Fig. 4. – The final observed intensity when averaged over all possible phase differences.

chromatic. When the excitation is produced by a uniform distribution, the incoming packet is well localized in space, and the time of the excitation of the atom can be determined with high certainty. As the mean life of the excited state is of the order $\hbar\gamma_0^{-1}$ and is the only time uncertainty in the process, the energy uncertainty in the fluorescent packet is of the order γ_0. The spectral distribution is that of the characteristic line. The other cases of Section 4 and the Lennuier experiment are intermediate examples. The atomic process reduces the time uncertainty and the fluorescent spectrum is then broadened. The frequency ω_0, favoured by resonance phenomena, appears then in the outgoing packet.

* * *

The author is deeply indebted to Dr. J. A. Balseiro for suggesting this investigation and for his constant advice and illuminating discussions. He wishes also to acknowledge some useful discussions with Dr. V. Heine and Dr. J. Westerkamp and the help of Dr. M. Balanzat in the solution of some mathematical difficulties.

Appendix

To study the fluorescent dispersion of a one photon packet we consider the solution of the time-dependent Schrödinger equation with the initial conditions of Table I.

Table I. – *States, energies and initial conditions for fluorescence resonance.*

State			Initial condition $b_n(0)$	Energy E_n
Label	Atom	Photon		
ki	Ground state	k	λ_k	$\hbar\omega_k$
0	Excited state	none	0	$\hbar\omega_0$
kf	Ground state	k	0	$\hbar\omega_k$

The states ki and kf are the same states of the system, but for the sake of clarity we add i or f according to whether the state is appearing as a component of the initial or final packet. The Schrödinger equation becomes

$$\text{(A.1)} \qquad i\hbar\dot{b}_n(t) = \sum_m H_{n,m} b_m(t) \exp\left[i(E_n - E_m)t/\hbar\right] + i\hbar b_n(0)\,\delta(t)\,.$$

In terms of the Fourier transform

$$b_n(t) = -\frac{1}{2\pi i}\int_{\infty}^{\infty} dE\, G_n(E)\, \exp[i(E_n - E)t/\hbar], \tag{A.2}$$

the equations becomes

$$(E - E_k)G_{ki}(E) = H_{ki,0}\, G_0(E) + \lambda_k\,, \tag{A.3}$$

$$(E - E_0)G_0\,(E) = \sum_k H_{0,kl} G_{ki}(E) + \sum_k H_{0,kf} G_{kf}(E)\,, \tag{A.4}$$

$$(E - E_k)G_{kf}(E) = H_{k',\gamma} G_0(E)\,. \tag{A.5}$$

We now put

$$G_n = \sum_k U_{0,ki} G_{ki}\zeta(E - E_0)\,, \tag{A.6}$$

$$G_{k'f} = \sum_k U_{k'f,ki} G_{ki}\,\zeta(E - E_{k'})\,, \tag{A.7}$$

where

$$\zeta(x) = \frac{\mathscr{P}}{x} - i\pi\,\delta(x)\,.$$

Substituting (A.6) and (A.7) into (A.4) and (A.5), and using

$$x\zeta(x) = 1$$

we obtain

$$U_{k'f,ki} = \frac{H_{k'f,0}H_{0,ki}}{E - E_0 + i\hbar\gamma_0/2}\,, \tag{A.8}$$

$$U_{0,ki} = \frac{(E - E_0)H_{0,ki}}{E - E_0 + i\hbar\gamma_0/2}\,, \tag{A.9}$$

where

$$\gamma_0 = 2i/\hbar \sum_k |H_{0,kf}|^2 \zeta(E - E_k) \tag{A.10}$$

is the natural line breadth of the excited atomic state. Substituting (A.9) and (A.6) into (A.4) we obtain

$$G_{ki} = \frac{\lambda_k}{E - E_0 + i\hbar\gamma_k/2}\,, \tag{A.11}$$

where

$$\gamma_k = 2i/\hbar \frac{|H_{ki,0}|^2}{E - E_0 + i\hbar\gamma_0/2}\,, \tag{A.12}$$

and where we have neglected terms of the order $e^2/\hbar c$. We are interested in the values of $b_{kf}(t=\infty)$ which are proportional to the coefficients in the final packet. From (A.2), (A.7), (A.8) and (A.11), letting $t \to \infty$, and using

$$\lim_{t\to\infty} \zeta(x) \exp[-ixt] = -2\pi i\, \delta(x)\,,$$

the final result (18) is obtained.

RIASSUNTO (*)

Si studia il campo elettromagnetico quantistico della radiazione per il caso della distribuzione spettrale dell'energia e dell'impulso. Si introducono e si classificano i pacchetti di fotoni. Si discutono alcune delle loro proprietà di coerenza associando ad ogni pacchetto un campo fisico equivalente. Si studia l'emissione e la dispersione di tali pacchetti sottolineando la risonanza di fluorescenza a frequenze prossime a quella atomica. Si mostra che un pacchetto che ha subito lo scattering contiene frequenze che non sono presenti nella radiazione incidente, come è stato trovato sperimentalmente da R. Lennuier, e si vede che l'apparente non-conservazione dell'energia è una conseguenza del principio di indeterminazione di Heisenberg.

(*) *Traduzione a cura della Redazione.*

Independent Particle Model and Photonuclear Giant Resonance.

E. Eberle, M. Nagasaki (*) and L. Sertorio

Istituto di Fisica dell'Università - Catania
Centro Siciliano di Fisica Nucleare - Catania

(ricevuto il 12 Dicembre 1959)

Summary. — A calculation of the Migdal mean energy of the photonuclear absorption cross section is made by using a harmonic oscillator shell model, without any complicated mathematical treatment, and the conditions under which this independent particle model can give account of the behaviour of the peak of the giant resonance in the photonuclear reactions are analyzed.

1. – Introduction.

The giant behaviour observed in nuclear photoeffects has been, as is well known now, interpreted by Goldhaber and Teller [1] as a resonance due to the oscillation of protons in a nucleus as a whole relative to neutrons, or considered by Steinwedel, Jensen and Jensen [2] as a resonance due to the oscillation of the densities of protons and neutrons with respect to their mean values.

Due to the recent success of the optical model and the independent particle model in explaining various experimental data on nuclear reactions, many effects [3-6] (*), have been made to investigate how the independent particle model could account for the giant resonance in nuclear photoeffects.

(*) On leave of absence from University of Rikkyo, Tokyo.

[1] M. Goldhaber and E. Teller: *Phys. Rev.*, **74**, 1046 (1948).

[2] H. Steinwedel, J. H. D. Jensen and P. Jensen: *Zeits. Natur.*, 5 a, 413 (1950).

[3] J. S. Levinger: *Phys. Rev.*, **97**, 122 (1955).

[4] D. H. Wilkinson: *Physica*, **22**, 1039 (1956).

[5] S. Rand: *Phys. Rev.*, **107**, 208 (1957).

[6] D. Brink: *Nucl. Phys.*, **4**, 213 (1957).

(*) For complete references one is referred to the review articles: J. S. Levinger: *An. Rev. Nucl. Sci.*, **4**, 13 (1954); V. De Sabbata: *Suppl. Nuovo Cimento*, **5**, 243 (1957); D. H. Wilkinson: preprint (1959).

LEVINGER (7) has calculated the mean energy of photoabsorption cross-section defined by MIGDAL (8,9). He has shown that the Migdal mean energy calculated using the Fermi gas model gives the same result as the one obtained by MIGDAL with the two-fluid model, provided that the Fermi energy E_F is equal to three times K, the coefficient of the symmetry energy term, $(N-Z)^2/A$ in the Weizsäcker mass formula.

In view of the fact that this condition is not satisfied by actual nuclei it may be interesting to see if some other simple model, than the Fermi gas model used by LEVINGER, can give a better result. In fact we are going here to consider this possibility by calculating the MIGDAL mean energy without any complicated mathematical treatment by means of the harmonic oscillator shell model, which, as BRINK (6) has shown, can give account of the collective aspects of nuclear dipole oscillations.

2. – Calculation of E_M.

MIGDAL defines the mean energy of the electric dipole absorption of photons by a nucleus as:

$$E_M = (\sigma_{\text{int}}/\sigma_{-2})^{\frac{1}{2}},$$

where:

$$\sigma_{\text{int}} = \int \sigma \, \mathrm{d}E,$$

is the integrated cross-section and

$$\sigma_{-2} = \int (\sigma/E^2) \, \mathrm{d}E.$$

It can be shown in general that σ_{-2} is related to the nuclear polarizability through the equation

$$\sigma_{-2} = (2\pi^2/\hbar c)\alpha,$$

valid in the 2-nd order of e, the electrostatic coupling constant of the nucleon.

In terms of the harmonic oscillator shell model, the nuclear polarizability can be easily calculated; the hamiltonian of the model is:

$$H = T_Z + T_N + (1/2)k\left[\sum_i \boldsymbol{r}_i^2 + \sum_j \boldsymbol{r}_j^2\right], \tag{1}$$

(7) J. S. LEVINGER: *Nucl. Phys.*, **8**, 428 (1958).
(8) A. MIGDAL: *Žurn. Éksp. Teor. Fiz.*, **15**, 81 (1945).
(9) J. S. LEVINGER: *Phys. Rev.*, **107**, 554 (1957).

where T_Z and T_N are the kinetic energies of protons and neutrons respectively, and the indices i and j refer to the co-ordinates of protons and neutrons respectively.

The hamiltonian (1) is modified as follows in the presence of an external electrostatic field $\boldsymbol{\epsilon}$:

$$H' = T_Z + T_N + \tfrac{1}{2} k \left[\sum_i \boldsymbol{r}_i^2 + \sum_j \boldsymbol{r}_j^2 \right] - \boldsymbol{Q} \cdot \boldsymbol{\epsilon} ,$$

where $\boldsymbol{Q}$ is

$$\boldsymbol{Q} = e \sum_i (\boldsymbol{r}_i - \boldsymbol{R}) = \frac{eN}{A} \sum_i \boldsymbol{r}_i \frac{eZ}{A} \sum_j \boldsymbol{r}_j ,$$

because the energy shift due to the recoil of the center of mass is not involved in the calculation of α.

The Hamiltonian H' can be rewritten as:

$$H' = T_Z + T_N + \tfrac{1}{2} k \left[\sum_i \boldsymbol{r}_i'^2 + \sum_j \boldsymbol{r}_j'^2 \right] - \frac{e^2}{2k} \varepsilon^2 \frac{NZ}{A} , \tag{2}$$

where

$$\boldsymbol{r}_i' = \boldsymbol{r}_i - \frac{N}{A} \frac{e}{k} \boldsymbol{\epsilon} ,$$

$$\boldsymbol{r}_j' = \boldsymbol{r}_j + \frac{Z}{A} \frac{e}{k} \boldsymbol{\epsilon} .$$

From the comparison of H and H' as given by (2), one sees that the energy shift ΔE due to the electrostatic field is given by the last term of eq. (2). The nuclear polarization is therefore:

$$\alpha = - \Delta E / (\varepsilon^2/2) = \frac{e^2}{k} \cdot \frac{NZ}{A} .$$

If one uses for σ_{int} the classical theoretical value ([10]), which is valid for a system of interacting nucleons through forces of non-exchange character, given by:

$$\sigma_{\text{int}}^{\text{class}} = \frac{NZ}{A} \frac{2\pi^2 e^2 \hbar}{Mc} ,$$

where M is the mass of a nucleon, the Migdal mean energy is

$$E_M = \hbar \sqrt{k/M} = \hbar\omega . \tag{3}$$

([10]) J. S. LEVINGER and H. A. BETHE: *Phys. Rev.*, **78**, 115 (1950).

This is the same expression as that obtained by BRINK (6) for the energy of the dipole oscillations.

Now, if we use for σ_{int} the formula obtained by LEVINGER and BETHE (10) by taking into account also interactions of exchange character among nucleons:

$$\sigma_{\text{int}} = \sigma_{\text{int}}^{\text{class}} (1 + 0.8x) , \quad (*) \tag{4}$$

where x is the fraction of exchange forces present in neutron-proton interaction.

In this case:

$$E_M = \hbar \sqrt{\frac{k\,(1 + 0.8x)}{M}} . \tag{5}$$

Introducing the usual definition of the well depth of the harmonic oscillator potential,

$$V_0 = \tfrac{1}{2} k R^2 , \qquad R = r_0 A^{\frac{1}{3}} , \tag{6}$$

into eq. (5), E_M becomes

$$E_M = \frac{\hbar}{A^{\frac{1}{3}}} \sqrt{\frac{2}{M}\left(\frac{V_0}{r_0^2}\right)(1 + 0.8x)} . \tag{7}$$

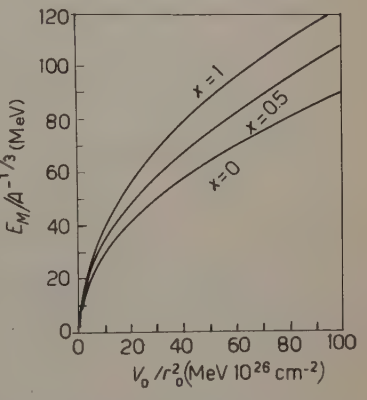

Fig. 1. – $E_M/A^{-\frac{1}{3}}$ in MeV *vs.* (V_0/r_0^2) in MeV$\cdot 10^{26}$ cm^{-2}. V_0 is the well depth defined by eq. (6), and r_0 is the nuclear radius parameter, x is the fraction of exchange force.

Fig. 1 gives the value $E_M/A^{\frac{1}{3}}$ in MeV as a function of the parameter (V_0/r_0^2) for the allowed range of x between 0 and 1.

3. – Discussion.

There are not experimental results to be compared directly with the present calculation of E_M. But the experimental values of E_M may be estimated as follows: an analysis (9) of experimental data on (γ, n), (γ, p), (γ, 2n), (γ, f) and

(*) The numerical value 0.8 was obtained by Levinger and Bethe for the Fermi gas model. This numerical coefficient is somewhat model dependent, but, as Levinger (3) has observed, it takes values not very different from that of Levinger and Bethe for the harmonic oscillator model.

(γ, γ) cross-sections up to 150 MeV excitation energy gives for heavy nuclei:

$$\sigma_{-2} = \int \sigma(E) E^{-2}\, \mathrm{d}E = 3.5 A^{5/3}\ \mu\mathrm{b/MeV}\,, \tag{8a}$$

$$\sigma_{-1} = \int \sigma(E) E^{-1}\, \mathrm{d}E = 0.30 A^{4/3}\ \mathrm{mb}\,. \tag{8b}$$

The σ_{-2} and σ_{-1} are generally related with σ_{int} through the relation:

$$\sigma_{\mathrm{int}} \geqslant \frac{\sigma_{-1}^2}{\sigma_{-2}}\,. \tag{9}$$

From eqs. (8) and (9), it is seen that

$$\sigma_{\mathrm{int}} \geqslant 26\ A\ \mathrm{mb \cdot MeV}\,.$$

Thus, if one uses these estimates for σ_{int} and σ_{-2}, the Migdal mean energy is estimated, for heavy nuclei, as:

$$E_M \geqslant 85 A^{-\frac{1}{3}}\ \mathrm{MeV}\,.$$

This estimate of the experimental value of E_M is confirmed by the peak energy of the photon scattering cross-section ([11]):

$$E_{\max} = 82 A^{-\frac{1}{3}}\ \mathrm{MeV}$$

for

$$23 \leqslant A \leqslant 238\,,$$

because it may be assumed ([11]) that the cross-section for scattering largely follows the cross-section for absorption, particularly for heavy nuclei, and the giant resonance is not one of very great width.

From the discussion given above, it seems reasonable to take for the present analysis

$$E_M \simeq 85 A^{-\frac{1}{3}}\ \mathrm{MeV}\,.$$

Then V_0/r_0^2 is required (see Fig. 1) to take a value between 50 and 90 $\mathrm{MeV \cdot 10^{26}\ cm^{-2}}$, owing to the possibility of x varying between 0 and 1.

([11]) E. G. FULLER and E. HAYWARD: *Phys. Rev.*, **98**, 1537 (1955); **101**, 692 (1956).

In order to fix further the values of the parameters V_0 and r_0, we now compare σ_{-2} given by the model with that from experiments.

In the present model, σ_{-2} is given by

$$\sigma_{-2} = 1.8 \cdot 10^2 \left(\frac{r_0^2}{V_0}\right) A^{5/3} \ \mu\text{b/MeV} \qquad (V_0 \text{ in MeV};\ r_0 \text{ in } 10^{-13} \text{ cm}). \tag{10}$$

Comparing this theoretical expression for σ_{-2} with the experimental result (8*a*), one observes that the parameter (V_0/r_0^2) should have the value $52\ \text{MeV} \cdot 10^{26}\ \text{cm}^{-2}$.

There is another relation, very simply derivable from the model which V_0 and r_0 must satisfy.

By fitting the mean square radius given by the model with $\frac{3}{5}R^2$ ([3,12]), and by using eq. (6), we have (*)

$$V_0 r_0 = 41\ \text{MeV} \cdot 10^{-26}\ \text{cm}^2 . \tag{11}$$

From this equation and the values $52\ \text{MeV} \cdot 10^{26}\ \text{cm}^{-2}$ of V_0/r_0^2 obtained above, we see that $V_0 = 46$ MeV and $r_0 = 0.95 \cdot 10^{-13}$ cm.

For these values of V_0 and r_0, the parameter x has to take the value $x = 0.92$ in order to reproduce the estimated experimental value of $E_M = 85 A^{-\frac{1}{3}}$ MeV. With this value of x, the theoretical integrated cross-section, eq. (5) takes the estimated experimental value $26\,A$ mb·MeV.

With these values of the parameters V_0, r_0 and x, the harmonic mean energy E_H given by the model:

$$E_H = \hbar \sqrt{\frac{\bar{k}}{M}} (1 + 0.8x),$$

becomes $110 A^{-\frac{1}{3}}$ MeV which is larger than $E_M \simeq 85 A^{-\frac{1}{3}}$ MeV. According to our assumption of $E_M \simeq 85 A^{-\frac{1}{3}}$ MeV, however, E_H must be roughly equal to E_M.

This discrepancy can be considered as due to the use of the harmonic oscillator potential which does not depend on the momentum of nucleons. The inclusion of the effect of the exchange force in σ_{int} means that the average potential acting on a nucleon can not be taken to be independent of the momentum of nucleons ([12,13]).

(*) This relation holds only for the lowest configuration but is expected not to change greatly for states of not too high excitation, because the nuclear density, as well as the average quantum number n, does not change greatly for such excitations.

([12]) V. F. Weisskopf: *Nucl. Phys.*, **3**, 423 (1957).

([13]) J. S. Levinger, N. Austern and P. Morrison: *Nucl., Phys.*, **3** 423 (1957).

We will now proceed to see the possibility that the harmonic oscillator potential with an effective mass, M_{eff}, which represents somehow the momentum dependence of the average potential, can account for the experimental data.

At first, we see that the effective mass M_{eff} should be equal to $M/1.74$ in order to reproduce the estimated value of σ_{int}.

The value $52\ \text{MeV}\cdot 10^{26}\ \text{cm}^{-2}$ of the parameter V_0/r_0^2, obtained by fitting σ_{-2} given by the model to the experimental one, is not changed, since the theoretical σ_{-2} does not depend on the mass. The use of the effective mass $M_{\text{eff}} = M/1.73$ changes eq. (11) to

$$V_0 r_0^2 = 71\ \text{MeV}\cdot 10^{-26}\ \text{cm}^2\ . \tag{11'}$$

Thus we have:

$$V_0 = 60\ \text{MeV}\ ,$$

$$r_0 = 1.1\cdot 10^{-13}\ \text{cm}\ .$$

The harmonic oscillator model with the effective mass M_{eff} gives $E_H = \hbar\sqrt{k/M_{\text{eff}}}$. With those values of the parameters the model gives

$$E_H = 85\,A^{-\frac{1}{3}}\ \text{MeV}\ , \quad \text{as well as} \quad E_H = E_M\ .$$

E_H is related to σ_{int} and σ_{-1} by the relation $E_H = \sigma_{\text{int}}/\sigma_{-1}$. With these values of E_H and σ_{int}, therefore, the experimental σ_{-1} is also reproduced by the model.

The resulting value of 60 MeV of the well-depth parameter V_0 is consistent with the value of the depths of optical potentials obtained from the analysis of nucleon scattering on nuclei.

The nuclear radius parameter r_0 seems to be a little smaller than the values, between 1.2 and $1.5\cdot 10^{-13}$ cm, usually taken for it.

There have been many observations ([14]), however, that the distribution of nuclear density is diffused around a distance of the order of $1.2\cdot 10^{-13}A^{\frac{1}{3}}$ cm, but the distance over which the nuclear density remains constant has been observed as $1.0\cdot 10^{-13}A^{\frac{1}{3}}$ cm.

The present model can not, naturally, give account for photo-nuclear pro-

([11]) Reports of the International Congress on Nuclear Size and Density Distributions, appeared in: *Rev. Mod. Phys.*, **30**, no. 2, (1958), part. 1.

cesses due to the rather extended distribution of nucleons around the nuclear surface ([15,16]) because the harmonic oscillator potential gives a constant attractive force for a nucleon even at distances much greater than the nuclear radius R.

One may argue, therefore, that the nuclear radius in the present model represents the central part of the nuclear density distribution.

The value 0.92 of the parameter x is greater than the value 0.5 usually taken for it, but is consistent with the nuclear saturation condition ([17]), $x \geqslant 0.8$, for the nuclear forces of pure Wigner and pure Majorana type.

It may be noted that, in the derivation of σ_{int} given by eq. (5), due to LEVINGER and BETHE, the possibility that the nuclear forces may include a repulsive hard core was not considered. It will be interesting, therefore, on the basis of recent investigations on the nuclear structure with the use of nuclear forces including hard cores, to investigate what value of x is necessary in order to reproduce the experimental values of σ_{int} and E_M, and to see whether that value of x is consistent or not with saturation conditions for nuclear forces with hard core.

As is noted in the introduction, the Fermi gas model has been shown to be equivalent to the liquid model for the photonuclear giant resonance under the condition

$$E_F = 3K \qquad (K \cong 23 \text{ MeV}).$$

If we estend our hypothesis of an effective mass to the Fermi gas model the condition $E_F = 3K$ can be considered no more in disagreement with data on actual nuclei. In fact if we substitute, $M/1.74$ to M we have:

$$E_F' = 68 \text{ MeV} \cong 3K .$$

In conclusion we can say that the present analysis, which is based on considerations without any mathematical complication, and which is connected with the use of the effective mass previously made by many people ([4,5,12]), may be perhaps useful in understanding the use of the independent particle model in order to explain some features of the photonuclear giant resonance.

([15]) A. AGODI, E. EBERLE and L. SERTORIO: *Nuovo Cimento*, **13**, 1279 (1959).

([16]) A. M. LANE: *Nucl. Phys.*, **11**, 625 (1959); A. M. LANE and J. E. LYNN: *Nucl. Phys.*, **11**, 646 (1959).

([17]) J. M. BLATT and V. F. WEISSKOPF: *Theoretical Nuclear Physics* (New York, 1952).

* * *

We would like to thank Prof. A. AGODI for his kind interest in this work and for useful discussions. One of us (M.N.) wishes also to thank Prof. R. RICAMO and the members of the C.S.F.N. for the kind hospitality.

RIASSUNTO

Si è calcolata l'energia media, quale è stata definita da Migdal, della sezione d'urto di assorbimento fotonucleare facendo uso del modello di oscillatore armonico e con calcoli matematici semplici. Si analizzano altresì le condizioni sotto cui il suddetto modello a particelle indipendenti può dar conto del picco della risonanza gigante nelle reazioni fotonucleari.

Influence de la chaleur sur la coloration des halos pléochroïques dans la biotite.

S. Deutsch

Laboratoire de Physique Nucléaire de l'Université Libre - Bruxelles

(ricevuto il 17 Dicembre 1959)

Summary. — The stability of pleochroic haloes in biotites heated in air and in nitrogen has been studied. The haloes can be erased by the heating process; the rate of this phenomenon increases with temperature and is greater in air than in nitrogen. A comparative study of the behaviour of haloes in different minerals would yield information on the thermal history of rocks.

1. – Introduction.

Dès les premières études du phénomène des halos et de leur application à la géologie, la stabilité à la chaleur de cette altération de la coloration de divers minéraux a été étudiée.

Dans la cordiérite et la hornblende, Gudden [1] a montré que vers 700 °C l'effacement des halos, avec une vitesse variable d'un minéral à l'autre, a lieu en 10 minutes environ.

Dans la biotite, le phénomène se complique du fait que ce minéral, même non irradié, se colore lors du chauffage à l'air au-dessus de 300 °C [1-3]. Jusqu'à cette température, la coloration des halos est stable pendant quelques heures au moins. Le comportement du halo, qui noircit et ne se distingue plus de la biotite, n'a pas été étudié à plus haute température.

Poole [3] a attribué au départ d'eau le phénomène de coloration à l'air de la biotite non irradiée; il a montré qu'il existe une relation directe entre les

---

(1) B. Gudden: *Thèse* (Göttingen, 1919).
(2) A. Michel-Levy: *Compt. Rend.*, **94**, 1196 (1882).
(3) J. H. Poole: *Phil. Mag.*, **5**, 132 (1928).

vitesses de départ de l'eau de ce minéral et celles de coloration en fonction de l'élévation de température. L'eau, à l'état gazeux avant son départ oxyderait le fer ferreux de la biotite en fer ferrique.

Rinne ([4]) avait également attribué à une telle oxydation la croissance de l'angle des axes optiques de la biotite avec le temps de chauffage à 1 000 °C. Il avait montré que ce phénomène est réversible à cette même température en atmosphère réductrice. Une étude en atmosphère de CO_2 a été faite par Memmel ([5]) qui a mis en évidence l'augmentation de l'indice de réfraction et de la couleur de la biotite avec la température (entre 440 et 700 °C).

De ces travaux, il ressort que certaines propriétés optiques et vraisemblablement la coloration de la biotite sont sensibles à l'atmosphère ambiante durant le chauffage de ce minéral. Mais les recherches sur la stabilité de cette coloration ont été faites durant des temps de chauffage courts et en atmosphère non contrôlée. La disparition des halos n'a pas été mise en évidence.

Nous avons fait une étude de la stabilité de la coloration des halos de quelques biotites en fonction de la température et du temps de chauffage dans l'air et dans une atmosphère d'azote.

Pour le chauffage dans l'azote, les lamelles de biotites obtenues par clivage sont disposées dans une tube de quartz en U, placé dans un four. Ce tube est relié au détendeur d'une bonbonne d'azote sec (teneur en $O_2 < 3 \cdot 10^{-6}$ g/g). Les lamelles de biotite chauffées à l'air sont disposées au fond du même four.

Le paramètre mesuré, à l'aide d'un microphotomètre à enregistrement continu ([6]), est ΔD, l'accroissement de la densité optique de la biotite chauffée par rapport à la biotite non chauffée. Il est proportionnel à l'épaisseur du cristal et calculé pour 30 μm.

Les biotites étudiées proviennent du granite de Vire (Normandie) et de La Bresse (Vosges) dans lesquels nous avons étudié les halos ([6]).

2. – Résultats.

2·1. *Stabilité de la coloration de la biotite.* – Les résultats des mesures faites sur la biotite de Vire, chauffée dans l'air et dans l'azote à des températures allant de 300 à 800 °C, sont donnés aux Figs. 1 et 2. ΔD y est porté en ordonnée et le logarithme du temps, en abscisse.

([4]) F. Rinne: *Ber. Verhandlungen Sächsischen Akad. Wissenschaften*, **76**, 261 (1924).

([5]) M. Memmel: *Chemie d. Erde*, **11**, 307 (1937).

([6]) S. Deutsch, D. Hirschberg et E. Picciotto: *Bull. Soc. Belg. Geol.*, **65**, 267 (1956).

Ces courbes montrent que, dans l'air comme dans l'azote, la densité optique de la biotite croît rapidement, passe par un maximum puis diminue. Ces variations surviennent d'autant plus rapidement que la température à laquelle est

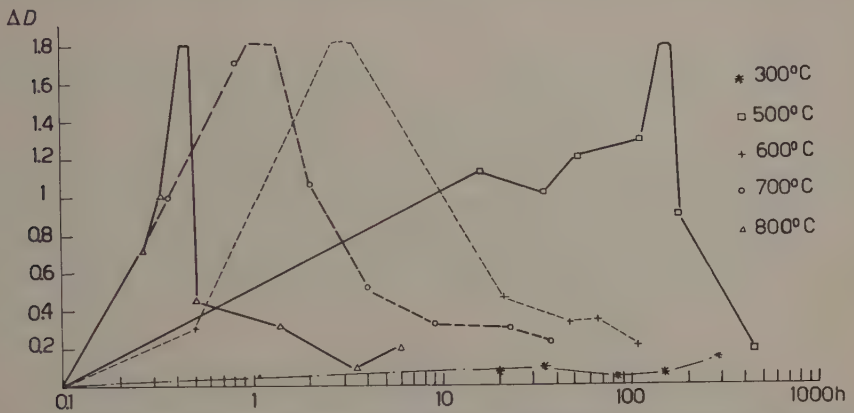

Fig. 1. - Variation de la densité optique de la biotite en fonction du temps de chauffage dans l'air, à diverses températures.

porté le minéral est plus haute. A 300 °C, le maximum n'est pas encore obtenu au bout de 300 heures, alors qu'il est atteint après moins d'une heure à une température supérieure à 700 °C.

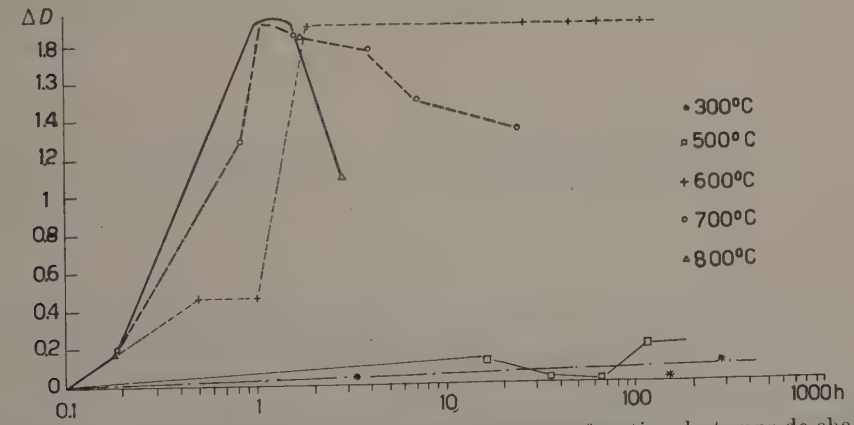

Fig. 2. - Variation de la densité optique de la biotite en fonction du temps de chauffage dans l'azote, à diverses températures.

Le temps nécessaire pour que la biotite chauffée à l'air retourne à sa coloration première ($\Delta D \simeq 0{,}2$) varie avec la température de chauffage; il est respectivement de 400, 100 et 2 heures à 500, 600 et 800 °C.

La comparaison des courbes correspondant à l'air et à l'azote, montre qu'à une même température, la variation de la coloration de la biotite est sensiblement plus lente en atmosphère inerte qu'en présence de l'oxygène de l'air. Le départ d'eau, semblable dans les deux cas, ne serait pas la cause de cette différence.

Notons que la biotite du granite de La Bresse réagit de manière semblable.

2·2. *Stabilité de la coloration des halos dans la biotite.* – Nous avons étudié la stabilité de la coloration des halos à des températures variant de 300 à 800 °C, en même temps que celle de la biotite non irradiée. Quelques-unes des mesures faites sur les profils enregistrés des halos sont données dans les Figs. 3 et 4. Elles montrent les divers profils d'un même halo au cours du

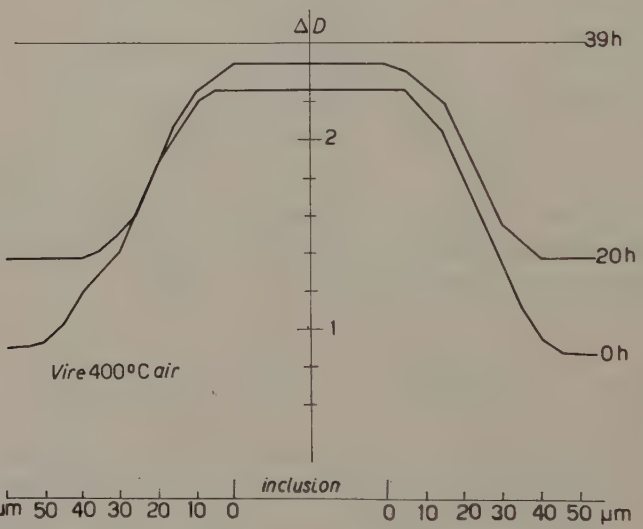

Fig. 3. – Profils de halo en fonction du temps de chauffage à 400° dans l'air.

temps de chauffage à 400 °C et à 700 °C. ΔD est porté en fonction de la distance au bord de l'inclusion radioactive autour de laquelle s'est formé le halo.

Les accroissements de densité optique de la biotite non irradiée y sont également donnés.

On peut conclure de l'ensemble des mesures qu'au début du chauffage dans l'air et dans l'azote, les densités optiques des différents points des halos augmentent, et ce d'autant plus lentement que leur densité optique est plus grande au départ. Puis le halo se confond avec la biotite qui a noirci également et atteint un maximum. Il ne réapparaît plus lorsqu'enfin la biotite s'éclaircit: la vitesse de la disparition du halo suit celle de la variation de coloration de la biotite, elle croît avec la température et en présence d'air.

Parfois, cependant, le halo se distingue encore de la biotite éclaircie environnante; il apparaît alors comme une plage légèrement plus claire que la biotite.

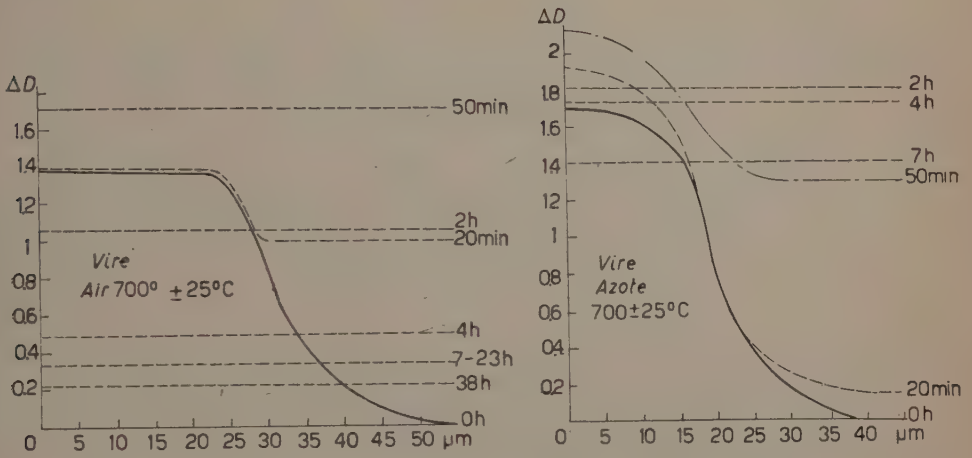

Fig. 4. - Profils de halo en fonction du temps de chauffage à 700° dans l'azote et dans l'air.

Ces résultats montrent que la coloration des halos dans la biotite est plus stable que dans la hornblende ou la cordiérite.

Une étude comparative du comportement à la chaleur des halos dans divers minéraux pourra donner des indications sur l'histoire thermique des roches.

* * *

Je remercie le Professeur KIPFER pour l'intérêt qu'il a porté à ce travail et M.lle J. STORMS pour son aide dans les mesures.

RIASSUNTO (*)

È stata studiata la stabilità degli aloni pleocroici nelle biotiti riscaldate in aria ed in azoto. Gli aloni possono essere cancellati dal riscaldamento; la velocità del fenomeno cresce con la temperatura ed in aria è maggiore che in azoto. Uno studio comparativo del comportamento degli aloni in diversi minerali potrebbe fornire informazioni sulla storia termica delle rocce.

(*) *Traduzione a cura della Redazione.*

IL NUOVO CIMENTO Vol. XVI, N. 2 16 Aprile 1960

A Technique for Eliminating the Variation of Mass with Velocity in Relativistic Problems.

S. Tyagaraja Rao

Department of Physics, University of Madras - Madras

(ricevuto il 21 Dicembre 1959)

Summary. — The solution of problems involving the relativistic change of mass with velocity is facilitated by the introduction of a new temporal parameter τ. When this parameter is used instead of t, the effective mass of the particle becomes a constant. The equation of motion of a relativistic particle in a given e.m. field is obtained using this formulation. This leads to a simple derivation of Sommerfeld's fine-structure formula, correct up to second order in α.

1. – Introduction.

The motion of a relativistic charged particle in a given electromagnetic field defined by the vector and scalar potentials $\boldsymbol{A}$, φ can be worked out starting from the standard relativistic Lagrangian. However, the resulting equations of motion are usually very complicated because of the variation of mass with velocity. In this paper an alternative approach to this problem is presented. The essential idea is to define a temporal parameter τ instead of the usual parameter t, where τ and t are related through an integral. The new velocity is the derivative of the position vector $\boldsymbol{r}$ with respect to τ. After this transformation one finds that the old problem is equivalent to a new one in which the mass of the particle is invariant and moves in a modified field defined by the potentials $\boldsymbol{A}'$ and φ'. The Lagrangian for this formulation can be written down and the equations of motion can be deduced from it. These are comparatively simple equations since the mass is now a constant and the position t of the particle $\boldsymbol{r}(\tau)$ as a function of τ can be obtained. The corresponding t in the old system can be obtained using the integral relation between τ and t. Thus the trajectory of the particle can be obtained.

The transformation from t to τ is not done in the Lorentz sense since the spatial co-ordinates are not affected by the transformation. Thus this transformation is useful in so far as it reduces a relativistic problem to a non relativistic one and the latter is more easily solvable.

2. – Formulation of the problem and equations of motion.

The standard relativistic Lagrangian for a particle of charge e moving in an e.m. field specified by the vector and scalar potentials $(\boldsymbol{A}, \varphi)$ with a velocity $\boldsymbol{v}$ is given by [1]

$$L = -m_0c^2(1-\beta^2)^{\frac{1}{2}} + \frac{e}{c}\boldsymbol{A}\cdot\boldsymbol{v} - e\varphi\,, \tag{1}$$

where $\beta = v/c$. The momentum is defined by

$$\boldsymbol{P} = \frac{\partial L}{\partial \boldsymbol{v}} = \frac{m_0}{(1-\beta^2)^{\frac{1}{2}}}\boldsymbol{v} + \frac{e}{c}\boldsymbol{A}\,, \tag{2}$$

and the Hamiltonian H is given by

$$H = \boldsymbol{P}\cdot\boldsymbol{v} - L = \frac{m_0c^2}{(1-\beta^2)^{\frac{1}{2}}} + e\varphi\,. \tag{3}$$

This is not in the canonical form. The corresponding equation of motion is defined by

$$\frac{\mathrm{d}}{\mathrm{d}t}\left(\frac{m_0}{(1-\beta^2)^{\frac{1}{2}}}\boldsymbol{v} + \frac{e}{c}\boldsymbol{A}\right) = -\operatorname{grad}\left(e\varphi - \frac{e}{c}\boldsymbol{A}\cdot\boldsymbol{v}\right). \tag{4}$$

Now, let us introduce a temporal parameter τ defined by

$$\tau = \int_0^t \mathrm{d}t(1-\beta^2)^{\frac{1}{2}}\,, \tag{5a}$$

so that

$$\frac{\mathrm{d}\tau}{\mathrm{d}t} = (1-\beta^2)^{\frac{1}{2}}\,. \tag{6}$$

The new velocity $\boldsymbol{v}'$ is given by

$$\boldsymbol{v}' = \frac{\mathrm{d}}{\mathrm{d}\tau}\boldsymbol{r} = \frac{\mathrm{d}t}{\mathrm{d}\tau}\cdot\frac{\mathrm{d}}{\mathrm{d}t}\boldsymbol{r} = \boldsymbol{v}/(1-\beta^2)^{\frac{1}{2}}\,. \tag{7}$$

(1) H. GOLDSTEIN: *Classical Mechanics* (Cambridge, Mass., 1953).

For a conservative system of energy E, eq. (3) gives

$$(E - e\varphi)/m_0c^2 = 1/(1-\beta^2)^{\frac{1}{2}} . \tag{8}$$

Let us now write equation (4) in terms of τ. Using (7) we get

$$\frac{\mathrm{d}}{\mathrm{d}\tau}\left(m_0\boldsymbol{v}' + \frac{e}{c}\boldsymbol{A}\right) = \frac{E - e\varphi}{m_0c^2}\,\mathrm{grad}\,(E - e\varphi) + \mathrm{grad}\,\frac{e}{c}\boldsymbol{A}\cdot\boldsymbol{v}' = \tag{9}$$

$$= -\,\mathrm{grad}\left[-\frac{(E - e\varphi)^2}{2m_0c^2} - \frac{e}{c}\boldsymbol{A}\cdot\boldsymbol{v}'\right].$$

This is the new equation of motion. This is extremely interesting, for now the effective mass is a constant equal to m_0 and this particle of charge e is effectively moving in an e.m. field defined by the potentials $\boldsymbol{A}'$, φ' where

$$\boldsymbol{A}' = \boldsymbol{A}\,, \tag{10}$$

$$\varphi' = -\,(E - e\varphi)^2/2m_0c^2e\,. \tag{11}$$

Thus only the scalar potential is modified and this modification is brought about by the energy which is a constant of motion.

It is to be noted, however, that the transformation $t \to \tau$ is not a Lorentz transformation since here the space co-ordinates are not at all affected. This will be of use in problems where the system is conservative and the particle is relativistic.

3. – Motional parameters in the new system.

In the previous section we established the relation between the velocity parameters in the two systems. Using that we find for the momentum

$$\boldsymbol{P}' = m_0\boldsymbol{v}' = m_0/(1-\beta^2)^{\frac{1}{2}}\cdot\boldsymbol{v} = m\boldsymbol{v} = \boldsymbol{P}\,. \tag{12}$$

Thus the linear momentum is unchanged. The energy function in the new system is given by the Hamiltonian

$$H' = \boldsymbol{P}'^2/2m_0 + e\varphi'\,. \tag{13}$$

Thus, the effective energy E' is given by

$$E' = \tfrac{1}{2}m_0v'^2 - (E - e\varphi)^2/2m_0c^2 = -\tfrac{1}{2}m_0c^2\,, \tag{14}$$

which is a constant independent of the state of motion and depends only on the rest energy of the particle. We further notice that

$$\left(1+\frac{v'^2}{c^2}\right)^{\frac{1}{2}}=\left(1+\frac{v^2}{c^2-v^2}\right)^{\frac{1}{2}}=1/(1-\beta^2)^{+\frac{1}{2}}, \tag{15}$$

so that we can put (5*a*) as

$$t=\int_0^\tau \mathrm{d}\tau\left(1+\frac{v'^2}{c^2}\right)^{\frac{1}{2}}. \tag{5b}$$

Now, the right side contains parameters for the new system. Similar results can be established for other parameters as well and they are summarized in Table I

TABLE I. – *Physical parameters in t and τ systems.*

Entity	*t*-system	*τ*-system
1. Mass	$m=m_0/(1-\beta^2)^{\frac{1}{2}}$	m_0
2. Position	$\boldsymbol{r}$	$\boldsymbol{r}$
3. Time	t	$\tau=\int_0^t \mathrm{d}t(1-\beta^2)^{\frac{1}{2}}$
4. Velocity	$\boldsymbol{v}=\frac{\mathrm{d}}{\mathrm{d}t}\boldsymbol{r}$	$\boldsymbol{v}'=\frac{\mathrm{d}}{\mathrm{d}\tau}\boldsymbol{r}=\boldsymbol{v}/(1-\beta^2)^{\frac{1}{2}}$
5. Momentum	$\boldsymbol{p}=m\boldsymbol{v}$	$\boldsymbol{p}'=m_0\boldsymbol{v}'=m\boldsymbol{v}=\boldsymbol{p}$
6. Total energy	$E=m_0c^2/(1-\beta^2)^{\frac{1}{2}}+e\varphi$	$E'=-\frac{1}{2}m_0c^2$
7. Vector potential	$\boldsymbol{A}$	$\boldsymbol{A}$
8. Scalar potential	Φ	$-(E-e\varphi)^2/2m_0c^2e$

Now, using (14) we get

$$\begin{aligned}-\frac{1}{2}m_0c^2&=\frac{1}{2}m_0v'^2-\frac{(E-e\varphi)^2}{2m_0c^2}\\&=\frac{(m_0v')^2}{2m_0}-\frac{(E-e\varphi)^2}{2m_0c^2}\\&=\frac{(mv)^2}{2m_0}-\frac{(E-e\varphi)^2}{2m_0c^2}\\&=\frac{1}{2m_0}\left(\boldsymbol{P}-\frac{e}{c}\boldsymbol{A}\right)^2-\frac{1}{2m_0c^2}(E-e\varphi)^2\,.\end{aligned}$$

Transposing, we obtain

$$(E - e\varphi)^2 = c^2 \left(\boldsymbol{P} - \frac{e}{c} \boldsymbol{A} \right)^2 + m_0^2 c^4 . \tag{16}$$

This is the standard expression relating E, $\boldsymbol{P}$, $\boldsymbol{A}$ and φ ([2]).

We notice that if the particle is at $\boldsymbol{r}$ at t then it is at $\boldsymbol{r}$ at τ if the origins of t and τ coincide. Thus, the distance moved in time $\mathrm{d}t$ (or $\mathrm{d}\tau$) is

$$\mathrm{d}\boldsymbol{r} = \boldsymbol{v}\,\mathrm{d}t = \boldsymbol{v}'(1 - \beta^2)^{\frac{1}{2}}\,\mathrm{d}t = \boldsymbol{v}'\,\mathrm{d}\tau . \tag{17}$$

Thus, the trajectories $\boldsymbol{r}(t)$ and $\boldsymbol{r}(\tau)$ are identical.

4. – Application to central orbits.

Let us now apply this result to the motion of an electron of charge $-e$ in the field of the nucleus of charge $+Ze$. The equations of motion are

$$m_0 \left[\frac{\mathrm{d}^2 r}{\mathrm{d}\tau^2} - r \left(\frac{\mathrm{d}\theta}{\mathrm{d}\tau} \right)^2 \right] = + \operatorname{grad} \frac{(E + e\varphi)^2}{2m_0 c^2} , \tag{18}$$

$$m_0 \frac{\mathrm{d}}{\mathrm{d}\tau} \left(r^2 \frac{\mathrm{d}\theta}{\mathrm{d}\tau} \right) = 0 . \tag{19}$$

Hence we get as usual

$$P = m_0 r^2 \frac{\mathrm{d}\theta}{\mathrm{d}\tau} = m r^2 \frac{\mathrm{d}\theta}{\mathrm{d}t} = m_0 h , \text{ a constant.} \tag{20}$$

Now

$$\operatorname{grad} \frac{(E + e\varphi)^2}{2m_0 c^2} = - \frac{Ze^2}{m_0 c^2} \left(\frac{E}{r^2} + \frac{Ze^2}{r^3} \right) \hat{\boldsymbol{r}} , \tag{21}$$

where $\hat{\boldsymbol{r}}$ is the unit vector along the radius vector.

Putting $u = 1/r$, we get the result

$$\frac{\mathrm{d}^2 u}{\mathrm{d}\theta^2} + u = \frac{Ze^2}{m_0 h^2 u^2} \left[\frac{E}{m_0 c^2} u^2 + \frac{Ze^2}{m_0 c^2} u^3 \right] = \frac{1}{m_0 h^2 u^2} \left[\frac{Ze^2}{m_0 c^2} E u^2 + \frac{Z^2 e^4}{m_0 c^2} u^3 \right] , \tag{22}$$

([2]) W. H. McCrea: *Relativity Physics* (New York, 1957).

comparing with the standard result

$$\frac{\mathrm{d}^2u}{\mathrm{d}\theta^2}+u=\frac{P}{m_0\hbar^2u^2}, \tag{23}$$

where P is the total force, we get the result that now there is an additional attractive force of magnitude $(Z^2e^4/m_0c^2)(1/r^3)$ which is equivalent tot he effect of the relativistic variation of mass with velocity.

Taking (22) and transposing we get

$$\frac{\mathrm{d}^2u}{\mathrm{d}\theta^2}+\left(1-\frac{Z^2e^4}{c^2P^2}\right)u=\frac{Ze^2}{P^2c^2}\cdot E\,. \tag{24}$$

Thus there is a precession of the orbit and the precession frequency ω_F is given in terms of ω, the frequency of the orbit, by

$$\omega_F=\omega\,\frac{1-\gamma}{\gamma}, \tag{25}$$

where

$$\gamma^2=1-\frac{Z^2e^4}{c^2p^2}\,. \tag{26}$$

Since, $Z^2e^4/c^2P^2\ll 1$ we get from (25),

$$\omega_F=\omega\cdot\frac{1}{2}\cdot\frac{Z^2e^4}{c^2p^2}\,. \tag{27}$$

Observing that the momenta are the same in the two descriptions, we get

$$\frac{1}{2m_0}\left(p_\gamma^2+\frac{1}{\gamma^2}\,p_\theta^2\right)-\frac{(E-e\varphi)^2}{2m_0c^2}=E'=-\frac{1}{2}\,m_0c^2\,. \tag{28}$$

Now put $E=m_0c^2+W$. Then,

$$\frac{(E-e\varphi)^2}{2m_0c^2}=\frac{1}{2}\,m_0c^2+\frac{(W-e\varphi)^2}{2m_0c^2}+(W-e\varphi)\,. \tag{29}$$

Substituting (29) in (28) we get

$$p_\gamma^2+\frac{1}{r^2}\,p_\theta^2=2m_0W+2m_0\frac{Ze^2}{r}+\frac{1}{c^2}\left(W+\frac{Ze^2}{r}\right)^2, \tag{30}$$

where we have set $e\varphi = Ze^2/r$. This is the equation obtained by SOMMERFELD ([3]) (p. 255) and gives the well-known fine-structure formula for H-like atoms.

5. – A derivation of Sommerfeld's fine structure formula using the $1/r^3$ force.

In this section, we give a simple derivation of the fine-structure formula of Sommerfeld correct up to terms of second order in α (*i.e.*) v/c.

The idea is to use the $1/r^3$ force mentioned above to replace the relativistic variation of mass with velocity. We use the circular Bohr orbits. To start with we put in the relativistic mass but annul it by an inverse cube *repulsive* field. But, since the orbit is constrained to be circular, the energy will change Then an *attractive* inverse cube field is superposed so that only the relativistic effect is present and the change in energy due to this is evaluated treating the force as a perturbation.

When we add the two energies, we get the required result. It may be mentioned that such a procedure automatically admits two quantum conditions.

We have the standard equations

$$m_0/(1-\beta^2)^{\frac{1}{2}} \cdot \frac{v^2}{r} = \frac{Ze^2}{r^2} - \frac{Z^2e^4}{m_0c^2} \cdot \frac{1}{r^3}, \tag{31}$$

$$m_0/(1-\beta^2)^{\frac{1}{2}} \cdot vr = n \cdot h/2\pi, \tag{32}$$

and the energy W' is given by

$$W' = m_0c^2 \left[\frac{1}{(1-\beta^2)^{\frac{1}{2}}} - 1 \right] - \frac{Ze^2}{r} + \frac{Z^2e^4}{2m_0c^2} \cdot \frac{1}{r^2}. \tag{33}$$

From (31) and (32) keeping throughout only terms up to second order in β, we get

$$m_0c^2\beta^2 = \frac{Ze^2}{r} - \frac{Z^2e^4}{m_0c^2} \cdot \frac{1}{r^2}, \tag{34}$$

$$m_0c\beta r = n \cdot h/2\pi. \tag{35}$$

Using (34) and (35)

$$\frac{1}{r} = \frac{2\pi m_0 c\beta}{nh} \left(1 + \frac{1}{2}\beta^2 \right).$$

([3]) A. SOMMERFELD: *Atomic Structure and Spectral Lines* (New York, 1934).

From (34), we get

$$\beta = \frac{Z\alpha}{n}\left(1+\frac{1}{2}\beta^2\right)\left(1+\frac{Z^2\alpha^2}{n^2}\right)^{-1}, \tag{37}$$

where $\alpha = 2\pi e^2/ch$ the fine structure constant. For the term containing β, we can use its Bohr value $\beta = Z\alpha/n$ so that (37) becomes

$$\beta = \frac{Z\alpha}{n}\left(1-\frac{1}{2}\frac{Z^2\alpha^2}{n^2}\right). \tag{38}$$

From (36) using (38) we see that

$$\frac{1}{r} = 2\pi m_0 c Z\alpha/n^2 h\,. \tag{39}$$

The energy level W' corresponding to this is given by (33)

$$W' = -\frac{Ze^2}{r} + \frac{Z^2e^4}{2m_0c^2}\cdot\frac{1}{r^2} + m_0c^2\left(\frac{1}{2}\beta^2+\frac{3}{8}\beta^4\right).$$

Using (33), (38), (39), we get

$$W' = -\frac{RZ^2}{n^2}\left(1-\frac{3}{4}\cdot\frac{Z^2\alpha^2}{n^2}\right), \tag{40}$$

where $R = 2\pi^2 m_0 e^4/h^2$, the Rybderg constant.

Now, applying the attractive force, we have for the change in energy from tha standard Hemilton-Jacobi theory [4] the expression

$$W'' = \oint \omega_F\,\delta J_F\,, \tag{41}$$

where J_F the angular momentum integral, is given by

$$J_F = \oint p\,\mathrm{d}\varphi = k\cdot h = p\cdot 2\pi\,. \tag{42}$$

From (27) we have

$$\omega_F = \omega\cdot\frac{1}{2}\cdot\frac{Z^2e^4}{c^2}\cdot\frac{1}{p^2} = 2\pi^2\omega\cdot\left(\frac{Ze^2}{c}\right)^2\cdot\frac{1}{J_F^2}\,. \tag{43}$$

---

[4] M. Born: *Mechanics of Atom* (London, 1927).

Substituting this in (41) and using the result that $\omega = 4\pi^2 m_0 Z^2 e^4/n^3 h^3$ we get

$$W'' = -\frac{RZ^2}{n^2}\frac{Z^2\alpha^2}{nk}. \tag{44}$$

Thus, the energy level $W(n;k)$ is given by

$$W(n;k) = W' + W'' = -\frac{RZ^2}{n^2}\left[1 + \frac{Z^2\alpha^2}{n^2}\left(-\frac{3}{4} + \frac{n}{k}\right)\right]. \tag{45}$$

This is the result sought for.

* * *

The author wishes to thank Prof. G. N. Ramachandran for interesting discussions and the Atomic Energy Commission for financial support which enabled this investigation to be carried out.

RIASSUNTO (*)

La soluzione dei problemi che comportano una variazione relativistica della massa con la velocità, è facilitata dall'introduzione di un nuovo parametro temporale τ. Quando si usa questo parametro invece di t, la massa effettiva della particella diviene una costante. Si ottiene l'equazione del moto di una particella relativistica in un dato campo elettromagnetico usando questo sistema di formulazione. Ciò porta a derivare in modo semplice la formula di Sommerfeld della struttura fina corretta sino al secondo ordine in α.

(*) *Traduzione a cura della Redazione.*

Gamma-Ray Transitions in ^{155}Gd.

B. N. Subba Rao

Tata Institute of Fundamental Research - Bombay

(ricevuto il 22 Dicembre 1959)

Summary. — Conversion coefficients of the 86 keV and 105 keV transitions following the β-decay of ^{155}Eu are determined to be $\alpha_{86}^{K}=0{,}49\pm0.075$ and $\alpha_{105}^{K}=0.29\pm0.054$ from studies with the intermediate image β-ray spectrometer and a scintillation spectrometer. In combination with L-subshell ratios, the mixing ratio, $\delta^2=M2/E1$, is found to be $\delta_{86}^2<0.04$ and $\delta_{105}^2<0.07$. These multipolarities are discussed on the basis of the spheroidal shell model.

1. – Introduction.

The present knowledge about the excited levels of ^{155}Gd based on studies of radioactive decay ([2,3-8]) of ^{155}Eu and ^{155}Tb and Coulomb excitation ([1]) is shown in Fig. 1. The assignments of spins and parities, and the asymptotic quantum numbers (N, n_z, Λ) are based on β-decay and a consideration of the level order, for the deformation parameters $\delta\simeq0.25$ and $N=91$, obtained from Mottelson and Nilson's diagrams ([14]). The 86 and 105 keV transitions

([1]) E. M. Bernstein and H. W. Lewis: *Phys. Rev.*, **105**, 1524 (1957); J. H. Bjerregaard and V. Meyer-Berkout, *Zeits. Naturfor.*, **11** *a*, 273 (1956).

([2]) E. L. Church: ANL-5497, 24 (1955); *Bull. Amer. Phys. Soc.*, **1**, 180 (1956).

([3]) B. Hermatz, T. H. Handley and J. W. Mihelich: *Phys. Rev.*, **114**, 1082 (195),

([4]) W. C. Rutledge, J. H. Cork and S. B. Burson: *Phys. Rev.*, **86**, 775 (1952).

([5]) M. R. Lee and R. Katz: *Phys. Rev.*, **93**, 155 (1954).

([6]) S. Y. Ambiye, M. C. Joshi and B. V. Thosar: *Proc. Ind. Acad. Sci.*, **50**, 342 1959).

([7]) J. W. Mihelich, B. Harmatz and T. H. Handley: *Phys. Rev.*, **108**, 989, (1957).

([8]) J. Juliano: UCRL-3733.

are the most intense in the decay of ^{155}Eu. The K/L ratios ([4-6]) and L-subshell ratios ([2-7]) of the 86 keV transition are not all in agreement and often they lead to ambiguous conclusions of its multipole nature. Only an upper

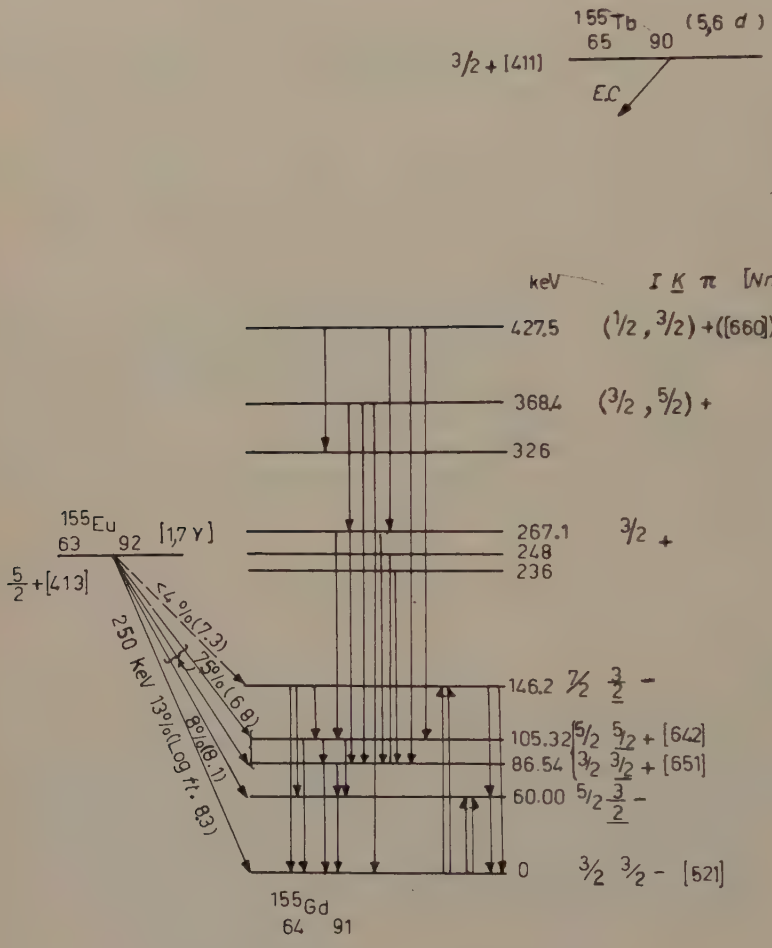

Fig. 1. – Level scheme of ^{155}Gd.

limit estimate of its conversion coefficient ($\alpha_{86}^{K} \ll 0.98$; < 0.75) has been reported by JULIANO ([8]). Much less is known about the 105 keV transition. JULIANO ([8]) has estimated its conversion coefficient to be $\alpha_{105}^{K} \ll 1.6$. Much indirect evidence, based on these estimates, L-subshell ratios and the level assignments based on Nilsson's spheroidal shell model, indicate that both these transitions may be possibly of $E1(+M2)$ type. A direct determination of their multipolarity would be a good verification of such level assignments.

It is, therefore, the purpose of this paper to discuss the multipolarity of these transitions, using the conversion coefficients determined in this work and L-subshell ratios ([2,7]).

2. – Source.

^{155}Eu (1.7 yr) was obtained as the decay product of ^{155}Sm (21 min) produced by irradiation of Sm_2O_3 (enriched in ^{154}Sm to 99.1%) with pile neutrons at ORNL. ^{153}Sm (27 h) and ^{156}Eu (15 days) were found to be present in the ^{155}Eu sample. So, the study of ^{155}Eu was started after five half-lives of ^{156}Eu had elapsed. (^{154}Eu activity was estimated to be present to the extent of about 2% of ^{155}Eu activity.)

3. – Experimental methods and results.

3·1. *β-ray spectrometer studies.* – The internal conversion spectrum was observedusing a thin source deposited on an aluminium backing (~ 160 μg/cm^2) with the intermediate image β-ray spectrometer. After applying corrections ([9]) for absorption in the Geiger counter window (~ 70 μg/cm^2) and for backscattering, the relative conversion electron intensities were determined to be $e_{K86}/e_{K105} = 2.7 \pm 0.1$.

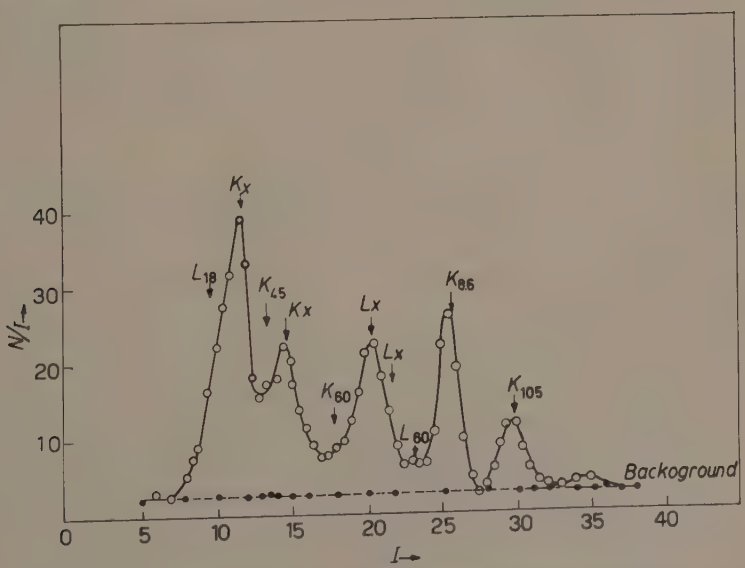

Fig. 2. – External conversion spectrum of radiations of ^{155}Gd in copper.

([9]) B. N. Subba Rao: *Proc. Ind. Acad. Sci.*, A **51**, 28 (1960).

External conversion spectra using thin copper ($\sim 100\ \mu g/cm^2$) and tin ($\sim 180\ \mu g/cm^2$) converters deposited over perspex discs ($290\ mg/cm^2$) were observed with the β-ray spectrometer. They are shown in Figs. 2 and 3.

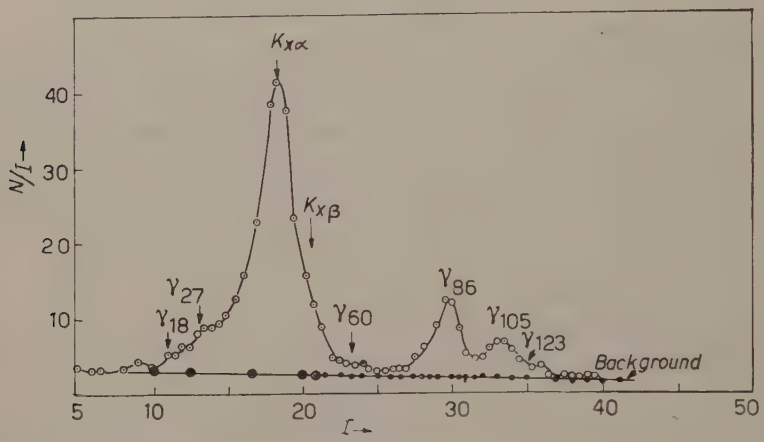

Fig. 3. – External conversion spectrum of radiations of ^{155}Gd in tin.

The source-converter separation was about 0.5 cm and the area of the converter was 3 cm². The source was 0.2 cm thick and had a cross-sectional area of 0.2 cm². The area under the photoelectron lines of 86 and 105 keV, ($P_{\gamma 86}$ and $P_{\gamma 105}$), corresponding to photoelectric effect in all shells and subshells in the case of copper, and corresponding to photoelectric effect in K-shell of tin, are related to the actual γ-intensity by the following relation:

$$\frac{\gamma_{105}}{\gamma_{86}} = \frac{P_{\gamma 105}}{P_{\gamma 86}} \frac{\tau_{\gamma 86}}{\tau_{\gamma 105}} \frac{C_{\gamma 86}}{C_{\gamma 105}}, \tag{1}$$

where τ's refer to photoelectric cross-sections in the atomic electron shell or sub-shell under consideration. The C's represent the effect of the longitudinal distribution of photoelectrons. The photoelectric cross-sections were taken from the tables due to WHITE ([10]). The ratio $C_{\gamma 86}/C_{\gamma 125}$ was evaluated by a graphical analysis of the distribution functions given by Sauter's relativistic equation ([11]) to be 1.00 ± 0.05. Thus, γ_{105}/γ_{86} turned out to be 0.66 ± 0.04 for the copper converter and 0.71 ± 0.04 for the tin converter and a value 0.68 ± 0.05 will be adopted for further consideration.

([10]) *Beta and Gamma-Ray Spectroscopy*, ed. K. SIEGBAHN, p. 859.
([11]) C. M. DAVISSON and R. D. EVANS: *Rev. Mod. Phys.*, **24**, 79 (1952).

3·2. *Scintillation spectrometer method.* – The scintillation spectrometer consisted of a $1\frac{1}{2}$ in.$\times\frac{1}{4}$ in. NaI(Tl) crystal optically coupled to a 6810A(RCA) photomultiplier with DC200 silicone fluid. The spectrum of electro-magnetic radiations of ^{155}Eu, taken with this arrangement with an energy resolution of 12% for 279 keV γ-rays of ^{203}Tl, is shown in Fig. 4.

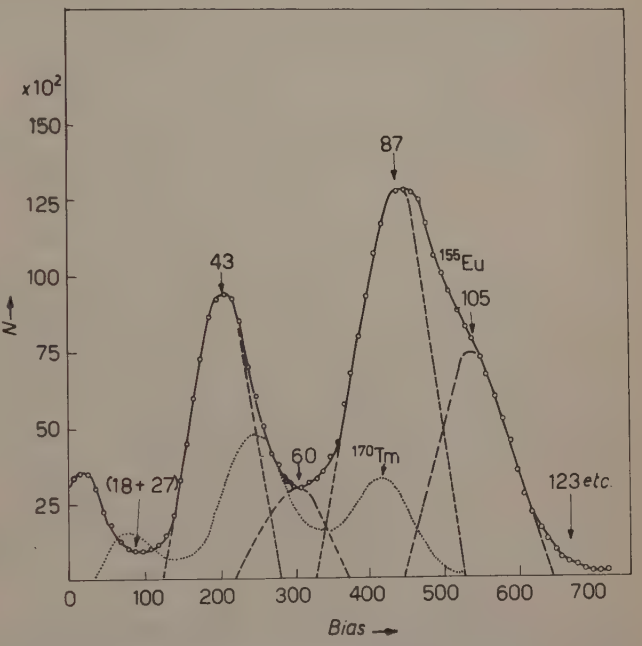

Fig. 4. – Spectrum of radiations of ^{155}Eu with scintillation spectrometer.

Since all the radiations considered were of low energy, corrections for the escape of Iodine X-rays were carefully evaluated. For this purpose, the calculations of AXEL [12] and the experimental determination of the ratio of escape peak to photopeak intensities using ^{170}Yb (51 keV) and ^{203}Tl (71 keV) X-rays and ^{170}Yb γ-rays (84 keV) with the present arrangement were used.

Corrections for absorption in the material surrounding the source and the actual crystal (such as aluminium can, neoprene and polyethylene padding and Al_2O_3 reflector) were calculated. After all these corrections, the relative intensities of X- and γ-rays were found to be as given in Table I.

TABLE I.

	Scintillation spectrometer	External conversion	Accepted value
K X-ray	97.5±3	—	97.5±3
60 keV γ-ray	5 ±0,5	—	5.0±0.6
86 keV γ-ray	100	100	100
105 keV γ-ray	58.5±6	68.5±5	63.5+7.5

[12] P. AXEL: BNL-271.

4. – Evaluation of conversion coefficients.

Table I shows the relative intensities of X- and γ-rays from external conversion and from scintillation spectrometer data, together with the values adopted for evaluation of conversion coefficients. These are in good agreement with the partial data of earlier workers ([8,13,14]).

The K X-ray intensity from the decay of ^{155}Eu is due to the K-shell internal conversion of 60 keV, 86 keV and 105 keV transitions, *i.e.*,

$$X_K = X_{K60} + X_{K86} + X_{K105} .$$

X_{K60} contribution may be extimated using the 60 keV γ-rays intensity relative to the intensity of the 86 keV γ-ray, from the relation $\gamma_{60} = X_{K60}(1/\omega_K \alpha_{60}^K)$, where ω_K, the K-shell fluorescence yield is 0.93 and α_{60}^K is obtained from the mixing ratio ([1,3,7]) $E2/M1$ of 5/95 together with theoretical conversion coefficients ([15]). Then, with the relative K-shell internal conversion electron intensities of the 86 keV and 105 keV transitions, conversion coefficients were evaluated from the following relations:

$$\alpha_{86}^K = \frac{1}{\omega_K}\left(\frac{C_{K86}}{C_{K86} + C_{K105}}\right)\left(\frac{X_{K86} + X_{K105}}{\gamma_{86}}\right), \tag{2}$$

and

$$\alpha_{105}^K = \left(\frac{C_{K105}}{C_{K86}}\right)\left(\frac{\gamma_{86}}{\gamma_{105}}\right)\alpha_{86}^K . \tag{3}$$

From these relations, the values shown in Table II were obtained. Table II also shows the theoretical values ([15]) and other available data ([8]).

TABLE II. – *Mixing ratios* $\delta^2 = M2/E1$.

		α_{86}^K	α_{105}^K
Experimental values	Present values	0.49 ± 0.075	0.29 ± 0.054
	Estimates of ref. ([8])	$\ll 0.098$ < 0.75	$\ll 1.6$
Theoretical ([15]) values	$E1$	0.365	0.20
	$M2$	25.76	10.73
	$E2$	1.626	0.95
	$M1$	2.685	1.39

([13]) F. BOEHM *et al.*: *Bull. Amer. Phys. Soc.*, **2**, 231 (1957).
([14]) A. BISI and L. ZAPPA: *Nucl. Phys.*, **6**, 252 (1958).
([15]) M. E. ROSE: *Internal Conversion Coefficients* (Amsterdam, 1958).

rom Table II, it is seen that experimental K-conversion coefficients con-ıvely indicate that both the transitions (86 keV and 105 keV) are of $E1$ ıature with possibly a small mixture of $M2$.

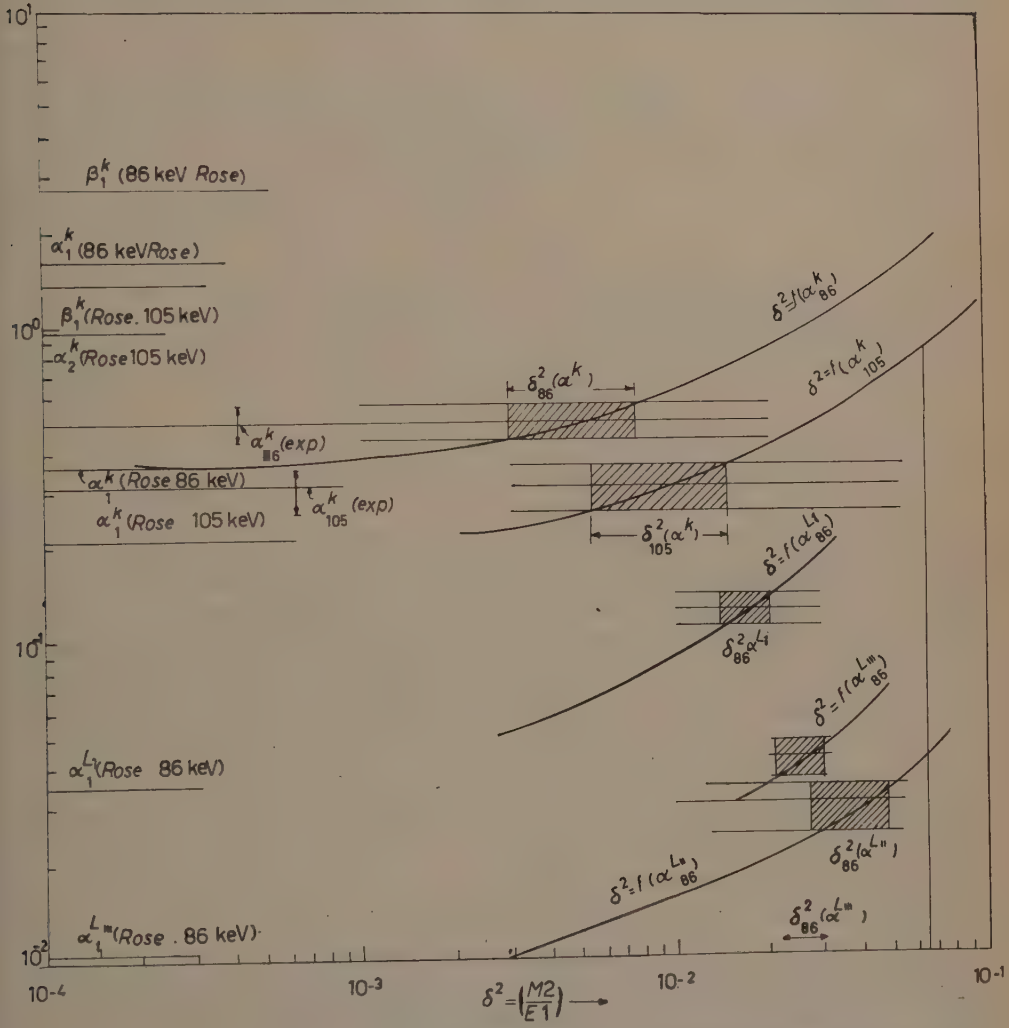

Fig. 5. – Graphical analysis of mixing ratio $\delta^2 = M2/E1$ of 86 keV and 105 keV transitions in ^{155}Gd.

The conversion ratios (7) $K/L_I/L_{II}/L_{III} = 12/3/0.7/1$ for the 86 keV transition and $(K/(L_I+L_{II})) = 5.1$ for the 105 keV transition (7) are combined with the respective α^K values determined here in an attempt to determine their multipole mixing ratios more accurately. Fig. 5 shows the various theoretical and experimental values. The function $\delta^2 = (\alpha^K - \alpha_1^K)/(\beta_2^K - \alpha^K)$, *i.e.*,

$\delta^2 = f(\alpha^K)$ indicates the variation of α^K with mixing ratio δ^2, predicted by theory. Similar functions $\delta^2 = f(\alpha^{L_I})$, $\delta^2 = f(\alpha^{L_{II}})$ and $\delta^2 = f(\alpha^{L_{III}})$ are shown for the 86 keV transition. In this figure $\delta^2 = f'(\alpha^K)$ and δ^2 for the $K/(L_I+L_{II})$ value are shown for the 105 keV transition. The expected values are shown in Table III, for all these parameters.

TABLE III. – *Mixing ratios.*

Mixing ratio	Parameter used					
	α^K	$\frac{K}{L_I+L_{II}}$	$\frac{L_I+L_{II}}{L_{III}}$	α^{L_I}	$\alpha^{L_{II}}$	$\alpha^{L_{III}}$
δ^2_{86}	$0.005^{+0.0035}_{-0.003}$	0	0	0.016	0.04	0.025
δ^2_{105}	0.010 ± 0.005	0.064	—	—	—	—

5. – Discussion and conclusions.

From these results, the 86 keV and 105 keV transitions are seen to be of predominantly $E1$ multipolarity. This is thus a proof of the existence of even parity states at 86 keV and 105 keV. Since such low lying opposite parity states do not occur in the framework of the spherical shell model, the existence of such levels point to the validity of the spheroidal shell model. On the basis of the multipolarity alone, the levels at 86 keV and 105 keV may be assigned $\frac{1}{2}+$, $\frac{3}{2}+$ or $\frac{5}{2}+$, with the respective asymptotic quantum numbers (Nn_zA) of (660), (651) or (642) on the basis of Mottelson and Nilsson's [16] calculations. The last two assignments are to be preferred on the basis of the large ft values of the β-transitions [16]. The assignments to these levels, thus, are left with a choice between the two configurations.

Similar low energy $E1$ transitions have been studied in greater detail in the actinide region. The 91 proton nuclei ^{231}Pa and ^{233}Pa have many features of their level structure and electromagnetic transitions similar to the 91 neutron ^{155}Gd. However, it may be noted that the hindered $E1$ transitions of these actinide nuclei have anomalous K, L_I and L_{II} conversion coefficients while they have a normal L_{III} conversion coefficient. This appears to be a general rule [17,18] in other $E1$ transitions that have been studied so far. On the basis

[16] B. R. MOTTELSON and S. G. NILSSON: *Mat. Fys. Skr. Dan. Vid. Selsk.*, **1**, 8 (1959).

[17] S. G. NILSSON and J. O. RASMUSSEN: *Nucl. Phys.*, **5**, 617 (1958).

[18] F. ASARO *et al.*: UCRL-8786 (1959).

of the selection rules for the asymptotic quantum numbers, both 86 keV and 105 keV transitions will be hindered. The variation in the values of δ^2 should then be expected to be due to the anomalous conversion coefficients in such transitions. On the basis of the general finding ([17,18]) referred to above, assuming $\alpha^{L_{III}}$ to be normal, δ^2_{86} should be 0.025. The range of values indicated by other parameters is from 0 to 0.04 for this (86 keV) transition. Since L_{III} values were not available for the 105 keV transition, it is only observed that δ^2_{105} ranges from about 0.01 to 0.064. It is, therefore, concluded that $\delta^2_{86} < 0.04$ and $\delta^2_{105} < 0.07$. Accurate L-subshell conversion ratio data are still needed for both these transitions.

* * *

I am much indebted to Dr. B. V. Thosar for some discussions. I am also thankful to Mr. M. C. Joshi and Mr. R. K. Gupta for some suggestions. My thanks are also due to Mr. S. D. Bhagwat, who prepared some of the converters.

Note added in proof.

Beta-group intensities, indicated in Fig. 1, had been obtained from Kurie plot analysis of the observed β-spectrum. Adopting these values, together with the relative γ-ray and conversion electron intensities, and $(K/L+M)_{105} = 3.1 \pm 0.5$, it was found that $\alpha^K_{105} = 0.30 \pm 0.1$ and $\alpha^K_{86} = 0.49 \pm 0.18$. These are in good agreement with those obtained by the method of this paper, indicating that partial β-group intensities are correct, within experimental errors.

RIASSUNTO (*)

I coefficienti di conversione delle transizioni ad 86 keV e 105 keV successive al decadimento β del ^{155}Eu sono stati determinati con uno spettrometro a raggi β ad immagine intermedia ed uno spettrometro a scintillazione ottenendo i valori $\alpha^K_{86} = 0.49 \pm 0.075$ e $\alpha^K_{105} = 0.29 \pm 0.054$. In combinazione con i rapporti dei sotto-strati L, il rapporto di mescolanza, $\delta^2 = M2/E1$, viene determinato in $\delta^2_{86} < 0.04$ e $\delta^2_{105} < 0.07$. Si discutono queste multipolarità sulla base del modello a strati sferoidali.

(*) *Traduzione a cura della Redazione.*

Cosmic Ray and Geomagnetic Disturbances from July 1957 to July 1958.

PART I. - The Cosmic Ray Events and their Correlation with the Geomagnetic Events.

F. BACHELET, P. BALATA, A. M. CONFORTO and G. MARINI

Istituto di Fisica dell'Università - Roma
Istituto Nazionale di Fisica Nucleare - Sezione di Roma
Commissione Italiana Anno Geofisico Internazionale - Roma

(ricevuto il 28 Dicembre 1959)

Summary. — Cosmic Ray Storms (CRS), *i.e.* world-wide decreases of the C.R. intensity as measured by standard neutron monitors in Rome and in other parts of the world, were systematically investigated during the period July 1957 - July 1958, in correspondence with Magnetic Storms (MS). The correlations CRS → MS and MS → CRS were examined. The characteristic features of both classes of events were considered in order to find out which of them were preferential for the association itself. Some aspects of the correlation were approached by statistical method.

---

1. – Introduction.

Since FORBUSH [1] showed the world-wide character of the transient decreases of the cosmic ray intensity which in many cases take place during magnetic storms, many Authors have studied these C.R. events in themselves or in connection with geomagnetic disturbances.

Views on these phenomena have gradually evolved. At first [2-6] a common mechanism for the explanation of the two classes of events was sought in the

---

(1) S. E. FORBUSH: *Phys. Rev.*, **51**, 1108 (1937).
(2) S. CHAPMAN: *Nature*, **140**, 423 (1937).
(3) V. F. HESS, A. DEMMELMAIR and R. STEINMAURER: *Terr. Mag.*, **43**, 7 (1938).
(4) S. E. FORBUSH: *Terr. Mag.*, **43**, 203 (1938).
(5) G. O. ALTMAN, H. N. WALKER and V. F. HESS: *Phys. Rev.*, **58**, 1011 (1940).
(6) I. LANGE and S. E. FORBUSH: *Terr. Mag.*, **47**, 185 (1942).

effects of the ring current of CHAPMAN and FERRARO. Later ([7-11]), however, the conviction gained ground that the events of the two classes might indeed be triggered, sometimes simultaneously, by a common cause, *i.e.* the arrival of a beam of ionized particles emitted from active regions of the Sun, but by means of two independent mechanisms, related to the particular characteristics of each exciting beam.

Experimental material for the understanding of the mechanism can be provided not only by the study of the most spectacular or peculiar events ([12-15]), but, perhaps even more, by the systematic analysis of the association between C.R. and geomagnetic events. Several studies have been carried out so far on this line ([16-22]), employing different selection methods; the latter however, were generally not specified with sufficient accuracy, especially in the case of geomagnetic events, and most of the C.R. data concerned only the mesonic component. The numerical results obtained by different Authors, therefore, cannot be easily compared; yet, as a whole, available data suggest an association, but not a 1 to 1 correspondence.

The present paper deals with the C.R. and geomagnetic disturbances which occured in the period July 1957 to July 1958. This period seemed to offer particularly favourable conditions for a systematic analysis, which included an examination of all magnetic storms and C.R. events of a world-wide character and a classification meant to evidentiate characteristics connected with the association. In fact, in this period:

1) the high rate of occurrence of the events under study provided in a few months a sufficiently wide and complete sample of the various types of both classes of events;

([7]) For a complete review up to 1952 see: H. ELLIOT: *Progress in Cosmic Ray Physics*, vol. **1** (Amsterdam, 1952), chap. VIII, pp. 492-497 and references therein.

([8]) J. A. SIMPSON: *Phys. Rev.*, **94**, 426 (1954).

([9]) P. MORRISON: *Phys. Rev.*, **101**, 1397 (1956).

([10]) E. N. PARKER: *Phys. Rev.*, **103**, 1518 (1956).

([11]) L. I. DORMAN: *Cosmic Ray Variations* (Moscow, 1957).

([12]) K. J. MCCRACKEN and N. R. PARSONS: *Phys. Rev.*, **112**, 1798 (1958).

([13]) J. R. WINCKLER, L. PETERSON, R. HOFFMAN and R. ARNOLDY: *Journ. Geophys. Res.*, **64**, 597 (1959).

([14]) S. YOSHIDA and M. WADA: *Nature*, **183**, 381 (1959).

([15]) V. SARABHAI and R. PALMEIRA: *Nature*, **184**, 1204 (1959).

([16]) Y. SEKIDO, S. YOSHIDA and Y. KAMIYA: *Rep. Ion. Res. Japan*, **6**, 195 (1952).

([17]) E. S. GLOKOVA: *Trudy NIIZM*, **8**, 59 (1952).

([18]) B. TRUMPY: *Physica*, **19**, 645 (1953).

([19]) S. E. FORBUSH: *Journ. Geophys. Res.*, **59**, 525 (1954).

([20]) Y. SEKIDO, M. WADA, I. KONDOH and K. KAWABATA: *Rep. Ion. Res. Japan*, **9**, 174 (1955).

([21]) G. RAMASWAMI and S. D. CHATTERJEE: *Can. Journ. Phys.*, **36**, 635 (1958).

([22]) J. A. LOCKWOOD: *Phys. Rev.*, **112**, 1750 (1958).

2) it was possible to study the intensity of the nucleonic component, which notoriously presents greater variations and can be corrected more accurately for atmospheric effects;

3) C.R. and geomagnetic data have been collected simultaneously in a large number of world-wide stations according to the I.G.Y. program.

In consideration of what outlined above, particular emphasis is given not only to the careful choice of the criteria of selection and classification of the events, but also to their detailed description; these criteria, in fact, constitute the inevitable limit to the value of the results obtained.

The analysis of the C.R. data, including a morphological description of each event is reported in Section **2**. The classification of magnetic storms, outlined in Section **3** of this paper is diffusely described in Part II ([23]). In Section **4** the association between the two classes of events is analysed on the basis of the above classifications, and some of its aspects are examined by statistical methods.

2. – Classification of cosmic ray storms (CRS).

The phenomenological analysis of C.R. data for the selection of world-wide events, from July 1957 to July 1958, was based on a comparative inspection of the pressure corrected bihourly intensities as obtained by our neutron monitor in:

Rome, Italy (s.l.; 41.9° N, 12.5° E geogr.; 42° N geom. conv.),

and as provided by the following neutron monitor stations, distributed on three well spaced longitudinal bands:

Weissenau, Germany (s.l.; 47.8° N, 9.5° E, geogr.; 49° N geom. conv.)
Chicago, U.S.A. (s.l.; 41.9° N, 87.6° W, geogr.; 53° N geom. conv.)
Climax, U.S.A. (3411 m; 39.4° N, 106.2° W, geogr.; 49° N geom. conv.)
Huancayo, Peru (3350 m; 12.0° S, 75.3° W, geogr.; 1° S geom. conv.)
Mt. Norikura, Japan (2840 m; 36.1° N, 137.5° E, geogr.; 26° N geom. conv.)

The detailed features of individual events (*i.e.* onset time, amplitude, etc.) were checked in most cases by means of the 15 minute intensities of data obtained in Rome.

It was found that the world-wide events which occurred during that period of time, at sea level as well as at mountain altitudes, were generally decreases

([23]) F. BACHELET, P. BALATA, A. M. CONFORTO and G. MARINI: *Nuovo Cimento*, **16**, 320 (1960).

of intensity of the type of the so-called « Forbush-Decreases ». Only variations of this kind will be dealt with in this paper and will be indicated as Cosmic Ray Storms (CRS).

It is pointed out, however, that also other minor or more unusual phenomena were recorded; they often seemed to interfere with « true » CRS. Some of them were universal time (UT) perturbations. They have been tentatively classified as follows:

a) gradual diminutions of C.R. intensity which seem to occur during the days immediately preceding some of the CRS;

b) gradual increases of C.R. intensity, which seem to occur at the end of some of the CRS and to enhance the recovery phase; they are generally characterized by a sudden sequence of abnormal Diurnal Effects (DE);

c) other perturbations in the shape of small « bays », which last some days and appear more or less clearly at different stations;

d) UT peaks which sometimes occur within the drop of a CRS; their amplitude often depends upon the latitude.

Other perturbations appear as local time variations; they generally consist of enhanced diurnal effects, of strongly varying phase, and usually occur when the geomagnetic field is disturbed.

All these effects cannot be disregarded as they sometimes interfere with CRS to such a degree that they deform or conceal their characteristics, in a different way at different longitudes or latitudes. In this connection, it should be pointed out that any classification based on daily instead of on bihourly intensities might be misleading; in such cases, in fact, the significance of the selected events is doubtful and it might become hard even to define the main parameters.

The classification of all individual C.R. events was based on a balance of various elements deduced from the bihourly data of the different stations. In the case of CRS, the classification was based essentially on the features of the decreasing phase, *i.e.* the start and the slope. The amplitude of the event was taken into consideration only implicitly.

During the selected period of time, a total of 24 (*) « true » CRS and about two scores of perturbations of other kinds were recorded. The CRS were divided into 4 groups; no sharp discontinuity, however, could be established between one group and the next. The first 3 groups include the most clear-cut

(*) This figure includes the event of June 30, 1957, which actually occurred before the beginning of the selected period.

events, from the sharpest and steepest of type I to the more gradual ones of type III. Type X comprises less well defined CRS, *i.e.* events selected as such only because they undoubtedly consist of an abrupt drop of intensity on a world-wide scale; however, at different longitudes and latitudes they are variously deformed or even concealed by local-time variations or by other peculiar UT perturbations (DE or UT-peaks). Event X of Sept. 2 — see Fig. 1 — and, even more so, event X of Sept. 13 are typical in this respect.

Table I provides a list of the 24 CRS, ordered by type and, within each type, by date, with the addition of one « Strange Event », which escapes classification and appears like a huge trough occurring at all stations on a local-time scale.

The main parameters of the events, *i.e.* onset time, amplitude and duration are reported in the same Table, together with some notes concerning more specific features of individual CRS.

The world-wide onset time was assumed to be the center of an interval defined by inspection of the starting times recorded at the different stations; at best, it could be defined within two hours, *i.e.* within the resolving time of currently available data. However, for the sharpest events it was possible in Rome to define the starting times with uncertainties in the range of 15 minutes (values given in parenthesis in the Table).

Also the duration of a CRS was defined on inspection of data from all the stations. It was assumed to be represented by the total time interval after which the intensity either *a*) roughly recovered to the pre-storm level, *b*) partly recovered and settled on a new level slightly lower than the pre-existing one.

The amplitude was computed only for the events recorded in Rome and was defined as the difference between the intensities, averaged over convenient periods of time, immediately before and at the bottom of the drop. Averages were calculated for periods of 3 to 15 hours for type I, and of 24 hours or more for types II and III, aiming, for each determination, at a compromise between statistical requirements and the necessity of adequately measuring the event, without « flattening it out ». Amplitudes of type X events could be evaluated only with gross approximation.

Typical examples of the various categories of events are shown in Figs. 1 to 6 at 2 hour intervals for the stations listed in page 294 (*). Fig. 7 reproduces the decreasing phase, at 30 minute intervals, of the 4 most typical cases of type I events and, for the sake of comparison, of one event of type II, as recorded in Rome.

(*) The plot of the intensity of Huancayo has been omitted from Fig. 1 because many data were missing, while in Fig. 3 the graph recorded at Mt. Washington, 71° W, reproduced from J. A. Lockwood, reference ([22]), was added as a further evidence of the longitude dependence of some aspects of that event.

TABLE I. – *Cosmic Ray Storms.*

Date	Onset time (UT) (*)	Max Amplit. of Drop (**) in Rome (%)	Total Durat. (days)	General remarks
		CRS TYPE I		
30 June 57	06 ±2	(Missing data)	9.0	Fair, in spite of scarcity of data and small size.
29 Aug. 57	19 ±1 (19.15 ±0.30)	7.4±0.3	19.0	*Exceptionally marked* and steep. Hint of pre-storm UT peak. Two CRS of type X during recovery (Sept. 2 and 13). Two minor perturbations are included: slow decrease before event (Aug. 25-29) and enhanced rise (DE) at end of recovery (Sept. 16-21). *Figs. 1 and 7a.*
21 Sept. 57	16 ±4 (18.00 ±0.15)	6.5±0.4	7.0	Conspicuous, but not very clear, because of numerous large DE preceding the event. *Huge UT peak* at ~15 UT, Sept. 22, preceding bottom of drop.
21 Oct. 57	23 ±1 (22.30 ±0.30)	9.3±0.3	17.0	*Exceptionally marked* and steep. Second smaller fall at ~16 *UT*, Oct. 22. Longitude-dependent aspect of decreasing phase. End of rise enhanced by DE (Nov. 6-8). *Fig. 7b.*
26 Nov. 57	03 ±2 (02.00 ±0.30)	6.5±0.5	5.0	Fair. Hint of a latitude-dependent UT peak, preceding bottom of drop. Two minor perturbations are included: slow decrease before the event (Nov. 23-25) and enhanced rise (DE) at the end of recovery (Nov. 30 - Dec. 5).
19 Dec. 57	16 ±2 (18.00 ±1.00)	2.9±0.4	8.5	Fair, though not large. Notice the « Strange Event » immediately preceding storm (Dec. 17-18). End of recovery rise enhanced by sequence of large DE, most of which with reversed phase(Dec. 23-24). *Fig. 2.*

(*) The uncertainty of the world-wide onset time is determined by the sum of the uncertainties of the onset time at each station, and therefore it has somehow the character of a maximum error.
(**) The uncertainty of the amplitude in Rome is measured by the standard error.

TABLE I (*continued*).

Date	Onset time (UT) (*)	Max Amplit. of Drop (**) in Rome (%)	Total Durat. (days)	General remarks
11 Feb. 58	02 ± 1 (01.45 ± 0.15)	4.4 ± 0.5	6.0	*Conspicuous and exceptionally steep.* Superposition, at some stations, of a large DE and of a latitude-dependent *UT peak* at bottom of drop. Minor perturbations before (Feb. 6-10) and upon end of event (Feb. 16-19). *Figs. 3 and 7c.*
25 March 58	17 ± 1 (17.00 ± 1.00)	6.6 ± 0.4	15.5	*Exceptionally marked* and « clean ». Hint of pre-storm peak. Long recovery rise; fairly steady in spite of superposition of large DE with varying phase. *Figs. 4a and 7d.*
9 May 58	03 ± 2 Hu 07 ± 2 Cl, Ch, Mt. No 09 ± 2 W, Ro (09.30 ± 0.30)	4.4 ± 0.5	2.0	Fair. Longitude-dependence of whole decreasing phase, possibly because of superposition of large DE. Notice short recovery. *Fig. 4b.*
21 July 58	17 ± 2 (19.15 ± 0.15)	3.1 ± 0.7	2.0	Poorly defined, small-size event. Notice short recovery.
	CRS TYPE II			
3 Aug. 57	19 ± 5	5.0 ± 0.2	11.0	Characteristic « Type II » CRS. Large DE of varying phase during whole event; at some stations they conceal onset time. *Fig. 5.*
29 Sept. 57	00 ± 4	3.4 ± 0.2	11.5	Average. Large DE during whole event.
14 March 58	13 ± 5	2.9 ± 0.2	4.5	Average. Large DE during recovery enhance rise. Rather short recovery. *Fig. 7e.*
29 May 58	01 ± 5	3.6 ± 0.2	7.0	Average. Large DE of varying phase.
8 July 58	07 ± 5	4.2 ± 0.2	4.0	Average. Particularly quick recovery. *Fig. 6a.*

TABLE I (*continued*).

Date	Onset time (UT) (*)	Max Amplit. of Drop (**) in Rome (%)	Total Durat. (days)	General remarks
		CRS TYPE III		
19 July 57	10 ± 8	2.0±0.2	8.5	Average. No special features. Minor perturbation at end of recovery. *Fig.* 6*b*.
16 Jan. 58	06 ±12	3.2±0.2	12.0	Rather poor. Minor perturbations at lower level (Jan. 20-21) and upon end of recovery (Jan. 27-29).
		CRS TYPE X		
2 July 57	07 ± 3	(Missing data)	2.5	Very confused because of scarcity of data.
2 Spet. 57	05 ± 3	3	5.0	Superposition of a large DE and of a UT peak, during drop, conceals features of event. Notice the different time association of the two phenomena at different longitudes. *See Fig.* 1.
13 Sept. 57	03 ± 6	1	3.5	Large latitude-dependent *UT peak* during drop; at lower latitude stations it almost conceals all changes of level.
25 Apr. 58	14 ± 6	1	10.5	At some stations local effects almost conceal event.
7 June 58	06 ±12	1.5	9.0	Same as previous event but more perturbed especially at lower latitude stations.
28 June 58	12 ± 5	2	9.5 (?)	Same as previous event but with even larger perturbations during whole event.
26 July 58	16 ±12	1.5	3.5	Local perturbation all over.
17-18 Dec. 57		3.5		« Strange event ». *See Fig.* 2.

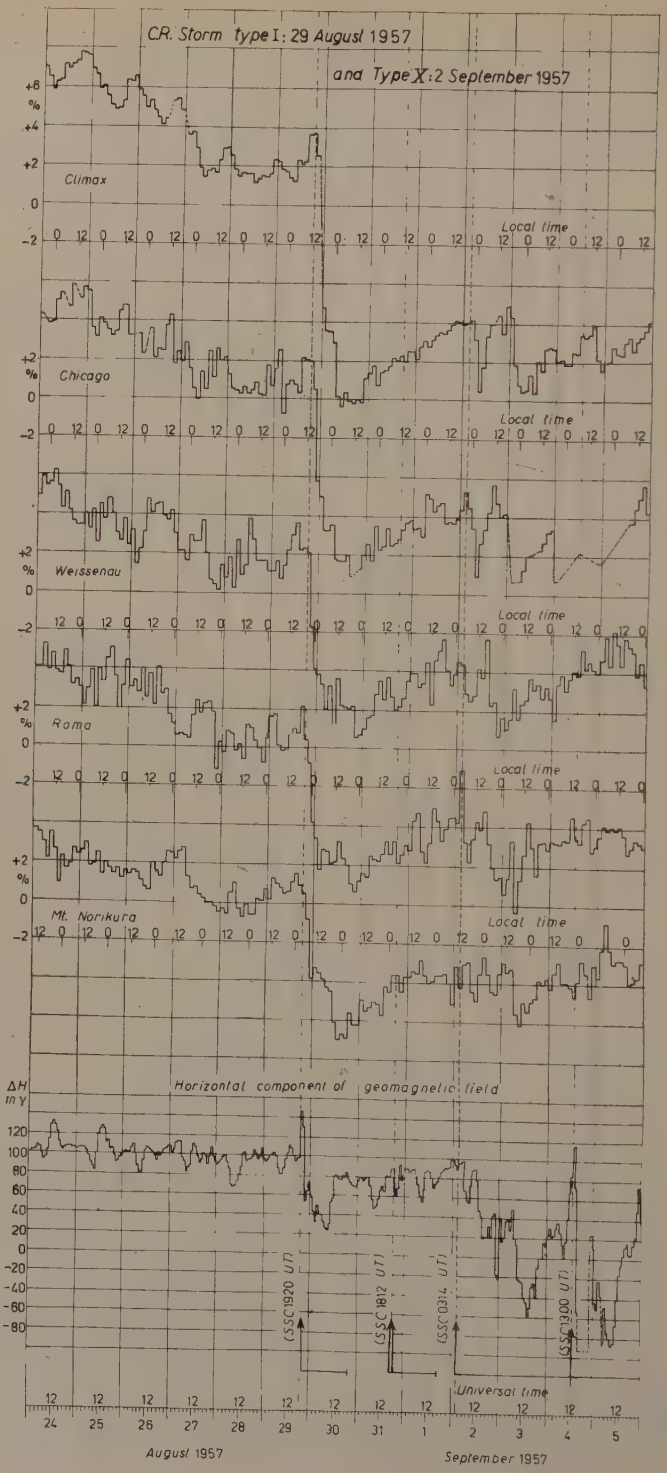
CR. Storm type I: 29 August 1957
and Type X: 2 September 1957
Climax
Chicago
Weissenau
Roma
Mt. Norikura
Local time
Horizontal component of geomagnetic field
ΔH in γ
(SSC 1920 UT)
(SSC 1812 UT)
(SSC 0314 UT)
(SSC 1900 UT)
Universal time
August 1957
September 1957

Fig. 1.

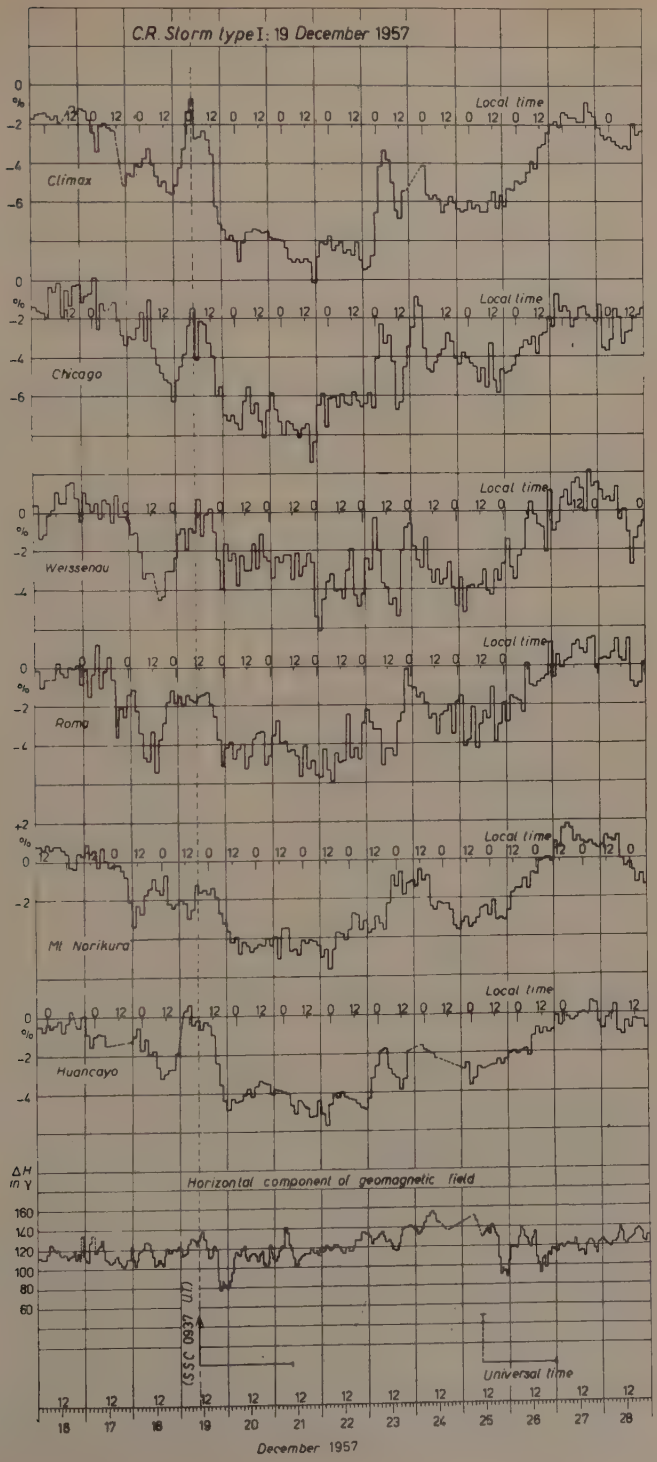
C.R. Storm type I: 19 December 1957
Local time
Climax
Chicago
Weissenau
Roma
Mt. Norikura
Huancayo
Horizontal component of geomagnetic field
ΔH in γ
(SSC 0837 U.T.)
Universal time
December 1957

Fig. 2.

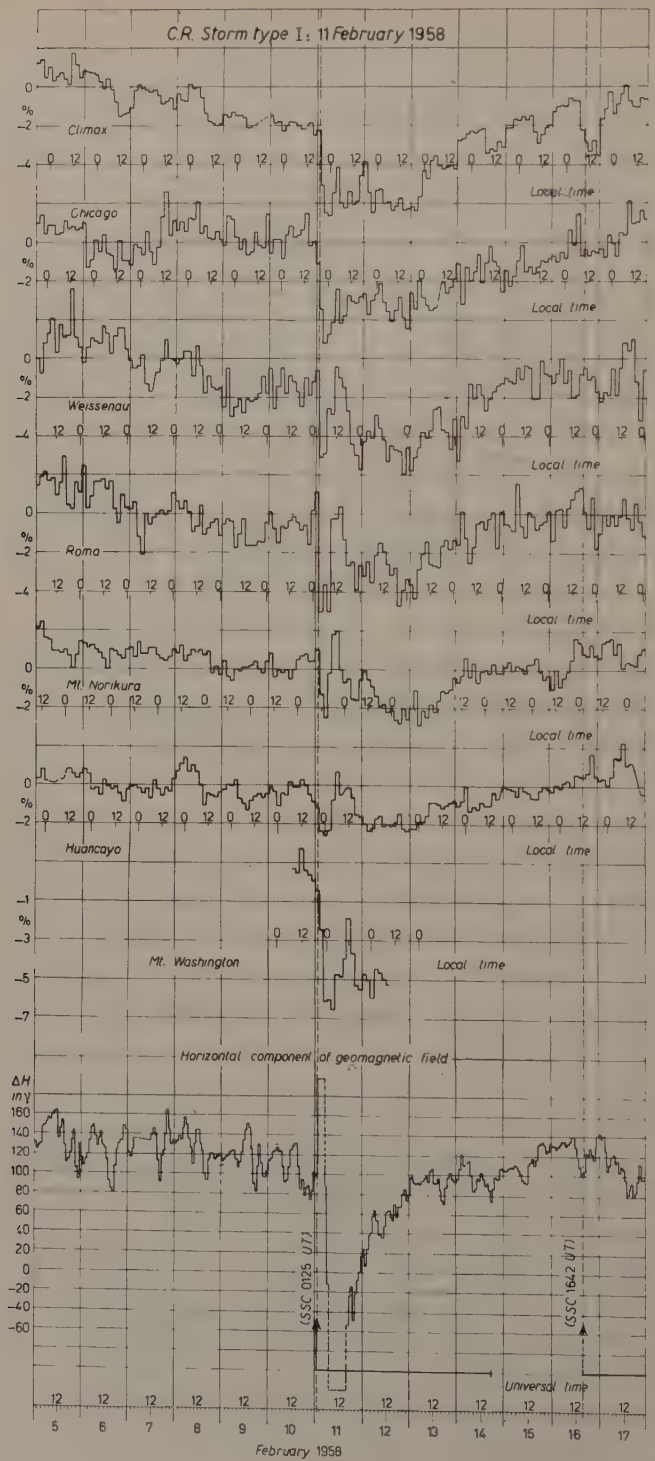
C.R. Storm type I: 11 February 1958
Climax
Chicago
Weissenau
Roma
Mt. Norikura
Huancayo
Mt. Washington
Local time
Horizontal component of geomagnetic field
ΔH in γ
(SSC 0125 U.T.)
(SSC 1642 U.T.)
Universal time
February 1958

Fig. 3.

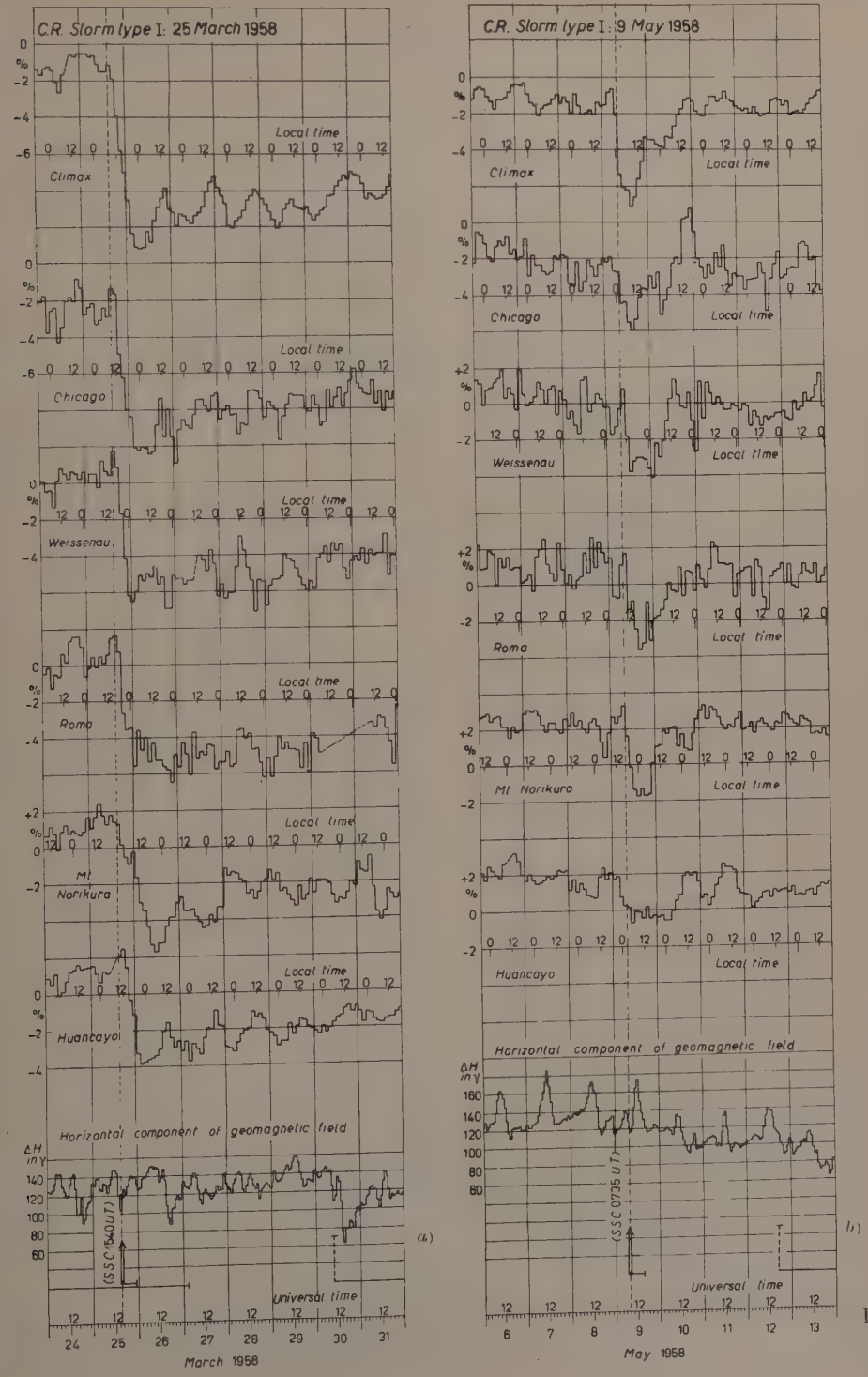
C.R. Storm type I: 25 March 1958
Local time
Climax
Chicago
Weissenau
Roma
Mt Norikura
Huancayo
Horizontal component of geomagnetic field
ΔH in γ
(SSC 1540 UT)
Universal time
March 1958
a)
C.R. Storm type I: 9 May 1958
Climax
Chicago
Weissenau
Roma
Mt Norikura
Huancayo
Horizontal component of geomagnetic field
(SSC 0735 UT)
May 1958
b)

Fig. 4.

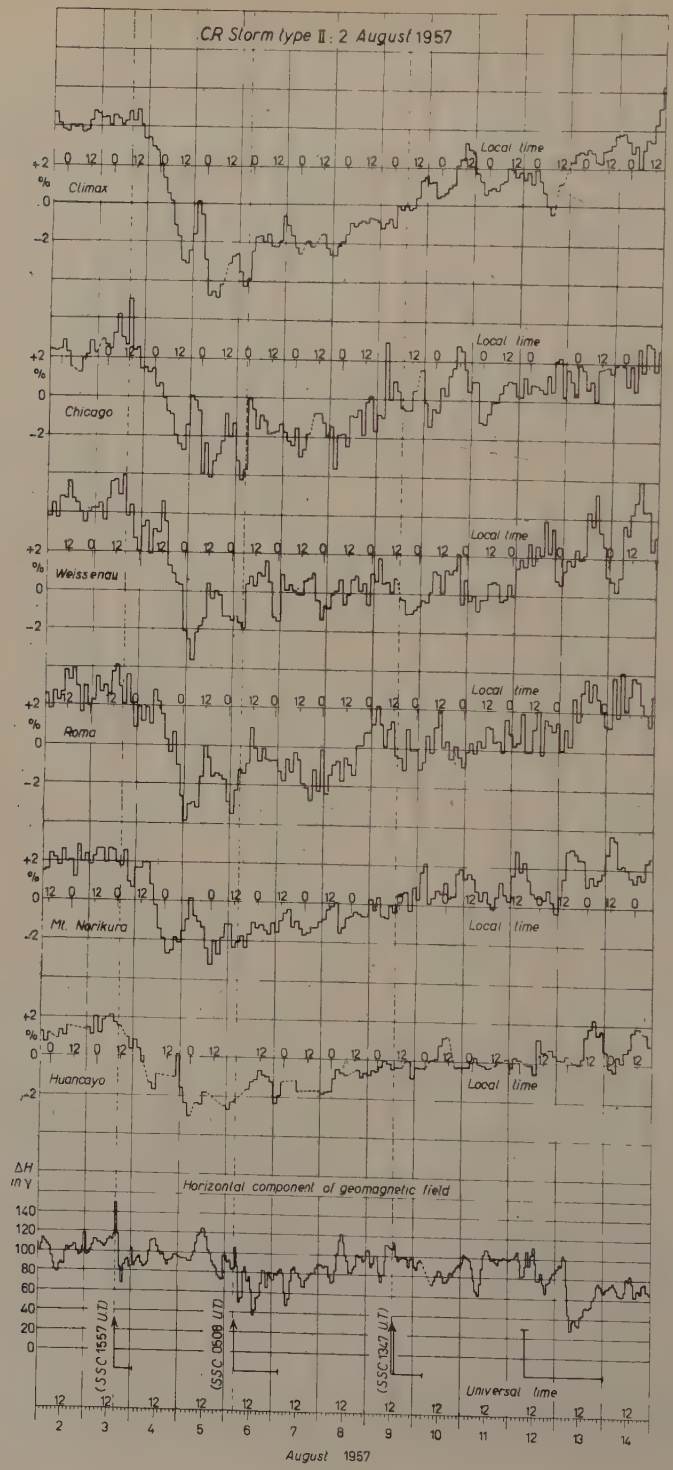
CR Storm type II: 2 August 1957
Local time
Climax
Chicago
Weissenau
Roma
Mt. Norikura
Huancayo
+2
%
0
-2
ΔH in γ
Horizontal component of geomagnetic field
140
120
100
80
60
40
20
0
(SSC 1557 UT)
(SSC 0508 UT)
(SSC 1327 UT)
Universal time
2 3 4 5 6 7 8 9 10 11 12 13 14
August 1957

Fig. 5.

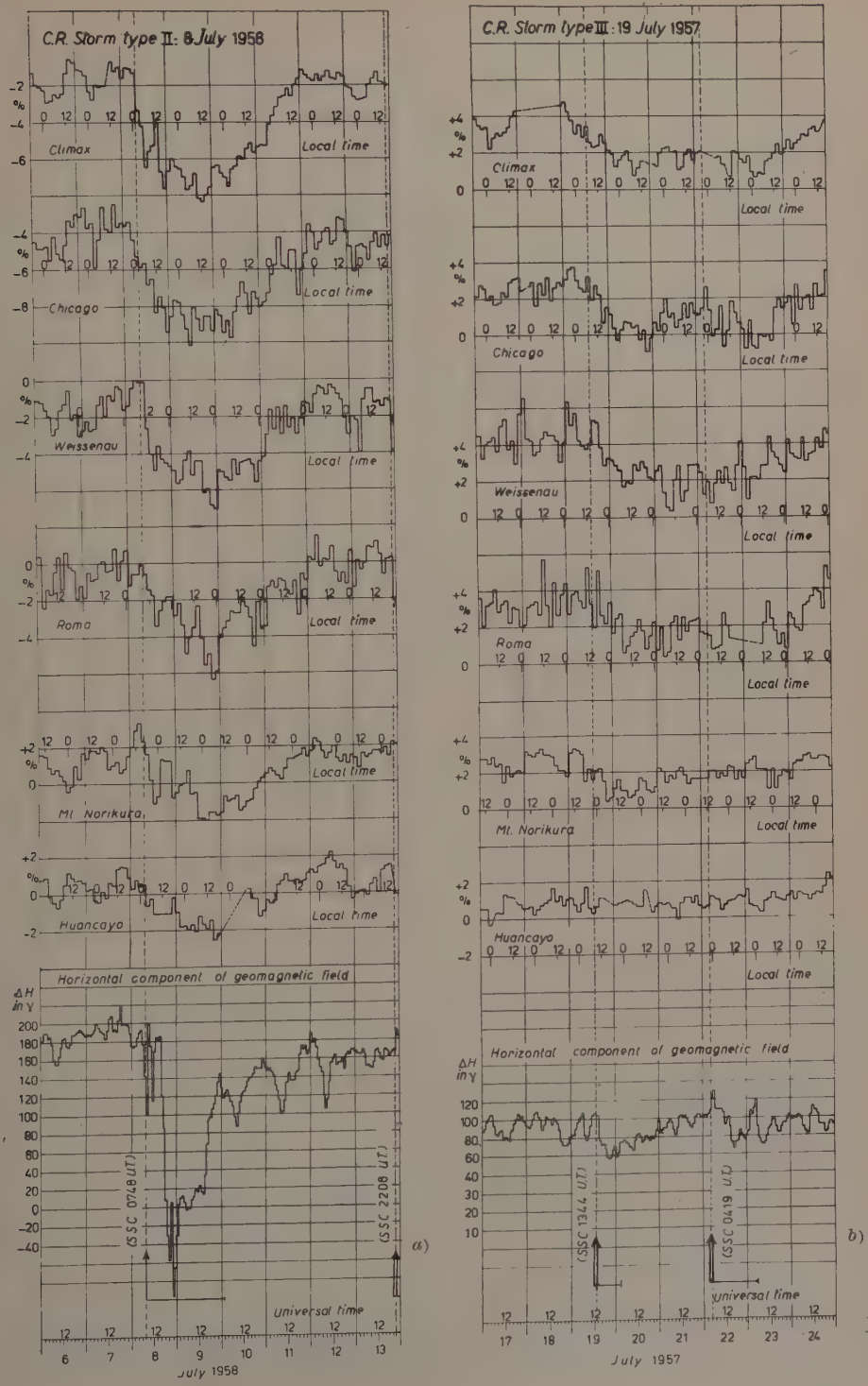
C.R. Storm type II: 8 July 1958
Climax
Local time
Chicago
Weissenau
Roma
Mt. Norikura
Huancayo
Horizontal component of geomagnetic field
ΔH in γ
(SSC 0748 U.T.)
(SSC 2208 U.T.)
Universal time
July 1958
a)
C.R. Storm type III: 19 July 1957
(SSC 1344 U.T.)
(SSC 0419 U.T.)
July 1957
b)

Fig. 6.

1339

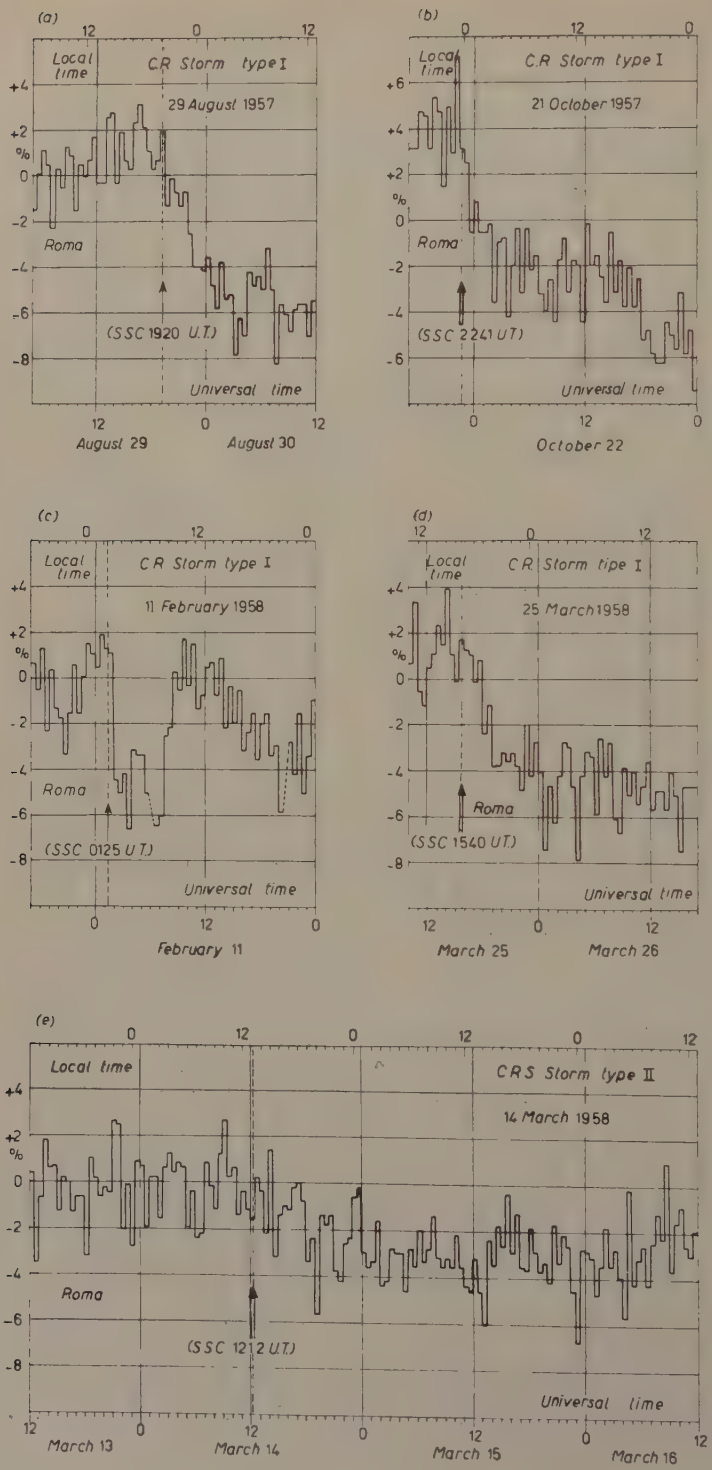
(a)
Local time
C.R Storm type I
29 August 1957
Roma
(SSC 1920 U.T.)
Universal time
August 29
August 30
(b)
Local time
C.R Storm type I
21 October 1957
Roma
(SSC 2241 UT)
Universal time
October 22
(c)
Local time
C.R Storm type I
11 February 1958
Roma
(SSC 0125 U.T.)
Universal time
February 11
(d)
Local time
C.R Storm tipe I
25 March 1958
Roma
(SSC 1540 UT.)
Universal time
March 25
March 26
(e)
Local time
C.R.S Storm type II
14 March 1958
Roma
(SSC 1212 U.T.)
Universal time
March 13
March 14
March 15
March 16

Fig. 7.

3. – Classification of magnetic storms (MS).

The July 1957–July 1958 period was analyzed from the geomagnetic standpoint both directly, by continuous recordings of the magnetic field carried out in four Italian Stations, and indirectly on the basis of the Reports of many other Stations located in different parts of the world and of the « International Data on Magnetic Disturbance » published in the *Journal of Geophysical Research*.

Part II of the present work is explicitly dedicated to the phenomenological study of the magnetic field and to the identification and classification of geomagnetic events. In order to study the correlation with cosmic ray events, it was thought profitable to classify all magnetic storms (MS) into five main types $\bar{A}$, $\bar{B}$, $\bar{C}$, A and C.

Only the main characteristics of each type will be outlined here:

type $\bar{A}$: it comprises classical MS in which the horizontal component H of the geomagnetic field presents a *sudden commencement* (SC), an *initial phase*, a *main phase* and a slow final recovery;

type $\bar{B}$: the *SC* is followed almost exclusively by an *initial phase* (the main phase is completely absent);

type $\bar{C}$: the storm presents a SC followed by great, irregular variations and lasts much longer than the previous types of MS;

types A and C differ respectively from the above types $\bar{A}$ and $\bar{C}$ only for the *absence of a SC*.

It should be pointed out that the recurrent storms, typical of the minimum solar activity, could suitably be included in types $\bar{C}$ and C.

The significance, objective value and limits of such a classification and the criteria employed to ascertain the world-wide extension of the events are discussed in Part II, which contains also the complete list of the 72 storms recorded during the investigated period; 26 MS were of type $\bar{A}$, 20 of type $\bar{B}$ 6 of type $\bar{C}$, 9 of type A and 11 of type C; moreover, about a score of « minor disturbances » were observed in that period.

The continuous recordings of the component H of the magnetic field registered in Italian Geomagnetic Observatories during some typical MS are also reported in Part II.

In the present paper, the diagrams of the hourly mean values of H for each of the CRS shown in Figs. 1 to 6 are given together with the bihourly means of the C.R. intensity.

In this connection it should be pointed out that while some types of storms (*e.g.* types $\bar{A}$ and A) can be clearly recognized also in the mean hourly tracings, storms of type $\bar{B}$ are so shaped that the operation of averaging generally deforms them beyond recognition and they are hardly apparent in hourly tracings of the magnetic field.

In the figures the MS are marked with the following symbols:

Type $\bar{A}$ ↑ Type $\bar{B}$ ⇑ Type $\bar{C}$ ⇡

Type A ⊤ Type C ⎺

The horizontal tract following each of these symbols in the figures represents the duration of the MS.

It should be added that the tracings of H have generally been obtained from Gibilmanna's magnetograms, excepting that of the MS of July 8, 1958 (Fig. 6-*a*) which was obtained from the magnetograms of L'Aquila.

4. – Correlation between C. R. and geomagnetic events.

4·1. – The study of the correlation between CRS and MS was first approached rom the phenomenological point of view considering the time association beween pairs of single events (Sections 4·2 and 4·3); the time association was xamined from two points of view:

1) CRS → MS: all CRS were considered in order to establish in which cases there was and in which there was not a coincidence with a MS;

2) MS → CRS: all magnetic storms were considered in order to establish in which cases there was and in which there was not a coincidence with a CRS.

Some aspects of such a correspondence were evidentiated also by a statistical approach (Section 4·4).

Eventually attempts were made to ascertain the existence of a linear correlation between the magnitudes of time associated pairs of events (Section 4·5).

4·2. *CRS → MS.* – In order to provide a direct view of the association between CRS and MS in the examined period, a list of all CRS previously specified in Section 2 is reported in chronological order in Table II, together with individual MS which were assumed to be associated with them. (The complete list of MS is given in Table I of Part II).

TABLE II.

Base No.	C.R. Storms			Associated Magnetic Storms						Δt (h)
	Date	Onset time UT (h)	Type	Onset time UT (h m)	Type	SC (γ)	Range (γ)	$a_{p\,max}$ (2γ)	Durat. (days)	
1	30 June 57	06 ± 2	I	05 28	$\bar{A}$	22.5 (G)	222.0 (G)	236	1.7	+ 0.5 ± 2
2	2 July	07 ± 3	X	08 57	$\bar{A}$	22.0 (G)	112.0 (G)	207	1.3	− 1.9 ± 3
3	19 July	10 ± 8	III	13 44	$\bar{B}$	8.8 (G)	72.0 (G)	39	0.5	− 3.7 ± 8
4	3 Aug.	19 ± 5	II	15 57	$\bar{A}$	43.3 (G)	101.0 (G)	94	0.4	+ 3.0 ± 5
5	29 Aug.	19 ± 1	I	19 20	$\bar{A}$	45.5 (G)	179.0 (G)	111	0.9	− 0.3 ± 1
6	2 Sept.	05 ± 3	X	03 14	$\bar{A}$	11.5 (G)	188.0 (G)	300	2.4	+ 1.8 ± 3
7	13 Sept.	03 ± 6	X	00 46	$\bar{A}$	69.9 (G)	465.0 (SV)	300	1.7	+ 2.2 ± 6
8	21 Sept.	16 ± 4	I	10 05	$\bar{A}$	55.1 (G)	240.0 (G)	154	1.2	+ 5.9 ± 4
9	29 Sept.	00 ± 4	II	00 16	$\bar{A}$	20.0 (G)	300.0 (SV)	300	2.6	− 0.3 ± 4
10	21 Oct.	23 ± 1	I	22 41	$\bar{B}$	71.7 (G)	104.0 (G)	111	0.5	+ 0.3 ± 1
11	26 Nov.	03 ± 2	I	01 55	$\bar{A}$	18.0 (G)	159.0 (G)	111	3.0	+ 1.1 ± 2
12	19 Dec.	16 ± 2	I	09 37	$\bar{A}$	16.5 (G)	77.0 (G)	39	2.0	+ 6.4 ± 2
13	16 Jan. 58	06 ± 12	III	—	—	—	—	—	—	—
14	11 Feb.	02 ± 1	I	01 25	$\bar{A}$	80.0 (G)	650.0 (SV)	400	3.7	+ 0.6 ± 1
15	14 March	13 ± 5	II	12 12	$\bar{B}$	38.0 (G)	112.0 (G)	67	1.3	+ 0.8 ± 5
16	25 March	17 ± 1	I	15 40	$\bar{B}$	38.0 (G)	52.0 (G)	80	0.3	+ 1.3 ± 1
17	25 Apr.	14 ± 6	X	—	—	—	—	—	—	—
18	9 May	03 ± 2 Hu 07 ± 2 Cl, Ch, Mt. No 09 ± 2 Ro, W	I	~07 35	$\bar{B}$	− 21.0 (G)	69.0 (G)	22	0.2	− 4.6 ± 2 Hu − 0.6 ± 2 Cl, Ch, Mt. No + 1.4 ± 2 Ro, W
19	29 May	01 ± 5	II	00 00	A	–	180.0 (A)	94	1.2	+ 1.0 ± 5
20	7 June	06 ± 12	X	00 46	$\bar{A}$	27.5 (G)	171.0 (G)	179	1.0	+ 5.2 ± 12
21	28 June	12 ± 5	X	07 13	$\bar{B}$	12.5 (G)	30.0 (G)	27	0.4	+ 4.8 ± 5
22	8 July	07 ± 5	II	07 48	$\bar{A}$	30.8 (G)	370.0 (A)	400	1.7	− 0.8 ± 5
23	21 July	17 ± 2	I	16 37	$\bar{B}$	93.1 (A)	128.0 (A)	154	0.8	+ 0.4 ± 2
24	26 July	16 ± 12	X	—	—	—	—	—	—	—

(G): Gibilmanna - (SV): S. Vittorino - (A): L'Aquila.

Table II gives the date, world-wide onset time and type of each CRS and MS; some fundamental parameters of the MS, *i.e.* the amplitude of the SC, the range and the highest values reached during the storm by the three-hourly planetary index a_p. Also the intervals Δt between onset times are reported for each pair of events; these time intervals are expressed as the delays of C.R. events with respect to geomagnetic events with an uncertainty equal to that of the determination of the starting time of the respective CRS.

It is necessary to point out that for each C.R. event, the « associated » geomagnetic storm was assumed to be the event which started *a*) at the closest time distance from the onset of the CRS, and *b*) when the time distance was of a few hours or, at most, of the same order of the uncertainty with which the onset time of the corresponding CRS could be determined.

Fig. 8 reproduces the distribution of Δt (with their errors) for the MS which, occurring within an interval of $\pm$ 36 hours from the onset of 24 CRS, might be possibly associated with it.

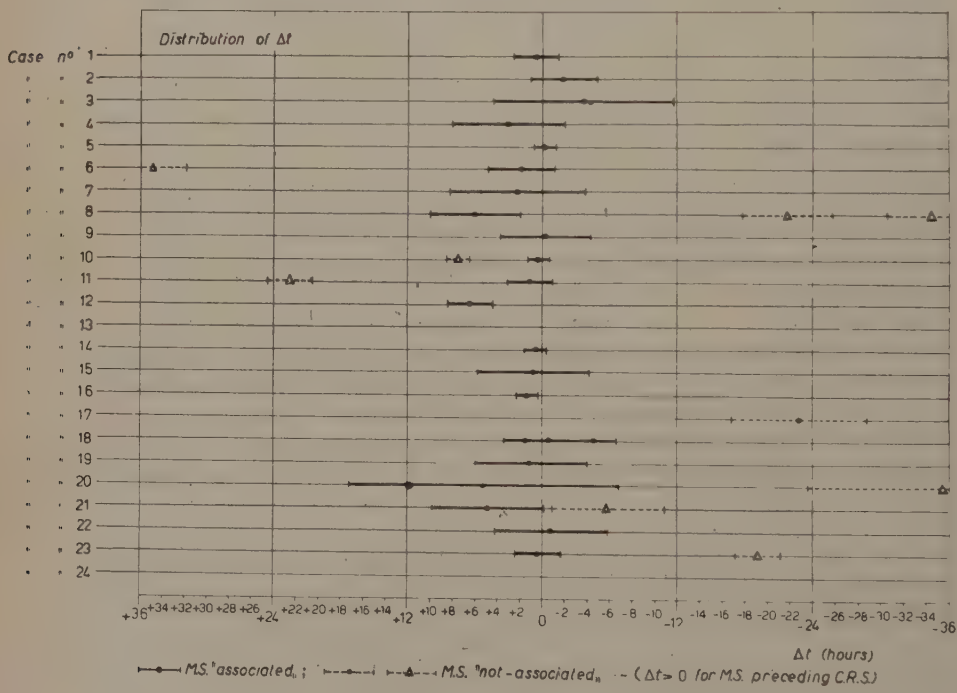

Fig. 8.

It is worth-while noting the close time correlation between the two classes of events occurring in this period; out of 24 CRS, in fact, 21 were « associated » with a MS, in spite of the strict limits chosen. In the three cases of « no-asso-

ciation », the Δt between the CRS and the closest MS varied from a minimum of — 23 hours for case no. 17 to a maximum of — 111 hours for case no. 13.

Concerning the sign of Δt for the association cases, positive values show a marked predominance, indicating that MS tend to *precede* CRS. The authors are aware of the fact that, as pointed out previously, most of these figures are within the experimental uncertainties, but at least in three cases (cases no. 8, 12, 16) the MS precedes the associated CRS of an interval which seems to be beyond the experimental error. This impression is confirmed in the case of events recorded in Rome, where at least for the more clear-cut events, the onset times were determined with greater accuracy.

It is moreover important to observe that, while CRS of the « highest quality » (a total of 15 cases of type I and II) are all correlated with MS, the three cases of no-association happen to correspond to less well defined events.

Finally, one more consideration can be drawn from Table II: with the exception of one event, all of the associated CRS seem to « prefer » association with geomagnetic events characterized by a SC, *i.e.* with MS of type $\bar{A}$ (13 cases) and $\bar{B}$ (7 cases). This is a point of considerable interest that will be dealt with again in the next sections.

4·3. *MS → CRS.* — 71 MS (*) were identified in the investigated period and taken into consideration in order to establish their correlation with the 24 CRS recorded in the same period.

The study of the MS → CRS correlation is therefore the most complex part of the whole investigation. In this case, in fact, it is necessary to analyze in detail the various characteristics of the MS and to investigate whether some of them are connected with the simultaneous occurrence of CR events.

It was realized that, besides the morphological features on which the classification in types was based (see Section 3), one further circumstance seems to play an important role, *i.e.* whether the MS begins at a time when the C.R. intensity can be assumed to be normal or, instead, when a C.R. event is already on its course. From now on these two alternatives will be indicated by the expression « free » and « non-free » MS.

In practice, the following criterion was followed to assign the different MS events to either of the two groups: MS were considered to be « non-free » when, while occurring during a CRS, they had started after the uncertainty interval of the onset time of the latter.

Table III shows the number of cases of association and no-association of MS (« free » and « non-free ») with a CRS. For a more complete vision of

(*) The last of the 72 magnetic storms listed in Part II (July 31, 1958) was not taken into consideration here because it occurred at the end of the investigated period.

the situation, in cases of no-association with a CRS, also the presence or absence of minor C.R. perturbations was reported. Both MS and CRS are subdivided according to their morphological types.

« Free » and « non-free » MS. – It seems evident that « non-free » MS give a tiny contribution to the number of cases of association with CRS: 18 out of 21 association cases correspond, in fact, to « free » MS.

Moreover, a comparison of the two parts of Table III shows a tendency of « non-free » MS to be associated, if so, with less sharp and important C.R. events than those corresponding to « free » MS: this tendency is displayed,

TABLE III.

	Magnetic Storms		Associated with CRS (I, II, III, X)	Not associated with CRS	
	Type	Total		Minor perturbation present	Nothing present
(a) « FREE »	$\bar{A}$	12	10 (6, 3, 0, 1)	0	2
	$\bar{B}$	9	7 (4, 1, 1, 1)	2	0
	$\bar{C}$	2	0	1	1
	A	8	1 (0, 1, 0, 0)	1	6
	C	8	0	2	6
	Total	39	18	6	15
(b) « NON-FREE »	$\bar{A}$	14	3 (0, 0, 0, 3)	5	6
	$\bar{B}$	10	0	2	8
	$\bar{C}$	4	0	3	1
	A	1	0	0	1
	C	3	0	1	2
	Total	32	3	11	18

within each type, by a shift of significative numbers to the columns at the right when passing from part *a*) to part *b*) of the Table.

In particular, the only three cases of association with true CRS recorded among « non-free » MS belong to type X (cases no. 2, 6, 7 of Table II). This in spite of the fact that the MS corresponding to them are far from being small, as shown, for instance, in Fig. 1 for the MS of September 2, 1957.

In conclusion, it seems that some cause, connected with the MS being « non-free », decreases, other conditions being equal, the probability of the simultaneous occurrence of a CRS, and, even more, the probability of the occurrence of a conspicuous and well-defined one.

This observation has to be kept in mind all through the following discussion.

MS with and without SC. – In Section 4·2 we pointed out the marked prevalence of cases of association of CRS with sudden commencement MS: 20 cases out of a total of 21. The observation should now be added that all type I storms (*i.e.* the 10 best defined events) were associated with MS characterized by SC. Moreover, an examination of the MS → CRS correspondence shows that this prevalence remains sharp and significant also when the association cases are referred to the corresponding totals of MS.

In fact the separate addition of cases of MS with and without SC (see Table III) gives the following results:

with SC, $(\bar{A} + \bar{B} + \bar{C})$: 17 associations out of 23 cases,

without SC, $(A + C)$: 1 association out of 16 cases;

while, for « free » and « non-free » MS,

with SC, $(\bar{A} + \bar{B} + \bar{C})$: 20 associations out of 51 cases,

without SC, $(A + C)$: 1 association out of 20 cases.

The slight worsening of the latter distribution, from the point of view of a preferential association with events characterized by a sudden commencement, is clearly due to the inclusion of « non-free » MS.

MS typical of the maximum and minimum solar activity. – Another relevant fact shown by Table III is the complete absence of associations with storms of type $\bar{C}$ and C. Considering only « free » MS we find:

$\bar{A} + \bar{B} + A$: 18 associations out of 29 cases,

$\bar{C} + C$: 0 association out of 10 cases.

This result, definitely against an association of type $\bar{C}$ and C magnetic storms with CRS, is of particular interest ([20]) considering that these storms are

typical of the period of minimum solar activity and can be referred to the M regions and not to activity centers of the sun, like the typical storms $\overline{A}$, $\overline{B}$ and A of the activity maximum.

This result, however, can lose much of its statistical significance if what has been previously found about the importance of the SC is taken into account: in fact, by singling out MS with SC among « free » MS, only a very small sample is found of cases of MS typical of the minimum solar activity.

MS with and without the Main Phase. – An attempt was made to establish the importance of the presence or absence of the main phase in MS, in relation to association with CRS.

Taking in consideration only « free » MS, we have:

with main phase $(\overline{A} + A)$: 11 associations out of 20 cases

without main phase $(\overline{B} + \overline{C} + C)$: 7 associations out of 19 cases.

It does not seem, therefore, that magnetic storms with the main phase are correlated with CRS in an appreciably different way than MS without this morphological feature.

Type $\overline{A}$ and $\overline{B}$ MS. – Since these types of MS include almost all cases of association with CRS (20 cases on a total of 21) it is obviously interesting to compare the relative contribution of each type. Once again, by taking into consideration only « free » MS, it is found:

$\overline{A}$: 10 associations out of 12 cases

$\overline{B}$: 7 associations out of 9 cases.

It is evident therefore that type $\overline{A}$ and type $\overline{B}$ magnetic storms are associated with CRS in comparable proportions. Even for what concerns the « quality » of the associated CRS, Table III clearly shows that the distribution of the various types of CRS is practically the same.

This result is of particular interest if we consider the remarkable structural differences between the two types of MS. It is important to recall, in fact, that the two types are, by definition, morphologically different: moreover, by examining all MS occurring in the period under study, (see Part II, Section 4) it becomes apparent that $\overline{A}$ events are by far the most relevant, while $\overline{B}$ events are the most modest, both for the intensity and duration and for the degree of the perturbation; thus, for instance, the mean value of $K_{p\,\max}$ is equal to 7_+ for $\overline{A}$ and equal to 5_0 for $\overline{B}$ events.

In spite of this considerable difference from the magnetic point of view, type $\overline{B}$ MS seem to be equally important as storms of type $\overline{A}$ for what concerns the association with CRS. It is clear therefore that, in the study of the

correlation of geomagnetic events with C.R. events, it is essential to take into account also type $\overline{B}$ magnetic storms, which might easily escape to an identification based exclusively on the determination of the $K_{\parallel}$ indices.

4·4. *Statistical approach.* – A Chree analysis, *i.e.* the method of superposed epochs, was applied to the C.R. data recorded in Rome (*) by taking as time zero the onset times of the MS.

MS with and without SC. – Fig. 9 reproduces, for the sake of comparison, the graphs obtained grouping together all C.R. data relative to MS with SC (curve *a*), 50 events) and without SC (curve *b*), 20 events).

It is clear that, while in curve (*a*) the SC is immediately followed by a sharp drop of the intensity, no such fall of intensity appears in curve (*b*) after the beginning of MS with a gradual commencement.

This result confirms, by a different method, the conclusion that had been reached in the previous comparison between single events about the importance of SC.

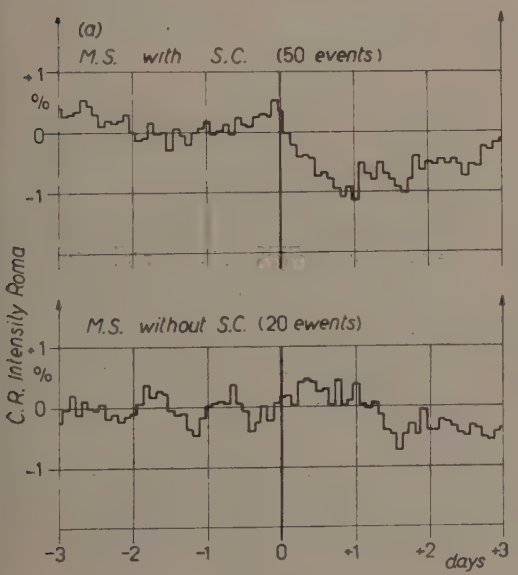

Fig. 9.

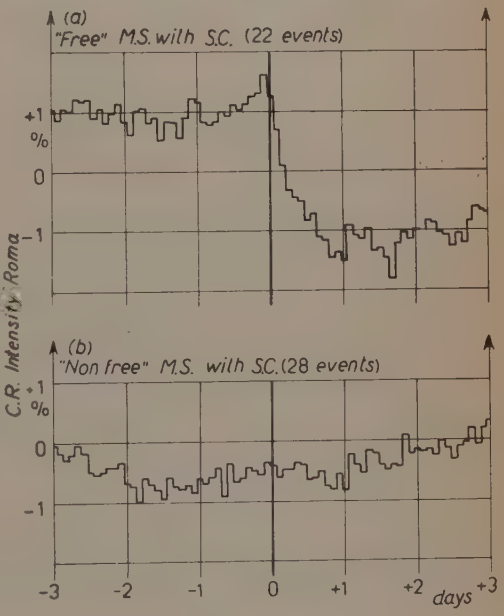

Fig. 10.

The amplitude of the average fall of C.R. intensity immediately after the SC (curve (*a*)) appears rather small, about 1%; this is essentially due to the in-

(*) Respecting the list of MS reported in Part II, the type $\overline{A}$ magnetic storm of June 30, 1957 and the MS of type $\overline{B}$ of July 7, 1958 were not included in this calculation, the former because the C.R. data recorded in Rome were lacking, the latter because it had been omitted also in the previous analysis (Sect. 4·3).

clusion of C.R. data for « non-free » storms with SC (28 out of 50), which, as previously pointed out, present only three cases of association with CRS. This fact is clearly shown in Fig. 10, which reproduces the curves for « free » (22 events) and « non-free » (28 events) MS with SC. The amplitude of the intensity fall for « free » MS is about 2.5%, while no intensity decrease is observed with « non-free » MS in correspondence to the SC: on the contrary, a slow rise is visible in the last case, as foreseen by the very definition of « non-free » MS; it should be recalled, in fact, that we considered « non-free » the MS which begin in a period when a CRS is already in course, and often in its recovery phase.

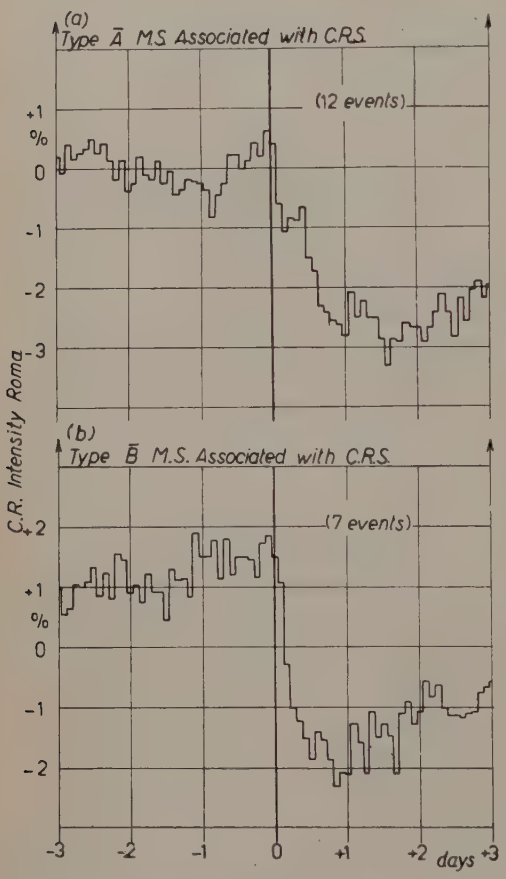

Fig. 11.

Tipe $\bar{A}$ and type $\bar{B}$ MS. Finally, it should be remarked that the Chree analysis confirms the previous observation of an equivalence of behaviour of the C.R. intensity in correspondence with MS of type $\bar{A}$ and $\bar{B}$.

This is shown by Fig. 11, reproducing the curves for type $\bar{A}$ (curve *a*)) and $\bar{B}$ (curve *b*)) events obtained exclusively with data relative to magnetic storms associated with a CRS. It is hardly necessary to point out that both the shape and mean amplitude of the fall are substantially identical in the two curves.

4·5. *Correlation between magnitudes of associated CRS and MS.* – The lack of a close parallelism between C.R. and geomagnetic field intensities in known from the literature and can be easily seen also in Figs. 1-6 of the present paper.

Moreover confining ourselves exclusively to the cases of association, the results obtained in the present work on the equivalence of type $\bar{A}$ and $\bar{B}$ MS in their correspondence with CRS, provide further evidence against the exis-

tence of a close correlation between the amplitude of the CRS and the « importance » of the associated MS.

Actually, a linear regression analysis between the amplitude of the CRS in Rome and either of the two parameters range and $a_{p\,\max}$ of the associated MS (see Table II) gives the correlation coefficients

$$r_{\text{range}} = -0.05\,, \qquad r_{a\,p\,\max} = -0.04\,.$$

It might be remarked that of the two parameters selected to represent the « importance » of the MS, the ranges we used can be inclusive of local effects, while the $a_{p\,\max}$ indices, though of a planetary character, do not always represent the total variation of H during the storm, for the very fact of being threehourly indices.

On the other hand these parameters proved to be well correlated with each other not only in the sample of the 72 identified storms ($r = +0.84$) but also, and with a coefficient of comparable value ($r = +0.85$), in the smaller sample of associated cases; this shows that the two indices, as a whole, correctly represent the world-wide importance of the MS.

It can be concluded, therefore, that in the analyzed period there is no correlation between the amplitude of the CRS and the « importance » of the MS, as previously found by several authors ([16 19,22]).

A priori it seemed more promising to attempt a correlation analysis between the amplitude of the CRS and the amplitude of the SC; this in consideration of the finding that the very presence of the SC in a MS is determinant for the association with a CRS, and that both the distribution and the mean value of the amplitude of the SC are very similar for MS of type $\bar{A}$ and $\bar{B}$.

Yet the linear correlation coefficient turns out to be very low also in this case ($r_s = +0.28$). Here however it is not possible to infer about the influence of local effects, which can be quite large, and are actually very difficult to correct. Consequently, the individual values of the selected parameters (*i.e.* the amplitude of the SC as measured in Italian stations) might not be a very satisfactory representative of the world-wide magnitude of the SC and the failure to find a correlation cannot be considered conclusive.

5. – Conclusions.

The main results obtained in the present work of correlation between cosmic ray and geomagnetic events during the July 1957–July 1958 period can be summarized as follows:

1) The degree of time-correlation of CRS to MS is particularly high: out of a total of 24 CRS, 21 are associated with MS at very close time inter-

vals. Among the few data published in the literature ([19,22]) about this point, we recall those of SIMPSON ([8]), who reported a larger proportion of no-associations; his study however, covered a different period of time and was based on a smaller sample.

2) The correlation of MS to CRS is far from being as tight as that of CRS to MS; the 21 cases of association, in fact, were found in a total of 71 MS. This result provides further evidence that the correspondence of geomagnetic and cosmic ray events is not of the one to one type. As for the period of time selected for the present research, a period of maximum solar activity, *i.e.* with a rather high rate of MS occurrence, it was possible to notice an interesting fact: it seems important if not determinant for the association of a MS with a true CRS that the MS be « free », or, in other words, that it does not start at a time when a CRS is already running: some cases of association can be found even with « non-free » MS, but only with less intense CRS or minor perturbations.

3) Among the morphological features of the recorded MS, the one which seems to play an essential role in favour of the association with a CRS is the world-wide presence of the sudden commencement at the start of the MS. Evidence of this can be obtained also from the data of different authors ([16,22]).

4) Neither the range of the magnetic event nor its degree of small time-scale disturbance (a_p or K_p) play an important role in the association: this is particularly evident if we consider that magnetically different events like type $\bar{A}$ and $\bar{B}$ are comparable from the point of view of their association with CRS.

5) Finally, there is a general indication that the MS precedes the associated CRS of a very short interval. This would seem to be in agreement with the findings of some other authors ([24,16,22,25]). In order to establish this point more clearly, it might be helpful to dispose of C.R. data with a better resolving rime, yet compatible with the requirement of statistics. Moreover it would be interesting to investigate more thoroughly some apparent discrepancies noticed in the onset times of the same events at different longitudes and the appearance of certain local time asymmetries (see for instance the events of October 21, 1957 and of May 9, 1958), which might reflect some sort of anisotropy of the phenomenon itself.

We think that some of the aspects revealed by this phenomenological analysis might be useful for the interpretation of the phenomena triggered by

([24]) A. R. HOGG: *Memoires of Commonwealth Observ. Camberra*, n. 10 (1949).

([25]) A. G. FENTON, K. G. MC CRACKEN, D. C. ROSE and B. G. WILSON: *Can. Journ. Phys.*, **37**, 970 (1959).

the arrival of a beam of solar ionized particles in the proximity of the Earth. Other aspects of the same problem concerning the emission of a corpuscular beam from the sun will be dealt with in a future paper.

* * *

We are indebted to the whole staff of the laboratory for continuous operation of the neutron monitor in Rome and for computational assistance. All the geomagnetic data from the observatories of the Istituto Nazionale di Geofisica were greatly appreciated; in particular we wish to thank Dr. F. MOLINA for several stimulating discussions. We are also grateful to Drs. J. A. SIMPSON, A. EHMERT and Y. MIYAZAKI for sending us the C.R. data from their stations and for permitting their pubblication.

RIASSUNTO

Si riporta un'analisi sistematica condotta, per il periodo Luglio 1957 - Luglio 1958, sull'intensità dei Raggi Cosmici quale misurata da rivelatori standard della componente nucleonica a Roma e in altre Stazioni in varie parti del mondo. Si sono identificati e classificati gli eventi di R.C. del tipo delle cosiddette diminuzioni alla Forbush, e si è studiata la loro corrispondenza temporale con le tempeste magnetiche identificate nello stesso periodo (vedi Parte II). Si è esaminato quali particolari caratteristiche di ambedue le categorie di eventi risultano determinanti ai fini di tale associazione, ed alcuni aspetti di quest'ultima si sono messi in evidenza con metodo statistico.

Cosmic Ray and Geomagnetic Disturbances from July 1957 to July 1958.

Part II - The Geomagnetic Events.

F. Bachelet, P. Balata, A. M. Conforto and G. Marini

Istituto di Fisica dell'Università - Roma
Istituto Nazionale di Fisica Nucleare - Sezione di Roma
Commissione Italiana Anno Geofisico Internazionale - Roma

(ricevuto il 28 Dicembre 1959)

Summary. — The Magnetic Storms (MS) occurred in the period July 1957 - July 1958 are selected and classified in view of an analysis of their correlation with Cosmic Ray Storms. The methods and the criteria employed are described in detail. A list of all geomagnetic events thus identified is reported.

1. – Introduction.

For the purpose of setting out a correlation between geomagnetic phenomena and Cosmic Ray events [1], we have attempted to identify, with the criteria that will be explained below, all the world-wide Magnetic Storms (MS) included in the period July 1957–July 1958.

There were 72 MS compared with 24 Cosmic Ray Storms (CRS) occurring in the same period. The comparison of these two numbers shows that if some correspondence exists between MS and CRS, it must be sought between the Cosmic Ray events on the one hand and those MS on the other, which show some systematic characteristics.

---

[1] F. Bachelet, P. Balata, A. M. Conforto and G. Marini: *Nuovo Cimento*, **16**, 292 (1960).

We have therefore studied in detail, using the magnetograms at our disposal, all the geomagnetic events, in order to group them in categories corresponding to their common characteristics, and for the purpose of inquiring what role such characteristics play in the MS–CRS correlation.

2. – Classes of MS.

The facts to which we have paid particular attention are the following (2):

1) The MS may begin gradually or with a sudden commencement (SC).

2) During the MS the so-called « main phase » may or may not appear. It manifests itself in the horizontal component H of the magnetic field as a drop of intensity at a relatively short time from the beginning of the MS.

3) The disturbance may present a typical behaviour that is reproduced in various MS (*) and is relatively short (of the order of a day), or else it can show irregular variations, not at all systematic, that often last for several days.

On the basis of these characteristics all the MS are subdivided into five principal types that we will indicate with the symbols $\overline{A}$, $\overline{B}$, $\overline{C}$, A and C.

Types $\overline{A}$, $\overline{B}$ and $\overline{C}$ consist of all the MS that begin suddenly (*MS with SC*) and in their turn are differentiated by the different behaviour of the field H as follows:

Type $\overline{A}$: The classical MS belong to this category. In these, after the initial *SC*, H exhibits values greater than normal for a rather short time: *initial plase*. This is followed by an appreciable fall, often very rapid, to a level lower than the prestorm value (*main phase*). This second phase is in general of longer duration than the first. The storm ends with a gradual and slow recovery of H towards its initial value.

We note finally that the sum of these phases rarely exceeds 48 hours duration; moreover the MS of type $\overline{A}$ (of which an example is given in Fig. 1*a*) is often associated with rather high values of the three-hourly planetary indices, K_p, of geomagnetic activity.

Type $\overline{B}$: These are the MS of shorter duration in the sense that after a SC that can also be very marked and intense, it is possible to recognize

---

(2) For the current terminology and for the general study of geomagnetic phenomena, see S. Chapman and J. Bartels: *Geomagnetism* (Oxford, 1951) and, very recently, F. Mariani and F. Molina: *Ann. Geofis.*, **12**, 297 (1959).

(*) See types $\overline{A}$, A, $\overline{B}$ of the classification that follows, in which the same qualitative behaviour is reproduced in the various storms of the same type.

in H essentially an *initial phase* only (see Fig. 1*b*). The corresponding values of K_p are in general much less high than in the preceding case.

Type $\bar{C}$: The behaviour of H in these storms has nothing typical: in fact the *SC* is followed by large and irregular fluctuations, of rather a long period, that often last for several days (at times up to 8 or 9) and end by gradually dying away. Fig. 1*c* shows the beginning of an event of this type.

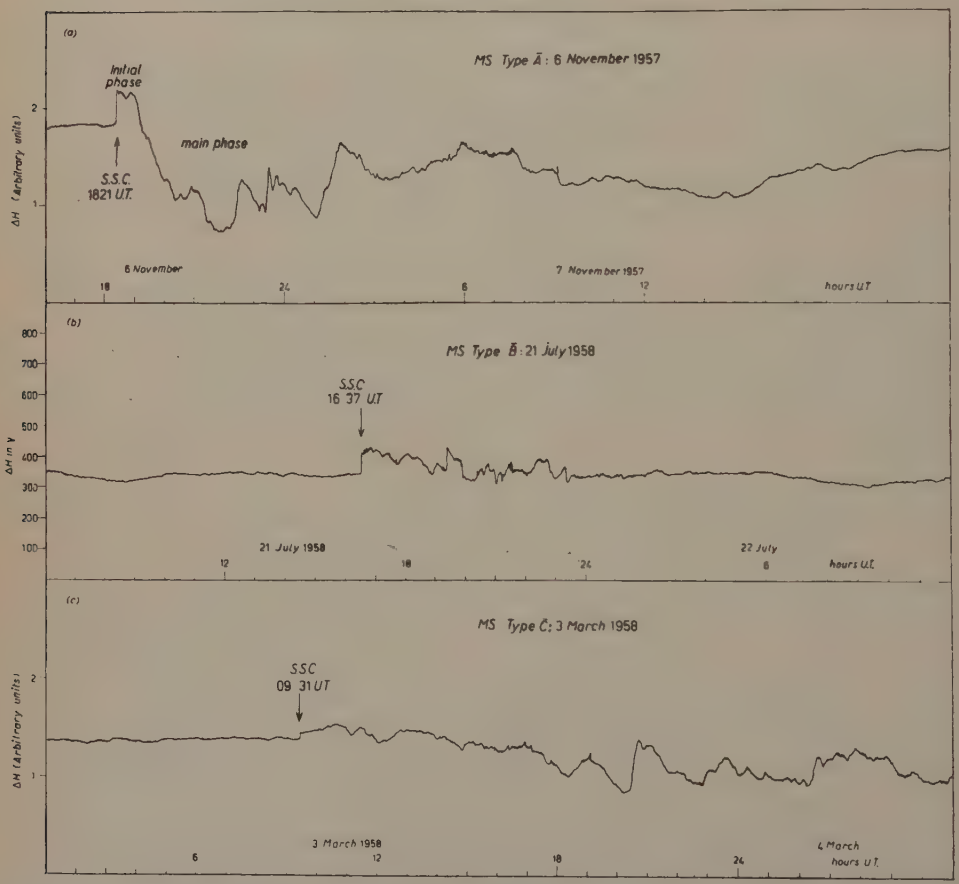

Fig. 1. – Examples of MS of types $\bar{A}$, $\bar{B}$ and $\bar{C}$: horizontal component H of the geomagnetic field at Gibilmanna ($\bar{A}$ and $\bar{C}$) and at L'Aquila ($\bar{B}$). The arbitrary unit indicated in the graphs of Gibilmanna corresponds to about 100 γ.

Contrary to the preceding types the storms of types A and C are essentially characterized by the lack of SC (*MS without SC*). For the rest, their behaviour does not differ from that of the homonyms $\bar{A}$ and $\bar{C}$ respectively.

It is pointed out that types $\bar{C}$ and C of our classification, turn out to be the categories to which practically all the recurrent MS taking place during the period of minimum solar activity would belong.

Besides the types of disturbance illustrated above, that cover all the events classified by us as MS, the field H can sometimes show periods of activity more intense than normal without the disturbance reaching such a level as to be considered a storm. Moreover, variations of the level of the magnetic field can suddenly appear (SI: sudden impulse) unaccompanied by any particular activity. We have grouped all these cases under the heading of « Minor geomagnetic disturbances ».

We wish at this point to emphasize that the preceding subdivision, although undoubtedly useful for the present purpose, is not meant to have more than a phenomenological value. When one wishes, as we do, to examine and to classify all the geomagnetic events that take place in a certain period, it is not always easy to attribute without ambiguity each MS to one of the categories indicated above, but on the contrary the transition from one class of MS to the other and from MS to minor disturbances occurs with a certain continuity. For this reason, in practice, one is inevitably confronted by a certain number of doubtful cases that need to be solved each time, possibly also with the intervention of subjective factors. It seemed to us therefore very important, for the valuation of the results that are derived from our analysis, to describe in detail the method employed and the criteria selected with the aim of attaining the maximum objectivtiy.

3. – Identification and classification of the events.

3·1. *General remarks.* – The objective of this analysis is to arrive at a list, subdivided into categories according to the preceding definitions, of the MS of world-wide character that happened in the period July 1957–July 1958.

For such a purpose we had at our disposal two different kinds of information:

I – Direct information: Continuous recordings of the earth's magnetic field, more precisely of the three magnetic elements H, Z and D (*), as obtained in the observatories of:

Gibilmanna (Italy)	38.0° N,	14.0° E, grog.;	38.5° N, geom.
L'Aquila, S. Vittorino (Italy)	42.4° N,	13.3° E, geog.;	42.9° N, geom.
Asiago (Italy)	45.9° N,	11.5° E, geog.;	46.6° N, geom.

(*) Z is the vertical component and D the declination of the field.

Such magnetograms have been kindly put at our disposal by Dr. F. MOLINA of the Istituto Nazionale di Geofisica, Roma.

II – Indirect information:

a) Chronological lists of the SC (**) and of the SI specifying for each case the numbers of world-wide observatories which on that date reported SC and SI respectively. (Reports prepared by the International Association of Geomagnetism and Aeronomy and published by the *Journal of Geophysical Research*).

b) Lists of the geomagnetic planetary indices K_p by Dr. J. BARTELS.

c) Lists of the principal MS reported in the magnetic bulletins of about fifteen observatories scattered throughout the world.

The main part of the work of identifying the events has been carried out directly on the magnetic recordings (Information I).

Information II has been used with two purposes: to confirm the world-wide character of the selected disturbances themselves and their characteristics; and, viceversa, to avoid the possibility that in the examination of the magnetograms some event should be missed that, following our criteria, is to be considered on a world-wide basis as a MS. With these data the possibility of checking and confirming the world-wide nature of the MS with a sudden commencement and that of the storms with a gradual commencement was quite different. In fact, while the international reports of the SC sum up the information of about a hundred observatories, for the MS with a gradual commencement, the only possibility of checking was given by the lists of MS (information II-*c*) that refer to a much smaller number of stations. In consequence of this, different criteria were adopted for selection in the two cases and it is therefore convenient to explain them separately.

3·2. *MS with SC.* – By a comparison and suitable valutation, case by case, criteria have been derived from various pieces of information that have allowed us to put some SC as « certain », others as « uncertain » and yet others as « non-existent ».

In the following we have reported in brackets case by case the number of events that in the period of examination satisfied these criteria.

MS with « certain » SC (44 events in all) have been considered those MS at the onset of which

either at least 20 stations gave SC (40 cases),

or $N_{SC} + N_{SI} \geqslant 30$, with $N_{SC} \geqslant 10$ (4 cases).

(*) In the magnetic bulletins the notation now used is SSC (storm sudden commencement).

(The symbols N_{SC} and N_{SI} indicate, here and in the following, the number of stations that reported SC or SI respectively). In correspondence to all these events, the SC appeared clear and unmistakable also on the magnetograms examined by us.

MS with « uncertain » SC (8 events in all) have been considered those, not included among the preceding, for which:

$$N_{SC} + N_{SI} \geqslant 15 , \quad \text{with} \quad N_{SC} \geqslant 5 .$$

Also in these cases the SC could always be identified on the magnetograms, though in general less distinct than in the preceding cases.

« *Non-existent* » *SC* have been considered all cases not satisfying the preceding criteria.

Among these we quote some events that were given on the world-wide reports essentially as SI only, though at times by a large number of stations (up to $N_{SI} = 43$). In such cases, there appeared on the magnetograms a sudden variation of level not followed by any noticeable activity. As decided above, these cases have been considered « minor disturbances ».

In regard to the remaining events it is interesting to observe that while one passes with a certain continuity from the MS with « certain » SC to those with « uncertain » SC, below the limits fixed for the « uncertain » cases one notes a distinct gap, in the sense that, in the period considered, there was no case in which

$$15 \geqslant N_{SC} + N_{SI} \geqslant 10$$

with a comparable number of SC and SI.

These events have been re-examined as possible MS with gradual commencement.

The MS with SC so selected have then been subdivided according to the preceding definitions into types $\bar{A}$, $\bar{B}$ and $\bar{C}$ on the basis of the records of the magnetic field. We checked finally that the attribution of each storm to one of these types was compatible with the corresponding behaviour of the indices K_p.

3·3. *MS without SC.* – As we have already noted, the confirmation of the MS with gradual commencement was sought for on the lists of the principal MS as provided by the various geomagnetic observatories (see Section 3·1 II*c*). Also in this case we have established the criteria by which some events have been considered as « certain » MS, others as « uncertain » MS and others simply as minor disturbances.

1) The more evident disturbances on the magnetograms—« *certain* » *MS. without SC*—were reported in general among the principal storms by at least 50% of the observatories taken into consideration (17 events in all).

2) The disturbances not included among the preceding cases, and considered as MS in the examination of the magnetograms, although more uncertain, were also given as principal in at least 25% of the other observatories. These have been considered by us as « *uncertain* » *MS without SC* (3 events in all).

3) We have included all the remaining events among the « minor disturbances »; it is interesting to note that none of these was reported in the lists of more than 2 of the observatories considered.

On the basis of the examination of the magnetograms and of the corresponding behaviour of K_p, the MS without SC were finally subdivided into types *A* and *C*.

4. – The MS of the period July 1957 - July 1958.

The results of the analysis described are reported in Table I. It represents, within the limits of the criteria described in the preceding section, the list of all the MS of the period July 1957–July 1958 (*). In it are reported for every storm: date, onset time, type, duration and a valuation of importance.

For this valuation are used:

1) $a_{p\,\max}$, that is the maximum value of the three-hourly index a_p (**) during the disturbance.

2) A qualification decided arbitrarily on the basis of the range of the MS, *i.e.* on the basis of the maximum excursion of H during the event, measured on the magnetograms of the Italian stations:

w = weak	for	Range $< 100\,\gamma$
m = moderate	»	$100\,\gamma \leqslant$ Range $< 200\,\gamma$
ms = moderately severe	»	$200\,\gamma \leqslant$ Range $< 300\,\gamma$
s = severe	»	$300\,\gamma \leqslant$ Range .

(*) More precisely among the 72 MS reported there, is also included the MS type $\bar{A}$ of June 30, 1957.

(**) It seemed more significant to report here, instead of the K_p, the a_p indices, that are expressed in a linear scale in the variation of H.

TABLE I. – *Magnetic Storms.*

Date	Onset time UT (h m)	Type with SC	Type without SC	Notes	Duration (days)	Importance $a_{p\,max}$	Importance range qual.	N_{SC}	N_{SI}
30 June 57	05 28	$\bar{A}$			1,7	236	ms	36	
2 July	08 57	$\bar{A}$			1,3	207	m	42	
5 July	00 42	$\bar{A}$			0,9	154	m	21	
16 July	07 14	$\bar{A}$			0.9	27	w	44	
19 July	13 44	$\bar{B}$			0.5	39	w	27	
22 July	04 19	$\bar{B}$			1.1	67	w	34	
27 July	19 59	$\bar{B}$			0.2	27	w	41	
3 August	15 57	$\bar{A}$			0.4	94	m	55	
6 August	05 08	$\bar{A}$			0.9	67	w	42	
9 August	13 47	$\bar{B}$			0.6	39	w	41	
12 August	08 30		A		1.6	67	m		
20 August	09 30		A	(*)	1.4	56	w		
29 August	19 20	$\bar{A}$			0.9	111	m	53	
31 August	18 12	$\bar{B}$			0.9	132	w	28	
2 September	03 14	$\bar{A}$			2.4	300	m	48	
4 September	13 00	$\bar{A}$			1.6	400	ms	50	
6 September	11 21	$\bar{A}$			0.7	67	w	25	
13 September	00 46	$\bar{A}$			1.7	300	s	48	
21 September	10 05	$\bar{A}$			1.2	154	ms	47	
22 September	13 45	$\bar{A}$			0.5	236	m	44	
23 September	02 35	$\bar{A}$			2.6	300	ms	27	
29 September	00 16	$\bar{A}$			2.6	300	s	48	
14 October	04 40	$\bar{A}$			0.9	94	m	21	
21 October	15 00 16 00		A		1.4	27	m		

(*) «Uncertain» MS without SC according to the criteria describe din Sect. 3·3.

TABLE I (*continued*).

Date	Onset time UT (h m)	Type		Notes	Duration (days)	Importance		N_{SC}	N_{SI}
		with SC	without SC			$a_{p\,max}$	range qual.		
21 October 57	22 41	$\overline{B}$			0.5	111	m	30	25
6 November	18 21	$\overline{A}$			1.1	132	m	60	
8 November	07 30		C		7.7	48	w		
25 November	04 30		A	(*)	0.9	56	m		
26 November	01 55	$\overline{A}$			3.0	111	m	16	12
1 December	03 36	$\overline{B}$		(**)	0.3	67	w	14	
9 December	00 00		C		7.0	67	m		
19 December	09 37	$\overline{A}$			2.0	39	w	37	
25 December	10 00		C		1.6	32	w		
31 December	01 00		A		2.7	94	m		
9 January 58	10 00		C		9.6	48	w		
20 January	21 43	$\overline{C}$		(**)	3.0	111	m	8	13
25 January	10 50	$\overline{A}$			0.4	32	w	27	8
4 February	13 04	$\overline{C}$			6.5	48	m	22	2
11 February	01 25	$\overline{A}$			3.7	400	s	57	1
16 February	16 42	$\overline{C}$			7.2	48	w	37	6
3 March	09 31	$\overline{C}$			5.2	111	w	39	3
11 March	11 00		C		1.5	132	m		
13 March	00 00		A		1.0	67	m		
14 March	12 12	$\overline{B}$			1.3	67	m	52	2
17 March	07 50	$\overline{C}$		(**)	4.8	80	m	13	3
22 March	23 00		C		4.2	56	w		
25 March	15 40	$\overline{B}$			0.3	80	w	42	4
30 March	09 00		C		8.7	67	w		

(*) « Uncertain » MS without SC according to the criteria described in Sect. 3·3.
(**) MS with « uncertain » SC » » » 3·2.

TABLE I (*continued*).

Date	Onset time UT (h m)	Tipe with SC	Tipe without SC	Notes	Duration (days)	Importance $a_{p\,max}$	Importance range qual.	N_{SC}	N_{SI}
14 April 58	09 30		*C*		5.6	80	w		
26 April	12 47	$\overline{B}$			0.4	39	w	38	5
27 April	14 00		*C*		4.5	56	w		
9 May	07 35	$\overline{B}$		(**)	0.2	22	w	5	22
12 May	17 00		*C*		6.3	67	w		
25 May	15 15		*C*		2.6	111	m		
29 May	00 00		*A*		1.2	94	m		
31 May	16 52	$\overline{A}$			1.5	207	m	64	
2 June	04 09	$\overline{A}$			0.7	39	w	13	29
7 June	00 46	$\overline{A}$			1.0	179	m	42	6
8 June	17 28	$\overline{C}$		(**)	3.3	80	w	9	9
14 June	18 28	$\overline{B}$			0.5	48	w	51	5
15 June	05 09	$\overline{B}$		(**)	0.6	56	w	11	8
19 June	16 00	$\overline{B}$			0.5	18	w	14	26
21 June	02 06		*A*		2.1	94	m	(8)	
28 June	07 13	$\overline{B}$			0.4	27	w	46	10
28 June	17 42	$\overline{A}$			2.2	207	ms	33	9
3 July	16 03	$\overline{B}$		(**)	1.3 (?)	39	w	5	11
8 July	07 48	$\overline{A}$			1.7	400	s	65	
13 July	22 08	$\overline{B}$			0.2	22	w	14	32
18 July	02 21		*A*	(*)	1.0	56	w	(8)	
21 July	16 37	$\overline{B}$			0.8	154	m	67	
22 July	12 07	$\overline{B}$		(**)	0.5	48	w	6	8
31 July	15 29	$\overline{B}$			0.2	56	w	44	15

(*) « Uncertain » MS without SC according to the criteria described in Sect. 3·3.
(**) MS with « uncertain » SC » » » 3·2.

Finally the values N_{SC} and N_{SI} are reported, which, as already said, indicate the number of stations that at the beginning of the MS gave a SC or a SI respectively.

It is interesting to examine Table I to study the distribution of the various types of MS according to the two parameters which we have chosen to indicate their importance.

The range taken into consideration, although relative to a particular station, gives an indication of the magnitude of the storm, while the three-hourly index $a_{p\,\max}$ represents the degree of perturbation on a world-wide scale. These parameters are therefore in some ways complementary for the purpose of specifying the importance of the event.

The distribution with respect to the ranges results from Table II in which the various types of storms are reported, subdivided into weak, moderate, moderately severe, severe, according to the preceding definitions.

TABLE II.

MS type	Total no.	w	m	ms	s
$\bar{A}$	26	7	10	5	4
A	9	2	7	0	0
$\bar{C}$	6	3	3	0	0
C	11	8	3	0	0
$\bar{B}$	20	17	3	0	0

As regards the indices $a_{p\,\max}$, on inspection of Table I one notes that the highest values of these indices correspond as a rule to the MS of type $\bar{A}$ while those of type $\bar{B}$ are generally associated with the lowest indices.

One can quantitatively describe this observation taking into consideration, for every type of storm, the value $a_{p\,\max}$ averaged over the various events; one obtains:

MS type	$\bar{A}$	$\bar{C}$	C	A	$\bar{B}$
$\bar{a}_{p\,\max}$	184	80	69	68	58
$\bar{K}_{p\,\max}$	7_+	6_0	6_-	6_-	5_0

where we have also reported, with obvious meaning of the symbol, the mean values of $K_{p\,\max}$.

From the preceding it is found that, at least in this period, the various types of MS do not present the same distribution neither in respect to the

ranges nor in respect ot the indices $a_{p\,\max}$, but that on the contrary a situation of asymmetry exists between the various types, which is analogous in the two cases.

One concludes from this that in an eventual classification of MS based on their importance the extreme positions would be occupied by type $\overline{A}$ and $\overline{B}$, the first as those by far the most important, the second as the least important, while the remaining types A, $\overline{C}$ and C would represent as a rule the intermediate positions.

* * *

Our thanks are due to Dr. F. Molina, not only for the large amount of material put at our disposal, but above all for the advice and discussions that have been essential for the realization of this work.

RIASSUNTO

Le tempeste magnetiche che si presentano nel periodo Luglio 1957 - Luglio 1958 sono state identificate e classificate morfologicamente in vista della loro correlazione temporale con le cosiddette tempeste di raggi cosmici dello stesso periodo (vedi Parte I). Si descrivono in dettaglio i metodi e i criteri seguiti e si presenta un elenco completo degli eventi geomagnetici selezionati.

IL NUOVO CIMENTO Vol. XVI, N. 2 16 Aprile 1960

Note on Divergenceless Currents and Muon Polarization in $K_{\mu 3}$ Decays (*).

S. Hatsukade, R. E. Marshak, S. Okubo (**) and E. C. G. Sudarshan

Department of Physics and Astronomy - University of Rochester

(ricevuto il 2 Gennaio 1960)

Summary. — The hypothesis of conserved current in weak interaction is examined for the strangeness non-conserving decays. This hypothesis enables the unambiguous calculation of the longitudinal polarization of a muon in $K_{\mu 3}$ decay as a function of the pion energy. Its dependence on the muon energy is also studied. The result is compared with that of Okun and Martinyan who did not use a conserved current.

1. – Introduction.

The decay of non-strange particles is now more or less quantitatively understood in terms of the chirality invariant $V-A$ interaction (1). The qualitative features of strange particle decays is also consistent with a universal $V-A$ interaction, but precise quantitative tests are lacking chiefly because of the unknown renormalization effects due to the strong interactions. Various authors have, however, proposed (2) direct tests for the current-current structure of this $V-A$ interaction, particularly as regards the isotopic spin transformation properties of the strangeness-violating current. One may, in addition, impose dynamical constraints which do not depend on the renormal-

(*) This work was supported in part by the U. S. Atomic Energy Commission.

(**) Now at University of Naples, Naples.

(1) See, for example, *Present status of weak interactions* by R. E. Marshak, *Proceedings of the Kiev Conference on High Energy Physics* (1959).

(2) S. Okubo, R. E. Marshak, E. C. G. Sudarshan, W. B. Teutsch and S. Weinberg: *Phys. Rev.*, **112**, 665 (1958).

ization effects and a natural assumption is that the strangeness-violating current is divergenceless ([3]). We have discussed elsewhere ([4]) the implications of such a constraint for the pion-neutrino correlation in $K_{\mu 3}$ and K_{e3} decays. In this note we wish to discuss the predictions of this hypothesis for the muon polarization in $K_{\mu 3}$ decay.

The muon polarization in $K_{\mu 3}$ decay is interesting even if one does not consider divergenceless currents in kaon decay. The chirality invariant ($V-A$) theory ([5]) suggests that in all weak interactions the fermions tend to come out with negative helicity while antifermions come out with positive helicity (since only the positive chiral projections are involved in the weak coupling). In allowed β-decay this suggestion is borne out since the electrons always possess negative helicity while the positrons possess positive helicity. However, in the $K_{\mu 2}$ and $\pi_{\mu 2}$ decays, the conservation of linear and angular momentum forbids negative helicity for the negative muon and the decay proceeds only by virtue of the chirality-violating mass term; this feature is responsible for the considerable suppression of the two-body electron modes of the kaon and the pion. This suppression no longer obtains in the decay modes $K_{\mu 3}$ and K_{e3} since there are now three particles in the final state. We note that at a given muon energy irrespective of the details of the decay mechanism, the negative

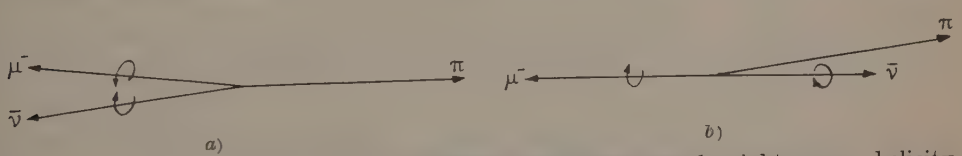

Fig. 1. – *a*) $K_{\mu 3}$ decay configuration of maximum pion energy and « right » muon helicity. *b*) $K_{\mu 3}$ decay configuration of minimum pion energy and « wrong » muon helicity.

muon in $K_{\mu 3}$ decay has negative helicity for the configuration of maximum pion energy while it has positive helicity for the configuration of minimum pion energy (see Fig. 1). If some additional restrictions (like divergenceless currents) are involved, one will be able to specify the detailed manner in which the muon polarization varies for configurations intermediate between these two extremes.

([3]) S. S. Gerstein and J. B. Zeldovich: *Žurn. Èksp. Teor. Fiz.*, **29**, 698 (1955); *Sov. Phys. Journ. Exp. Theor. Phys.*, **2**, 576 (1957); R. P. Feynman and M. Gell-Mann: *Phys. Rev.*, **109**, 193 (1958).

([4]) S. Weinberg, R. E. Marshak, S. Okubo, E. C. G. Sudarshan and W. B. Teutsch: *Phys. Rev. Lett.*, **1**, 25 (1958).

([5]) E. C. G. Sudarshan and R. E. Marshak: *Proceedings of the Padua-Venice Conference on Mesons and Newly Discovered Particles* (September, 1957); R. P. Feynman and M. Gell-Mann: *Phys. Rev.*, **109**, 193 (1958); S. Okubo, R. E. Marshak, E. C. G. Sudarshan, W. B. Teutsch and S. Weinberg: *Phys. Rev.*, **112**, 665 (1958).

1357

2. – Muon polarization as a function of pion energy.

Within the framework of the current-current structure ([5]), the $K_{\mu 3}$ decay matrix element is

$$\langle \pi \mu \nu | H_w | K \rangle = V^\lambda \bar{u}_\mu \gamma_\lambda (1+\gamma_5) u_\nu ,$$

with

$$V^\lambda = \{ f(p^\lambda - q^\lambda) + g p^\lambda \} ,$$

where p and q are the kaon and pion momenta respectively and f and g are invariant functions of $(p-q^2)$, so that in the rest system they may be considered as functions of the pion energy. If the kaon is pseudoscalar (scalar), only the vector (axial vector) current contributes to this matrix element. If this current is conserved, it follows that the invariant functions f and g satisfy the relation ([4]):

$$(p-q)^2 f + (p^2 - pq) g = 0 . \tag{1}$$

Consequently, the decay matrix element is now completely determined except for an unknown multiplicative factor depending on the pion energy; we have

$$V^\lambda = \left\{ p^\lambda \left(\frac{q_0}{\Delta} - \frac{m_\pi^2}{m_K q_0} \right) - q^\lambda \right\} f(q_0) , \tag{2}$$

where q_0 is the pion energy and

$$\Delta = m_K - q_0 .$$

The pion and muon energies essentially determine the decay configuration and the muon polarization can now be evaluated as a function of these two quantities. The calculation is straightforward and yields for the longitudinal muon polarization

$$P(k_0, q_0) = -\frac{1}{|\boldsymbol{k}|} \left\{ k_0 + \frac{2(\Delta^2 - a)(k_0 a - m_\mu^2 \Delta) m_\mu^2}{[2k_0 a - (m_\mu^2 + a)\Delta]^2 - a(\Delta^2 - a)(a - m_\mu^2)} \right\} , \tag{3}$$

where

$$a = (m_K - q_0)^2 - q_0^2 + m_\pi^2 = \Delta^2 - |\boldsymbol{q}|^2 .$$

This expression for the polarization is plotted in Fig. 2 as a function of the pion energy q_0 for fixed k_0.

We may now calculate the muon polarization as a function of the pion energy by integrating over the muon energy spectrum for a fixed pion energy.

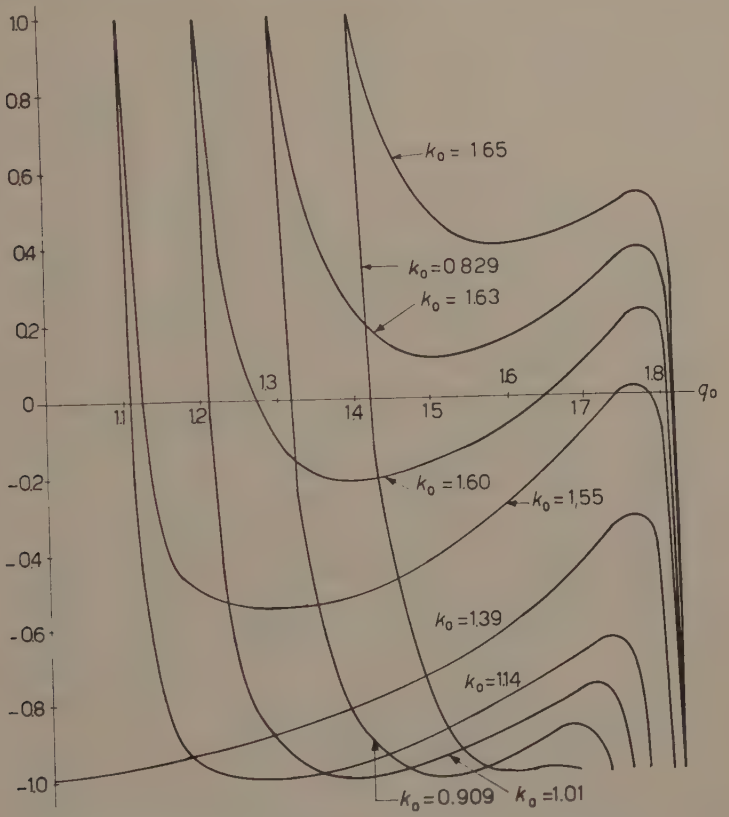

Fig. 2. - Muon longitudinal polarization $P(k_0, q_0)$ as a function of pion and muon energies.

This integration is facilitated by the observation that after the angle integrations are carried out, the kinematic weight factor for the configuration (q_0, k_0) is a constant in the allowed domain and zero outside. The allowed domain is indicated in Fig. 3 and corresponds to the restriction

$$(4) \qquad (\Delta - |\boldsymbol{q}|) + \frac{m_\mu^2}{(\Delta - |\boldsymbol{q}|)} \leqslant 2k_0 \leqslant (\Delta + |\boldsymbol{q}|) + \frac{m_\mu^2}{\Delta + |\boldsymbol{q}|} .$$

Integrating (3) over k_0 gives:

$$(5) \qquad P(q_0) = \frac{F(q_0, k_0') - F(q_0, k_0'')}{G(q_0, k_0') - G(q_0, k_0'')} ,$$

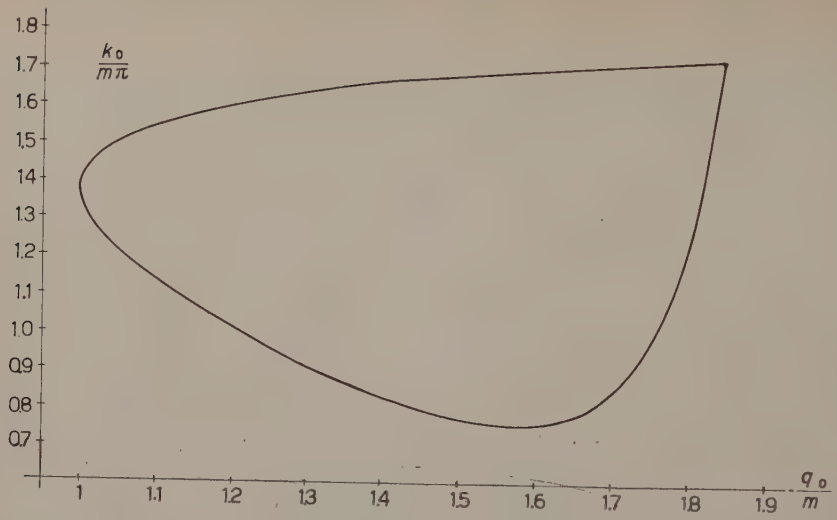

Fig. 3. – The allowed decay configurations.

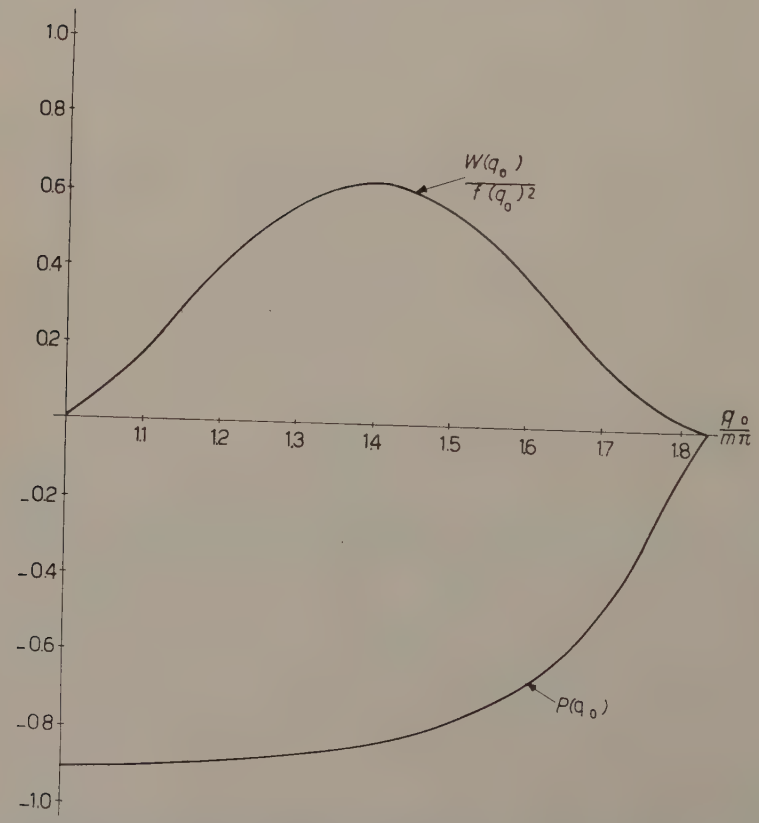

Fig. 4. – Integrated muon longitudinal polarization and differential energy spectrum as a function of pion energy.

where

$$F(q_0, k_0) = \tfrac{2}{3} a^2 k_0^2 |\boldsymbol{k}| - (a + m_\mu^2) a \Delta k_0 |\boldsymbol{k}| + \\ + \{\tfrac{1}{2}(a + m_\mu^2)^2 \Delta^2 - \tfrac{1}{2} a(a - m_\mu^2)(\Delta^2 - a) + (\Delta^2 - a) a m_\mu^2 + \tfrac{4}{3} a^2\} |\boldsymbol{k}| - \\ - \{(a + m_\mu^2) a + (\Delta^2 - a) m_\mu^2\} m_\mu^2 \log (k_0 + |\boldsymbol{k}|) ,$$

$$G(q_0, k_0) = \frac{1}{2} a(\Delta^2 - a)(a - m_\mu^2) k_0 - \frac{2}{3a} \left\{ k_0 a - \frac{1}{2} (a + m_\mu^2) \Delta \right\}^3$$

and k_0' (or k_0'') is the maximum (or minimum) value of k_0 given by eq. (4).

This function is plotted in Fig. 4 along with the differential pion energy spectrum divided by the square of the (unknown) function $|f(q_0)|^2$. One notices that the polarization is large and negative over most of the spectrum.

3. – Muon polarization as a function of muon energy.

It is perhaps of greater interest experimentally to determine the muon polarization as a function of the muon energy. Since the matrix element for decay is known only within a multiplicative factor depending on the pion energy, this polarization computation can be carried through only if some form is assumed for the function $f(q_0)$. The two obvious choices are to take either $f(q_0)$ or $g(q_0)$ to be a constant. The integration over the pion energies now gives, respectively:

$$P_f(k_0) = -\frac{k_0}{|\boldsymbol{k}|} + \frac{m_\mu^2 \{F_1(\Delta'', k_0) - F_1(\Delta', k_0)\}}{|\boldsymbol{k}| \{G_1(\Delta'', k_0) - G_1(\Delta', k_0)\}} , \tag{6}$$

where

$$F_1(\Delta, k_0) = \tfrac{1}{2}(2 m_K k_0 - m_\mu^2)\Delta^2 - (5 m_K^2 k_0 - m_\pi^2 k_0 - 2 m_K m_\mu^2)\Delta + \\ + (4 m_K k_0 - m_\mu^2)(m_K^2 - m_\pi^2) \log \Delta + (m_K^2 - m_\pi^2)^2 \frac{k_0}{\Delta} ,$$

$$G_1(\Delta, k_0) = -\frac{m_K}{2} \{3 m_\mu^2 + 4 m_K^2 - 8 m_K k_0\} \Delta^2 + \\ + \left\{ \left(6 m_K^2 + \frac{3}{2} m_\mu^2 \right)(m_K^2 - m_\pi^2) + 2 m_K^2 m_\mu^2 - \frac{1}{2} m_\mu^4 - 4 m_K (2 m_K^2 - 2 m_\pi^2 - m_\mu^2) k_0 - 8 m_K^2 k_0 \right\} \Delta + \\ + (m_K^2 - m_\pi^2) \{8 m_K k_0^2 + 2(m_K^2 - m_\pi^2 - m_\mu^2) k_0 - m_K (3 m_K^2 - 3 m_\pi^2 + 2 m_\mu^2)\} \log \Delta - \\ - \frac{(m_K^2 - m_\mu^2)^2}{2} \{m_K^2 - m_\pi^2 + m_\mu^2 - 4 k_0^2\} \frac{1}{\Delta} ,$$

with

$$\Delta'' = m_K - q_0'' ,$$

$$\Delta' = m_K - q_0' ,$$

and q_0', q_0'' are the maximum and minimum values of q_0 for a given k_0, and

$$P_e(k_0) = -\frac{k_0}{|\boldsymbol{k}|} + \frac{m_\mu^2\{F_2(a'', k_0) - F_2(a', k_0)\}}{m_K|\boldsymbol{k}|\{G_2(a'', k_0) - G_2(a', k_0)\}}, \tag{7}$$

$$F_2(a, k_0) = \frac{1}{2}(2m_K k_0 - m_\mu^2)a^2 + \{-4m_K(m_K^2 + m_\pi^2)k_0 - 3m_\mu^2(m_K^2 - m_\pi^2) + 4m_\mu^2 m_K^2\}a +$$
$$+ (m_K^2 - m_\pi^2)\{(m_K^2 - m_\pi^2)(2m_K k_0 - 3m_\mu^2) + 4m_\mu^2 m_K\}\log a + m_\mu^2(m_K^2 - m_\pi^2)^3\frac{1}{a},$$

$$G_2(a, k_0) = \frac{1}{2}(8m_K k_0 - 4m_K^2 - 3m_\mu^2)a^2 +$$
$$+ \{8m_K(m_K^2 - m_\pi^2 + m_\mu^2)k_0 - 16m_K^2 k_0^2 - (2m_K^2 - 6m_\pi^2)m_\mu^2\}a -$$
$$- (m_K^2 - m_\pi^2)m_\mu^2(3m_K^2 - 3m_\pi^2 + 2m_\mu^2 - 8m_K k_0)\log a + (m_K^2 - m_\pi^2)^2 m_\mu^4\frac{1}{a},$$

where

$$a = m_K^2 + m_\pi^2 - 2m_K q_0$$

and a' and a'' denote the values of a at q_0' and q_0''.

These expressions are plotted in Fig. 5 along with the differential muon energy spectrum.

These assumptions of a divergenceless current and constancy of $f(q_0)$ or $g(q_0)$ may be compared to the approximation employed by other authors that $f(q_0)$ and $g(q_0)$ are both constants independent of q_0. Then the ratio f/g can be obtained by matching the branching ratio of the $K_{\mu 3}$ and K_{e3} modes ([6]). In this manner, FUJII and KAWAGUCHI ([6]) obtained:

$$f/g = -4.9 \quad \text{or} \quad 0.56. \tag{8}$$

This gives two alternative predictions for the decay matrix element and muon polarizations ([7]). We give, for comparison, the muon polarization

$$P_{fs}(k_0) = -\frac{k_0}{|\boldsymbol{k}|} + \frac{m_\mu^2\{F_3(\Delta'', k_0) - F_3(\Delta', k_0)\}}{|\boldsymbol{k}|\{G_3(\Delta'', k_0) - G_3(\Delta', k_0)\}}, \tag{9}$$

$$F_3(\Delta, k_0) = \left\{\frac{1}{2}(2m_K k_0 - m_\mu^2)\Delta^2 - (m_K^2 - m_\pi^2)k_0\Delta\right\}f^2 +$$
$$+ m_K^2(\Delta^2 - 2K_0\Delta)fg + m_K^2\left(\frac{\Delta^2}{2} - k_0\Delta\right)g^2,$$

([6]) R. GATTO: *Phys. Rev.*, **111**, 1426 (1958); S. ONEDA: *Nucl. Phys.*, **9**, 476 (1959); A. FUJII and A. KAWAGUCHI: *Phys. Rev.*, **113**, 1156 (1959).

([7]) L. OKUN and S. G. MATINIAN: *Žurn. Èksp. Teor. Fiz.*, **36**, 1317 (1959); *Sov. Phys. Journ. Exp. Theor. Phys.*, **9**, 933 (1959).

$$G_3(\Delta, k_0) = \frac{m_\mu^2 m_K}{2}(\Delta^2 - 2K_0\Delta)f^2 + 2m_\mu^2 m_K\left(\frac{\Delta^2}{2} - k_0\Delta\right)fg +$$

$$+ m_K^2\left\{(\Delta^2 - 2k_0\Delta)k_0 - \frac{1}{2}m_K(\Delta^2 - 2K_0\Delta)\right\}g^2 ,$$

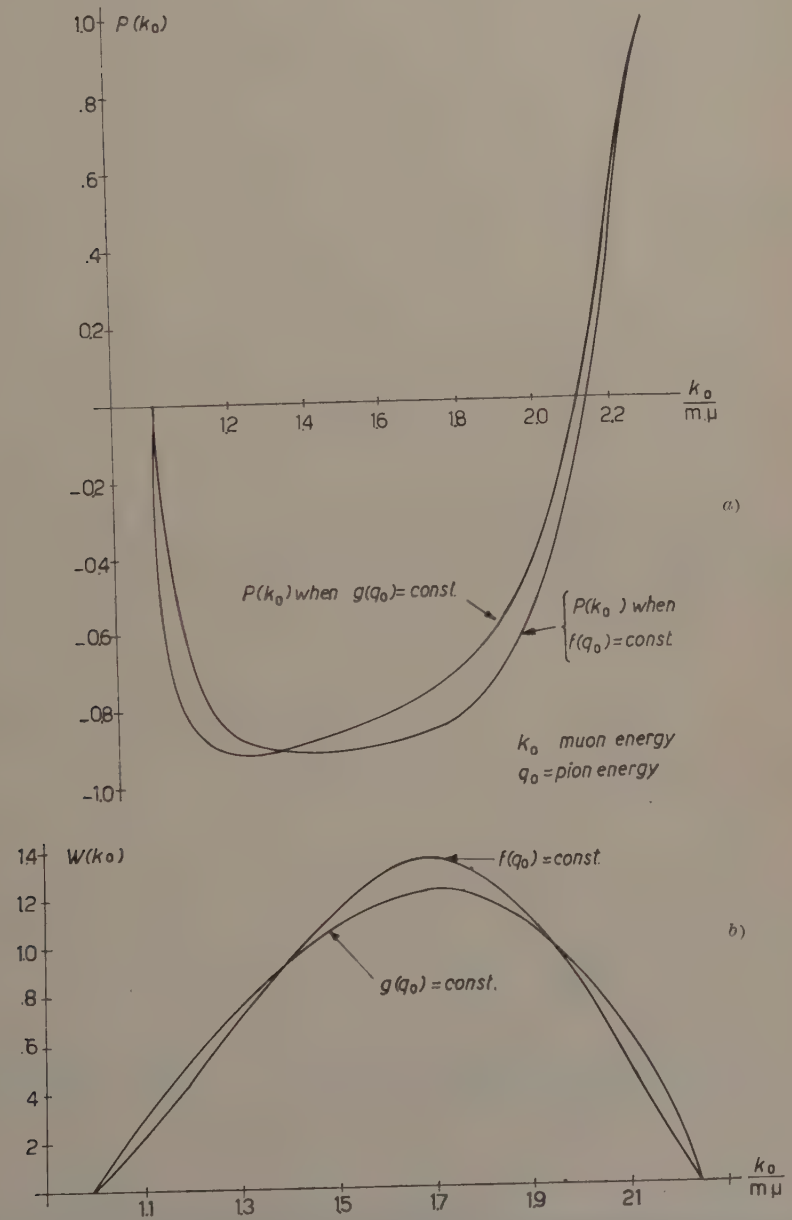

Fig. 5. – Integrated muon longitudinal polarization and energy spectrum as a function of muon energy.

where $K_0 = (m_K^2 - m_\pi^2 + m_\mu^2)/2m_K$ is the maximum muon energy, in Fig. 6. It may be possible to discriminate among the theoretically predicted expressions P_f, P_g and P_{fg} by direct measurement of the muon polarization. It

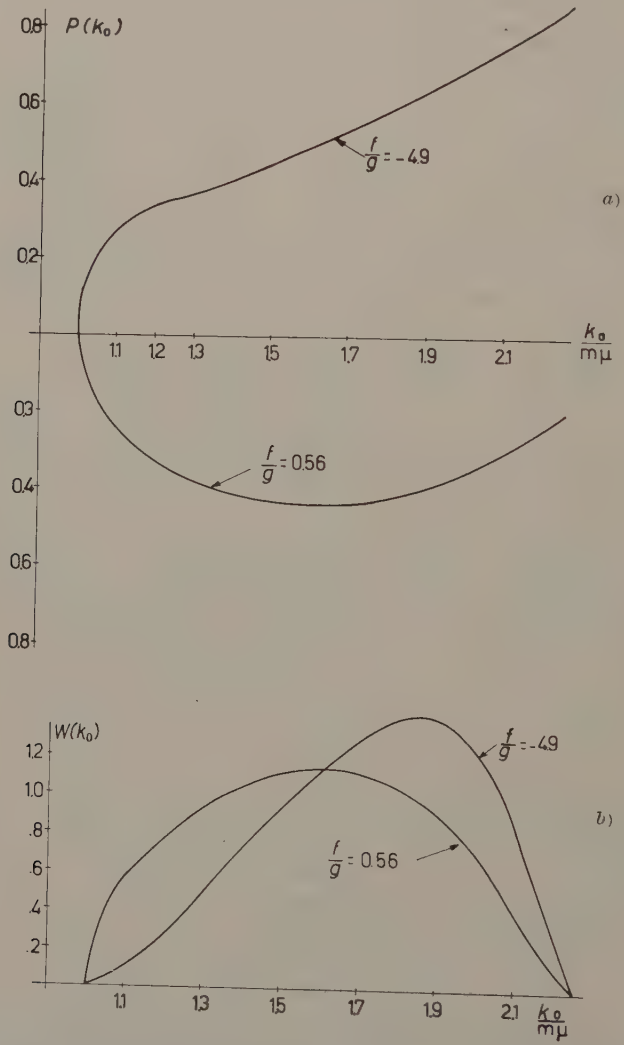

Fig. 6*a*). – Integrated muon longitudinal polarization as a function of muon energy under the assumption of constant $f(q_0)$ and $g(q_0)$. *b*) Muon energy spectrum under the assumption of constant $f(q_0)$ and $g(q_0)$.

appears that the polarization measurement may be easier than the pion-neutrino correlation measurement for testing the divergenceless current hypothesis. It may be noted that independent of the isotopic spin transformation pro-

perties of the interaction current, the polarization in the decays $K \to \pi^0 + + \mu^- + \bar{\nu}$ and $K^0 \to \pi^+ + \mu^- + \bar{\nu}$ are the same under the « divergenceless »-current hypothesis.

Finally, it should be remarked that we have derived the relation between the functions $f(q_0)$ and $g(q_0)$ under the assumption of a divergenceless current (2). However, a strictly conserved divergenceless current is not really required; it is sufficient that the divergence of the current has a vanishing matrix element between the one-kaon and one-pion states (8).

---

(8) Compare the discussion by S. Okubo: *Nuovo Cimento*: **13**, 292 (1959).

RIASSUNTO (*)

Si esamina l'ipotesi della corrente conservata nelle interazioni deboli nei decadimenti che non conservano la stranezza. Questa ipotesi rende possibile un calcolo non ambiguo della polarizzazione longitudinale del muone nel decadimento $K_{\mu 3}$ in funzione dell'energia del pione. I risultati vengono confrontati con quelli di Okun e Martinyan che non fecero uso della corrente conservata.

(*) *Traduzione a cura della Redazione.*

IL NUOVO CIMENTO Vol. XVI, N. 2 16 Aprile 1960

The Binding Energy of Λ-Particles in Nuclear Matter.

J. D. Walecka (*)

Department of Physics, Stanford University - Stanford, Cal.

(ricevuto il 4 Gennaio 1960)

Summary. — From an analysis of the existing data on the binding energy of Λ particles in hyperfragments a fairly reliable value of the binding energy of Λ particles in nuclear matter can be obtained. This value is $V_0 \approx 22$ MeV. It is proposed that this number gives an independent check on the validity of potentials deduced from the very light hyperfragments. Some simple calculations using the techniques of Brueckner *et al.* are carried out with the potential of Lichtenberg and Kovacs (which contains a hard core). It is found that if only s wave interactions are considered one finds good agreement with the above number. If higher partial waves are included one obtains far too much binding energy and it is suggested that the Λ-nucleon interaction may be weakened by an exchange force in these states.

1. – Analysis of experimental data.

The general behavior of the binding energy of Λ particles in hypernuclei as a function of the mass number has been discussed by Tati and Tati [1]. Their analysis can be extended so that one can obtain a fairly accurate value of the binding energy of Λ particles in nuclear matter even though the present data [2] do not run above $N = 12$. If one adopts the model in which the nucleons provide a potential well of depth V_0 for the Λ and in which if more nucleons are added the only effect is to change the radius of the well and not

(*) National Science Foundation Postdoctoral Fellow.

(1) T. Tati and H. Tati: *Nuovo Cimento*, **3**, 1136 (1956).

(2) *Proceedings of the Annual International Conference on High Energy Physics at CERN* edited by B. Ferretti, CERN (Geneva, 1958) pag. 182.

its depth, then by taking a radius parameter from the studies of the electromagnetic structure of nuclei (3) one can determine the parameter V_0 which gives the best fit to the data. The charge radius is used because of the short range of the Λ-nucleon force. One solves the elementary quantum mechanical problem

$$\left[-\frac{\hbar^2\nabla^2}{2\mu_\Lambda}+V(r)\right]\psi(\boldsymbol{r})=\varepsilon\psi(\boldsymbol{r}), \tag{A.1}$$

where

$$\begin{cases} V(r)=-V_0 & \text{for} \quad r<R=r_0(N-1)^{\frac{1}{3}} \\ V(r)=0 & \text{for} \quad r>R \end{cases} \tag{A.2}$$

and μ_Λ is the reduced mass of the Λ-nucleus system. One calculates the ground-state eigenvalues $\varepsilon_{V_0}(N)$ and, by comparing with the observed binding energy $B_\Lambda(N)$, the best value of V_0 can be obtained. $\varepsilon_{V_0}(N)$ is easily found by solving

$$s=\frac{1}{\sqrt{1-x}}\,ctn^{-1}\left[-\sqrt{\frac{x}{1-x}}\right], \tag{A.3}$$

where

$$s=\left[R^2\left(\frac{\hbar^2}{2\mu_\Lambda V_0}\right)\right]^{\frac{1}{2}}=(N-1)^{\frac{1}{3}}\left[\frac{(N-1)}{(N-1)+1.18}\right]^{\frac{1}{2}}\left[r_0^2\left(\frac{2m_\Lambda V_0}{\hbar^2}\right)\right]^{\frac{1}{2}}, \tag{A.4}$$

$$x=\frac{\varepsilon_{V_0}(N)}{V_0}$$

and the angle must lie between $\pi/2$ and π. Note that for large R one has

$$\varepsilon_{V_0}(N)=V_0-\frac{\hbar^2\pi^2}{2\mu_\Lambda R^2}\left[1-\frac{2}{s}+\frac{3}{s^2}+O\left(\frac{1}{s^3}\right)\right], \tag{A.5}$$

where the physical interpretation of the first two terms is self-evident.

The results are given in Fig. 1. A value of $r_0=1.3\cdot10^{-13}$ cm was used for the radius parameter. For the best fit (*)

$$V_0=21.7\ \text{MeV}. \tag{A.6}$$

---

(3) R. HOFSTADTER: *Rev. Mod. Phys.*, **28**, 214 (1956).

(*) After this work was completed, the author discovered that this value was already known to V. A. FILIMONOV: *Žurn. Eksp. Teor. Fiz.*, **36** (9), 1113 (1959), English translation.

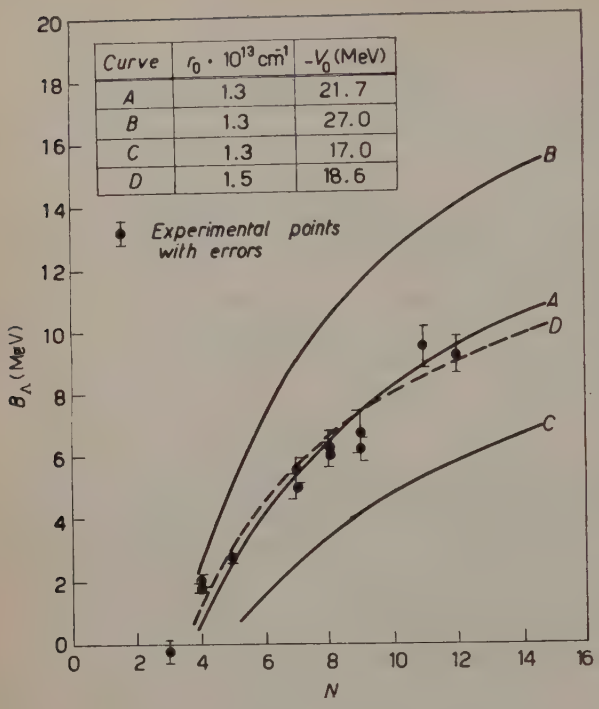

One point in favor of this analysis is that if V_0 is changed by 5 MeV in either direction curves are obtained which lie far outside of the experimental variation (see Fig. 1) and thus this value of V_0 seems quite reliable. Also plotted on Fig. 1 (for comparison) is a curve obtained for $r = 1.5 \cdot 10^{-13}$ cm V=18.6 MeV. This curve indicates that the value of V_0 is not oversensitive to the choice of radius parameter.

Fig. 1. – Binding energy of Λ particle *vs.* mass number of the hyperfragment.

2. – Theoretical analysis.

Very extensive work has been carried out on the analysis of the binding energy of Λ particles in the very light hyperfragments ($N < 5$) and its implications for the Λ-nucleon potential by DALITZ and DOWNS ([4]), LICHTENBERG ([5]), TRUONG ([6]), and others. On the other hand there has been considerable success recently, using methods developed by BRUECKNER and others, in calculating binding energies of nucleons in nuclear matter from the nucleon-nucleon interaction ([7-9]). It is proposed that the same techniques can be applied to Λ particles in nuclear matter and that V_0 provides an independent check on the validity of the Λ-nucleon potential as deduced from the light hyperfragments. For example, the analysis of the light hyperfragments determines chiefly the

([4]) R. DALITZ and B. DOWNS: *Phys. Rev.*, **111**, 967 (1958).
([5]) D. LICHTENBERG: *Nuovo Cimento*, **8**, 463 (1958).
([6]) T. TRUONG: *Effect of a hard core in the Λ-nucleon potential* (preprint).
([7]) K. BRUECKNER and J. GAMMEL: *Phys. Rev.*, **109**, 1023 (1958). (See this paper for earlier ref.).
([8]) H. BETHE and J. GOLDSTONE: *Proc. Roy. Soc.*, A **238**, 551 (1957).
([9]) L. C. GOMES, J. D. WALECKA and V. F. WEISSKOPF: *Ann. Phys.*, **3**, 241 (1958).

s wave Λ-nucleon interaction [4], while the present analysis is quite sensitive to the interaction in the higher angular momentum states.

In this paper only a few simple calculations will be carried out to provide an orientation. The potential of LICHTENBERG and KOVACS will be used [10](*)

$$\text{(B.1)}\qquad \begin{cases} v = \infty\,, & r < c\,, & v_0^1 = -\,672\ \text{MeV}\,, \\ v = v_0 \exp\,[-\,sr]\,, & r > c\,, & v_0^3 = -\,336\ \text{MeV}\,, \\ s = 1.62\,, & & \\ c = \ .6\,, & & \bar{v}_0 = \tfrac{1}{4}\,[3v_0^3 + v_0^1] = -\,420\ \text{MeV}\,, \end{cases}$$

where all lengths are measured in units of K_F^{-1} and from (9)

$$\text{(B.2)}\qquad K_F = 1.48 \cdot 10^{13}\ \text{cm}^{-1}\,.$$

For the Λ in its ground state, which in nuclear matter means the Λ at rest, there can be no real scattering as the Λ interacts with any of the nucleons, since even though there is no Pauli principle restricting the states of the Λ there is one for the nucleons. Therefore, there will be no phase shift in this state and the energy shift for the interaction with a nucleon in the state $\boldsymbol{K}_{\mathcal{N}}$ is given by [9]

$$\text{(B.3)}\qquad \Delta E = \frac{1}{\Omega}\int \exp\,[-\,i\boldsymbol{K}_0 \cdot \boldsymbol{x}]\, v(x)\, \psi(\boldsymbol{x})\, \mathrm{d}\boldsymbol{x}\,,$$

where ψ is the solution to the Bethe-Goldstone equation

$$\text{(B.4)}\qquad \begin{cases} \dfrac{\hbar}{2\mu}\,(\nabla^2 + K_0^2)\,\psi(\boldsymbol{x}) = v(x)\,\psi(\boldsymbol{x}) - \displaystyle\int G_{\mathrm{P}}(\boldsymbol{x}-\boldsymbol{y})\, v(y)\, \psi(\boldsymbol{y})\, \mathrm{d}\boldsymbol{y}\,, \\ G_{\mathrm{P}}(\boldsymbol{x}-\boldsymbol{y}) = \dfrac{1}{(2\pi)^3}\displaystyle\int_{\Gamma} \exp\,[i\boldsymbol{K}\cdot(\boldsymbol{x}-\boldsymbol{y})]\, \mathrm{d}\boldsymbol{K}\,. \end{cases}$$

Γ is the region in $\boldsymbol{K}$ space, $\boldsymbol{K} = \boldsymbol{K}_{\mathcal{N}} - (m_{\mathcal{N}}/(m_{\mathcal{N}} + m_{\Lambda}))\boldsymbol{P}$, such that $\boldsymbol{P}$ is held fixed and $\boldsymbol{K}_{\mathcal{N}}$ is given all values $|\boldsymbol{K}_{\mathcal{N}}| \leqslant K_F$. The following definitions are

---

[10] J. KOVACS and D. LICHTENBERG: *Nuovo Cimento*, **13**, 371 (1959).

(*) v_0 has been reduced by 15% in accordance with the footnote in ref. [10].

used:

$$\text{(B).5}\qquad \begin{cases} \boldsymbol{K} = \dfrac{1}{m_\Lambda + m_\mathcal{N}} [m_\Lambda \boldsymbol{K}_\mathcal{N} - m_\mathcal{N} \boldsymbol{K}_\Lambda] ; \\ \boldsymbol{P} = \boldsymbol{K}_\mathcal{N} + \boldsymbol{K}_\Lambda , \\ \boldsymbol{K}_0 = \left[\dfrac{1+\eta}{2}\right] \boldsymbol{K}_\mathcal{N} , \\ \eta = \dfrac{m_\Lambda - m_\mathcal{N}}{m_\Lambda + m_\mathcal{N}} , \\ \dfrac{1}{\mu} = \dfrac{1}{m_\mathcal{N}} + \dfrac{1}{m_\Lambda} . \end{cases}$$

The total energy shift is obtained by summing over all nucleons. By charge symmetry the Λ-n force is the same as the Λ-p force and by taking this to be the spin average $\bar{v}_0$ one finds

$$\text{(B.6)}\qquad E = \frac{4\Omega}{(2\pi)^3} \int_0^{K_F} \mathrm{d}\boldsymbol{K}_\mathcal{N} \Delta E(\boldsymbol{K}_0, \boldsymbol{P}) .$$

If one considers first the problem of a hard sphere Λ in a nucleus of hard spheres the energy shift can be written (*)

$$\text{(B.7)}\qquad E = \frac{\hbar^2 K_F^2}{2\mu} \cdot \left[\frac{8c}{3\pi} + \frac{8c^2}{\pi^2}\left(\frac{1}{3} - \frac{1}{2(1-\eta)}\left\{\frac{3-\eta^2}{6\eta} - \frac{1}{3} - \frac{(\eta^2-1)^2}{4\eta^2} \ln \frac{1+\eta}{1-\eta}\right\}\right) + O(c^3)\right] .$$

These first two terms in the power series expansion should be exact and can be obtained by studying the s wave projection of the B-G equation. p waves will begin to contribute in order c^3 and the leading term will be

$$\text{(B.8)}\qquad E_c^p = \frac{\hbar^2 K_F^2}{2\mu}\left[\frac{8c^3}{5\pi}\left(\frac{1+\eta}{2}\right)^2\right] .$$

It was shown in (9) that in the nuclear case one could get a good approximation to ψ by taking the solution to the hard-core problem alone. This is because the wave function must vanish at the core and go over to $\exp[i\boldsymbol{K}_0 \cdot \boldsymbol{x}]$ at distances $\approx \lambda_\pi$ and the attractive potential, which enters as $v_A/(\hbar^2 K_F^2/2\mu)$

(*) For a detailed treatment of the method of calculation see ref. (11).

(11) J. D. WALECKA: *Thesis* (Massachussetts Institute of Technology, 1958).

cannot do much to change things. The same approximation will be made here. This means

$$\Delta E = \frac{1}{\Omega}\int \exp\left[-i\boldsymbol{K}_0\cdot\boldsymbol{x}\right]\left[v_c(r)\,\psi_c(\boldsymbol{x}) + v_A(r)\,\psi_c(\boldsymbol{x})\right]\mathrm{d}\boldsymbol{x} = \Delta E_c + \Delta E_A \,. \tag{B.9}$$

and the energy separates into a part coming from the hard core and a part coming from the attractive well. For the former the power series expansion from above will be used. For the latter, the integral was evaluated for various analytical approximations to ψ_c. Considering first only the s wave interaction, since this is what the work on the light hyperfragments is sensitive to, one finds

$$\left\{\begin{array}{lll} & \underline{\psi_c^s} & \underline{E_A^s} \qquad\qquad \underline{E_A^s} \\ 1) & j_0(K_0x) & .267\bar{v}_0 \quad -112\ \text{MeV}\,. \\ 2) & \dfrac{\sin K_0(x-c)}{K_0x} & .162\bar{v}_0 \quad -68\ \text{MeV}\,. \\ 3) & j_0(K_0x) - j_0(K_0c)\,\dfrac{si(\beta x)}{si(\beta c)} & .216\bar{v}_0 \quad -91\ \text{MeV}\,. \end{array}\right. \tag{B.10}$$

where $\beta = 1.1$ and $si(x) = -\left[(\pi/2) - Si(x)\right]$.

Expression (3) gives a very good approximation to ψ_c for all $\boldsymbol{K}_0$ and $\boldsymbol{P}$ in the nuclear problem [12]. The actual correlation is essentially independent of $\boldsymbol{K}_0$ and $\boldsymbol{P}$ and since the Λ and nucleon see the same excluded volume Γ for $\boldsymbol{P} = 0$, expression (3) should also be a good approximation for the Λ-nucleon hard core problem.

To evaluate E_c one needs to know μ. If one takes into account the fact that the nucleon moves in a momentum-dependent potential, then $m_{\mathcal{N}}$ is replaced by an effective mass [8]

$$m^*_{\mathcal{N}} = 0.68\,m_{\mathcal{N}}\,. \tag{B.11}$$

No effective mass will be used for the Λ for two reasons. First, there are no exchange integrals arising from the Pauli principle as there are in the nuclear case and, second, it shall be assumed (to start with) that the Λ-nucleon space-exchange force is negligible. These are the major contributing factors in the nuclear case. Inserting this result gives

$$E_c = 68\ \text{MeV} \tag{B.12}$$

---

[12] L. C. GOMES: *Thesis* (Massachusetts Institute of Technology, 1958).

and combining this with the most reliable result, case 3, for the attractive energy yields

$$B_\Lambda^S = 23 \text{ MeV} . \tag{B.13}$$

in fairly close agreement with experiment.

If one now calculates the contributions to the binding energy coming from the higher angular momentum states,

$$\psi_c^{l>0} = \exp[-i\boldsymbol{K}_0 \cdot \boldsymbol{x}] - j_0(K_0 x) , \tag{B.14}$$

$$E_A^{l>0} = .103\, v_0 = -43 \text{ MeV} \tag{B.15}$$

$$E_c^P = 5 \text{ MeV} \tag{B.16}$$

and one finds far too much binding energy. Corrections to E_c coming from higher partial waves will be negligible. It is therefore difficult to see where the additional repulsion can come from unless the Λ-nucleon force is weakened in the higher angular momentum states. This would help in two ways. It cuts down $E_A^{l>0}$ and gives the Λ an effective mass which increases E_c (*).

The question arises whether one can find any evidence for such an exchange force coming from field theory. LICHTENBERG and ROSS have calculated the contribution of a Λ meson exchange to the Λ-nucleon force ([13]). They find that if the K is pseudoscalar, then in lowest order the force is attractive in s states and repulsive in p states which is just what is needed above (if the K is scalar the effect is reversed in the more heavily weighted triplet state). This correction appears to be too small to give the cancellation indicated by the above argument. These authors also include the effect of exchanging one π as well as one K. For pseudoscalar K this contribution is much larger than the lower order term and has the same sign in the singlet state while reversing sign in the triplet state (for a scalar K both singlet and triplet central potentials have the « wrong » sign, being repulsive in s states and attractive in p states). Since the effect of including one π exchange along with a K exchange is much larger than the effect of including only one K exchange and does not appreciably alter the *range* of the force, it is difficult to see what the effect of including more π mesons will be. There is also no reason here to expect that such effects will be suppressed as in the nucleon-nucleon case for whereas s wave $\pi + \mathcal{N} \to \pi + \mathcal{N}$ is known experimentally to be small, the Λ polarization in $\pi + \mathcal{N} \to \Lambda + \mathrm{K}$ indicates that s and p waves are of comparable importance in the production.

The preceding analysis indicates that the net result should be a Λ-nucleon exchange force attractive in s states and repulsive in p states.

(*) If $m_\Lambda^* = 0.68 m_\Lambda$ for example, then $E_c = 80$ MeV and $E_c = 4$ MeV.

([13]) D. LICHTENBERG and M. ROSS: *Phys. Rev.*, **109**, 2163 (1958).

3. – Conclusion.

From an analysis of the curve $B_\Lambda(N)$ it appears that the depth parameter determining the binding energy of Λ particles in nuclear matter is

$$V_0 \approx 22 \text{ MeV} .$$

This can be well accounted for by considering the s wave Λ-nucleon interaction through a potential determined from the light hyperfragments. When higher partial wave interactions are included, one obtains far too much binding energy and it is suggested that a weakening of the Λ-nucleon interaction in these states may be necessary to counteract this.

* * *

The author is greatly indebted to Professor S. D. Drell for several interesting discussions and suggestions.

RIASSUNTO (*)

Da un'analisi dei dati esistenti sull'energia di legame delle particelle Λ negli iperframmenti si può ottenere un valore abbastanza attendibile dell'energia delle particelle Λ nella materia nucleare. Questo valore è $V_0 \approx 22$ MeV. Si avanza l'ipotesi che questo valore offra un controllo autonomo sull'attendibilità del valore dei potenziali dedotti da iperframmenti molto leggeri. Alcuni semplici calcoli usando le tecniche di Brueckner *et al.* vengono eseguiti col potenziale di Lichtenberg e Kovacs (che contiene un « hard core »). Se si considerano solo interazioni dell'onda s si trova un buon accordo con il dato precedente. Se si includono onde parziali superiori si ottiene una energia di legame troppo elevata e si suggerisce quindi che l'interazione Λ-nucleone possa essere indebolita da una forza di scambio fra questi stati.

(*) *Traduzione a cura della Redazione.*

IL NUOVO CIMENTO Vol. XVI, N. 2 16 Aprile 1960

Circular Polarization of External Bremsstrahlung from Beta Emitters.

A. Bisi, A. Fasana and L. Zappa

Istituto di Fisica del Politecnico - Milano

(ricevuto il 12 Gennaio 1960)

Summary. — The results of an investigation concerning the circular polarization-energy relation of the external bremsstrahlung radiation produced by β-rays from various β-emitters are reported. It was found that at the upper limit of the spectra the circular polarization of the EB quanta corresponds to a longitudinal polarization of β^--rays equal to: $-(1.05\pm0.04)\,v/c$ (^{32}P); $-(0.98\pm0.03)\,v/c$ (^{90}Y); $-(0.98\pm0.02)\,v/c$ (^{170}Tm). At the lower energy side of the spectra the circular polarization was found very high and larger than that estimated on the basis of present knowledge. Account is given of the attempts made by us to ascertain how the events which occur before an EB quantum is radiated contribute to the measured polarization-energy relation.

1. – Introduction.

A number of works on circular polarization of external bremsstrahlung (EB) produced by β-rays have appeared in literature ([1-6]). These works seem to have been mainly intended to demonstrate the existence of the EB circular polarization and to show that its amount is as large as should be expected on the basis of our present knowledge.

The intrinsic difficulties of these measurements, added to the fast developing techniques for analyzing polarization, give rise to large errors that

([1]) M. Goldhaber, L. Grodzins and A. W. Sunyar: *Phys. Rev.*, **106**, 826 (1957).

([2]) H. Schopper and S. Galster: *Nuclear Physics*, **6**, 125 (1958).

([3]) F. Bohem and A. H. Wapstra: *Phys. Rev.*, **109**, 456 (1958).

([4]) S. C. Cohen, R. Wiener, M. Wald and M. Shmorak: *Proc. Rehovoth Conf. Nucl. Structure* (Amsterdam, 1958), p. 404.

([5]) A. Bisi and L. Zappa: *Nuclear Physics*, **10**, 331 (1959).

([6]) U. Amaldi jr., M. Bernardini, P. Brovetto and S. Ferroni: *Nuovo Cimento*, **11**, 415 (1959).

affect the results as a whole. Some information in fact is available as a by-product obtained when checking the polarimeter in the course of investigations on β-γ circular polarization correlation.

Though we are quite aware that further improvements in the experimental apparatus can be reached, a careful use of some of the present techniques can actually give a polarization versus EB energy relation with an accuracy of 5% or thereabout. Such an accuracy is quite sufficient when investigating up to where the present theories and calculations can account for the experimental results. From this comparison it is not convenient to attempt to extract information on the longitudinal polarization of the β-particles, as there are direct methods to obtain the β-ray polarization. The comparison is however quite useful because of the intrinsic interest of the bremsstrahlung process and since other phenomena affect the experimental results when EB is produced in thick targets.

To clarify this point let us summarize the events which occur before the EB quantum is radiated. The phenomenon starts with the emission of a β^- particle from a radioactive nucleus, having a degree of longitudinal polarization equal to $-v/c$; then the particle penetrating matter loses energy and is deviated from its original direction. A decrease in polarization follows, which depends on the atomic number of the target and the length of the electron path. At this point we are interested in the emission of an EB quantum whose energy is nearly the same as that of the radiating electron; as it is well known the emission cross-section is a function of the electron and quantum energies and of the atomic number of the target. It turns out that the longitudinal polarization of the electron gives rise to a right circular polarization of the external bremsstrahlung, the transfer efficiency from electron longitudinal polarization to photon circular polarization depending on the ratio of photon to electron energy and the emission angle.

In the following sections we shall give an account of the attempts made by us to see how the events just described contribute in yielding the measured relation between EB circular polarization and energy. For this investigation we have employed samples of ^{32}P, ^{90}Y and ^{170}Tm whose β^- decay is well known.

2. – Measuring techniques and results.

The features of the β sources and of the targets used to produce EB were as follows:

^{32}P: a sample of about 30 mC with a specific activity greater than 1 C/mg was used. The active area was about 1 cm^2. The sample was backed and covered with iron targets, as the same sample was employed for a different investigation.

^{90}Y: a β sample of 40 mC of ^{90}Sr in equilibrium with its daughter ^{90}Y was used. The ^{90}Sr-carbonate was dispersed in a layer of silver 0.05 cm thick; it was backed with silver and covered by targets of Al, Fe, Cu, Ag, Pb respectively in the various measurements.

^{170}Tm: a disc of 4 mm$\times$0.4 mm containing 50 mC of ^{170}Tm as Tm_2O_3 enclosed in a Birmabright aluminium alloy capsule was used. The EB was produced mainly in the source itself. A layer of silver (570 mg/cm^2 thick) covered the sample so as to reduce the intensity of low energy γ- and X-rays arising from the decay.

The circular polarization of the EB quanta was analyzed through forward Compton scattering with polarized electrons in magnetized iron; the experimental apparatus and the experimental procedure were the same as described in a previous work ([5]). Here we summarize only the essential points which interest the discussion of the experimental results.

In general the apparatus is sensitive to circular and plane polarization of quanta, the sensitivity being only in the first case dependent on the magnetic field direction ([7]). Then the percentage differences of counting rates for opposite directions of polarimeter magnetization yield to EB circular polarization degree when the absence of planeness of the radiation is assured. In this connection it shall be pointed out that the EB plane polarization is detectable when the emission plane is fixed and that its degree depends on the emission angle, dropping to zero for emission angle equal to zero ([8]). In our case we are observing mainly forward bremsstrahlung and are not making selection of emission plane because of the geometric features of sources and targets.

The polarimeter circular polarization efficiency ε, defined as the fractional change in intensity of scattered quanta on reversing the field direction for a source of completely right polarized γ-rays, can be calculated as a function of the fraction of polarized electron per atom, v/Z and of the initial and final photon momenta $\boldsymbol{k}_0$ and $\boldsymbol{k}$ ([5]). Then the degree of EB circular polarization P_c is given by

$$P_c = 2\,\frac{\Delta}{\Sigma}\cdot\frac{1}{\varepsilon}\,, \tag{1}$$

where Δ and Σ are respectively the difference and the sum of the counting rates obtained on reversing the polarimeter magnetization, when corrected for the intrinsic resolution of the scintillation spectrometer, the Compton electron distribution and the energy spread of the polarimeter.

([7]) H. A. Tolhoek: *Rev. Mod. Phys.*, **28**, 277 (1956).
([8]) J. W. Motz and R. C. Placious: *Phys. Rev.*, **112**, 1039 (1958).

The Δ and Σ pulse distributions were measured by means of a $1\frac{1}{2}$ in. diameter per 1 in. thick NaI(Tl) crystal coupled through a 10 cml ucite light pipe to an EMI 9514 photomultiplier. After amplification the pulses were fed into a ten channel pulse height analyzer. In order to eliminate any residual influence of the magnetic stray field on the photomultiplier, three iron shields and a compensating coil were used coaxially with the photomultiplier.

Table I contains the measured polarization P for the three β sources, as a function of the quantum energy together with the calculated ones according to the method discussed in the next section. As an example Fig. 1 shows these polarizations in the case of ^{32}P.

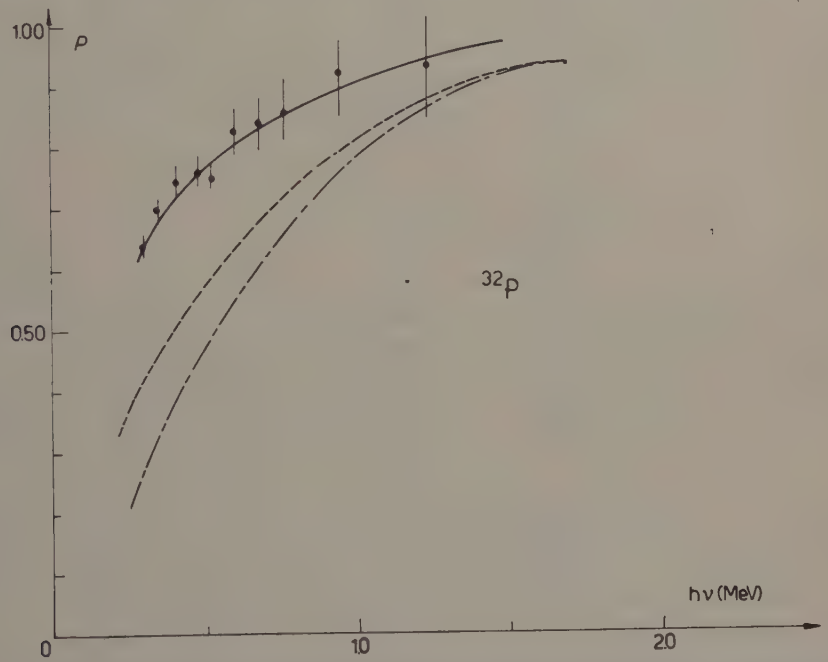

Fig. I. – Circular polarization of EB from β-rays of ^{32}P as a function of quantum energy. The upper dashed line represents the calculated relation for $Z=0$, the lower one that for $Z=25$.

As regards the accuracy of the present measurements a few comments are necessary. Errors can arise from: *a*) the uncertainty in the number of polarized electrons per iron atom. In our case the v/Z ratio was determined with the polarimeter in working conditions and the accuracy is probably better than 2%; *b*) the uncertainty in the calculation of the polarimeter efficiency. The error involved is not likely to be greater than a few percent; *c*) the influence of the polarimeter magnetic stray field on the photomultiplier. As a typical result of the percentage difference of the counting rates when the

TABLE I. - *Comparison between P calculated and P measured versus quanta energy for various β emitters.*

β emitter (atomic number of the target)	EB quantum energy (MeV)	P (calculated) %		P (measured) %	
		eq. (11)	eq. (6)		
^{32}P ($Z = 26$)	0.300	26.5	—	63.7	(1.3)
	0.345	31.0	—	69.7	(1.5)
	0.410	37.0	—	74.2	(1.9)
	0.480	43.5	—	75.6	(2.1)
	0.525	47.0	—	75.2	(2.7)
	0.600	53.2	—	83.2	(3.8)
	0.680	59.5	—	83.8	(4.2)
	0.755	65.0	—	85.9	(5.0)
	0.940	76.1	—	92.0	(6.9)
	1.230	87.5	—	9.30	(9.8)
^{90}Y ($Z = 47$)	0.540	34.0	41.2	61.2	(1.2)
	0.715	47.0	—	68.8	(1.7)
	0.930	60.0	—	76.0	(2.3)
	1.10	68.7	68.2	81.7	(2.9)
	1.23	74.5	—	82.1	(3.5)
	1.36	79.0	—	90.8	(4.5)
	1.51	83.7	83.5	88.5	(5.4)
	1.69	88.5	—	93.0	(6.5)
	1.88	92.0	—	88.8	(8.4)
	2.09	94.5	94.5	87.6	(11.3)
^{170}Tm ($\bar{Z} = 37.2$)	0.230	13.0	—	24.4	(1.22)
	0.280	21.0	—	34.6	(1.48)
	0.340	29.5	—	41.8	(1.9)
	0.400	38.0	—	45.8	(2.3)
	0.460	45.5	—	52.2	(2.8)
	0.540	54.7	—	61.8	(4.2)
	0.610	61.7	—	63.3	(5.4)
	0.660	66.2	—	68.0	(6.4)
	0.720	71.0	—	72.9	(7.5)
	0.780	75.0	—	81.0	(9.6)

polarimeter magnetization is reversed we have obtained: $(4 \pm 8) \cdot 10^{-4}$; *d*) the uncertainty in the corrections to be applied to the measured Δ and Σ distributions in order to obtain the « true » ones. As the correction is small (less than 10% in the energy ranges of interest), it affects the polarization values to an extent amounting to one or two percent.

In Table I, in parenthesis, and in the graphs the quoted errors are only statistical and represent the standard deviations of the mean. They were

found quite consistent with what is to be expected on the basis of both the counting rates and the drifts of the whole electronic apparatus.

When the various sources of errors are considered, one can estimate that the curves fitting the experimental points and shown in Figs. 1, 3, 4, 5, are accurate within about 5%.

3. – Calculated polarizations.

For the purpose of correlating the photon circular polarization with energy, the following considerations on the events occurring before the emission of an EB quantum, which have been summarized in Section **1**, are made:

a) *Depolarization of electrons in matter.* The depolarizing effect of the matter on the electron is described by the following equation, where ζ_l is the net electron longitudinal polarization

$$\zeta_l = (-v/c)\cdot\exp\left[-\int_{E_0}^{E}\gamma\left(\frac{\mathrm{d}E}{\mathrm{d}x}\right)^{-1}\mathrm{d}E\right] = (-v/c)\exp\left[G(E_0)-G(E)\right] \tag{2}$$

if initially the polarization is $-v/c$ and the energy E_0; $\mathrm{d}E/\mathrm{d}x$ represents the energy loss and does not require particular comments. The quantity γ was firstly calculated by ROSE and BETHE [9]; recently the electron depolarization was reinvestigated by various authors. In particular, NEAMTAM [10] has given a useful tabulation of the function $G(E)$ for various atomic numbers, which we shall use in what follows.

b) *Emission cross-section.* The EB spectral distribution observed by us consists mainly of hard quanta to which corresponds a very low final energy of the electron. Then the cross-sections interesting our problem are those typical of the high frequency limit to which corresponds the break-down of the well known Bether-Heitler [11] formula. Though there are more approximate expressions, we shall use for our calculations the following rough formulae:

$$\begin{cases} a) \quad \sigma \propto \dfrac{1}{h\nu}, \\ b) \quad \sigma \propto \dfrac{1}{h\nu}\left(1-\dfrac{3}{4}\dfrac{h\nu}{E}\right), \\ c) \quad \sigma \propto \dfrac{1}{h\nu}\left(1-0.86\dfrac{E}{h\nu}\right)\dfrac{E+mc^2}{E}. \end{cases} \tag{3}$$

---

[9] M. E. ROSE and H. A. BETHE: *Phys. Rev.*, **55**, 277 (1939).
[10] S. M. NEAMTAM: Private communication.
[11] H. BETHE and W. HEITLER: *Proc. Roy. Soc.*, A **146**, 83 (1934).

The first one takes into account only the dependence on quantum energy, the second was given by WYARD ([12]) and the third is intermediate between those given by BETHE and HEITLER ([11]) and by ELWERT ([13]).

c) Transfer efficiency from electron longitudinal polarization to photon circular polarization. The transfer efficiency $P_{c,l}/\zeta_l$ was calculated by MCVOY ([14]) and by FRONSDAL and ÜBERALL ([15]). Their results showed that the efficiency is nearly 0.95, at least for forward quanta and at high frequency limit. Numerical computations made by them for initial electron energy $E = 2.0$, 2.5 MeV and for emission angles 0°, 2°, 5°, 10°, 30° showed that the transfer efficiency is little affected by the emission angle and rises with the quantum energy with a nearly linear trend. In view of the failure of more extensive numerical computations we shall assume for our purpose the independence of transfer efficiency from the emission angle, as also a linear trend for any values of the electron energy. That is, we shall use the expression

$$\frac{P_{c,l}}{\zeta_l} = \frac{h\nu}{E}\left(1 + \frac{1-\beta}{2-\beta}\cdot\frac{E+2mc^2}{E}\right)^{-1} . \tag{4}$$

Starting with an electron of initial energy E_0, the circular polarization of a photon of energy $h\nu$ emitted when the electron has attained an energy E, can be written as

$$P_c = \frac{\int_E^{E_0} \zeta_l \sigma \frac{P_{c,l}}{\zeta_l} \frac{\mathrm{d}x}{\mathrm{d}E}\,\mathrm{d}E}{\int_E^{E_0} \sigma \frac{\mathrm{d}x}{\mathrm{d}E}\,\mathrm{d}E} . \tag{5}$$

By considering that the β spectrum is continuous, the expression (5) must be weighted over the β spectral distribution, so that

$$\overline{P} = \int_{E_0}^{E_{\max}} P_c I(E_0)\,\mathrm{d}E_0 . \tag{6}$$

Numerical calculations of eqs. (5) carried out in the case of ^{90}Y, by using the cross-sections 3 *a*), *b*), *c*), have shown that eq. (5) is rather insensitive to

---

([12]) S. J. WYARD: *Proc. Phys. Soc.*, A **65**, 377 (1952).
([13]) G. ELWERT: *Ann. d. Phys.*, **34**, 178 (1939).
([14]) K. W. MCVOY: *Phys. Rev.*, **106**, 828 (1957); **111**, 1484 (1958); **110**, 1333 (1958).
([15]) G. FRONSDAL and H. ÜBERALL: *Phys. Rev.*, **111**, 580 (1958).

the assumptions made about the dependence of the cross-section on energy. That holds even more for eq. (6). The reason for this insensitivity lies in the fact that the dominant contribution to eq. (6) comes from the transfer efficiency and from the β spectral distribution. As an example, we are reporting in Fig. 2 the calculated value of P_c as a function of E_0 for ^{90}Y.

These results suggest that a different approximate calculation should be made, which besides being numerically easier and faster, allows us moreover to deal separately with the events which occur before the emission of an EB quantum. We proceed by considering that a quantum of energy $h\nu$ can be radiated by an electron whose initial energy E_0 lies in the range between $h\nu$ and E_{max}. The mean value of E_0 is

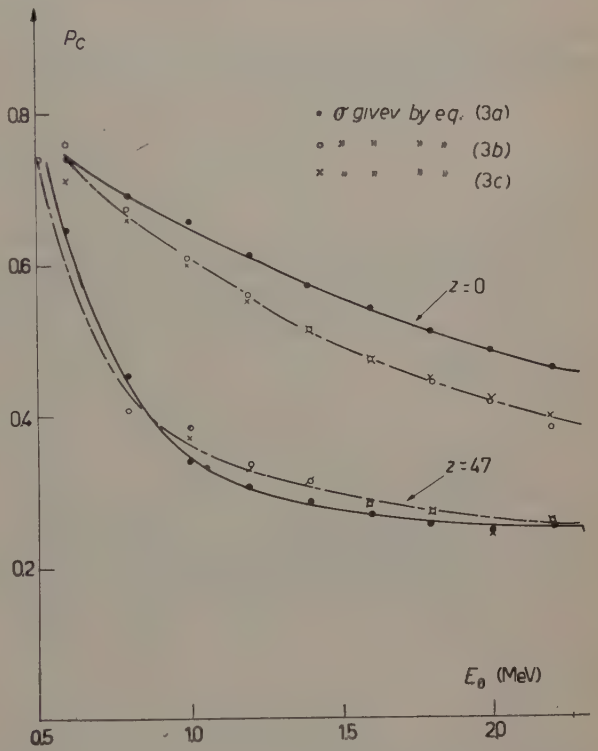

Fig. 2. – Calculated values of P_c from eq. (5) as a function of β-ray energy with different approximations for the EB cross-section.

$$\bar{E}_0 = \int_{h\nu}^{E_{max}} E_0 I(E_0)\, dE_0 . \tag{7}$$

The fictitious electron of energy $\bar{E}_0$ radiates a quantum of energy $h\nu$ when it has attained an energy $\bar{E}$ where

$$\bar{E} = \frac{\int_{h\nu}^{\bar{E}_0} E\sigma\, dE}{\int_{h\nu}^{\bar{E}_0} \sigma\, dE} . \tag{8}$$

By using eq. (3*b*), one obtains numerically:

$$\bar{E} = 0.559\, \bar{E}_0 + 0.441 \left(\frac{h\nu}{mc^2} + 1 \right) . \tag{9}$$

With these values of $\bar{E}_0$ and $\bar{E}$, the depolarizing effect of the matter is described by

$$P(\bar{E}) = P(\bar{E}_0) \exp\left[G(\bar{E}_0) - G(\bar{E})\right], \tag{10}$$

and the transfer efficiency is given by eq. (4) evaluated at $E = \bar{E}$. Then the circular polarization of the EB quanta results to be

$$\bar{P} = P(\bar{E}) \cdot \left(\frac{P_{c,l}}{\zeta_l}\right)_{E=\bar{E}} \qquad (\bar{E} \geqslant h\nu) . \tag{11}$$

In Table I the values calculated according to eq. (11) in the case of ^{90}Y are compared with those obtained with the more exact numerical calculations: as can be seen the rough approximation gives about the same results as the second one. For that reason we shall make use of eq. (11) to discuss our experimental results.

4. – Conclusions.

The comparison between our experimental results and the rough calculation just described is shown in Figs. 3, 4 and 5 in which the measured values are plotted against the calculated ones. The measured values fit, within the errors, a straight line. We shall now discuss separately the upper limit of the polarizations, which occur at the end point of the β and EB spectra, and the slope of the obtained straight lines.

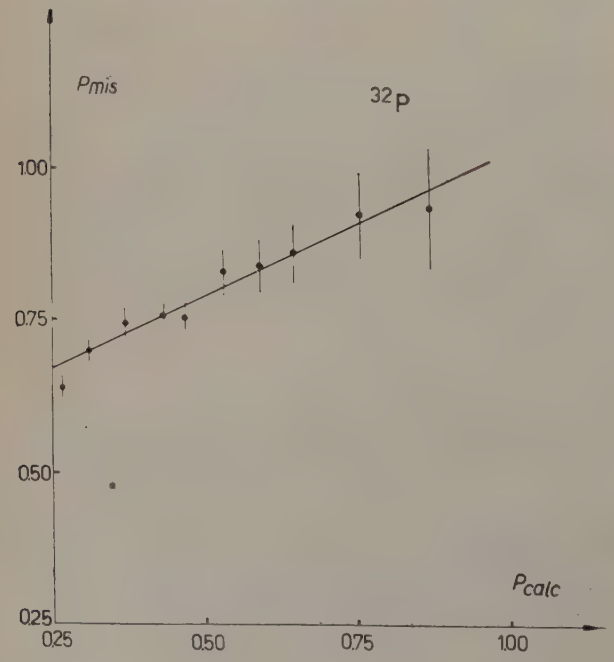

Fig. 3. – Measured polarizations of EB from β-rays of ^{32}P in Fe versus calculated ones.

a) *Upper limit of the spectra.* The quanta at the high frequency limit of EB spectra are emitted

from β^--rays at the spectral end point, that is from electrons which lose their whole energy in a radiative collision. Obviously only the transfer efficiency given by eq. (4) is of interest in establishing the degree of photon circular polarization P_{max}. As a direct measurement of P_{max} is impracticable, its value can be obtained with a total error not exceeding 5%, by extrapolating the straight lines to the polarization calculated at the end point of the β^--spectrum. The corresponding longitudinal polarizations of the β^--rays are collected in Table II.

As can be seen, our results are quite consistent with full $-v/c$ electron polarization and do not seem to be affected by systematic errors exceeding a few percent. This favourable check warrants the reliability of the facts on the basis of which the following subsection is discussed.

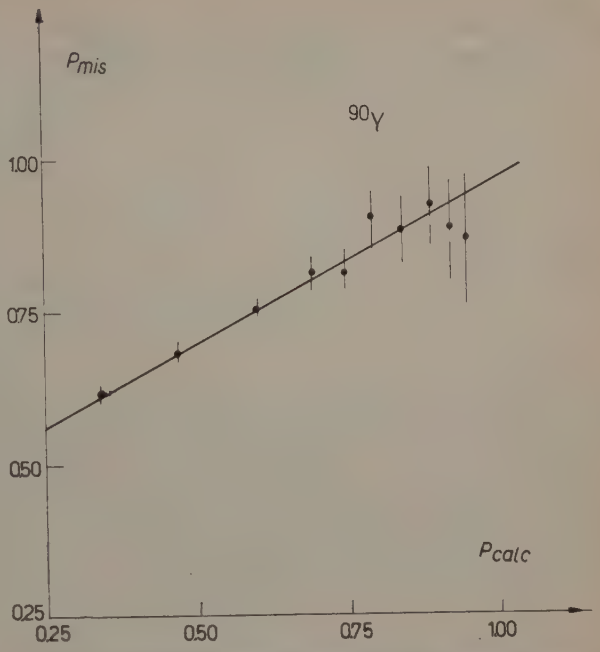

Fig. 4. – Measured polarizations of EB from β-rays of ^{90}Y in Ag versus calculated ones.

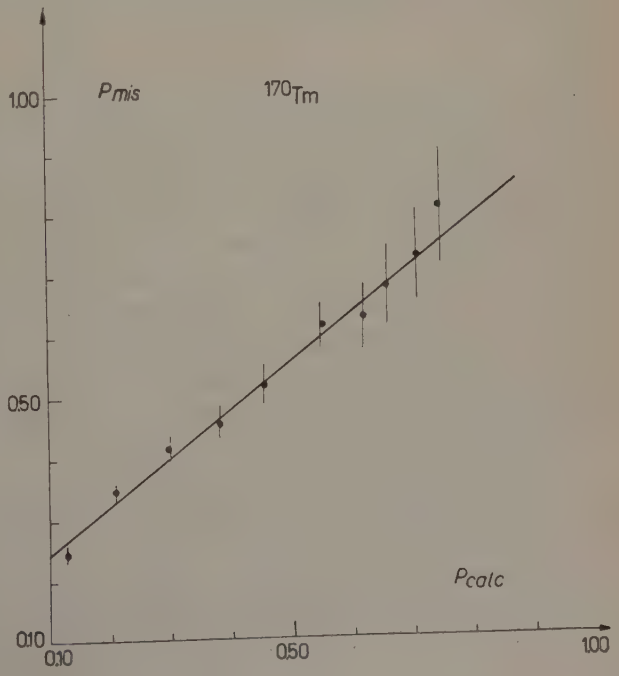

Fig. 5. – Measured polarizations of EB from β-rays of ^{170}Tm in Tm_2O_3 versus calculated ones.

TABLE II. – *Longitudinal polarization of β^--rays at the upper limit of the spectra, deduced by EB measured circular polarization.*

Source	Target	Longitudinal polarization of β^--rays at the upper limit of the spectra
^{32}P	Fe	$-(1.05 \pm 0.04)\, v/c$
^{90}Y	Al	$-(0.96 \pm 0.03)\, v/c$
	Fe	$-(0.99 \pm 0.02)\, v/c$
	Cu	$-(1.04 \pm 0.04)\, v/c$
	Ag	$-(0.94 \pm 0.03)\, v/c$
	Pb	$-(0.93 \pm 0.04)\, v/c$
^{170}Tm	Tm_2O_3	$-(0.98 \pm 0.02)\, v/c$

b) *Slope of the straight line.* The slopes of all the obtained lines are larger than unity showing that the measured values disagree from the calculated ones to an extent which increases with decreasing energy. The desagreement reaches a factor of about 2.5 at the lower energy side of the measured spectra.

By considering the role which the different factors quoted in the preceding section play in the calculation of the polarization degree, it appears reasonable to assume that the disagreement arises from the drastic assumptions regarding the transfer efficiency as given by eq. (4). In fact an incorrect estimation of the depolarizing effect of matter does not seem to be called in question, because for ^{32}P and ^{90}Y the measured polarizations are larger (at least near the lower energy side) even than those calculated under the extreme assumption of an ideal undepolarizing matter. A transfer efficiency with a rather flat dependence on energy at least near the high frequency limit, would account satisfactorily for our measurements, but at present there is no theoretical consideration justifying a similar hypothesis.

Another point which should be taken into account is the dependence of the transfer efficiency on the emission angle: conceivably an angular dependence, at electron energies lower than 2.0 MeV, more prominent than that shown by FRONSDAL and ÜBERALL, could effect the numerical calculation of eq. (5). It must be emphasized that the calculations of MCVOY and of FRONSDAL and ÜBERALL, whose results we have used in approximating eq. (4), are based

on the Born approximation and are numerically available only for 2.0 and 2.5 MeV electrons: therefore a generalization to our practical cases would have been rather arbitrary.

RIASSUNTO

Sono riportati i risultati di una ricerca per la determinazione sperimentale della relazione polarizzazione circolare-energia della bremsstrahlung esterna prodotta da vari emettitori β^-. Si è trovato che al limite superiore dello spettro la polarizzazione circolare dei quanti di bremsstrahlung corrisponde a una polarizzazione longitudinale delle particelle β^- rispettivamente uguale a: $-(1.05 \pm 0.04)\, v/c$ (^{32}P); $-(0.98 \pm 0.09)\, v/c$ (^{90}Y); $-(0.98 \pm 0.02)\, v/c$ (^{170}Tm). Nella regione di bassa energia dello spettro il grado di polarizzazione misurato è superiore al valore calcolato in base alle attuali conoscenze. Si esaminano infine i diversi eventi che precedono l'emissione del quanto discutendone la possibile influenza sul grado di polarizzazione misurato.

IL NUOVO CIMENTO Vol. XVI, N. 2 16 Aprile 1960

On the Origin of Super-Selection Rules.

S. T. Epstein

University of Nebraska - Lincoln, Nebr.

(ricevuto il 9 Febbraio 1960)

Summary. — It is shown that all the usually assumed super-selection rules follow from the fact that in any experiment one starts with definite numbers of each kind of particle.

In this note we wish to point out that the fact (1) that *in any experiment one starts with definite numbers of each kind of particle* (2) is already sufficient to lead to the usually assumed super-selection rules (3). Before demonstrating this we will first sketch some of the background for our considerations.

Some time ago Wick, Wightman and Wigner (3) suggested that there probably exists a set of observables W which commutes with all observables (and thus is a set of mutually commuting constants of motion since the energy is certainly an observable) and showed that the existence of this set would lead to what are called super-selection rules. Quantities which have been sug-

(1) From an experimental point of view the use of the word « fact » seems quite justified. To attempt to give it a deeper theoretical basis would presumably involve a considerable discussion of the measuring process. See also G. Feinberg and S. Weinberg: *Nuovo Cimento*, **14**, 571 (1959).

(2) By « particle » we mean any localizable, recognizable entity, stable or unstable elementary or compound. Note also that in a single set-up there may be several experiments each with a different starting situation. For example, we may start a meson production experiment by having two protons collide, and we may then start a meson decay experiment by isolating one of the produced mesons.

(3) G. C. Wick, A. Wightman and E. P. Wigner: *Phys. Rev.*, **88**, 101 (1950).

gested as belonging to this set include charge, baryon number, lepton number, and fermion parity (± 1 as one is dealing with an even or an odd number of fermions). However except for the case of fermion parity no proof [4] was offered that they *must* belong to the set W. It is with this problem of proof that our note is concerned.

First of all we remark that the original definition of W as the set of observables commuting with all observables is a circular one unless we make more precise what we mean by an observable [5]. However this definition is sufficient to imply that every realizeable pure state must be an eigenstate of W. Namely we suppose we could prepare a state ψ which is not an eigenstate of W:

$$\psi = \psi_1 + \psi_2 ,$$

where ψ_1 and ψ_2 are eigenstates of W belonging to different eigenvalues. Now the point is that this state is an eigenstate of its own projection operator P ($P\psi = \psi$, $P\psi' = 0$ if ψ' is orthogonal to ψ) and since, by hypothesis, we can prepare the eigenstates of P, P must certainly be counted as an observable, whence we have a contradiction since P obviously does not commute with W. Thus we may say that the set W is more than conserved, it is superconserved since one is always in an eigenstate of W. Conversely if a quantity R is superconserved, then it belongs to W.

With this background the proof of our opening statement becomes very simple: First of all it is now clear that if a quantity R is such that i) every state containing definite numbers of each kind of particle is an eigenstate of R, and ii) it is conserved, then R is a member of W. Namely from i) it follows that we always start with an eigenstate of R and from ii) it follows that we stay in an eigenstate whence R is super-conserved and hence belongs to W. Finally it is trivial to verify that, with the usually assumed Hamiltonians, the only operators satisfying these conditions are just those Already suggested. *q.e.d.*

In conclusion we remark that energy, momentum and angular momentum satisfy ii) but not i) whereas the number of protons, for example, satisfies i) but not ii). Thus the quantities which are super-conserved according to i) and ii) differ from those which are merely conserved in that the former are determined only by the nature of the particles involved (in field theory they generate simple constant phase gauge transformation) and not by their state of motion, whereas the latter depend on the state of motion.

---

(4) For possible criticism of this proof see E. Fabri: *Nuovo Cimento*, **13**, 326 (1959).

(5) For some remarks along these lines see N. Kemmer, J. C. Polkinghorne and D. L. Pursey: *Rep. Progr. Phys.*, **22**, 368 (1959).

* * *

I wish to thank Professor G. FEINBERG and Professor G. C. WICK for their criticisms.

RIASSUNTO (*)

Si dimostra che tutte le regole di superselezione, che di solito si assumono, derivano dal fatto che in ogni esperimento si parte con numeri definiti di ciascuna specie d particella.

(*) *Traduzione a cura della Redazione.*

LETTERE ALLA REDAZIONE

(La responsabilità scientifica degli scritti inseriti in questa rubrica è completamente lasciata dalla Direzione del periodico ai singoli autori)

An Attempt at Universal Four-Fermion Interaction (*).

J. C. PATI and S. ONEDA (**)

University of Maryland - College Park, Md.

(ricevuto il 22 Giugno 1959)

The discussion of the Λ-decay by OKUBO *et al.* [1] on the basis of $V-A$-Interaction extended to the tetrahedron-scheme reveals that the main features of the Λ-decay can be explained surprisingly well by considering only such types of diagrams as shown in Fig. 1. We may then ask the following questions:

1) Can we explain both Λ and $\Sigma^{\pm}$-decays by treating all the hyperons as equally basic (subject to selection rules) for the weak-interactions and by still assuming that the diagrams of type of Fig. 1 are the most important ones for all the hyperon decays?

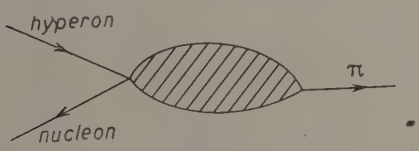

Fig. 1. – Hyperon decay. The shading represents virtual pionic effects.

2) Can we explain the approximate validity of the $|\Delta I| = \frac{1}{2}$ rule for the $K \to 2\pi$ decays? This problem seems to be the essential obstacle for the scheme treated in the ref. [1].

In the first place, if we believe in the assumption mentioned in 1), the vanishing asymmetry parameters for $\Sigma^{\pm} \to n + \pi^{\pm}$-decays [2] found experimentally force us to introduce positive chiral currents of the form $\bar{A}\gamma_\alpha(1-\gamma_5)B$ in addition to the usual negative chiral currents of the form $\bar{A}\gamma_\alpha(1+\gamma_5)B$. The purpose of this note is mainly to convey the results of a more or less desperate attempt to obtain any conceivable scheme of the interaction currents, which can explain the characteristics of the strange-particle decays by allowing the above-mentioned modification of the chiral nature of the currents, which participate in the primary weak interactions. To facilitate the arguments we shall assume:

1) The main features of hyperon-decays may be described in terms of Fig. 1, which includes renormalization effects inside the loop, but neglects them outside the loop.

(*) This research was supported in part by the U.S. Air Force through the Air Force Office of Scientific Research of the Air Research and Development Command.

(**) On leave of absence from the Institute of Theoretical Physics, Kanazawa University, Japan.

(1) S. OKUBO, R. E. MARSHAK and E. C. G. SUDARSHAN: *Phys. Rev.*, **113**, 944 (1959); see also J. J. SAKURAI: *Nuovo Cimento*, **7**, 649 (1958).

(2) R. L. COOL, B. CORK, J. W. CRONIN and W. A. WENZEL: *Phys. Rev.*, **114**, 912 (1959).

2) Global symmetry of strong pion-baryon interactions [3] hold and the contributions of the various baryon-anti-baryon loops are equal [4] to each other.

3) The weak-interaction current J_α is composed of all possible combinations of the fields $\nu, e; \mu, p, n, \Sigma^+, Y, Z, \Sigma^-, \Xi^0$ and Ξ^- subject to the conditions $\Delta S=0, \pm 1$ and $\Delta Q=\pm 1$ where [3]

$$Y=\frac{\Lambda-\Sigma^0}{\sqrt{2}} \quad \text{and} \quad Z=\frac{\Lambda+\Sigma^0}{\sqrt{2}}.$$

4) The chirality of a current (positive or negative) is uniquely fixed by the two fields composing the current.

5) Currents of opposite chiralities do not couple with each other, so thas the interaction can be written in the form [5]

$$(1)\quad H_{\text{weak}}=(f/\sqrt{2})(J_\alpha^{(+)}J_\alpha^{*(+)}+J_\alpha^{(-)}J_\alpha^{*(-)})+ \\ +\text{H.C.}$$

where $J_\alpha^{(-)}$ is composed of all currents having negative chirality and $J_\alpha^{(+)}$ of all currents having positive chirality.

With these assumptions an attempt was made to examine if there exists any possible assignment of chiralities to the various currents, which explains the observed asymmetry parameters, absolute decay rates and branching ratios of the various modes of Λ and $\Sigma^\pm$ decays. The results obtained could be summarized as follows:

There does exist essentially one and only one solution [6] which explains reasonably well the magnitudes of asymmetry parameters, decay rates and branching ratio of the various modes of Λ and $\Sigma^\pm$-decays. This solution however, leads to the following restrictions:

a) The currents $(\bar{\Sigma}^+ \text{n})$ and $(\bar{\Xi}^0 \Sigma^-)$ satisfying $\Delta S/\Delta Q=-1$ should be included in J_α.

b) The $(\bar{\Sigma}^+ \text{n})$-current should have negative chirality, while the $(\bar{\text{n}}\,\Sigma^-)$ current should have positive chirality, so that by assumption (5) Σ^+ is expected to decay to $\text{n}+\text{e}^+ +\nu$ with universal rate, while Σ^- cannot go to $\text{n}+\text{e}^-+\bar{\nu}$ in the lowest order, since the leptonic currents necessarily have negative chirality if we assume the two-component theory of the neutrino.

c) The pion-asymmetry parameters in the decays $\Lambda\to\text{p}+\pi^-$ and $\Lambda\to\text{n}+\pi^0$ should be equal in magnitude, but opposite in sign, the former being negative and the latter positive.

d) Symmetry of the strong K-meson interactions should have to be imposed in addition to the global symmetry for pion-interactions [assumption (2)] in order to explain the slowness of $\text{K}^+\to\pi^+ +\pi^0$ compared to $\text{K}_1^0\to 2\pi$ and the approximately 2 : 1 ratio of

$$\text{K}_1^0\to 2\pi^0/\text{K}_1^0\to\pi^+ +\pi^-$$

Probably the present experiments are not definite enough to rule out (*a*) and (*b*). However, the recent measurements of

---

(3) M. GELL-MANN: *Phys. Rev.*, **106**, 1296 (1957); J. SCHWINGER: *Ann. Phys.*, **2**, 407 (1957).

(4) This should strictly be the case if one could neglect the virtual kaonic effects.

(5) This assumption is equivalent to demanding that the four-fermion interaction $(\bar{\text{A}}\text{B})(\bar{\text{C}}\text{D})$ is form-invariant under the interchange of B and D, and is crucial to limiting the possible alternatives for the assignment of chiralities to the various currents.

(6) For the details see Physics Department Technical Report no. 139, University of Maryland. At the time when this work was completed (June 1959) only magnitudes of the asymmetry parameters were known.

the sign ([7]) of the pion asymmetry parameter in $\Lambda \to p + \pi^-$-decay shows that it should be positive. Moreover, the sign and magnitude of the asymmetry parameter of $\Lambda \to n + \pi^0$-decay seems ([8]) to be nearly equal to those of $\Lambda \to p + \pi^-$-decay. Both of these data are in contradiction with (*c*). As regards the symmetry of the strong kaon interactions, it has been shown by PAIS ([9]) that very high symmetry of both pion and kaon interactions is not compatible with experiments unless one is inclined to complicate the situation by introducing interactions violating charge independence like $KK\pi$ or $KK\pi\pi$.

Thus the above arguments show that the attempt at four-fermion interactions based on assumptions 1 through 5 do not seem to be compatible with experiments. This, together with the fact that the Fig. 1 does not provide an explanation of the $K \to 2\pi$-decays in the tetrahedron scheme (since the matrix element for Fig. 1 contains an appreciable amount of $|\Delta I| = \frac{3}{2}$-part), might be thought of as an indication that the class of diagrams shown in Fig. 1 may not be the dominant class contributing to the non-leptonic processes. The consideration of some important set of diagrams (which may satisfy the strict $|\Delta I| = \frac{1}{2}$-rule) may be missing entirely from the discussion of strange particle-decays.

Added Note.

The above work had been completed by June, 1959. In the meantime the authors have examined the possible importance of a class of diagrams which satisfies the strict $|\Delta I| = \frac{1}{2}$-rule. The investigation (*) reveals that at least for the tetrahedron scheme, a class of diagrams, which leads to an effective $(\bar{n}\,\Lambda)$-interaction, seems to be more important than Fig. 1. This makes it easier to explain the approximate validity of the $|\Delta I| = \frac{1}{2}$-rule and furthermore provides a way to explain the slowness of the strangeness-violating leptonic processes, as shown by recent experiments.

([7]) E. BOLDT, H. S. BRIDGE, D. D. CALDWELL and Y. PAL: *Phys. Rev. Lett.*, **1**, 256 (1958); R. W. BIRGE and W. B. FOWLER: *Bull. Am. Phys. Soc.*, **4**, 355 (1959).

([8]) J. W. CRONIN, B. CORK, L. KERTH, W. A. WENZEL and R. L. COOL: *Bull. Am. Phys. Soc.*, **5**, 11 (1960).

([9]) A. PAIS: *Phys. Rev.*, **110**, 574 (1958); **112**, 624 (1958).

(*) B. SAKITA and S. ONEDA: to be published. S. ONEDA, J. C. PATI and B. SAKITA: University of Maryland, Physics Department Technical Report no. 160.

On the High Energy Behavior in Field Theory (*).

E. Kazes

Physics Dept., The Pennsylvania State University - University Park, Pa.

(ricevuto il 22 Febbraio 1960)

The high energy behavor of cross-sections and vertices is of great interest in dispersion theory and bears heavily on the consistency problem of field theory (1). Using the method of Lehmann, Symanzik and Zimmermann (2) we show that the $\pi \to \mathcal{N} + \overline{\mathcal{N}} + \pi$ vertex cannot go to the Born approximation result in the limit of infinite invariant momentum transfer.

Starting from (2)

$$\langle \Omega | \varphi(x)\varphi(y) | \Omega \rangle = \int \Delta'_F(x-\xi) F(\xi-\eta) \Delta'^*_F(\eta - y) \, \mathrm{d}\xi \, \mathrm{d}\eta \,,$$

where the Fourier transform of $F(\xi - \eta)$ is

$$F(-k^2) = \sum_n F_n(-k^2) \,,$$

$$F_n(-k^2) = \frac{(2\pi)^4}{(2\pi)^{3n}} \int \delta(k - q_1 - q_2 \ldots - q_n) \, \mathrm{d}q_1 \ldots \mathrm{d}q_n \cdot$$

$$\cdot |\mathscr{M}(q_1 + q_2 + \ldots q_n, \; q_2 + \ldots q_n, \ldots, q_n)|^2 \theta(q_1^0) \, \delta(q_1^2 + \mu_i^2) \ldots \theta(q_n^0) \, \delta(q_n^2 + \mu_j^2).$$

The intermediate states in

$$\langle \Omega | \varphi(x)\varphi(y) | \Omega \rangle = \sum_n \langle \Omega | \varphi(x) | n \rangle \langle n | \varphi(y) | \Omega \rangle \,,$$

consisting of a nucleon-antinucleon pair and a pion contribute

$$F_3(-k^2) = \frac{1}{(2\pi)^5} \int \delta(k - p - p' - k') \, \frac{m^2}{2E(p)\, E(p')\, \omega(k')} \cdot$$

$$\cdot \sum_{\substack{\text{spin} \\ \text{sum}}} |\bar{v}(p') \mathscr{M}(p + p' + k', \; p' + p, \; k') \, n(p)|^2 (\mathrm{d}p')^3 (\mathrm{d}p)^3 (\mathrm{d}k')^3 \,.$$

(*) Supported in part by the Un. States Atomic Energy Commission Contract no. AT(30-1)-2399.

(1) G. Källén *CERN Symposium*, **2**, 187 (1956).

(2) H. Lehmann, K. Symanzik and W. Zimmermann: *Nuovo Cimento*, **2**, 425 (1955).

Since

$$\int \frac{F(x^2)}{(x^2-1)^2}\,\mathrm{d}x^2 < \infty\,(^2)\,,$$

where $x^2 = -k^2$, $F_3(-k^2)$ cannot be proportional k^2 as $k^2 \to \infty$. Because k is time like we can choose it to have zero space components, this simplifies the calculations appreciably. If it is assumed that

$$\lim_{k0\to\infty} \bar{v}(p')\mathscr{M}(p+p'+k',\ p+p',\ k')u(p) \to \text{Born approximation}\,,$$

then it follows that $F_3(k_0^2) \to k_0^2$ which is in contradiction with the result of ref. (2). The same result is also obtained if an intermediate state consisting of 3π's is considered and the Born approximation corresponding to a $\lambda\varphi^4$ type interaction is assumed.

As pointed out by ARAMAKI (3) if the meson propagator should be proportional to $(k^2)^n$, $n \geqslant 0$ as $k^2 \to \infty$ then $F(-k^2)$ has to vanish faster than k^2, thus validating our conclusions even in this case. It is thus concluded that the Born approximation cannot be valid for the $\pi \to \mathcal{N} + \overline{\mathcal{N}} + \pi$ and the $\pi \to \pi + \pi + \pi$ direct process in the limit of infinite momentum transfer.

Added in proof.

This conclusion does not contradict the conjecture of ref. (1) since the quantity $N(Q^2)$ which appears in eq. (12) of that paper may go to zero as $-Q^2 \to \infty$, whereas our Born approximation for infinite momentum transfer is assumed to have an effective coupling constant that is different from zero. We thank Prof. G. KÄLLÉN for kindly emphasizing this fact.

---

(3) S. ARAMAKI: *Progr. Theor. Phys.*, **22**, 485 (1959). We also like to thank Dr. S. WEINBERG for informing us of similar conclusions.

IL NUOVO CIMENTO Vol. XVI, N. 2 16 Aprile 1960

Radiative Corrections to the e-e Scattering (*).

YUNG SU TSAI

Institute of Theoretical Physics, Department of Physics, Stanford University - Stanford, Cal.

(ricevuto il 25 Gennaio 1960)

The radiative corrections to the e-e clashing beam experiment are calculated assuming the following experimental conditions. The experiment is done with two intersecting 500 MeV electron beams. The detectors for the scattered electrons are Čerenkov counters facing each other with equal circular apertures subtending the same solid angle and arranged for coincidence (see Fig. 1). Čerenkov counters are assumed to have no energy resolution. Angular distributions from 35 to 90° are taken.

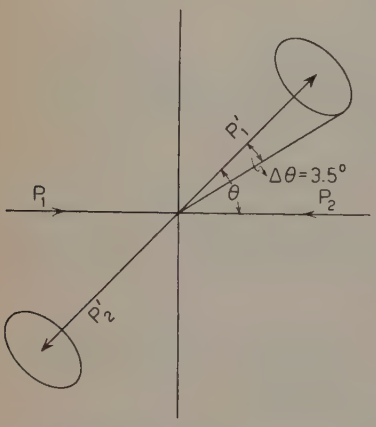

Fig. 1. – Electron-electron clashing beam experiment with Čerenkov counters arranged for coincidence.

The experiment described above is in progress at Stanford, and is being conducted by O'NEILL, BARBER, GITTELMAN, PANOFSKY and RICHTER. It is designed to test the validity of quantum electrodynamics at small distances, or to find out if the electron has any finite size (form factor) down to $\sim 0.5 \cdot 10^{-14}$ cm. The elastic parts of the radiative corrections to order α^3 are calculated by using a high-energy approximation (1), *i.e.*, $\eta, -q^2, -q'^2 \gg m^2$, where $\eta=(p_1+p_2)^2$, $q^2=(p_1-p_1')^2$ and $q'^2=(p_1-p_2')^2$. Only logarithmic terms are kept in the calculation of the two-photon exchange diagrams. In this approximation, the results of REDHEAD (2) and POLOVIN (3) for the elastic parts have been confirmed. It is found that the two- photon exchange diagrams (crisscross and non-crisscross) contribute negligibly to the cross section after cancellation with the corresponding soft real photon contribution (see the discussion below).

To calculate the inelastic contribution to the cross section, we observe that the

(*) Supported in part by the United States Air Force through the Air Force Office of Scientific Research.

(1) We use units in which $\hbar=c=1$ and the metric $AB=A_0B_0-\boldsymbol{AB}$.

(2) M. L. G. REDHEAD: *Proc. Roy. Soc.* (*London*), A **220**, 219 (1953).

(3) R. V. POLOVIN: *Soviet Phys. Journ. Exp. Theor. Fys.*, **4**, 385 (1957).

minimum energy of the photon which can be emitted in the p_1 or p_2 direction is $2E_1\Delta\theta/(\sin\theta+\Delta\theta)$, where $\Delta\theta$ is the half angle of the counter (see Fig. 1); and in the p_1' or p_2' direction $k_{\max}\approx E_1$. Thus we divide the calculation into two steps. First, calculate the soft photon contribution $\mathrm{d}\sigma_{\text{soft}}$ in which terms like k/p_ik in the matrix elements are neglected and $k_{\max}$ is assumed to have isotropic distribution (the same for all directions) and is equal to $\Delta E = 2E_1\Delta\theta/(\sin\theta+\Delta\theta)$. Next, calculate the contribution from hard photons emitted along the p_1' and p_2' directions and integrate it from ΔE to E_1. Terms like k/p_ik in the matrix elements are included in this calculation. Denote the contribution from hard photons to the cross section by $\mathrm{d}\sigma_{\text{hard}}$. Summing over the contribution from elastic and inelastic parts, we get the expression for the cross section

$$\mathrm{d}\sigma = \mathrm{d}\sigma_{\text{elastic}} + \mathrm{d}\sigma_{\text{soft}} + \mathrm{d}\sigma_{\text{hard}},$$

where

$$\mathrm{d}\sigma_{\text{elastic}} + \mathrm{d}\sigma_{\text{soft}} = \frac{r_0^2}{8}\frac{m^2}{E_1^2}\cdot$$

$$\cdot\mathrm{d}\Omega\left[\left(\frac{\eta^2+q'^4}{q^4}+\frac{\eta^2}{q'^2q^2}\right)\left[1-\frac{4\alpha}{\pi}\left\{\frac{23}{18}-\frac{11}{12}\ln\frac{-q^2}{m^2}+\left(\ln\frac{q^2q'^2}{\eta m^2}-1\right)\ln\frac{E_1}{\Delta E}\right\}+\frac{\alpha}{\pi}f(x)\right]+\right.$$

$$\left.+\text{ terms obtained by the interchange } x\leftrightarrow 1-x;\ q^2\leftrightarrow q'^2\right],$$

r_0 is the classical radius of an electron,

$$f(x) = -\left(\frac{3+(1-x)^2}{2x^2}+\frac{1}{x(1-x)}\right)\ln^2\frac{1}{x}+\frac{1-x}{x}\ln\frac{1}{x}+$$

$$+\left(\frac{3(1-x)^2+1}{2x^2}+\frac{1+(1-x)^2}{2x(1-x)}\right)\ln^2\frac{(1-x)}{x}+\frac{1}{x(1-x)}\ln\frac{(1-x)}{x},\qquad x=\frac{-q^2}{\eta},$$

and

$$\mathrm{d}\sigma_{\text{hard}} = \frac{r_0^2}{8}\frac{m^2}{E_1^2}\mathrm{d}\Omega\left(\frac{\eta^2+q'^4}{q^4}+\frac{2\eta^2}{q'^2q^2}+\frac{\eta^2+q^4}{q'^4}\right)\cdot$$

$$\cdot\frac{2\alpha}{\pi}\left[\left(\ln\frac{\eta}{m^2}-\ln\frac{16E_1^2}{(\Delta E)^2\sin^2\theta}\right)\left(\ln\frac{E_1}{\Delta E}-1\right)-2\ln\frac{E_1}{\Delta E}+\ln^2\frac{E_1}{\Delta E}\right].$$

$f(x)+f(1-x)$ is the contribution from the two-photon exchange diagrams after cancellation with the corresponding soft real photon contribution. As mentioned before, it is very important to notive that its contribution to the cross section is negligible, namely, 0.1, 0.03, and 0 per cent, respectively, at $\theta=90°$, 35° and 0°.

Since we can neglect the two-photon exchange terms $f(x)+f(1-x)$, we can understand the rest of the terms in our formula for $\mathrm{d}\sigma_{\text{elastic}}+\mathrm{d}\sigma_{\text{soft}}$ in the following way. If one replaces the term $\ln q^2q'^2/\eta m^2$ by $\ln(-q^2/m^2)$, the result is essentially the same as Schwinger's [4] corrections to the electron nucleus scattering with the

---

[4] J. SCHWINGER: *Phys. Rev.*, **76**, 790 (1949), eq. (2.105).

contributions from bremsstrahlung and vertex parts doubled but the vacuum polarization term undoubled. This is because in Schwinger's corrections there are one lowest-order diagram, two bremsstrahlung diagrams, one vertex and one vacuum polarization diagrams; whereas in the e-e scattering we have two lowest-order diagrams, eight bremsstrahlung diagrams, four vertex diagrams, and two vacuum polarization diagrams. Thus our result is very plausible.

The numerical results are as follows. Let $\delta(\theta)$ be the radiative corrections to the Møller cross section such that $d\sigma = d\sigma_{\text{Møller}}(1 - \delta)$, then for $E_1 = 500$ MeV and $\Delta\theta = 3.5°$, $\delta(90°) = 9.5\%$, $\delta(35°) = 6.0\%$. The error is estimated to be less than 2%, which arises from non-logarithmic terms which we have neglected in the calculation of inelastic and two-photon exchange diagrams.

The fact that the angular dependence of the radiative corrections is rather small is very important experimentally. It shows that the effect due to the radiative corrections does not mar significantly the measurement of the effect due to the possible finite size of the electron which the experiment was originally designed to investigate.

Remarks about Redhead and Polovin's paper: Redhead and Polovin's results for the e-e scattering with the target electron at rest contain terms [5] like $\alpha \ln^2(-q^2/m^2)$. This kind of term cancels out in our final expression. The source of this kind of term in their results was found to be due to their special assumption that $k_{\max}$ is isotropic and $\ll m$ in the lab system. Neither of these two conditions on $k_{\max}$ can be satisfied in most experiments at high energies. We have calculated the radiative corrections for the high-energy e-e scattering with the target electron at rest and one of the outgoing electrons undetected and the other outgoing electron selected by a slit and then momentum-analyzed by a spectrometer. (This experiment is being carried out by E. B. Dally at Stanford.) In this case we found no terms like $\alpha \ln^2(-q^2/m^2)$ remaining in the final result. This work will be published later.

* * *

It is my great pleasure to express my gratitude to Professors S. D. Drell, D. R. Yennie, and Drs. J. D. Bjorken, S. C. Frautschi and H. Suura for helpful discussions.

---

[5] Brown and Feynman's results on the radiative corrections to Compton scattering also contain terms like $\alpha \ln^2(-q^2/m^2)$. This is also due to their special assumption that $k_{\max}$ is isotropic and $\ll m$. See L. M. Brown and R. P. Feynman: *Phys. Rev.*, **85**, 231 (1952).

IL NUOVO CIMENTO Vol. XVI, N. 2 16 Aprile 1960

Dislocation Relaxation in Zinc Single Crystals.

P. G. Bordoni

Istituto di Fisica Matematica dell'Università - Pisa

M. Nuovo and L. Verdini

Istituto Nazionale di Ultracustica - Roma

(ricevuto il 28 Gennaio 1960)

The relaxation effect due to dislocations has been observed until now only in cubic metals of the face-centered type (1) (Pb, Al, Cu, Ag, Au, Pd, Pt). The evidence of the same effect in magnesium (hexagonal c.p. lattice) cannot be considered satisfactory, as the only experimental curve known (2) was obtained for a polycrystalline specimen under the large intergrain stresses due to the anysotropy of thermal expansion and without considering the influence of anneal and pre-strain.

It may be observed that the existence of the effect in non-cubic lattices has a basic significance for the theory of dislocation motion (3). A new investigation has been started to decide if the effect is present in zinc (hexagonal c.p. structure). To avoid intergrain thermal stresses the specimens used during this research are single crystals, in the shape of flat circular plates, with their bases normal to the hexagonal axis within two degrees. The plates are cut by means of a chemical saw (4) from longer crystals (5) and the value of Q^{-1} is measured with the same technique employed in previous investigations (6).

At room temperature the vibration frequency and the Q^{-1} are amplitude-dependent even when the maximum strain is of the order of 10^{-6} as is shown in Fig. 1 for a plate of 25 mm diameter and 6.2 mm thickness vibrating on its fundamental flexural mode with one

(1) For a review of the experimental evidence of the theory of the effect see: P. G. Bordoni: *Dislocation Relaxation at High Frequencies*, Reports of the A.S.M. Convention, Chicago, 1959; W. P. Mason: *Physical Acoustics and the Properties of Solids* (New York, 1958), pp. 266-271.

(2) H. L. Caswell: *Journ. Appl. Phys.*, **29**, 1210 (1958).

(3) L. J. Bruner: *Low Temperature Internal Friction in F.C.C. and B.C.C. Metals.* Thesis submitted to the Dept. of Physics at the Institute for the Study of Metals (Chicago, Ill., 1959).

(4) R. Maddin and W. R. Asher: *Rev. Sci. Instr.*, **21**, 881 (1950).

(5) The single crystals have been grown in the shape of bars with circular cross section (diameter 1 in., lenght 6 in.) by the Virginia Institute for Scientific Research, Richmond, Va.

(6) P. G. Bordoni, M. Nuovo and L. Verdini: *Nuovo Cimento*, **14**, 273 (1959).

nodal circle (6). However the low-temperature measurements have been made in the *linear* range, where f and Q^{-1} are independent of strain, as it has been done in the previous investigation on f.c.c. metals.

between two rubber sheets in a vice until a permanent pre-strain is observed and glide-lines appear on the etched bases, a large increase of Q_m^{-1} is found, its value being more then twice the original value before annealing (Fig. 2,

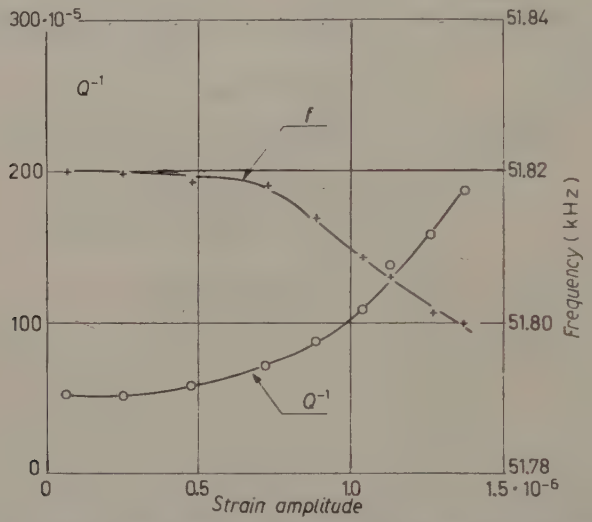

Fig. 1. – Strain amplitude dependence of the resonant frequency and attenuation at room temperature. Abscissa: strain component e_{xx}, computed at the center of one base and normally to the plate axis.

After the plate has been cut from the crystal and before any other treatment, a broad peak is found in Q^{-1} as a function of the temperature, with its maximum Q_m^{-1} at a value T_m of about 210 °K. The attenuation Q_m^{-1} of the peak is about six times larger than the room temperature value (Fig. 2, curve A). The corresponding frequency-temperature curve (Fig. 3, heavy line) has an inflexion in the temperature range of the attenuation peak, showing that the latter is due to a temperature-dependent relaxation effect. To prove that this effect is related to the presence of dislocations the influence of anneal and pre-strain has been considered. An anneal of half an hour at the temperature of 300 °C reduces the Q_m^{-1} to about one third of its original value (Fig. 2, curve B). If the plate is successively compressed

curve C). Hence, as in the case of f.c.c. metals, dislocations seem to be responsible for the relaxation effect (7).

While further investigations are in progress to evaluate the activation energy W of the process through the frequency dependence of T_m, a first approximate evaluation of W may be obtained from the available data, observing that in every metal in which the effect has been found the limiting value τ_0^{-1} of the inverse of the relaxation time τ for high temperatures is of the same order of magnitude as the Debye frequency ν_D computed by means of the equation $\nu_D = k\theta_D/h$ (θ_D = characteristic temperature). Assuming approximately $\tau_0^{-1} = \nu_D$ the error made in

(7) See the first paper quoted in footnote (1).

the evaluation of W is small, the latter parameter being proportional to $\log_e \tau_0^{-1}$.

With the above hypothesis and from the experimental values of T_m and f_m (Fig. 2, curve A and Fig. 3) one finds an activation energy $W = 0.33$ eV, which is near enough to those measured in f.c.c. metals [1] (from 0.11 for aluminium to 0.26 for palladium).

A lower boundary for W may also be obtained from the shape of the attenuation-temperature curves assuming that the effect has a single relaxation time. From the high temperature branch of the curves A and C of Fig. 2, which are less influenced by the additional low-temperature peak of the Niblett and Wilks type [6], one finds that $W > 0.10$ eV, in agreement with the previous approximate evaluation. The ratio between the last value and the approximate evaluation of W obtained above gives the parameter γ which characterizes the relaxation spectrum according to the Fuoss and Kirkwood theory [6]. In the present case the value found for γ is 0.3 which is intermediate between those measured in f.c.c. metals [1] (from 0.266 for silver to 0.426 for platinum).

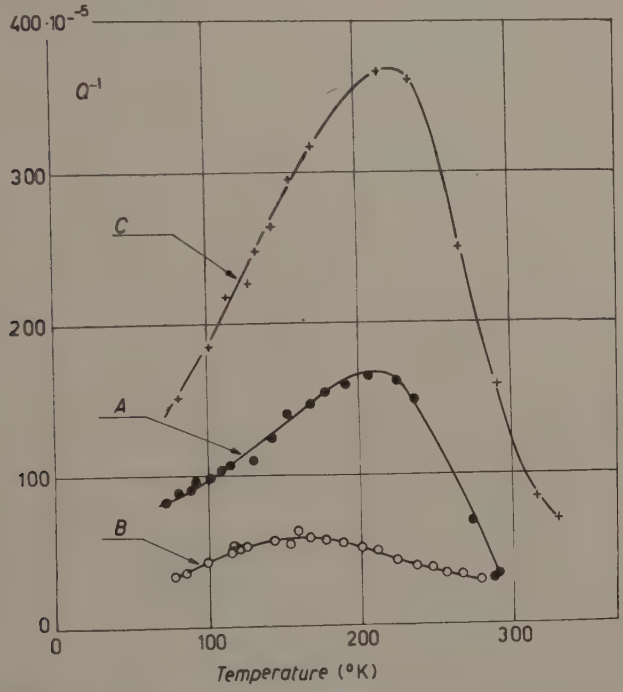

Fig. 2. – Attenuation as a function of the absolute temperature. Curve A: after the chemical cut of the specimen from the single crystal; B: after a 30 min anneal at 300 °C; C: after a permanent compressional strain.

The experimental curves of Fig. 2 have the following features in common with those obtained in f.c.c. metals.

1) A slight decrease is observed in T_m when Q_m^{-1} decreases owing to the anneal. The opposite happens if Q_m^{-1} is increased by pre-strain.

2) The low temperature branch is higher than the high-temperature one.

The asymmetry is larger when the attenuation is plotted as a function of the *universal* variable (6) $Wk^{-1}(T_m^{-1} - T^{-1})$.

The dependence 1) of T_m upon Q_m^{-1} can be explained, as it was done in previous cases (6), by the reasonable

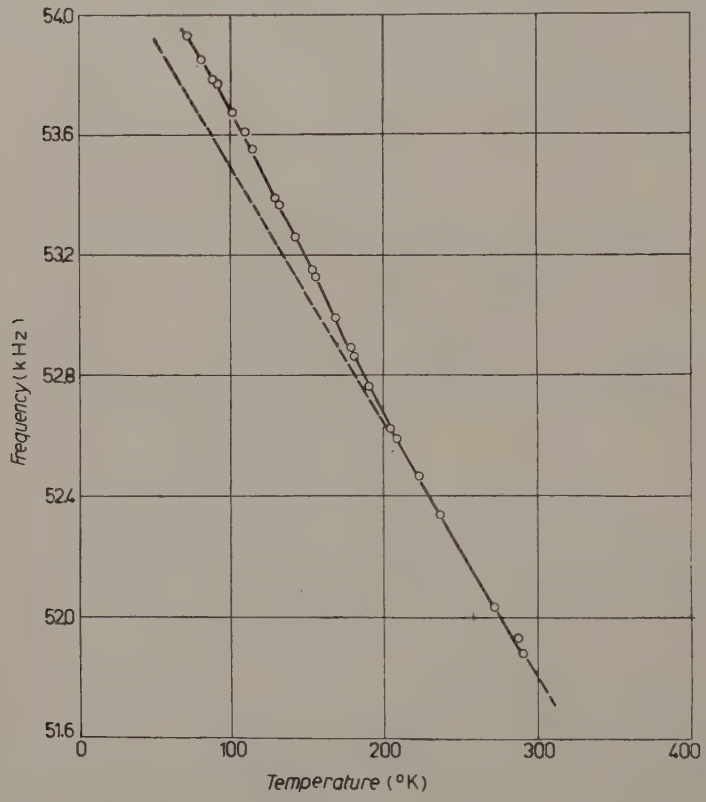

Fig. 3. – Resonant frequency as a function of the absolute temperature. Heavy line: experimental values; dotted line: slope of the curve near room temperature.

3) The attenuation values measured when the specimen is heated are somewhat larger than the corresponding values obtained during the previous cooling process. However this disagreement is only a temporary one as the former values of the attenuation decrease in time at constant temperature, reaching an equilibrium value which coincides with the attenuation measured at the same temperature when the specimen is cooled from the room temperature.

assumption that the anneal cancels more easily the effect of the dislocations associated with the larger values of the relaxation time τ.

In f.c.c. metals the asymmetry 2) has been related to a second low-temperature peak of the Niblett and Wilks type. No mention has yet been made of the effect 3), the differences between the attenuation measured with opposite time-changes of temperature being much less evident than those observed in zinc.

It is now suggested that a relation may exist between 2) and 3). During the cooling process of the specimen new dislocations are introduced by the thermal stresses due to temperature gradients or to crystal imperfections. The attenuation is then measured for a number of dislocations which increases when T decreases, and this may account, at least in part, for the asymmetry of the attenuation curves in the low-temperature branch. When the specimen is heated up, the effect of some of the new dislocations is cancelled. For every value of T this process requires some time, and this can explain the time-dependence observed in the attenuation values measured at constant temperature.

On the $^{196}Au^{m}$ Isomeric State.

M. Ademollo, M. Bocciolini, G. Di Caporiacco and M. Mandò

Istituto Nazionale di Fisica Nucleare - Sottosezione di Firenze
Istituto di Fisica dell'Università - (Firenze)

(ricevuto il 30 Gennaio 1960)

The ground state of ^{196}Au (5.55^{d} E.C. and β^{-}) has been thoroughly investigated ([1-4]).

Until recently, however, little was known about the isomeric state $^{196}Au^{m}$, except that it was about 14^{h} half-life and emitted X-rays or soft γ ([5,6]). A search was made for the properties of this isomeric state and its production in the reactions (n, 2n) and (γ, n). Preliminary results were presented in october 1959 at the Pavia meeting of the Italian Physical Society, where R. A. Ricci was so kind as to communicate us the results of an investigation on the same nuclide carried out at Amsterdam, which at the time were still in press and have now appeared in printed form ([7]). These results are more complete and extended than ours and substantially agree with ours. It is thought, however, worthwhile to report here briefly also our results, as an independent confirmation of those findings, which differed from the older ones for the appreciation of the half-life. Besides we have obtained an estimation of the production branching in the (n, 2n) reaction, and an upper limit for the production of the excited state in the (γ, n) reaction; finally there is a point on which our results differ from those of the Amsterdam group; this point, if confirmed, would indicate a still more complicated decay scheme than that proposed by them.

First of all the attempt to produce the $^{196}Au^{m}$ isomeric state by bombarding a gold target with 30 MeV bremsstrahlung gammas was unsuccessful; the upper limit for the branching ratio for production of $^{196}Au^{m}$ with respect to the ground state ^{196}Au (5.5^{d}) comes out from our results to be $< 10^{-2}$ of the corresponding ratio in the (n, 2n) reaction. This in turn cannot be evaluated exactly until the decay scheme is better established; assuming however that on the average 1.4 conversion K-X ray per disintegration is emitted (which is

---

([1]) R. M. Steffen, O. Huber and F. Humbel: *Helv. Phys. Acta*, **22**, 167 (1949).

([2]) P. Stähelin: *Phys. Rev.*, **87**, 374 (1952).

([3]) R. M. Steffen: *Phys. Rev.*, **89**, 665 (1953).

([4]) M. T. Thieme and E. Bleuler: *Phys. Rev.*, **101**, 1031 (1956).

([5]) E. M. McMillan, M. Kamen and S. Ruben: *Phys. Rev.*, **52**, 375 (1937).

([6]) G. Wilkinson: *Phys. Rev.*, **75**, 1019 (1949).

([7]) R. Van Lieshout, R. K. Girgis, R. A. Ricci, A. H. Wapstra and E. Ythier: *Physica*, **25**, 703 (1959).

probably a lower limit), the (n, 2n) production branching isomeric to ground state comes out to be $(5 \pm 1) \cdot 10^{-2}$.

reaction, that is neutrons of about 14.5 MeV.

A simple γ-ray spectrum with NaI(Tl)

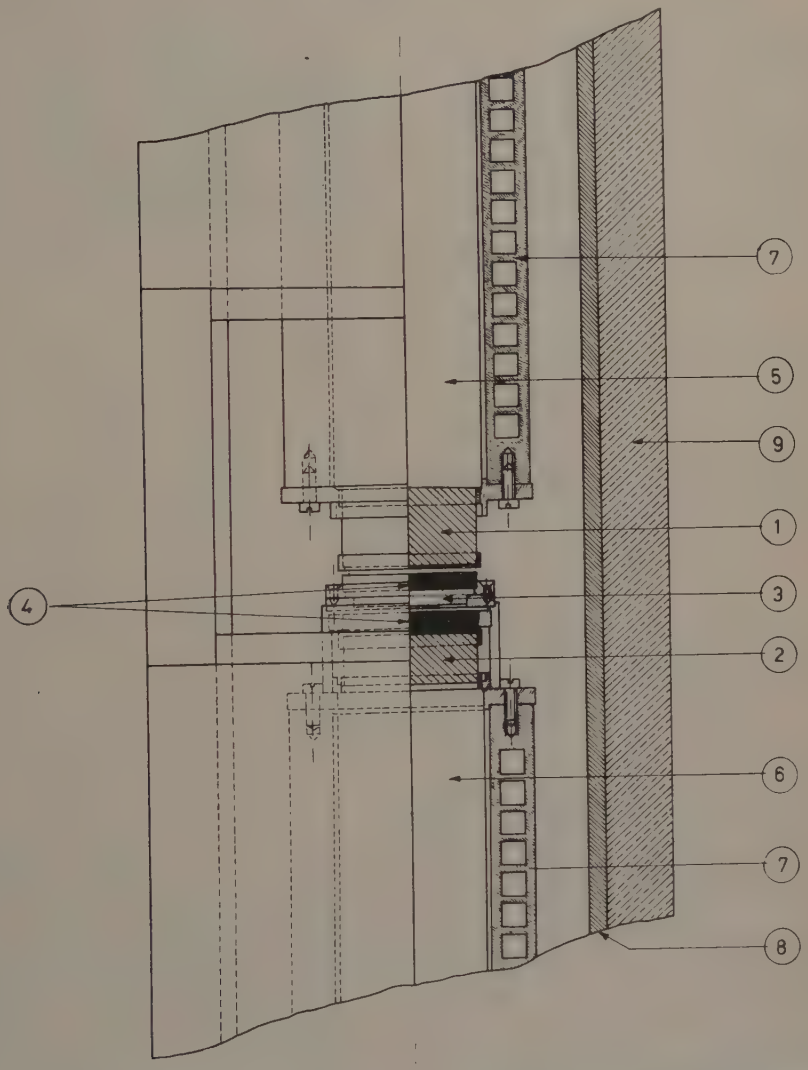

Fig. 1. – Counting geometry: 1) NaI main crystal (Levinthal); 2) NaI coincidence pilot (Harshaw); 3) Au foil container; 4) Graphite absorber (0.94 g/cm²); 5) Ph.M. 5819 R.C.A.; 6) Ph.M. 6292 DuMont; 7) Ph.M. cooling container; 8) Iron; 9) Lead shield.

This ratio refers to the production of the isomeric state $^{196}Au^m$ and of the ground state ^{196}Au by bombardment of a gold foil with neutrons from the (D.T)

crystal $1\frac{1}{2}$ in. in diameter and 1 in. thick was taken with a 10 channel pulse height analyzer; it showed two peaks at $\gamma_1 = (149 \pm 2)$ keV and $\gamma_2 = (188 \pm 2)$ keV,

γ_2 being less intense, in perfect agreement with the findings of the Amsterdam group (Fig. 2); the decay time for these

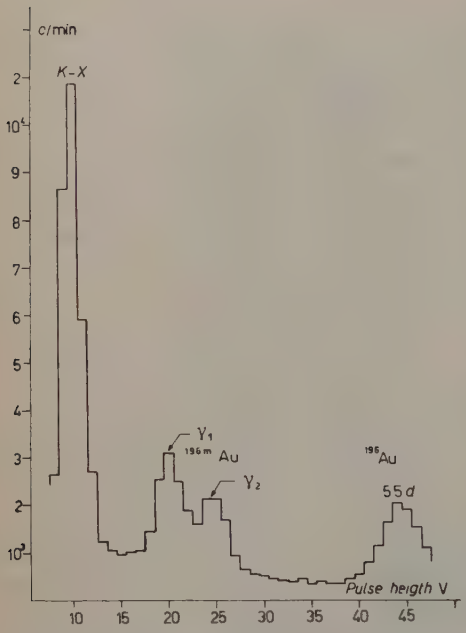

Fig. 2. – Typical spectrum of gold foil, irradiated 4 h with 14.5 MeV neutrons, taken after 4 h from end of irradiation.

activities, duly corrected for background and residual long-life activity was about 10^h; a component of the same half-life was also present in the K-X line; the same half-life was also present in some measurements taken with a thin window Geiger, which mainly responded to soft conversion electrons or betas as was shown by absorption in a thin plexiglas sheet.

As an average of various runs, and by detecting in turn γ_1, γ_2, X line and (with the Geiger counter) conversion electrons our best result for the half-life is (9.8$\pm$0.3) hours; the quoted error is not, of course, the statistical one, but has been evaluated from the internal consistency of the various runs and various type of measurements; (it is rather an upper limit, than a probable error).

Both γ_1 and γ_2 were shown to be in coincidence among themselves and with the K-X line (resolving time 5 μs); this is also in agreement with the results of the Amsterdam group.

Our measurements, however, definitely indicate also an apparent γ_1-γ_1 coincidence, (cfr. Fig. 3) which we are unable to explain unless we assume that there are actually two γ of about this energy in cascade.

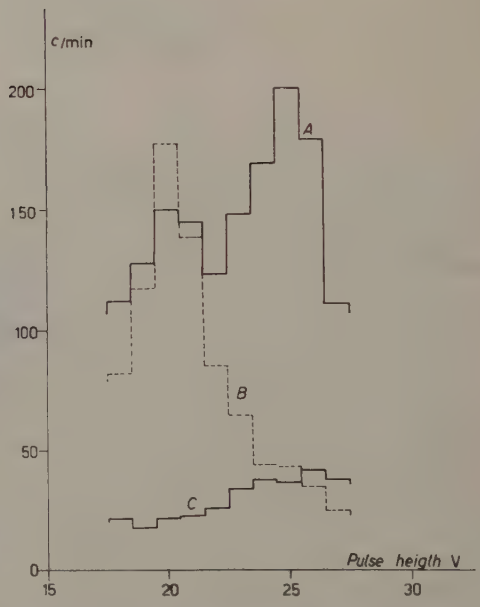

Fig. 3. – Typical coincidence spectrum: *a*) with gate centered on γ_1 line; *b*) with gate centered on γ_2 line; *c*) correction to *a*) for back-scattering contribution from 5.5 d activity and accidentals.

Variation of the resolving time from 3.7 to 7.8 μs showed no difference in the coincidence rate (allowance being made, of course, for accidental coincidences).

Different geometries were also used without changing the relative coincidence rate. Although the conditions of the experiment did not allow accurate measurements of intensities and, in

fact, these appeared to differ in the various runs, the apparent γ_1-γ_1 coincidence rate was in every case too strong (never less than one half γ_1-γ_2 coincidence rate) to be accounted for as a spurious event in spite of the poor geometry and therefore points to a decay-scheme still more complicated than that proposed by the Amsterdam group.

We hope that further measurements with a different technique may help to clarify this point.

* * *

Our warmest thanks are due to Prof. G. PUPPI, Director of the Sezione di Bologna of the I.N.F.N., for his kind permission to carry out freely repeated irradiations at their accelerator and to Prof. S. PETRALIA for friendly advice on its use.

The constant encouragement of Professor S. FRANCHETTI is also gratefully acknowledged. Finally we would like to thank M. G. BALDINI for his careful operation of the accelerator.

IL NUOVO CIMENTO Vol. XVI, N. 2 16 Aprile 1960

Fluctuations of Space-Time Metric.

D. I. Blohinčev
Joint Institute for Nuclear Research - Dubna

(ricevuto il 10 Marzo 1960)

1. – Introduction.

In those regions of space where there are powerful turbulent motions of matter accompanied by considerable changes in the density of matter or having large irregular velocities of motions (v/c is not small!), the metric tensor $g^{\mu\nu}$ is a random quantity. This implies that the interval of time t_{AB} and the distance x_{AB} separating two physical world-points A and B also become random quantities. Therefore, one may speak only of the probability that $t_{AB}=t$, $x_{AB}=l$.

In the microworld such a statistical character of the metric may be due to the statistical features of the vacuum, or in other words, to the « zero » oscillations of the quantized fields. However, we face here a very intricate problem and it is probable that the statisticalf eatures of the metric which reflect zero vacuum oscillations are essential only in the extremely small volumes which are likely to be beyond the limits of quantum theory.

Nevertheless, it seems interesting to make a theoretical attempt to enter this region. It is sufficient for the time being to restrict oneself to the simplest problem.

2. – Fluctuations of metric.

We will assume that the energy tensor of matter $T^{\mu\nu}$ may be expanded into two terms

$$T_0^{\mu\nu} = T^{\mu\nu} + \delta T^{\mu\nu}, \tag{1}$$

so that $T_0^{\mu\nu}$ describes the global motion of matter characterized by large scales L and periods of time T, whereas the term $\delta T^{\mu\nu}$ is due to the turbulent motion of matter characterized by small scales and short periods τ ($\lambda \ll L$, $\tau \ll T$). The mean value of $\delta T^{\mu\nu}$ by the time intervals comparable with T or by the scales comparable with L is assumed to be zero. Therefore,

$$\langle T^{\mu\nu} \rangle = T_0^{\mu\nu}, \qquad \langle \delta T^{\mu\nu} \rangle = 0, \tag{2}$$

where $\langle ... \rangle$ means the averaging over the turbulent motion. Correspondingly the metric tensor (1) may be decomposed into two parts:

$$\mathfrak{G}^{\mu\nu} = \mathfrak{G}_0^{\mu\nu} + g^{\mu\nu} + \dots . \tag{3}$$

The magnitude of the turbulent fluctuations of matter $\delta T^{\mu\nu}$ is also assumed to be small, thus the quantities $g^{\mu\nu}$ are also small compared with $\mathfrak{G}_0^{\mu\nu}$ determining the global space-time metric. Under these assumptions the Einstein gravitational equation may be put as

$$-\tfrac{1}{2}\Box^2 g^{\mu\nu} = \varkappa t^{\mu\nu} . \tag{4}$$

Here:

$$\varkappa = \frac{8\pi\gamma}{c^2} , \qquad \gamma = 6.7\cdot 10^{-8}\,\frac{au^3}{2 - au^2}\ \mathrm{cm^3\cdot g^{-1}\cdot s^2} ,$$

is the Newtonian gravitational constant;

$$\Box^2 = \mathfrak{G}_0^{\alpha\beta}\frac{\partial}{\partial x_\alpha}\frac{\partial}{\partial x_\beta} ,$$

and the tensor

$$t^{\mu\nu} = \delta T^{\mu\nu} - \tfrac{1}{2}\mathfrak{G}_0^{\mu\nu}\,\delta T , \tag{5}$$

where

$$\delta T = \mathfrak{G}_0^{\alpha\beta}\,\delta T_{\alpha\beta} ,$$

is an invariant.

From (4) we find

$$g^{\mu\nu}(x) = -2\varkappa\Box^{-2} t^{\mu\nu}(x) , \tag{6}$$

where $\Box^{-2}$ is the operator, reverse to $\Box^2$. According to (6) we can write now for the correlations of the metric tensor components at the two space-time points x and x':

$$\langle g^{\alpha\beta}(x)\, g^{\mu\nu}(x')\rangle = 4\varkappa^2\,\Box_x^{-2}\Box_{x'}^{-2}\,\langle t^{\alpha\beta}(x)\, t^{\mu\nu}(x')\rangle . \tag{7}$$

Because of the smallness of $g^{\mu\nu}(x)$, the interval between the two physical world-points A and B

$$S_{AB} = \int_A^B \sqrt{\mathfrak{G}^{\mu\nu}\,\mathrm{d}x_\mu\,\mathrm{d}x_\nu} , \tag{8}$$

may be represented as follows

$$S_{AB} = S^0_{AB} + \frac{1}{2}\int_A^B \frac{g^{\mu\nu}\,\mathrm{d}x_\mu\,\mathrm{d}x_\nu}{\sqrt{\mathfrak{G}^0_{\mu\nu}\,\mathrm{d}x_\mu\,\mathrm{d}x_\nu}} + \dots . \tag{9}$$

The mean value of $\langle S_{AB} \rangle$, in the linear approximation, is equal to S^0_{AB}, whereas the root-mean-square deviation $\langle (S_{AB} - S^0_{AB})^2 \rangle = \Delta S^0_{AB}$, according to (9), may be written as

$$\Delta S^2_{AB} = \frac{1}{4} \int_A^B \mathrm{d}x_\mu \int \mathrm{d}x'_\mu \langle g_{\mu\mu}(x)\, g_{\mu\mu}(x') \rangle \,. \tag{10}$$

Here the direction of the interval S^0_{AB} is taken along the $0x_\mu$ axis.

Making use of (7) we express now ΔS^2_{AB} in terms of the matter fluctuations

$$\Delta S^2_{AB} = \frac{\varkappa^2}{2} \int_A^B \mathrm{d}x_\mu \int_A^B \mathrm{d}x'_\mu \Box_x^{-2} \Box_{x'}^{-2} \langle t^{\mu\mu}(x)\, t^{\mu\mu}(x') + t^{\mu\mu}(x')\, t^{\mu\mu}(x) \rangle \,. \tag{11}$$

Thus, in the linear approximation, the problem reduces to the calculation of the double correlations of the tensor $t^{\mu\nu}(x)$.

3. – An estimation of metric fluctuations in the macroworld.

The motion of matter will be treated as a motion of a perfect compressible fluid. The tensor of matter for this case reads:

$$T^{\mu\nu} = \left(\varrho + \frac{P}{c^2} \right) \frac{u^\mu u^\nu}{c^2} - \frac{P}{c^2} g^{\mu\nu} \,. \tag{12}$$

Here ϱ is the rest mass density of the medium, $P = f(\varrho)$ is the pressure, u^μ are the velocity components of the medium. From (5) and (12) we obtain

$$t^{\mu\nu}(x) = A^{\mu\nu}(x)\, \delta\varrho + B(x)\, \frac{\delta(u^\mu u^\nu)}{c^2} \,, \tag{13}$$

where

$$A^{\mu\nu}(x) = \left(1 - \frac{v^2}{c^2} \right) \left(\frac{u^\mu u^\nu}{c^2} - \frac{1}{2} \mathfrak{G}^{\mu\nu}_0 \right) ,$$

and

$$B(x) = \left(\varrho + \frac{P}{c^2} \right) , \qquad v^2 = \frac{\mathrm{d}P}{\mathrm{d}\varrho} \,,$$

is the square of the velocity of sound. Note, that the density fluctuations $\delta\varrho$, by the order of magnitude, are equal to $(\delta u^2 / v^2)\varrho$.

Consider now the tensor correlations $g^{\mu\nu}$ outside the volume Ω occupied by the turbulent matter. According to (7), we get

$$\langle g^{\nu\nu}(x)\, g^{\nu\nu}(x') \rangle = 4\varkappa^2 \iint_\Omega \frac{\mathrm{d}^3 y\, \mathrm{d}^3 z}{R(x, y)\, R(x', z)} \langle t^{\nu\nu}([t], y)\, t^{\nu\nu}([t'], z) \rangle \,, \tag{14}$$

where $R(x, y)$ and $R(x', z)$ are the distances between x and y, x' and z, while

$$[t] = t - \frac{R(x, y)}{c}, \qquad [t'] = t' - \frac{R(x', z)}{c},$$

are the retarded moments of time.

If δu^2 is not small compared with v^2, but still appreciably less than c^2, then among the components $t^{\mu\nu}$ only the term t^{44} is important. At the same time $A^{44} \simeq \frac{1}{2}$, $B^{44} \ll A^{44}$, therefore: $\langle t^{44}(y) t^{44}(z)\rangle \simeq \langle \delta\varrho(y)\, \delta\varrho(z)\rangle$.

When the medium is sufficiently homogeneous this quantity will depend weakly upon $\frac{1}{2}(y+z)$ and essentially depend upon $(y-z)$. Passing now in (14) to the coordinates $\frac{1}{2}(y+z)$ and $(y-z)$, it is not difficult to obtain an estimate of (14) for

$$x = (\boldsymbol{x}, t), \qquad x' = (\boldsymbol{x}, t'),$$

$$\langle g^{44}(t, \boldsymbol{x})\, g^{44}(t', \boldsymbol{x})\rangle \simeq \frac{\varkappa^2 \Omega \omega(t'-t)\, \delta\varrho^2}{R^2}. \tag{15}$$

Here $\Omega = (4\pi/3)R^3$ is the volume of the medium, $\omega(t'-t)$ is the correlation function, which is equal, at $t=t'$, to the fluctuation volume (λ^3), $\delta\varrho$ is the amplitude of the medium density fluctuation. As is seen from (15), the fluctuations of the metric tensor are proportional to $\sim R^{\frac{1}{2}}\lambda^{\frac{3}{2}}$, where R are the linear dimensions of the medium, λ is the linear scale of turbulentness. Correspondingly:

$$\Delta S_{AB}^2 \simeq \frac{\varkappa^2 \Omega \omega \tau\, \delta\varrho^2}{R^2}\, t \simeq \varkappa^2 \omega\tau \cdot \delta\varrho^2 \cdot R \cdot t, \tag{16}$$

where τ is the time scale of turbulentness.

4. – An estimation of metric fluctuations in the microworld.

Let us now evaluate the correlation between the quantities g^{44} at the points x and x' which is due to the oscillations of the scalar field μ, with the non-zero rest mass.

In this case the Lagrange function is

$$\mathscr{L} = \frac{1}{2}\sqrt{\mathfrak{G}}\left(\mathfrak{G}^{\alpha\beta}\, \frac{\partial\psi}{\partial x_\alpha}\, \frac{\partial\psi}{\partial x_\beta} - \mu^2\psi^2\right), \tag{17}$$

and the tensor of matter equals

$$T^{\mu\nu}(x) = \mathfrak{G}_0^{\mu\alpha}\, \mathfrak{G}_0^{\nu\beta}\, \frac{\partial\psi}{\partial x_\alpha}\, \frac{\partial\psi}{\partial x_\beta} - \delta T^{\mu\nu} \cdot \mathscr{L}. \tag{18}$$

Due to the nature of the vacuum the quantities $\mathfrak{G}_0^{\mu\nu}$ have now the Galilean values. It is not the tensor $T^{\mu\nu}$ but only its fluctuations $\delta T^{\mu\nu}$ we are interested in. In order to obtain $\delta T^{\mu\nu}$ from (18) it is sufficient to mean by $(\partial\psi/\partial x_\alpha)(\partial\psi/\partial x_\beta)$, ψ^2 etc. the

normal products of these operators. Therefore, according to (5) and (18), we get

$$t^{44}(x) = \frac{1}{2}\,\mathfrak{G}_0^{\alpha\beta}\,\frac{\partial\psi}{\partial x_\alpha}\,\frac{\partial\psi}{\partial x_\beta} - \mu^2\psi^2\,, \tag{19}$$

here the products of the operators are considered already normal.

Expanding, as usual, the field ψ into a Fourier series

$$\psi = \frac{1}{V^{\frac{1}{2}}}\sum_k\sum_{k'}\left(\frac{\hbar}{2\omega_k}\right)^{\frac{1}{2}}\left(a_k \exp\left[i(k,x)\right] + a_k^+ \exp\left[-i(k,x)\right]\right), \tag{20}$$

where V is the normalized volume, $\omega_k = c\sqrt{k^2+\mu^2}$, $k=(\boldsymbol{k},\omega)$, a_k, a_k^+ are the annihilation and production operators of the field particles. A substitution of (20) into (19) yields

$$t^{44}(x) = \frac{1}{V}\sum_k\sum_{k'}\left(\frac{\hbar^2}{2\omega_k\omega_{k'}}\right)^{\frac{1}{2}}\left\{A_{kk'}(x)a_k a_{k'} + B_{kk'}(x)a_k^+ a_{k'} + B^*_{kk'}(x)a_{k'}^+ a_k + A^*_{kk'}(x)a_k^+ a_{k'}^+\right\}, \tag{21}$$

and

$$A_{kk'}(x) = -\tfrac{1}{2}\left[2\mu^2 + (k,k')\right]\exp\left[i(k+k',x)\right], \tag{22}$$

$$B_{kk'}(x) = -\tfrac{1}{2}\left[2\mu^2 - (k,k')\right]\exp\left[-i(k-k',x)\right]. \tag{22'}$$

From (21) and (7) and by averaging over the vacuum, we find

$$\tfrac{1}{2}\langle g_{44}(x)g_{44}(x') + g_{44}(x')g_{44}(x)\rangle = \tag{23}$$
$$= \hbar^2\varkappa^2\iint\frac{\mathrm{d}^3k\,\mathrm{d}^3k'}{\omega_k\omega_{k'}}\left[\frac{2\mu^2+(k,k')}{(k+k',k+k')}\right]^2\cos\left(k+k',x-x'\right).$$

For $x=(\boldsymbol{x},ct)$, $x'=(\boldsymbol{x},ct')$, $t'-t=T$ we get

$$\tfrac{1}{2}\langle g_{44}(x)g_{44}(x') + g_{44}(x')g_{44}(x)\rangle = \tag{24}$$
$$= \frac{2\pi\hbar^2\varkappa^2}{c^2}\int_0^K\int_0^K\frac{k^2\,\mathrm{d}k\,k'^2\,\mathrm{d}k'}{\omega\omega'}\left\{\frac{1}{2} + \frac{\mu^2}{2kk'}\lg\frac{\mu^2+\omega\omega'+kk'}{\mu^2+\omega\omega'-kk'} + \frac{\mu^2}{\mu^2+k^2+k'^2}\right\}\cos\left(\omega+\omega',T\right).$$

This integral is divergent at the upper limit, by $K\to\infty$.

If the rest mass of the field particles is zero ($\mu=0$), then for $KcT\gg 1$ the integral in (16) is tending to zero like $1/T^2$, whereas for small times $KcT\ll 1$ it behaves like K^4 *viz*:

$$\begin{cases} \tfrac{1}{2}\langle g_{44}(t)g_{44}(t') + g_{44}(t')g_{44}(t)\rangle = \dfrac{2\pi\hbar^2\varkappa^2}{c^2}\,\dfrac{K^4}{8}\,, & KcT\ll 1 \\ \qquad\qquad = \dfrac{2\pi\hbar^2\varkappa^2}{c^2}\,\dfrac{K^2}{c^2T^2}\cos 2KcT, & KcT\gg 1\,. \end{cases} \tag{25}$$

It is seen from here, that the metric fluctuations become essential, if $cT \ll 1/K = L_0$ and the scale L_0 is determined by the formula

$$L_0 = \left(\frac{\hbar\varkappa}{c}\right)^{\frac{1}{2}} = 0.82 \cdot 10^{-32} \text{ cm} . \tag{26}$$

This scale is much larger than the gravitational radii of particles $L_g = \varkappa\mu$ (μ is the mass of particles), which are usually treated as characteristic dimensions of that region of space in which the gravitational effects in the microworld could be essential. However, it is still considerably smaller even than those small scales which are characteristic of weak interactions ($\sim 10^{-16}$ cm).

Note, that the mass of the field particles is of no importance for the metric until the Compton length of the particle $L_c = \hbar/\mu c$ is longer than its gravitational radius L_g since $L_0 = (L_g L_c)^{\frac{1}{2}}$, then the condition $L_c > L_g$ is equivalent to the condition $L_0 > L_g$.

Pion Resonances (*).

J. J. Sakurai

The Enrico Fermi Institute and the Department of Physics
The University of Chicago - Chicago, Ill.

(ricevuto il 24 Marzo 1960)

In recent years it has become increasingly evident that no further progress in strong interaction physics will be made until we know something about interactions of pions among themselves. The present letter is concerned with possible « resonances » in two-pion and three-pion systems.

In an interesting paper Frazer and Fulco (1) have shown that a two-pion resonance in $T=1$, $J=1$ can account for the large isovector moment $(\mu_p - \mu_n)$ of the nucleon (2); in fact, as Chew (3) remarks, the Frazer-Fulco resonance appears to be « the only explanation of the situation that does not abandon local field-theory ». It is expected that this $T=1$, $J=1$ resonance would be helpful not only in understanding the isovector part of the nucleon structure but also in attacking the so-called two-pion contribution in $\mathcal{N}\mathcal{N}$ scattering and $\pi\mathcal{N}$ scattering.

One may naturally ask whether or not the two-pion contribution together with the « non-controversial » one-pion contribution is sufficient to account for the major features of the nuclear force down to the « core ». It is easy to see that the answer to this question is negative. A straightforward application of G conjugation invariance shows that, if the repulsive core in $\mathcal{N}\mathcal{N}$ interactions is due to an exchange of two pions (four, six pions, etc.), there must also be a repulsive core in $\mathcal{N}\bar{\mathcal{N}}$ interactions whereas, if it is due to an exchange of three pions (five, seven pions, etc.), there must be a very strong short-range attraction between a nucleon and an antinucleon. Recent antiproton experiments show that both the annihilation cross section and elastic cross section are « large » not only at (100÷300) MeV (which is not surprising in view of the work of Ball and Chew (4)) but also

(*) Work carried out under the auspices of the U.S. Atomic Energy Commission.

(1) W. R. Frazer and J. R. Fulco: *Phys. Rev. Lett.*, **2**, 365 (1959).

(2) The need for such an enhancement mechanism was first emphasized by S. D. Drell: *Annual International Conference on High-Energy Physics at CERN* (Geneva, 1958). See also P. Federbusch, M. L. Goldberger and S. B. Treiman: *Phys. Rev.*, **112**, 642 (1958).

(3) G. F. Chew: *Possible manifestations of a pion-pion interaction*, UCRL-9028, January 1960 (unpublished).

(4) J. S. Ball and G. F. Chew: *Phys. Rev.*, **109**, 1395 (1958).

in GeV regions [5] (which *is* somewhat surprising). If we are not to abandon local field theory, we would like to believe that the interaction radius of the annihilation region (the so-called « black hole ») is small ($\approx 0.5 \cdot 10^{-13}$ cm), and the observed large antiproton cross sections in GeV regions are reasonable only if there exists a short-range, very deep attractive well (in addition to the long-range one-pion-exchange tail of Ball and Chew) which is capable of drawing an incident antinucleon into the « black hole » even at higher (≈ 1 GeV) energies. Having ruled out a repulsive core in the $\mathcal{N}\mathcal{N}$ case, we conclude that the repulsive core in the $\mathcal{N}\mathcal{N}$ case is due to a three-pion state.

The three pions that are capable of producing anything like the hard core effect must necessarily be correlated. Using an elementary argument, one can convince oneself that, if the repulsive core (attractive well) in $\mathcal{N}\mathcal{N}$ ($\mathcal{N}\overline{\mathcal{N}}$) interactions is to exist in all angular momentum and parity states, it must be due to a state which has the same symmetry properties as a neutral vector meson ($T=0$, $J=1$, odd G conjugation parity) coupled to the nucleon via an effective vector-type coupling. We can readily construct a $\pi^+\pi^-\pi^0$ system (but not a $3\pi^0$ system) with the desired symmetry properties.

In this manner we are led to the view that there exists a three-pion resonance in $T=0$, $J=1$. Such a resonance also throws light on the isoscalar part of the nucleon structure as previously discussed by NAMBU in a similar context [6]. The « large » isoscalar charge radius and the « small » isoscalar moment can be understood if the effective coupling between the three pion resonance and the nucleon turns out to be of the vector type rather than of the tensor type in agreement with our nuclear force considerations. On the other hand, the strong effective tensor coupling between the Frazer-Fulco resonance and the nucleon required to produce the large isovector moment might not be surprising in view of the analytic properties of $\pi\mathcal{N}$ scattering amplitudes which exhibit the three-three resonance in the physical region. These superficial and qualitative remarks on the two-nucleon (nucleon-antinucleon) problem and the nucleon structure may have some value if they serve to encourage investigations of the « experts » who have hitherto regarded the three pion state as a state of uncomputable and unmanageable complexity.

Recently a new theory of strong interactions (hereafter denoted as VTSI, the vector theory of strong interactions) has been proposed which, among other things, unambiguously predicts the existence of one two-pion resonance in $T=1$, $J=1$ and two three-pion resonances both in $T=0$, $J=1$ [7]. Since a three-pion resonance (or bound state) has been also proposed by CHEW [8], it is worth emphasizing the differences between the Chew theory and VTSI.

(1) In the Chew theory the same attractive force between two pions in a p state is responsible for both the Frazer-Fulco two-pion resonance and Chew's three-pion resonance. In VTSI the three resonances are deeply rooted in the three internal conservation laws of strong inter-

---

[5] T. ELIOFF *et al.*: *Phys. Rev. Lett.*, **3**, 285 (1959).

[6] Y. NAMBU: *Phys. Rev.*, **106**, 1366 (1957).

[7] J. J. SAKURAI: *Ann. Phys.* (to be published). In an attempt to localize the conservation laws of isospin, hypercharge and baryon number in the sense of Yang and Mills [*Phys. Rev.*, **96**, 191 (1954)] there emerge three vector-type couplings such that in each case a vector field is coupled linearly to the conserved current in question. These vector fields are taken to be massive, and the corresponding quanta appear as resonances in two-pion and three-pion systems since they « decay strongly » into pions.

[8] G. F. CHEW: *Phys. Rev. Lett.*, **4**, 142 (1960).

actions — isospin conservation, hypercharge conservation, and baryon conservation — and are not related to each other.

(2) In the Chew theory there is only one $T=0$, $J=1$ three-pion resonance while VTSI predicts *two* $T=0$, $J=1$ three-pion resonances. The two theories are hardly distinguishable as far as the nuclear force problem and the nucleon structure problem are concerned. The empirical fact that there are *two* $T=\frac{1}{2}$ resonances and *one* $T=\frac{3}{2}$ resonance in $\pi\mathcal{N}$ interactions above the three-three resonance might be related to the *two* $T=0$ three-pion resonances and the *one* $T=1$ two-pion resonance that appear in VTSI.

(3) VTSI is far more specific in predictions as to how these resonances are dynamically coupled to strongly interacting particles; in fact the couplings are uniquely determined by the very existence of the three conservation laws. For instance, VTSI really predicts that the $K\mathcal{N}$ « potential » should be repulsive while the $\overline{K}\mathcal{N}$ « potential » should be attractive provided that the dominant parts of the $\overline{K}\mathcal{N}$ and $K\mathcal{N}$ forces are due to an exchange of one of the three-pion resonances. In contrast the Chew theory is phenomenological in character.

Every conceivable experimental attempt should be made to detect the conjectured resonances. Some of the possible experiments have already been discussed by CHEW ([3,8]). Frascati-type experiments to study $\gamma + p \to p + X^0$ should be carried out at various energies and angles ([9]). In $\mathcal{N}\overline{\mathcal{N}}$ annihilations pions interacting in these resonant states are expected to be produced abundantly ([10]), and they may well account for the unexpectedly large pion multiplicity. It is suggested that in future experiments with antiprotons directions and momenta of neutral pions as well as those of charged pions be studied so that the conjectured resonances may be unambiguously identified ([11]).

It is hoped that these pion resonances will throw light on all the questions in strong interactions of non-strange particles that cannot be answered on the basis of the Yukawa concept:

(1) Why is s wave $\pi\mathcal{N}$ scattering isospin dependent?

(2) Why is there an anomalous d wave scattering at 300 MeV? ([12]).

(3) Why does the static model with a direct $\pi\mathcal{N}$ interaction fail to explain the reaction $\pi^- + p \to \pi^+ + \pi^- + n$ at (250÷450) MeV? ([13]).

(4) Why is multiple pion production more copious than is to be expected from simple statistical considerations?

(5) Why are the « higher resonances » in $\pi\mathcal{N}$ interactions so sharp? Why are there only three « higher resonances »?

(6) What is the origin of the repulsive core? That of the spin-orbit force?

(7) Why are the antiproton cross sections so large not only at (100÷÷300) MeV but also in GeV regions?

([9]) C. BERNARDINI, R. QUERZOLI, G. SALVINI, A. SILVERMAN and G. STOPPINI: *Nuovo Cimento*, **14**, 268 (1959).

([10]) If these resonances exist, a set of correlation numbers recently invented by Pais [*Ann. Phys.* (to be published)] turn out to be an extremely useful tool for analyzing antiproton data.

([11]) According to G. GOLDHABER and D. A. GLASER experiments along this line may be feasible in a hydrogen bubble chamber with lead plates inside, or in a xenon bubble chamber with a small hydrogen target inside.

([12]) J. H. FOOTE, O. CHAMBERLAIN, E. H. ROGERS, H. M. STEINER, C. WYEGAND and T. YPSILANTIS: *Phys. Rev. Lett.*, **4**, 30 (1960).

([13]) W. A. PERKINS, J. C. CARIS, R. W. KENNEDY, E. A. KNAPP and V. PEREZ-MENDEZ: *Phys. Rev. Lett.*, **3**, 56 (1959).

(8) Why is the average pion multiplicity in $\mathcal{N}\,\bar{\mathcal{N}}$ annihilations higher than is to be expected from a « resonable » interaction volume? ([14]).

(9) Why is the isovector moment $(\mu_p - \mu_n)$ so large?

(10) Why is the charge radius of the proton so large? That of the neutron so small?

* * *

The author is indebted to Professor Y. NAMBU for interesting conversations. Thanks are also due to Dr. H. P. NOYES for informing the author of the nature and progress of work carried out by the Berkeley-Livermore group.

([14]) N. HORWITZ D. MILLER, J. MURRAY and R. TRIPP: *Phys. Rev.*, **115**, 472 (1959).

Production and Decay of an $\overline{\Sigma^+}$.

E. Amaldi, A. Barbaro-Galtieri, G. Baroni, C. Castagnoli, M. Ferro-Luzzi, A. Manfredini, M. Muchnik, V. Rossi and M. Severi

Istituto Nazionale di Fisica Nucleare - Sezione di Roma
Istituto di Fisica dell'Università - Roma

(ricevuto il 17 Aprile 1960)

1. – About one year ago we started a search for $\overline{\Sigma^+}$ by exposing emulsion stacks to antiproton beams of the Bevatron of the Radiation Laboratory in Berkeley. A first exposure, in March 1959, to a beam of 1.65 GeV/c momentum (1), did not give any positive result. A second exposure was made in October 1959 to the 2.05 GeV/c purified $\overline{\text{p}}$ beam (2). In the course of the scanning of this stack (175 G-5 emulsions 600 μm thick) we observed the event shown schematically in Fig. 1.

Track 1 belongs to the beam of negative incident particles, the composition of which corresponds, very roughly, to 1 antiproton for every 2 pions and 1 muon. The angle of dip of the incident particle is 1°; the center of star A is in emulsion No. 69, point C in emulsion No. 67 and the center of star B in emulsion No. 66.

Table I.

Track no.	Angle	Observed range (cm)	$p\beta$ (MeV/c)	w_0/w	n/n_0	β	Mass (MeV)	Identification
2	5° 10′	1.79	1 430±210	1.12±.04	1.09±.03	.76±.03	1 600±300	$\overline{\Sigma^+}$
3	2° 27′	0.85	685±100	1.18±.04	1.12±.03	.71±.03	970±190	$\overline{\text{p}}$

w_0 and n_0 correspond to measurements on tracks of the incident antiprotons.

Table I shows the $p\beta$ — derived from scattering measurements —, the mean gap-length w and the number of blobs n for tracks 2 and 3; it contains also the values of the corresponding masses, deduced by combining the $p\beta$ with the β

(1) T. Elioff, L. Agnew, O. Chamberlain H. Steiner, C. Wiegand and T. Ypsilantis: *Phys. Rev. Lett.*, **3**, 285 (1959).

(2) Our stack was exposed to the purified $\overline{\text{p}}$ beam prepared for the 72 inch Hydrogen Bubble Chamber of the Alvarez Group.

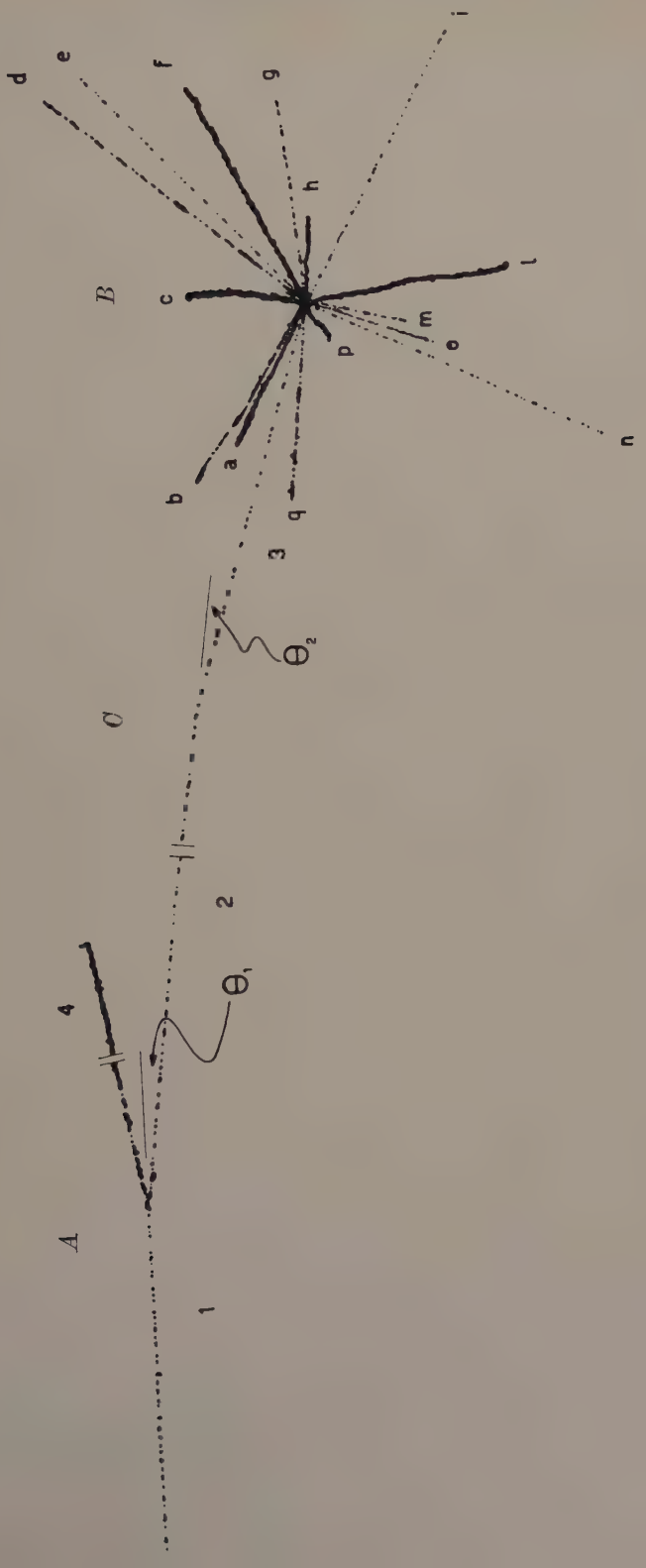
d
e
f
g
h
i
B
c
l
m
p
o
n
a
b
q
3
Θ_2
O
2
Θ_1
4
A
1

derived from the ionization measurements. The calibration curves for w and n have been derived from careful measurements of 15 incident particles identified as $\bar{p}$ from obvious annihilation stars, and 5 positive pions identified from the π-μ-e decay at rest. The error attached to the β values arises in part from the statistical error, and in part from the dispersion of the calibration points. Track 1 is too short (1 cm) for scattering measurements.

The features of stars A and B are collected in Table II.

2. – The experimental evidence suggests the following interpretation of the event. Star B is due to the annihilation of an antiproton (track 3) which is produced in the decay of an $\overline{\Sigma^-}$ (track 2) at C ($\theta_2 = 2° 27'$). The $\overline{\Sigma^+}$ is produced in star A by an incident antiproton (track 1).

Arguments in favour of such an interpretation are the following.

a) The mass of particle 3 is very close to that of a proton (Table I); if we attribute to particle 3 a protonic mass, the corresponding kinetic energy turns out to be

$$T_3 = (400 \pm 70) \text{ MeV} .$$

The visible energy of star B (Table II) is at least 1.2 GeV larger than T_3; therefore the star must to be due to

TABLE II.

Star	Track	Range (mm)	Identification	Kinetic energy (MeV)	Binding energy or rest mass (MeV)
A	4	41	p	118	8
	2	—	$\overline{\Sigma^+}$	910±150	1189
	Probable recoil	$\sim 10^{-3}$	—	—	—
B	a	1.55	p	18.0	8
	b	1.36	p	16.5	8
	c	0.21	p	5.6	8
	d	14.0	p	64.0	8
	e	—	π	280.0±80	139.6
	f	1.73	p	19.0	8
	g (*)	> 50.0	p	> 135.0	8
	h	0.15	p	4.5	8
	i	36.0	p	115.0	8
	l	0.4	p	8.2	8
	m (**)	> 18.5	p	> 175.0	8
	n	—	π	200.0±60	139.6
	o	23.0	p	85.0	8
	p	1.5	p	18.0	8
	q	29.6	p	98.5	8
				Total > (1242±100) MeV	383 MeV
				Total visible energy: > 1.6 GeV	

(*) The identification of this track is uncertain because it leaves the stack and is steeply dipping. The energy balance does not change appreciably if it is attributed to a pion.

(**) Leaves the stack.

an annihilation process. The argument is strengthened by considering, besides the visible energy, the energy taken away by neutral particles.

b) The value of the mass of particle 2 favours its interpretation as a hyperon (Table I).

c) The values of the momenta of tracks 2 and 3 — derived from the $p\beta$'s — and of the angle θ_2 agree, within one experimental error, with the kinematics of the decay process

$$\Sigma \to p + \pi^0 + 115.9 \text{ MeV} . \qquad (1)$$

At point *C* no electron, recoil or blob is visible; the tracks 2 and 3 are joined in an extremely clear region of the emulsion. Having established that track 3 is due to an antiproton, the observed reaction should be

$$\overline{\Sigma^+} \to \bar{p} + \pi^0 + Q . \qquad (1')$$

It is to be noticed that, if one assumes that the $\overline{\Sigma^+}$ has the same mean life as the Σ^+, the decay mean free path expected at the observed energy, is 3.9 cm; this should be compared to an observed path of 1.79 cm.

d) From the Lorentz transformation of the $\bar{p}$ velocity to the c.m.s. one derives a value of its emission angle compatible within one (large) experimental error, with the value deduced from transvers momentum consideration. The latter gives:

$$\sin \theta_2^* = 0.22 \pm 0.03 ; \quad \pi - \theta_2^* = 13^\circ \pm 1.5^\circ .$$

e) Track 1 should be due to a $\bar{p}$, since a π^- of 2.05 GeV/c momentum is below the threshold for production of $\overline{\Sigma}$'s.

3. – The energy balance of star *A* is the following:

Kinetic en. of $\overline{\Sigma^+}$ . .	(910 ± 150) MeV
Kinetic en. of track 4	118 MeV
$M_\Sigma - M_p$	251 MeV
Total	(1279 ± 150) MeV

This energy should be compared with the kinetic energy of the incident antiproton:

$$T_1 = 1320 \text{ MeV} ;$$

thus, about (40 ± 150) MeV are available in star *A* for the probable very short recoil (Table II) and for possible neutral-non visible-particles.

This energy balance agrees satisfactorily with the following interpretation of star *A*. The incident $\bar{p}$ collides with a neutron bound in a heavy nucleus of the emulsion, and gives rise to the process

$$\bar{p} + n \to \overline{\Sigma^+} + \Lambda^0 , \qquad (2)$$

with the Λ^0 bound in the heavy target nucleus.

The hyperfragment takes a kinetic energy of the order of one hundredth of the kinetic energy of the $\overline{\Sigma^+}$ and therefore should produce a recoil hardly visible. Then, in about 10^{-12} s, it decays through a typical non-mesonic decay, according to the scheme

$$\Lambda^0 + p \to n + p + 175 \text{ MeV} . \qquad (3)$$

The proton emitted in this reaction should have an energy distribution around 88 MeV. This value compares well with the 118 MeV of track 4. The neutron produced in process (3), as well as other possible evaporation neutrons, escape observation.

An alternative to process (3) for producing track 4 would be an elastic collision $\Lambda^0 + p$; but the energy balance excludes that the Λ^0 takes an energy large enough to produce track 4.

It is not improbable that process (2), in which the Λ^0 is produced bound in the heavy target nucleus, contributes a large percentage of all the processes of production of $\overline{\Sigma^+}$, especially near the threshold, since it is favoured by the larger *Q*-value which provides a larger phase-space volume.

Another alternative to process (2), in which a $\Sigma\overline{\Sigma}$ pair is produced, is com-

patible, within one experimental error, with the measured $p\beta$ of track 2, only assuming a maximum Fermi energy of the target proton; it is unfavoured with respect to process (2) by the higher threshold.

4. – Looking for an interpretation which avoids the assumption of the existence of the $\overline{\Sigma^+}$, we have found only a possibility which neglects, however, the measured mass difference between tracks 2 and 3. One can assume that tracks 1, 2 and 3 are all due to the same antiproton, which undergoes two inelastic scatterings in *A* and *C*. One should notice that this interpretation is unfavored by various facts. First the interpretation of the deflection in *C* as an inelastic scattering of an antiproton requires the disappearence of $\Delta T_{\bar{p}} \simeq$ $\simeq 500$ MeV, with respect to the initial energy $T_{\bar{p}} = 950$ MeV, without any visible excitation energy. A similar consideration holds for star *A* which, when interpreted as an inelastic $\bar{p}$ scattering, involves a $\Delta T_{\bar{p}}/T_{\bar{p}}$ of about 400 MeV/1300 MeV. Furthermore the kinematics of tracks 2 and 3 should be such as to simulate the kinematics of the decay process (1). And finally the value of the velocity deduced from the $p\beta$ for particle 2 interpreted as a $\bar{p}$, differs by 2.5 times the experimental error from the value derived from ionisation measurements.

The number of accidental cases fulfilling these conditions which we expect to find in our observed $\bar{p}$ sample, is extremely low.

Another possibility that one could consider, is that tracks 2 and 3 are due to an $\overline{\Sigma^\pm}$, which undergoes an inelastic scattering in *C* and annihilates in *B*. This interpretation does not avoid the assumption of the existence of an antihyperon nor the difficulties connected with the measured values of the masses and with the assumption of an inelastic scattering in which a very high fraction of the incident kinetic energy disappears without any visible energy.

* * *

We express our gratitude to Dr. WENZEL and the Bevatron staff, to Prof. L. ALVAREZ and his group, to Prof. O. CHAMBERLAIN and colleagues and to Prof. G. GOLDHABER for their precious assistance in arranging and carrying out the exposures of the stacks.

LIBRI RICEVUTI E RECENSIONI

L. R. B. Elton, Ph. D., F. Inst. P. *Introductory Nuclear Theory*. Pitman & Sons Ltd., London, £ 2.00.

Dopo due capitoli introduttivi sulle proprietà generali dei nuclei, quali energia di legame, momenti magnetici e di quadrupolo, spin, ecc., l'Autore dedica il 3° capitolo all'aspetto statico e dinamico del problema dei due nucleoni, e discute nel 4° capitolo il problema delle forze nucleari. Seguono tre capitoli sui modelli, sulle reazioni e sulle disintegrazioni nucleari (disintegrazione α e fissione).

Chiudono il libro altri tre capitoli riguardanti rispettivamente l'interazione dei nuclei col campo elettromagnetico, la teorica del decadimento beta e la teorica mesonica delle forze nucleari.

La varietà degli argomenti trattati, il modo di presentare i fatti sperimentali e proporne l'interpretazione teorica ed infine i numerosi problemi proposti alla fine di ogni capitolo rendono questa introduzione alla fisica nucleare un libro adeguato per un insegnamento annuale da svolgersi nei corsi superiori delle nostre Università, in preparazione a corsi più monografici e completi che attualmente vengono svolti nelle scuole di perfezionamento. A differenza di altri trattati di maggior mole, il libro si adatta ad una lettura diretta da parte dello studente, in quanto scritto con intendimento didattico, come risulta evidente dai paragrafi introduttivi sulla teoria dell'urto, teoria delle perturbazioni ed equazioni di Dirac premessi ai capitoli relativi al problema dei due nucleoni, all'interazione dei nuclei col campo elettromagnetico ed alla teoria del decadimento beta.

Non concordo con l'Autore nel trasferire gli attributi di simmetrico ed antisimmetrico dalle autofunzioni alle particelle o sistemi che esse rappresentano (p. 39), e, a meno di non applicare l'inversione rispetto alla variabile tempo, direi che il merito di avere introdotto il potenziale di tipo spin-orbita nelle forze nucleari (p. 100) va attribuito a Case e Pais (1950) e non a Marshak e Signell (1958).

E. Clementel

H. Goldstein – *Fundamental Aspects of Reactor Shielding*. Ed.: Addison-Wesley Publishing Company Inc. ($ 9.50).

Rivolgendosi ai fisici, come biglietto di presentazione, basterebbe dire che questo libro è dovuto allo stesso Autore di *Classical Mechanics*. Siccome però gli argomenti trattati interessano anche i biologi, i chimici e gli ingegneri nucleari, aggiungerò che pochi libri presentano con tanta chiarezza di esposizione una fusione armonica fra la parte teorica e quella applicativa. A differenza di altri testi sullo stesso argomento, sono più volte precisati i limiti di validità della teoria fondamentale, indicando anche quali dovrebbero essere le future linee di sviluppo per migliorare le soluzioni attuali

dei problemi di schermaggio nelle varie applicazioni.

Dopo due capitoli introduttivi di carattere generale, con particolare riguardo agli effetti biologici delle radiazioni, segue un capitolo sulle sorgenti, sia di neutroni che di raggi gamma, delle quali va tenuto conto nell'impostazione dei problemi di schermaggio di reattori od acceleratori. La parte centrale del libro è occupata da un capitolo dove sono descritti i dispositivi sperimentali usati ad Argonne e Brookhaven per la verifica sperimentale della teoria dell'attenuazione dei raggi gamma e dei neutroni, teoria discussa nei due successivi ed ultimi capitoli.

Fra i vari metodi, sono discussi in particolare il metodo dei momenti per la soluzione dell'equazione di Boltzmann ed il metodo di Montecarlo. Soprattutto per i fisici, gli ultimi due capitoli sono di interessante e piacevole lettura.

Chiudono il libro una serie di appendici, dove sono raccolte un grande numero di tabelle di estrema utilità dal punto di vista applicativo. Altre tabelle e numerosi grafici sono inseriti anche nel testo.

E. Clementel

J. M. Jauch and F. Rohrlich – *The Theory of Photons and Electrons*. Addison-Wesley Publishing Company (Cambridge, Mass., USA, 1955), pp. 488.

Nonostante che il notevole sviluppo dell'elettrodinamica quantistica — in certo senso la sua sistemazione — sia avvenuto dal 1947 al 1950, vari anni sono intercorsi prima che l'argomento sia stato esposto e trattato esaurientemente sotto forma di libro. Il testo di Jauch e Rohrlich — che è uno tra i primi in lingua inglese — è a giudizio del recensore la trattazione più completa di questo campo fondamentale della fisica teorica moderna.

Il libro è predominantemente concepito per uso dei fisici teorici, infatti è limitato il confronto dei risultati teorici con l'esperienza e la trattazione è alquanto minuziosa e particolarmente esauriente nei dettagli formali.

Lo schema del libro si differenzia da quello classico nel quale la quantizzazione è introdotta mediante il formalismo Hamiltoniano. Qui la quantizzazione è introdotta utilizzando lo schema Lagrangiano facendo uso essenziale del Principio d'Azione; il procedimento permette di mantenere evidente l'invarianza relativistica durante tutta la trattazione.

Un notevole spazio, e sforzo, è dedicato all'impostazione generale della teoria; questa non fa uso del metodo perturbativo sin dall'inizio e quindi rappresenta una presentazione della teoria dei campi più generale di quanto sia poi necessario per l'applicazione all'elettrodinamica o a teorie caratterizzate da un accoppiamento debole che permetta uno sviluppo iterativo. In questo modo, dopo la trattazione dei campi liberi e l'impostazione delle equazioni di campo per l'interazione tra elettroni e radiazione, si trovano analizzate isolatamente quelle proprietà dei campi in interazione che derivano da invarianze sotto particolari trasformazioni (di Lorentz, di misura, inversioni spaziali e temporali, coniugazione di carica, ecc.) ed inoltre una presentazione generale del formalismo della matrice S. A questo formalismo è poi applicato il metodo iterativo arrivando in questo modo all'introduzione dei diagrammi di Feynman e alle regole per la loro valutazione. È fatto anche un rapido cenno alla valutazione della matrice S in rappresentazione di Heisemberg. Nei due capitoli susseguenti gli AA. trattano le divergenze nella serie perturbativa e la loro rinormalizzazione a tutti gli ordini nel modo consueto (separazione e riduzione delle divergenze, rinormalizzazione

di massa, carica e funzione d'onda). Avendo in questo modo sviluppato il formalismo, gli AA. lo applicano a problemi specifici nei capitoli seguenti. Così vengono studiate la diffusione Compton semplice e doppia, la diffusione elettrone-elettrone ed elettrone-positrone (compreso lo studio del positronio), la diffusione luce-luce, ecc. e — dopo avere introdotto il formalismo della matrice S in presenza di campo esterno — la diffusione coulombiana, la bremsstrahlung, la produzione di coppie, ecc. Il libro finisce con lo studio di alcuni problemi speciali — tra i quali quello delle divergenze infrarosse — e una lunga serie di appendici matematiche.

In definitiva, questo trattato ha l'indubbio valore di vedere unita alla quanto mai accurata impostazione generale della teoria la sua applicazione sistematica alla maggioranza dei processi di interesse fisico. La sua generalità e la sua precisione fanno di questo libro un testo prezioso per ogni fisico teorico interessato a questi problemi o alla teoria dei campi in generale.

D. Amati

D. Cheng – *Analysis of Linear Systems*. Addison-Wesley Publ. Co. Inc., Cambridge, Mass., USA, 12 Maggio 1959, pp. xiii-431, prezzo $ 8.50.

Il libro è, per esplicita dichiarazione dell'autore, destinato ai corsi universitari o immediatamente post-universitari per studenti e laureati in ingegneria o fisica. Per tale motivo tutta la trattazione è in generale mantenuta su un piano relativamente elementare e intuitivo. L'autore presuppone soltanto una generica conoscenza di analisi matematica e di fisica elementare. In termini di programmi universitari italiani esso è certamente comprensibile agli studenti di ingegneria, di fisica e matematica che abbiano superato il 1° biennio.

Pregio notevole del libro è di essere dotato di numerosi esempi svolti dettagliatamente e di avere inoltre alla fine di ciascun capitolo una raccolta di esercizi (con risultati!); sia gli esempi che gli esercizi sono intelligentemente scelti per imprimere nella memoria dello studente le regole fondamentali.

Dopo aver introdotto il concetto di sistema lineare nel 1° capitolo e richiamato alcuni concetti sulle equazioni differenziali nel 2° capitolo, l'autore affronta nel 3° la descrizione dei sistemi elettrici; nel 4° capitolo viene invece analizzata la corrispondenza fra circuiti meccanici ed elettromeccanici e i circuiti elettrici. Nei successivi capitoli fino all'ottavo è la trattazione vera e propria dell'analisi dei sistemi lineari con la trasformata di Fourier e con quella di Laplace. Il 9° capitolo, nel quale vengono discussi i sistemi controreazionati, ci sembra il meno apprezzabile a causa di una certa superficialità; è certamente interessante l'idea di introdurre subito i grafici di flusso, ma nel caso specifico ne è risultato un eccessivo formalismo.

Molto interessante ed opportuno il 10° capitolo che introduce alla moderna analisi dei sistemi campionati.

L'ultimo capitolo è dedicato ai sistemi a costanti distribuite.

Nel complesso l'opera ci sembra organicamente disposta e consigliabile a chi voglia iniziare lo studio dei sistemi lineari.

C. A. Galtieri

U. Fano and L. Fano – *Basic Physics of Atoms and Molecules*. John Wiley and Sons, Inc., Publisher, 1959.

La fisica atomica è una musica complicata ma ben composta che, per il fatto di essere insegnata ai fisici sin dai primissimi anni dell'università, si radica profondamente nella mente di questi

specialisti i quali, al giorno d'oggi, l'adoperano ormai con grande disinvoltura. Viceversa, il chimico, il biologo, l'ingegnere, seguendo in media tutt'altra scuola, sono costretti ad impararla ad orecchio. E conservano naturalmente, nel servirsene, una certa diffidenza sulla liceità e portata dei metodi orecchiati. Gli autori di questo libro partono da questa constatazione e si propongono di ridimensionare la mole delle basi necessarie per intendere ed usare la fisica atomica; cioè di facilitarne ed affrettarne la digestione. È difficile dire se ci riescano o meno: ho l'impressione che a molti un libro così possa essere decisamente utile (ai chimici, in particolare). Ma l'espressione « a molti » non si deve intendere nel senso che il libro sia elementare. Tutt'altro! Lo è alla base di ogni argomento trattato ma non lo è leggendo delle pagine a caso.

Le notazioni lasciano un po' perplessi. Ridondanti, si direbbe a prima vista, ma poi si capisce che certa sovrabbondanza può essere mnemonicamente comoda a chi non fa di solito dei calcoli. Inoltre si tratta di digerire dei simboli più dettagliati del solito ma non diversi dal solito, e questo è poco male.

C. BERNARDINI

Handbuch der Physik – Encyclopedia of Physics; ed. by S. FLÜGGE, vol. XLIV; Nuclear Instrumentation I (E. CREUTZ co-editor). Springer Verlag, Berlin, 1959. Prezzo DM 125.

Questo volume della Enciclopedia edita da Flügge, dedicato in massima parte alle macchine acceleratrici, consta di ben otto articoli, tutti di autorevoli specialisti, sui seguenti argomenti:

I moltiplicatori di tensione, trattati da E. Baldinger (unico pezzo in tedesco del volume); e le macchine di Van de Graaf, a cura di R. G. Herb. Su ambedue gli argomenti era sinora difficile reperire una rassegna aggiornata; i moltiplicatori di tensione in particolare compaiono raramente nelle pubblicazioni propriamente per fisici ma piuttosto sulle riviste d'ingegneria elettrotecnica.

Vengono poi i ciclotroni ed i sincrociclotroni, di B. L. Cohen; ci sembra un po' troppo succinto il paragrafo dedicato all'estrazione del beam nei sincrociclotroni.

L'articolo « Sincrotroni per elettroni » di R. R. Wilson sembra scritto con uno stile decisamente più sbrigativo degli altri del volume. In 22 pagine si parla rapidamente dei principali problemi di queste macchine; dati costruttivi sono sparsi qua e là, riferendosi quasi sempre alla macchina di Cornell.

Segue « Il Betatrone », trattato da D. W. Kerst: è anch'esso in verità un articolo un po' succinto, che ricalca alcuni noti articoli del suo autore (apparsi già molti anni fa) con qualche spruzzatina di FFAG. Non è molto chiaro come al cap. 10, intitolato « The vacuum chamber », si attacchi un paragrafo sui betatroni FFAG.

G. K. Green e E. D. Courant hanno scritto sul protosincrotrone, di gran lunga la più completa e soddisfacente rassegna del volume. In circa 120 pagine si danno, oltre alle idee fondamentali, numerosissime notizie sulle effettive modalità di funzionamento delle principali macchine esistenti. Di queste, quattro sono sistematicamente raffrontate lungo il testo (cosmotrone, Bevatrone, Sincrofasotrone e PS Birmingham). Nell'ultimo paragrafo si riparla brevemente di macchine FFAG.

Un articolo sugli acceleratori lineari, a firma di Lloyd Smith, chiude la parte riservata agli acceleratori.

Infine, ecco « Reactor techniques », di D. J. Hughes: ci si chiede in un primo momento che cosa c'entra con il resto del volume. In realtà si possono trovare argomenti pro e contro l'inserzione di questo articolo; ma se si conviene di considerare il volume come dedicato alle

sorgenti di particelle per la ricerca, allora anche le sorgenti di neutroni trovano diritto di cittadinanza e la loro sistemazione tipografica non è poi così importante. Naturalmente nell'articolo si parla poco della sorgente e piuttosto dell'uso di beams di neutroni dai reattori: l'autore circoscrive molto accuratamente il suo argomento sin dalle prime righe introduttive.

Il volume, pur denso di contributi (ben otto rassegne, ripetiamo) sembra mancante di qualcosa. L'editore avverte subito del fatto che, al momento d'uscire, i manoscritti hanno già circa due anni di vita: ma non è questo forse il guaio. Già nel 1956 il mondo degli acceleratori, più che ogni altro un mondo di « unpublished reports » e di ricette tecniche, era pieno di idee nuove. Ebbene, ci sembra che manchi il cosiddetto « cappello », la panoramica introduttiva che guida per le strade di questa costosissima strumentazione nucleare. Inoltre in questa panoramica avrebbe forse trovato posto, accanto alle proposte di storage rings o di macchine a plasma, anche il trascurato microtrone che, se non altro, ha il vantaggio di funzionare.

C. BERNARDINI

Direttore responsabile: G. POLVANI Tipografia Compositori - Bologna

Questo Fascicolo è stato licenziato dai torchi il 10-V-1960